AD-A085 759 KAMAN AVIDYNE BURLINGTON MA F/G 17/2
STRUCTURAL MODELING AND RESPONSE OF COMMAND, CONTROL AND COMMUN--ETC(U)
MAR 80 J M CALLIGEROS, J P WALSH DAAD05-74-C-0744
UNCLASSIFIED KA-TR-151 ARBRL-CR-00421 NL

1 of 3

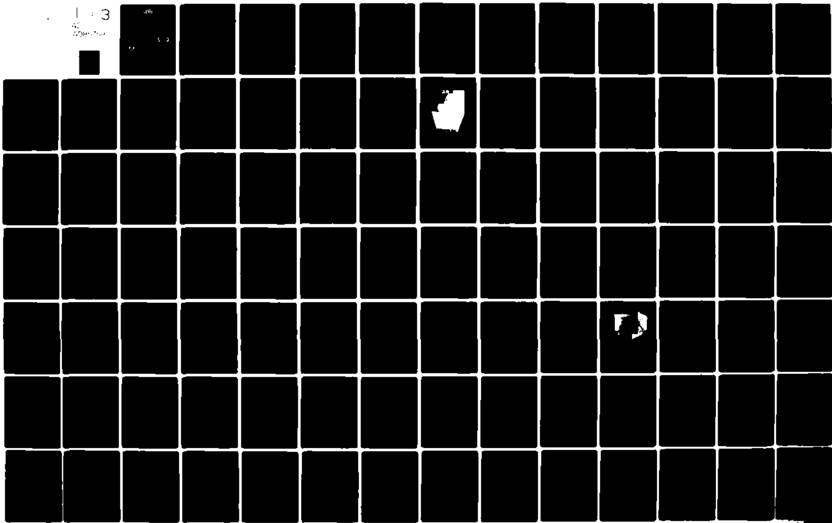

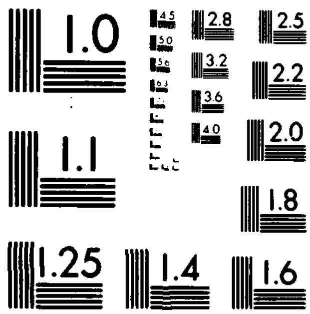

MICROCOPY RESOLUTION TEST CHART
NATIONAL BUREAU OF STANDARDS-1963-A

(12) LEVEL III

AD-E430442

AD

ADA085759

CONTRACT REPORT ARBRL-CR-00421

STRUCTURAL MODELING AND RESPONSE OF COMMAND, CONTROL AND COMMUNICATION SHELTER SYSTEMS FOR EVENT DICE THROW

Prepared by

Kaman AviDyne
83 Second Avenue
Burlington, MA 01803

March 1980

US ARMY ARMAMENT RESEARCH AND DEVELOPMENT COMMAND
BALLISTIC RESEARCH LABORATORY
ABERDEEN PROVING GROUND, MARYLAND

UNCLASSIFIED

SECURITY CLASSIFICATION OF THIS PAGE (When Data Entered)

REPORT DOCUMENTATION PAGE		READ INSTRUCTIONS BEFORE COMPLETING FORM
1. REPORT NUMBER CONTRACT REPORT ARBRL-CR-00421	2. GOVT ACCESSION NO. AD-A085 759	3. RECIPIENT'S CATALOG NUMBER
4. TITLE (and Subtitle) Structural Modeling and Response of Command, Control and Communication Shelter Systems for Event DICE THROW		5. TYPE OF REPORT & PERIOD COVERED Final Report 26 July 1977 - 1 March 1978
		6. PERFORMING ORG. REPORT NUMBER KA TR-151
7. AUTHOR(s) John M. Calligeros John P. Walsh Raffi P. Yeghiayan		8. CONTRACT OR GRANT NUMBER(s) DAAD05-74-C-0744
9. PERFORMING ORGANIZATION NAME AND ADDRESS Kaman AviDyne Division of Kaman Sciences Corporation 83 Second Avenue, Burlington, MA 01803		10. PROGRAM ELEMENT, PROJECT, TASK AREA & WORK UNIT NUMBERS
11. CONTROLLING OFFICE NAME AND ADDRESS U.S. Army Armament Research & Development Command U.S. Army Ballistic Research Laboratory ATTN: DRDAR-BL Aberdeen Proving Ground, Maryland 21005		12. REPORT DATE MARCH 1980
		13. NUMBER OF PAGES 271
14. MONITORING AGENCY NAME & ADDRESS(if different from Controlling Office)		15. SECURITY CLASS. (of this report) UNCLASSIFIED
		15a. DECLASSIFICATION/DOWNGRADING SCHEDULE

16. DISTRIBUTION STATEMENT (of this Report)

Approved for public release; distribution unlimited.

17. DISTRIBUTION STATEMENT (of the abstract entered in Block 20, if different from Report)

18. SUPPLEMENTARY NOTES

This research was sponsored by the U.S. Army Project DA No. 1L162118AH75, AMCMS Code 632306.11.H7200, Nuclear Weapons Effects for Army Applications, Blast and Shock.

19. KEY WORDS (Continue on reverse side if necessary and identify by block number)

Finite Element Modeling	Blast Response
Electronic Equipment Shelter	NASTRAN Modeling
Command Control Communication Systems	Structural Dynamics
DICE THROW	Blast Loading

20. ABSTRACT (Continue on reverse side if necessary and identify by block number)

Structural finite element models of the Army command, control, and communication systems AN/TRC-117, AN/TRC-110, AN/TCC-61 which utilizes the S-280 shelter, and the AN/TRC-145 and AN/GRC-142B, which utilize the S-250 shelter, were developed for NASTRAN. Loading models and dynamic response for overpressure levels experienced in the recent DICE THROW field test were determined for all but the AN/GRC-142B. Comparisons between measured and analytical accelerations are given for the AN/TRC-117 and the AN/TRC-145 at

DD FORM 1473, 1 JAN 73 EDITION OF 1 NOV 65 IS OBSOLETE

UNCLASSIFIED

SECURITY CLASSIFICATION OF THIS PAGE (When Data Entered)

an incident overpressure level of 41.4 kPa. The comparisons were generally poor for the AN/TRC-117 but much more favorable for the AN/TRC-145.

FOREWORD

This work was performed for Ballistic Research Laboratories, Aberdeen Proving Ground, Md., under Contract Number DAAD05-74-C-0744 by Kaman AviDyne, Burlington, MA., a division of Kaman Sciences Corporation. The technical monitor for BRL was Dr. W. Don Allison. Mr. John M. Calligeros was the project leader and principal investigator of the study which was performed in the Structural Mechanics Group of Kaman AviDyne headed by Mr. E. S. Criscione.

The authors are grateful to Dr. W. Don Allison and Dr. William Schuman for their support during the course of the contract and to Mr. Joseph Roma of ECOM, Fort Monmoth, N.J., for providing configurational data on the various shelter-rack systems. The authors also acknowledge the following Kaman AviDyne personnel: Mr. Lawrence J. Mente for developing the structural model of the AN/TRC-145, Mr. Michael Tomayko for processing the NASTRAN runs and machine plots, and Mr. William Lee for computer processing of the various loading models.

TABLE OF CONTENTS

PRECEDING PAGE BLANK-NOT FILMED

LIST OF ILLUSTRATIONS

LIST OF ILLUSTRATIONS (CONT'D)

LIST OF ILLUSTRATIONS (CONT'D)

LIST OF ILLUSTRATIONS (CONT'D)

LIST OF ILLUSTRATIONS (CONT'D)

LIST OF ILLUSTRATIONS (CONT'D)

LIST OF ILLUSTRATIONS (CONT'D)

LIST OF ILLUSTRATIONS (CONCL'D)

LIST OF TABLES

LIST OF TABLES (CONCL'D)

SECTION I

INTRODUCTION

An area of major concern to the Army is the blast response of acceleration sensitive equipment systems housed in truck mounted communication shelters. These systems include those for command, control and communications (C^3) and others such as S^3, TACFIRE, TOSS, and TRI-TAC. This subject is of considerable importance because the proper functioning of acceleration-sensitive equipment can be restricted by the shock-induced acceleration levels, resulting in negation of the mission of the Army system.

The blast response of electronic equipment housed in communication shelters is inherently complex since the equipment response is affected by the response of the supporting rack structure, the response of the shelter walls and by the motions of the truck. Currently, two complementary efforts are underway at Kaman AviDyne for BRL in this area. One effort, which is the primary subject of this report, is concerned with the detailed structural modeling and response of the shelter and of the equipment racks to the blast loads. Structural models of the shelter and racks are formulated with the finite element code NASTRAN as flexible interconnected structures subjected to the blast overpressure loads and to the base motions of the truck. The companion effort, on the other hand, is concerned with the development of the code TRUCK for predicting the nonlinear gross motions and possible overturning of a truck-shelter-rack system in response to blast. The base motions from the TRUCK code may be used as input data to the NASTRAN model to provide the base excitation experienced by the truck-mounted shelter system.

Several operational Army electronic communication shelter systems were modeled in the current study with NASTRAN for the DICE THROW field test. These include the AN/TRC-117, AN/TRC-110 and the AN/TCC-61 systems which are housed in the S-280 shelter, and the AN/TRC-145 system which is housed in the S-250 shelter. The S-280 systems are mounted on the M35A2 2½ ton truck and the S-250 system on the M715 1¼ ton truck. Each of these systems consists of a basic shelter structure whose side walls are of sandwich construction with internal stiffeners. Channel extrusions along each free edge of the shelter provide additional strength and stiffening. The shelters contain electronic equipment racks of open framework construction using standard extrusions. The racks are usually connected to the shelter floor and to an adjacent shelter wall(s). Various electronic equipment are supported on the racks and additional equipment and electrical apparatus are located within the shelter.

Typically, each of the S-280 systems has a mass of approximately 2300 kg, about twice the mass of the S-250 system. The dynamical degrees-of-freedom of the NASTRAN models ranged from approximately 150

for the AN/TRC-145 to 275 for the AN/TCC-61. In essence, the final number of degrees-of-freedom reflects a compromise between the desire to reproduce a high degree of detail in the structural model and the practical considerations regarding computer storage and running times. The NASTRAN version used was Level 15.5.1 for the SCOPE 3.3 operating system. In addition to the above mentioned systems, structural models were developed for the AN/GRC-142B system which utilizes the S-250 shelter and a hardening concept for the AN/TRC-145.

Four major stages were involved in developing each shelter-rack structural model. The first consisted in arriving at an understanding of the internal structural geometry of the system using engineering drawings provided by ECOM and photographs in technical manuals. This resulted in a definition of the structural load paths, connectivity of frame and panel members, structural cross-sections, stiffness and mass destributions, and rack geometry. The second area involved the actual layout of the NASTRAN model, selection of the appropriate NASTRAN structural elements, property calculations, grid point layout, boundary condition selection, etc. The third phase was concerned with the preparation of a blast loading model, starting with pressure-time history information, converting it to forces at the loaded grid points of the shelter and introducing the grid loads into NASTRAN. Finally, the TRUCK code was exercised to determine the base response from which base motion loading tables were prepared for NASTRAN.

Section 2 of the report describes the structural model developed for each system, including pertinent data on the truck. Section 3 discusses the blast loading and presents acceleration time histories for the modeled systems (except the AN/GR-142B for which there was no requirement) as obtained by NASTRAN for several selected overpressure levels of the DICE THROW test. Section 3 also presents comparisons between NASTRAN predictions and the DICE-THROW data for two systems, the AN/TRC-117 and the AN/TRC-145, each at an incident overpressure level of 41.4 kPa (6.0 psi). Finally, a summary and conclusions are given in Section 4.

SECTION 2

STRUCTURAL MODELS

2.1 S-280 SHELTER SYSTEMS

The AN/TRC-117, AN/TRC-110 and the AN/TCC-61 systems are each housed in the S-280 electronic equipment shelter. A photograph of the S-280 shelter is shown in Fig. 2.1 and overall dimensions are given in Figs. 2.2-2.4.

The S-280 shelter is basically a closed rectangular box whose side walls are of sandwich construction with internal hat stiffeners, containing channel extrusions along each edge of the shelter. The three systems mentioned above differ from each other with respect to the internally mounted electronic equipment, the rack frames used to support this equipment and in the installation of the rack frames within the shelter. The basic shelter, however, is structurally the same for each system.

2.1.1 Basic S-280 Shelter

A NASTRAN finite element model of the S-280 shelter was developed from engineering drawings provided by ECOM. The shelter walls and roof were modeled as flexible structures using the NASTRAN plate (CQUAD1) and beam (CBAR) elements; the floor, however, was assumed rigid. Though the shelter has mass symmetry, the inclusion of the rack structure destroys the symmetry of the complete system. Therefore, it was necessary to model the entire shelter structure without the benefit of symmetry for reducing the dynamical degrees-of-freedom. Previous S-280 shelter models prepared under the current effort made use of symmetry because they had symmetric rack arrangements.

The basic coordinate system of the structure was located as shown in Fig. 2.5 and in Figs. 2.2-2.4. The blast wave is assumed to travel in direction 3, impinging upon the roadside wall and subsequently enveloping the entire shelter. Figures 2.6-2.10 show the grid systems for the shelter walls and roof. Dimensions are shown to the midplanes of the walls and roof and to the centerlines of the beam members. A typical cross-section of a wall or roof panel is depicted in Fig. 2.11. The sandwich panel is constructed of 0.813 mm aluminum facing sheets with a urethane foam core. The density of the urethane core is 64 kg/m^3 in the roof and in the two outer bays of the roadside and curbside walls, and 32 kg/m^3 in the remaining bays of the curbside and roadside walls and in the front end and door end walls.

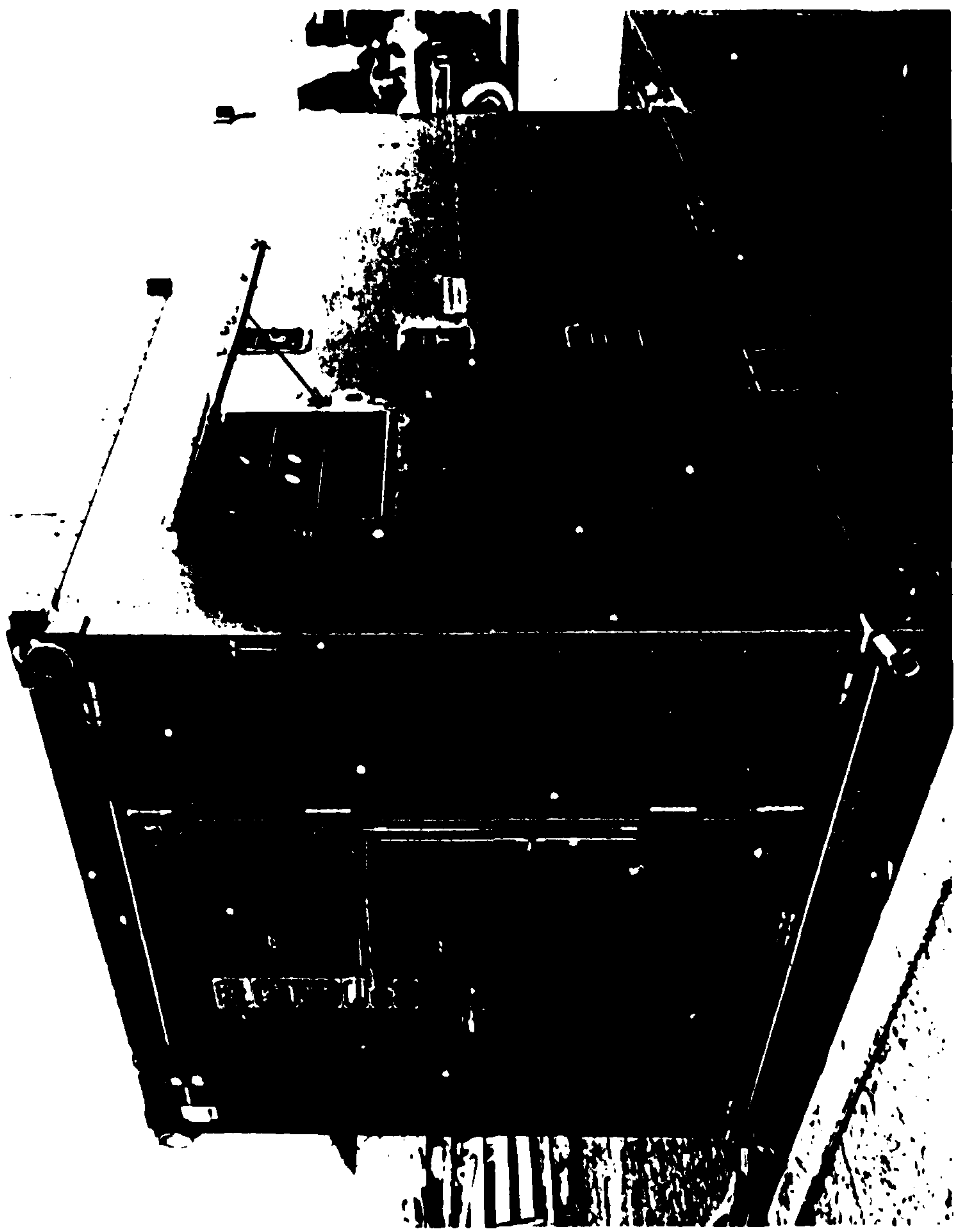

FIGURE 2.1. S-280 SHELTER

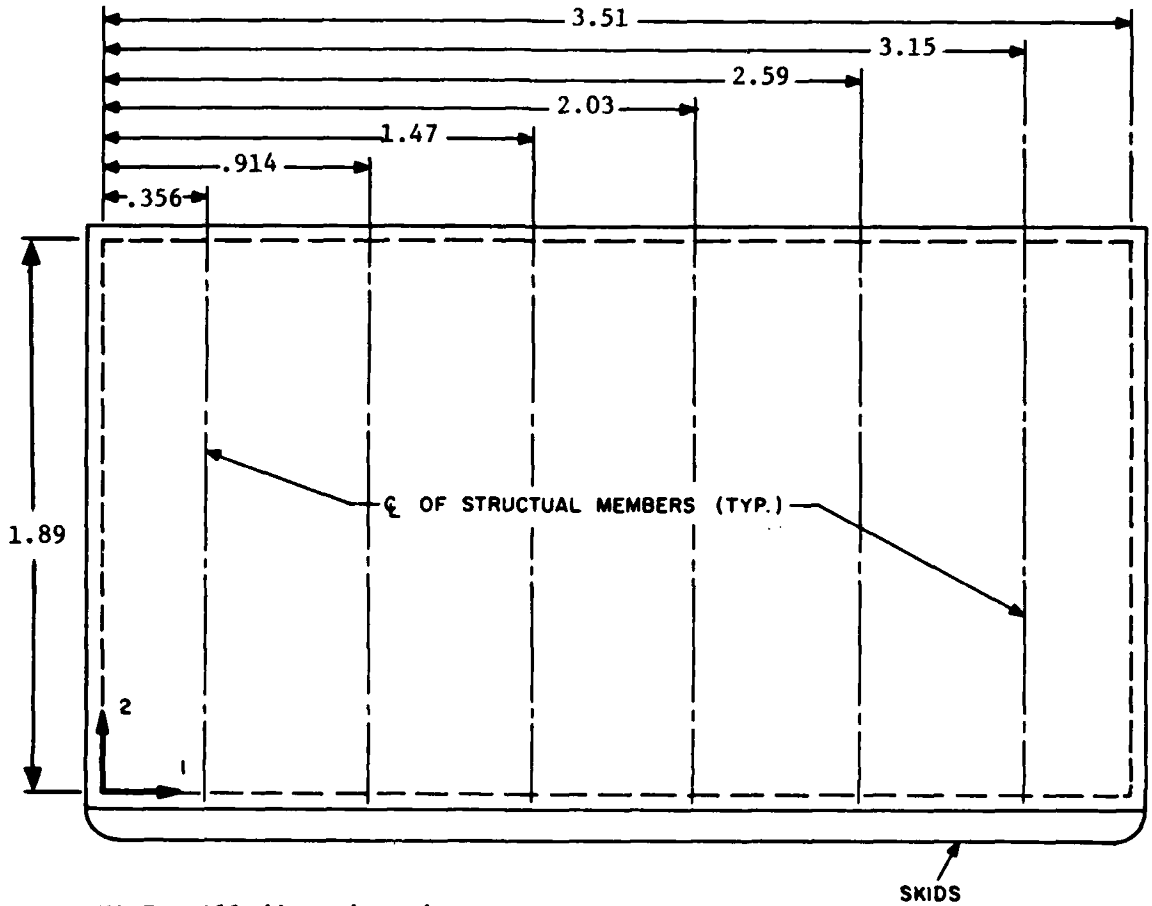

NOTE: All dimensions in metres

FIGURE 2.2 S-280 ROADSIDE AND CURBSIDE WALL DIMENSIONS

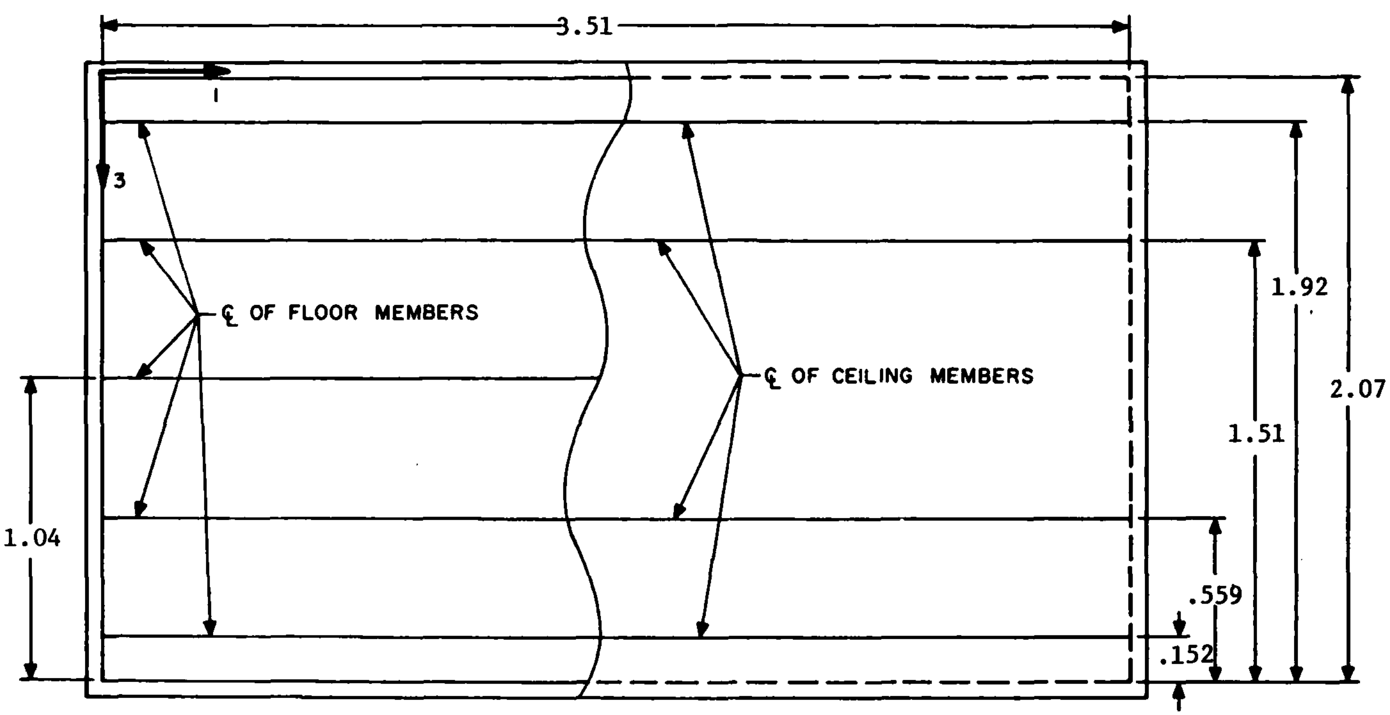

NOTE: All dimensions in metres

FIGURE 2.3 S-280 FLOOR AND ROOF DIMENSIONS

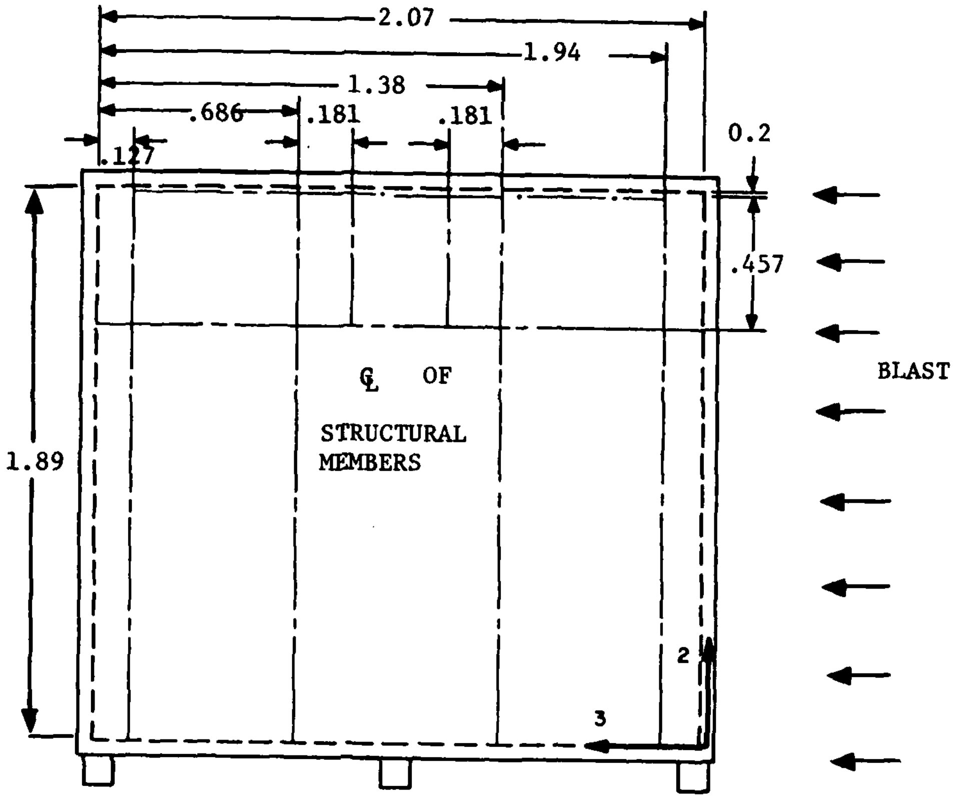

NOTE: All dimensions in metres

FIGURE 2.4. S-280 END WALL DIMENSIONS

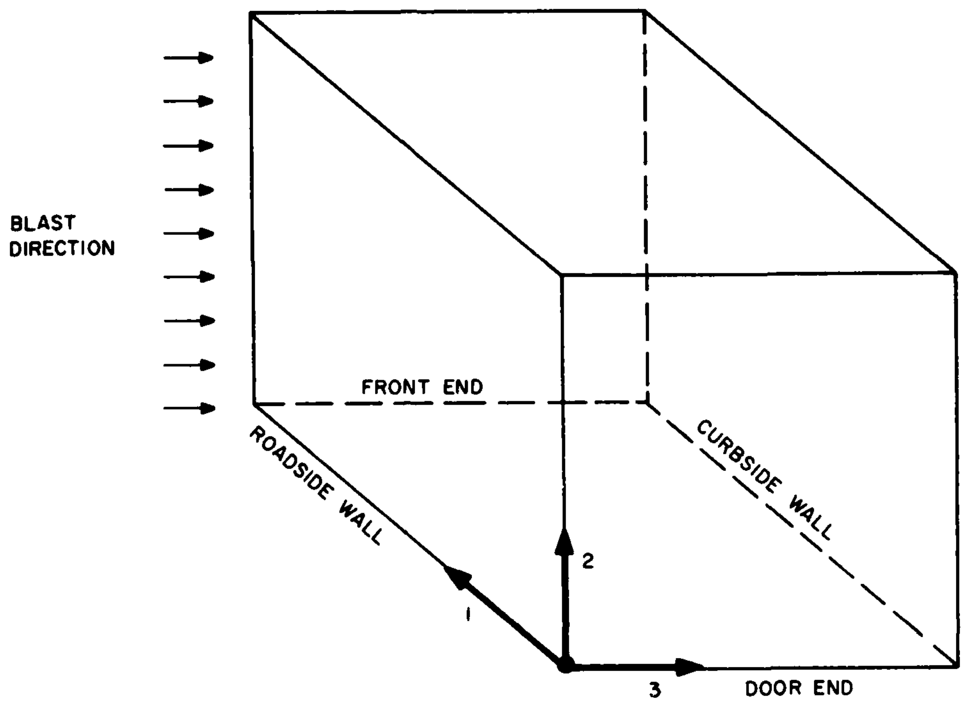

FIGURE 2.5. COORDINATE SYSTEM DEFINITION FOR AN/TRC-117, AN/TRC-110 AND AN/TCC-61 SYSTEMS

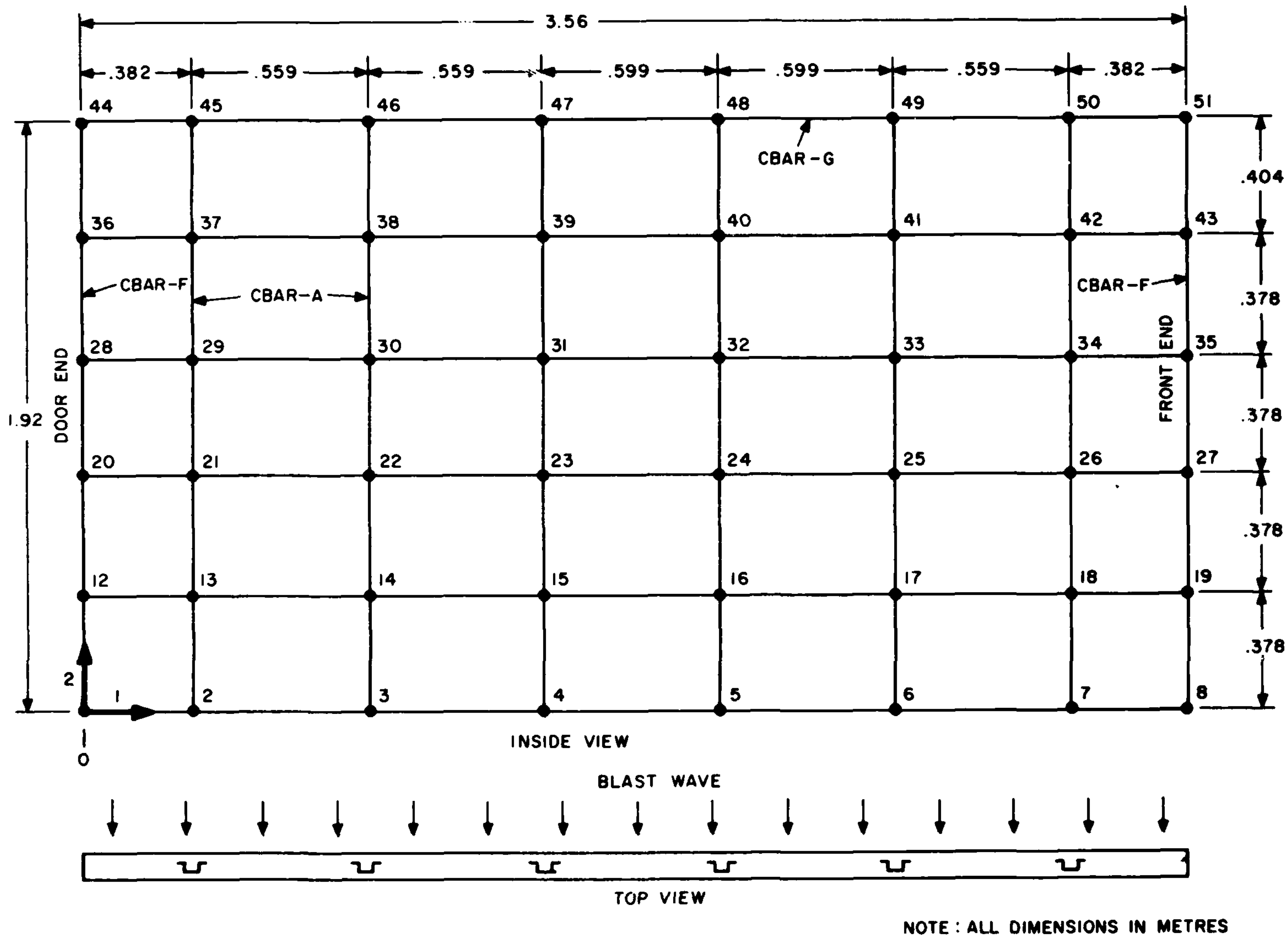

FIGURE 2.6. S-280 ROADSIDE WALL GRID SYSTEM

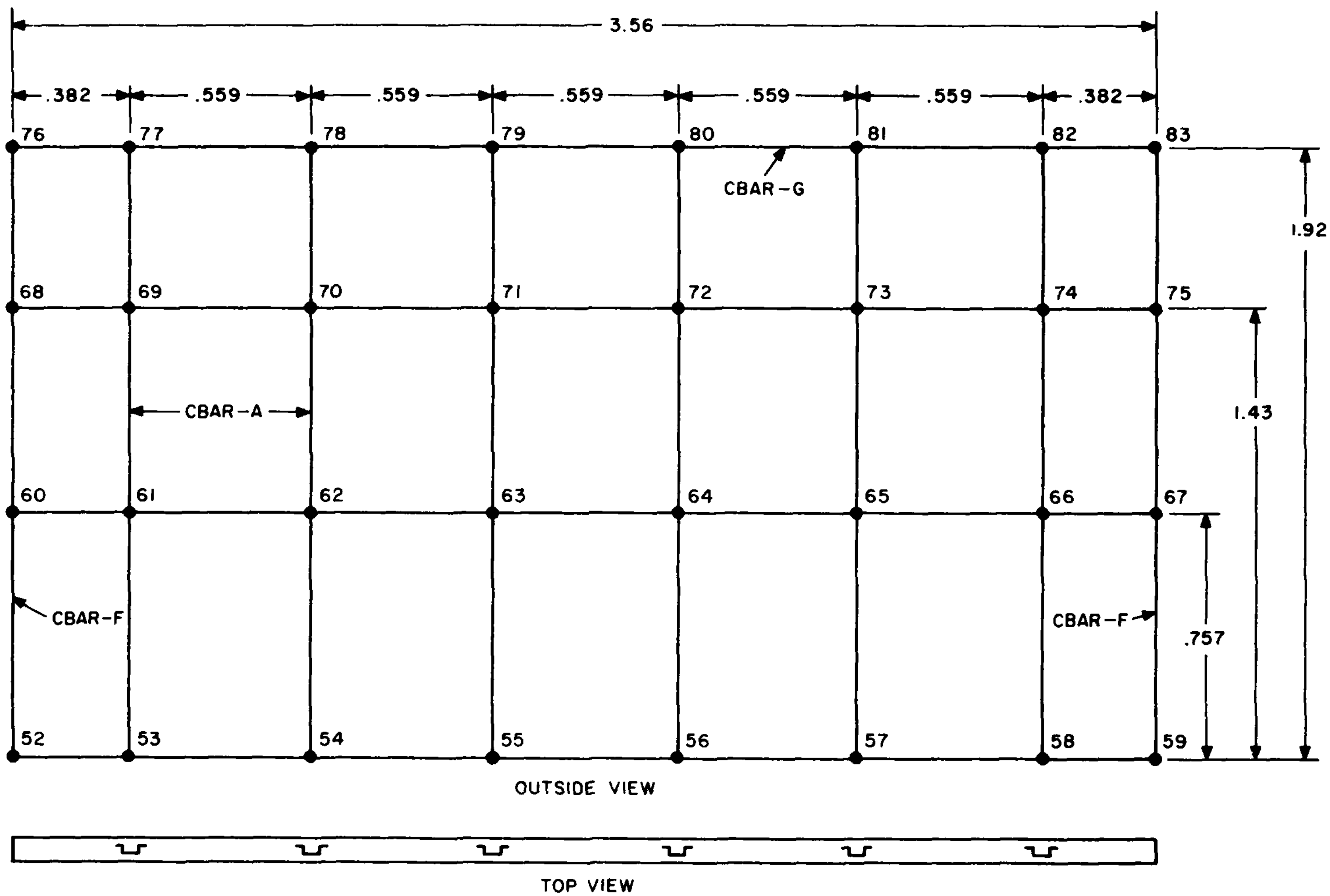

NOTE: ALL DIMENSIONS IN METRES

FIGURE 2.7. S-280 CURBSIDE WALL GRID SYSTEM

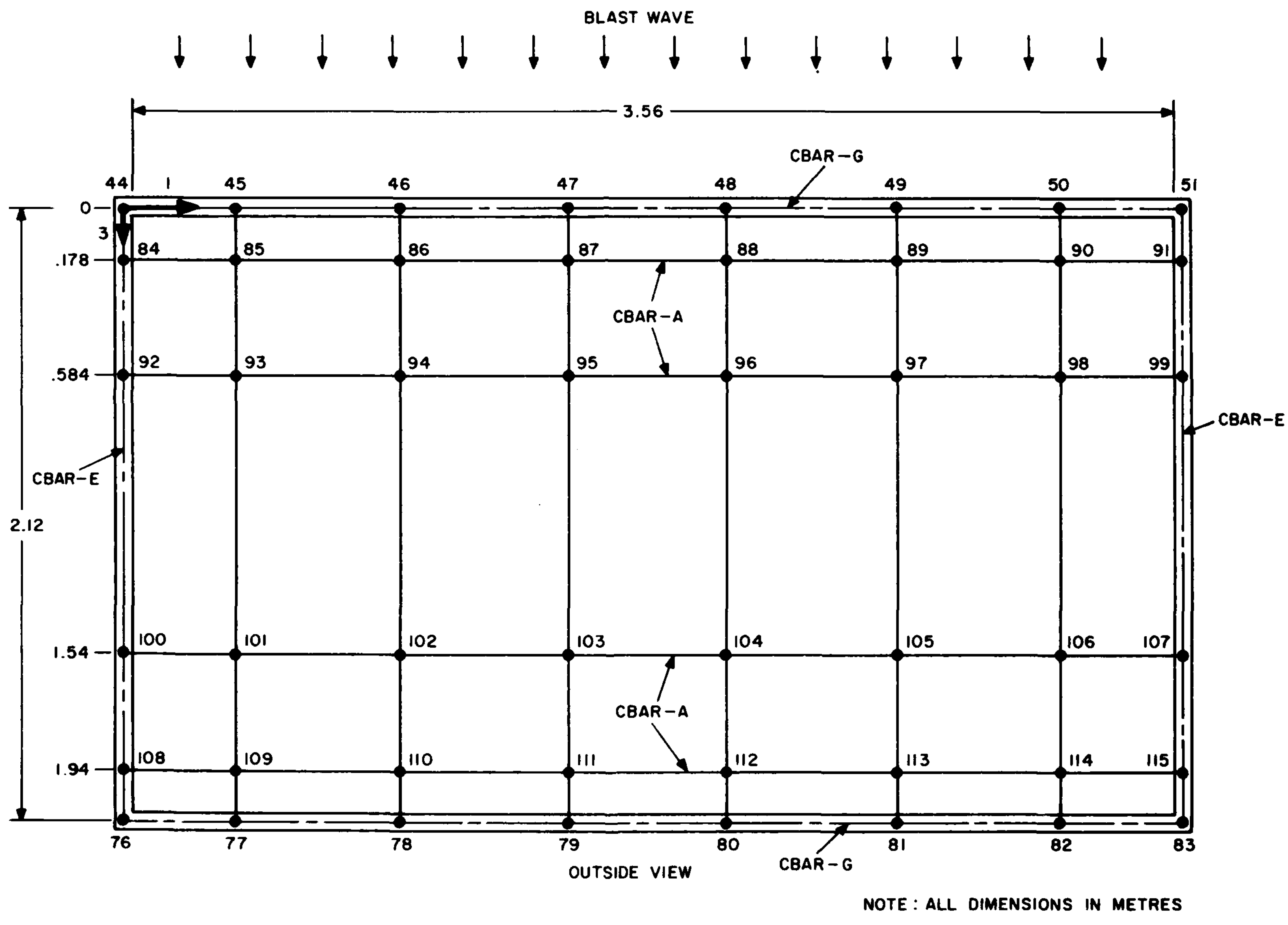

FIGURE 2.8. S-280 ROOF GRID SYSTEM

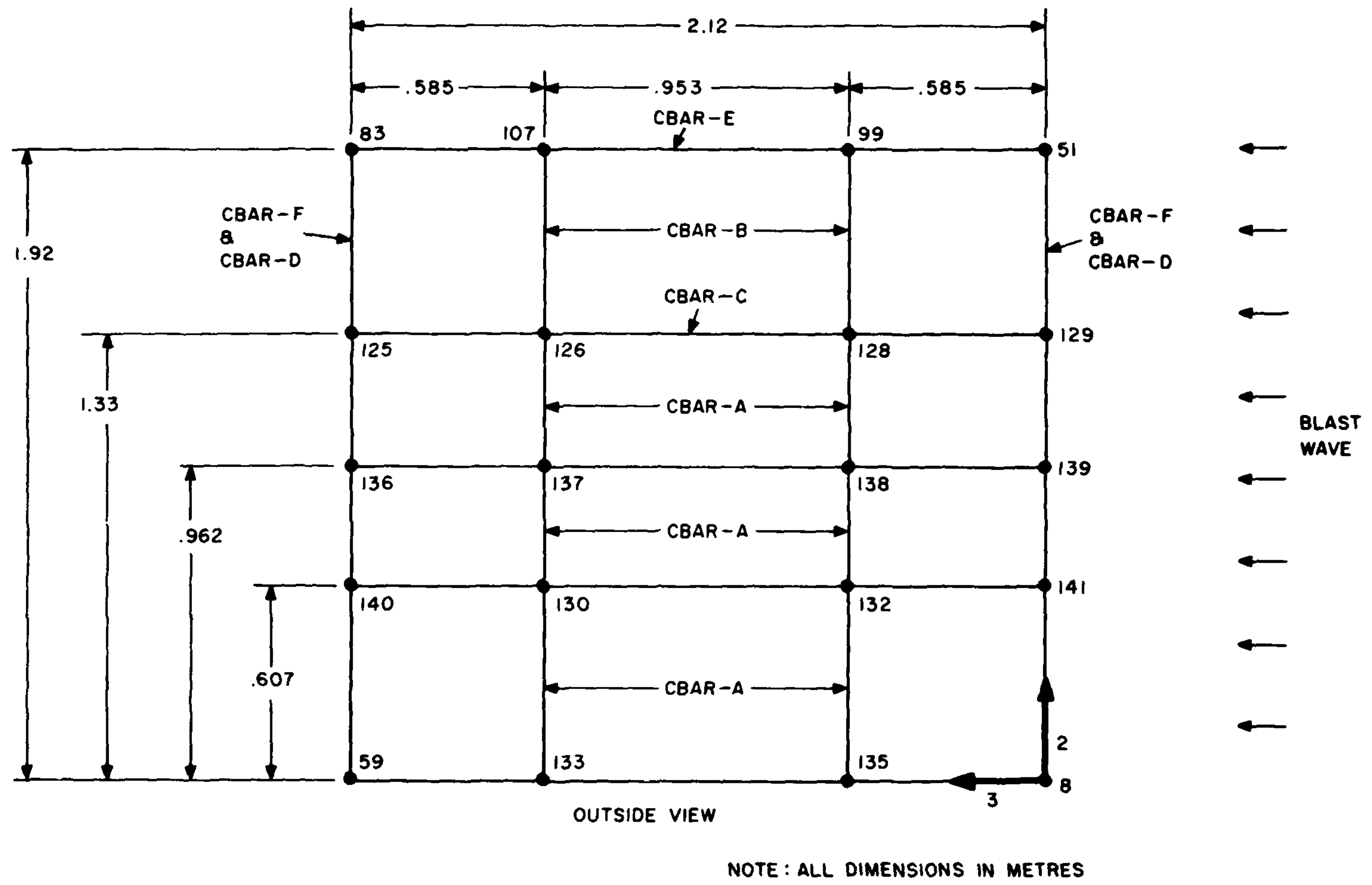

FIGURE 2.9. S-280 FRONT END WALL GRID SYSTEM

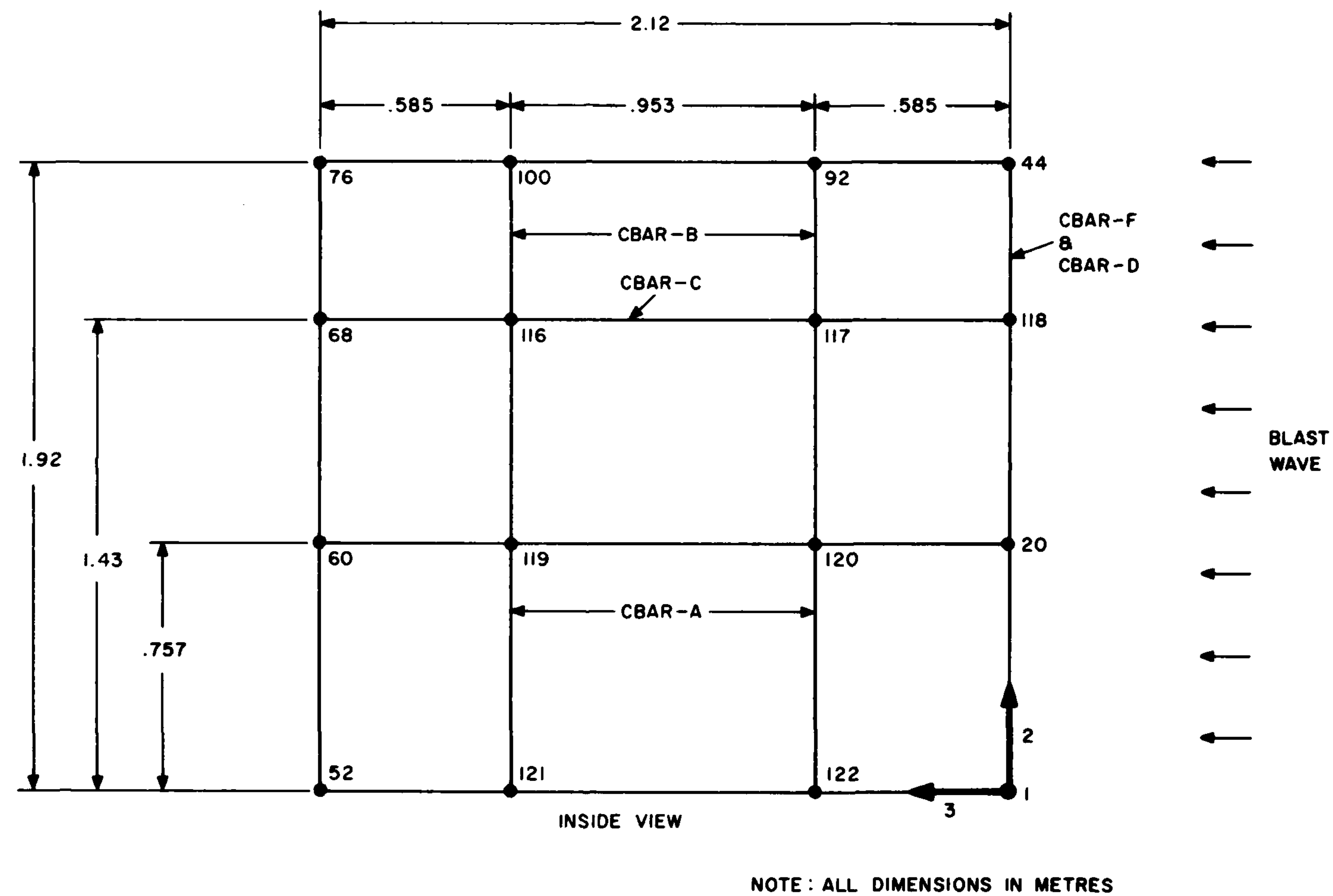

FIGURE 2.10. S-280 DOOR END GRID SYSTEM

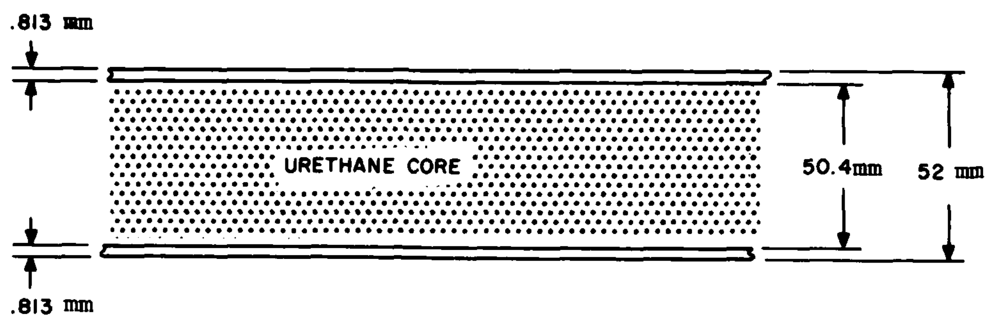

FIGURE 2.11. TYPICAL S-280 SANDWICH PANEL

The sandwich panel was modeled with the CQUAD1 plate element, which reproduced the bending, extensional and shear stiffnesses. Table 2.1 lists the panel properties, referring to the dimensions given in Fig. 2.11. Also tabulated is the panel mass density ρ

$$\rho = \frac{\rho_F t_F + 2\rho_S t_S}{T_1} \tag{2.1}$$

where ρ_F, t_F are the urethane core density and thickness, ρ_S, t_S are the skin density and thickness, and T_1 is the reference membrane thickness. It is seen that the core density affects only the panel mass density and the transverse shear stiffness. CQUAD1 plate elements were connected between the grid points of each surface in Figs. 2.6-2.10, i.e., 35 elements were used for the roadside wall, 21 for the curbside wall, 35 for the roof, 12 for the front end and 9 for the door end.

The shelter has vertical and horizontal beam members along its edges and within each wall panel and the roof. Table 2.2 lists the section properties of these beam members (CBAR elements) and Table 2.3 identifies their grid point connections.* Figures 2.6-2.10 may also be referred to for beam element identification.

The total weight of the modeled shelter structure as determined by the structural NASTRAN elements was 137 kg less than the actual weight, due to miscellaneous items such as hardware, weldments, fasteners, paint and adhesive which were not accounted for in the model. Concentrated mass cards (CONM2) were used to distribute the 137 kg at the grid points of the shelter walls and roof. The total weight of the S-280 shelter is 613 kg (Ref. 1).

The NASTRAN shelter model thus developed was used in each of the AN/TRC-117, AN/TRC-110 and AN/TCC-61 systems. Each system was then modeled by incorporating the appropriate racks and equipment within the basic shelter model. A description of each rack model is given in the following sections.

2.1.2 AN/TRC-117 Racks

The AN/TRC-117 system consists of two equipment racks located at the roadside wall and a double rack at the front end wall. The rear of each rack is bolted to the wall and the rack bases to the floor. A schematic of the rack arrangement is shown in Fig. 2.12 and the grid systems of the racks are given in Figs. 2.13 and 2.14 (dimensions shown are to the centerlines of structural members).

---

*Cross-section dimensional data may be obtained from the referenced ECOM drawings in Table 2.2.

Reference 1. Private Communication from Mr. Joe Roma of ECOM, Fort Monmouth, N. J.

TABLE 2.1

S-280 PANEL PROPERTIES (CQUAD1)

PROPERTY	CORE DENSITY	
	$\rho_F = 32\ kg/m^3$	$\rho_F = 64\ kg/m^3$
I (cm^4/cm)	2.70	2.70
T_1 (mm)	1.63	1.63
T_3 (mm)	50.4	50.4
E (GPa)	68.9	68.9
G (MPa)	1.38	2.76
ν	.33	.33
ρ $(\frac{Mg}{M^3})$	3.77	4.77

TABLE 2.2

PROPERTIES OF S-280 SHELTER BEAM ELEMENTS

CBAR	I_{zz} (cm^4)	I_{yy} (cm^4)	I_{yz} (cm^4)	J (cm^4)	K_y	K_z	A (mm^2)	ECOM DRAWING NO.
A 	10.8	13.3	0	12.7	.35	.65	363	SM-B-165318
B 	4.97	.951	0	.122	.50	.50	147	SM-B-165440
C 	4.02	7.34	0	.016	.63	.37	189	SM-B-165439
D 	14.7	18.3	$\pm$1.38	13.3	.42	.58	454	SM-B-508769
E 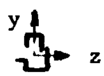	137.0	64.4	$\pm$5.61	.641	.60	.40	103	SM-B-165304 SM-B-165439
F 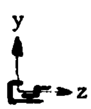	63.6	61.8	$\pm$1.74	45.8	.45	.55	101	SM-B-165304 SM-B-165310
G 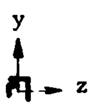	24.3	23.0	$\pm$9.59	.362	.50	.50	577	SM-B-165300 SM-B-165437

NOTE: The $\pm$ sign on I_{yz} is determined by the beam location, since the cross-section may be reversed.

TABLE 2.3

CBAR ELEMENT CONNECTIONS
FOR THE S-280 SHELTER

CBAR	GRID POINT CONNECTIONS	NUMBER OF ELEMENTS	LOCATION
A	2,13,21,29,37,45	5	
	3,14,22,30,38,46	5	
	4,15,23,31,39,47	5	ROADSIDE
	5,16,24,32,40,48	5	WALL
	6,17,25,33,41,49	5	
	7,18,26,34,42,50	5	
	53,61,69,77	3	
	54,62,70,78	3	CURBSIDE
	55,63,71,79	3	WALL
	56,64,72,80	3	
	57,65,73,81	3	
	58,66,74,82	3	
	84 → 91	7	
	92 → 99	7	ROOF
	100 → 107	7	
	108 → 115	7	
	133,130,137,126	3	FRONT END
	135,132,138,128	3	
	121,119,116	2	DOOR END
	122,120,117	2	

TABLE 2.3 (CONT'D)

CBAR	GRID POINT CONNECTIONS	NUMBER OF ELEMENTS	LOCATION
B	126,107 128, 99	2 2	FRONT END
	116,100 117, 92	2 2	DOOR END
C	125,126,128,129 68,116,117,118	3 3	FRONT END DOOR END
D	1,20,118,44 52,60,68,76	3 3	DOOR END
	8,141,139,129,51 59,140,136,125,83	4 4	FRONT END
E	44,84,92,100,108,76	5	INTERSECTION ROOF AND DOOR END
	51,91,99,107,115,83	5	INTERSECTION ROOF AND FRONT END
F	1,12,20,28,118,36,44	6	INTERSECTION ROADSIDE WALL AND DOOR END
	8,19,141,27,139,35, 129,43,51	8	INTERSECTION ROADSIDE WALL AND FRONT END
	52,60,68,76	3	INTERSECTION CURBSIDE WALL AND DOOR END
	59,140,67,136,125,75,83	6	INTERSECTION CURBSIDE WALL AND FRONT END
G	44 → 51	7	INTERSECTION ROADSIDE WALL AND ROOF
	76 → 83	7	INTERSECTION CURBSIDE WALL AND ROOF

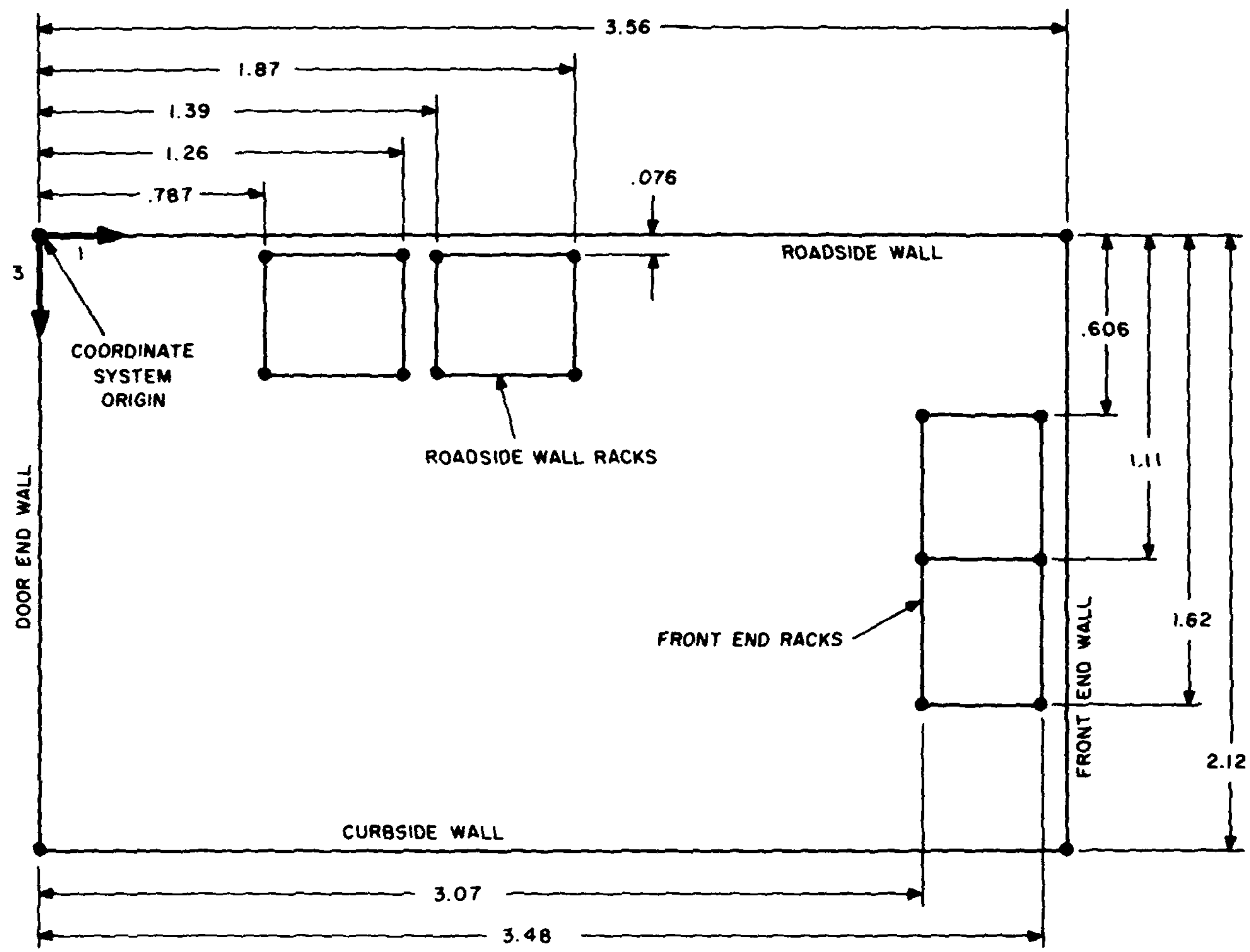

NOTE: ALL DIMENSIONS IN METRES

FIGURE 2.12. LOCATION OF THE AN/TRC-117 RACKS WITHIN THE S-280 SHELTER (TOP VIEW)

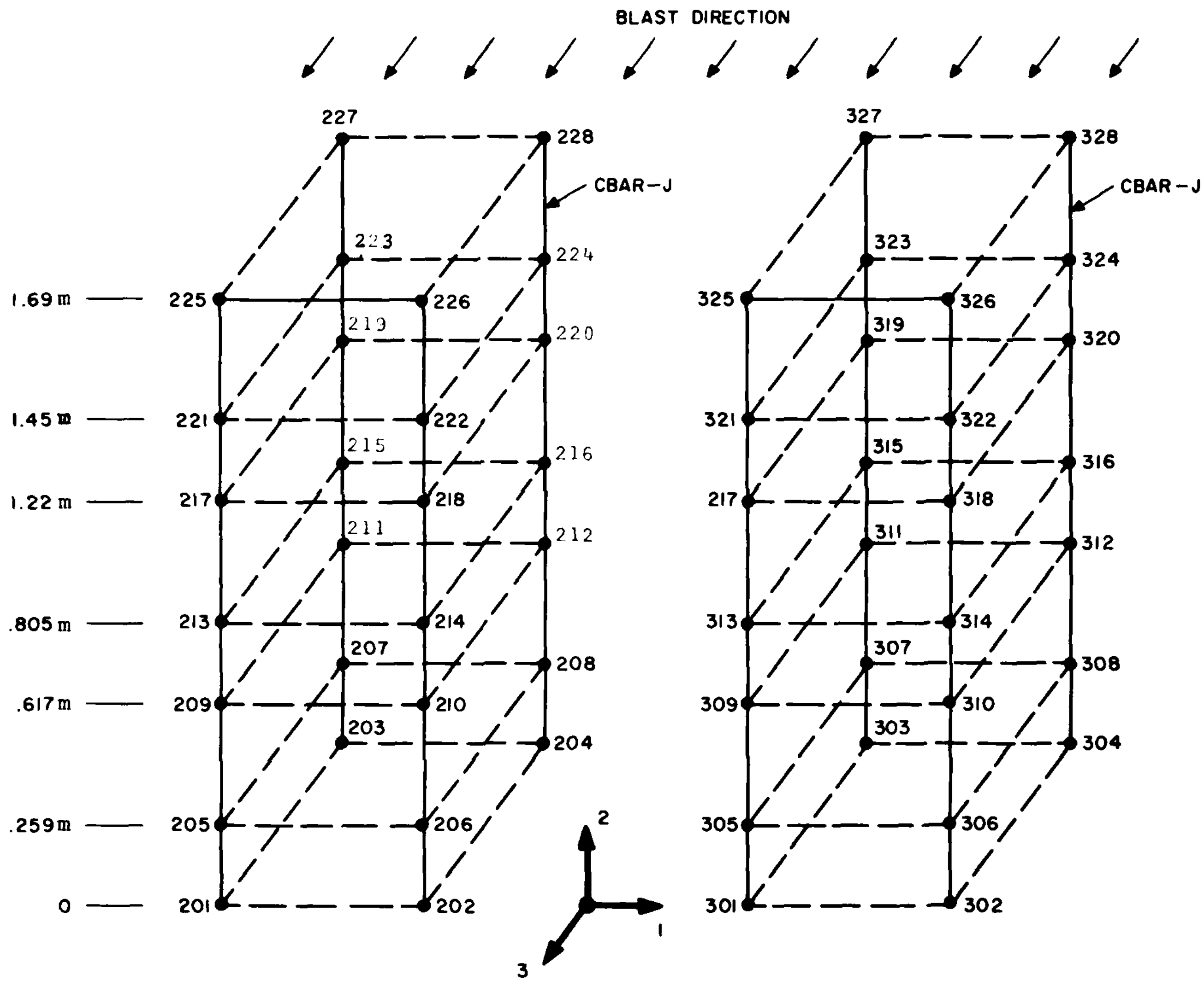

FIGURE 2.13. ROADSIDE WALL RACKS - AN/TRC-117

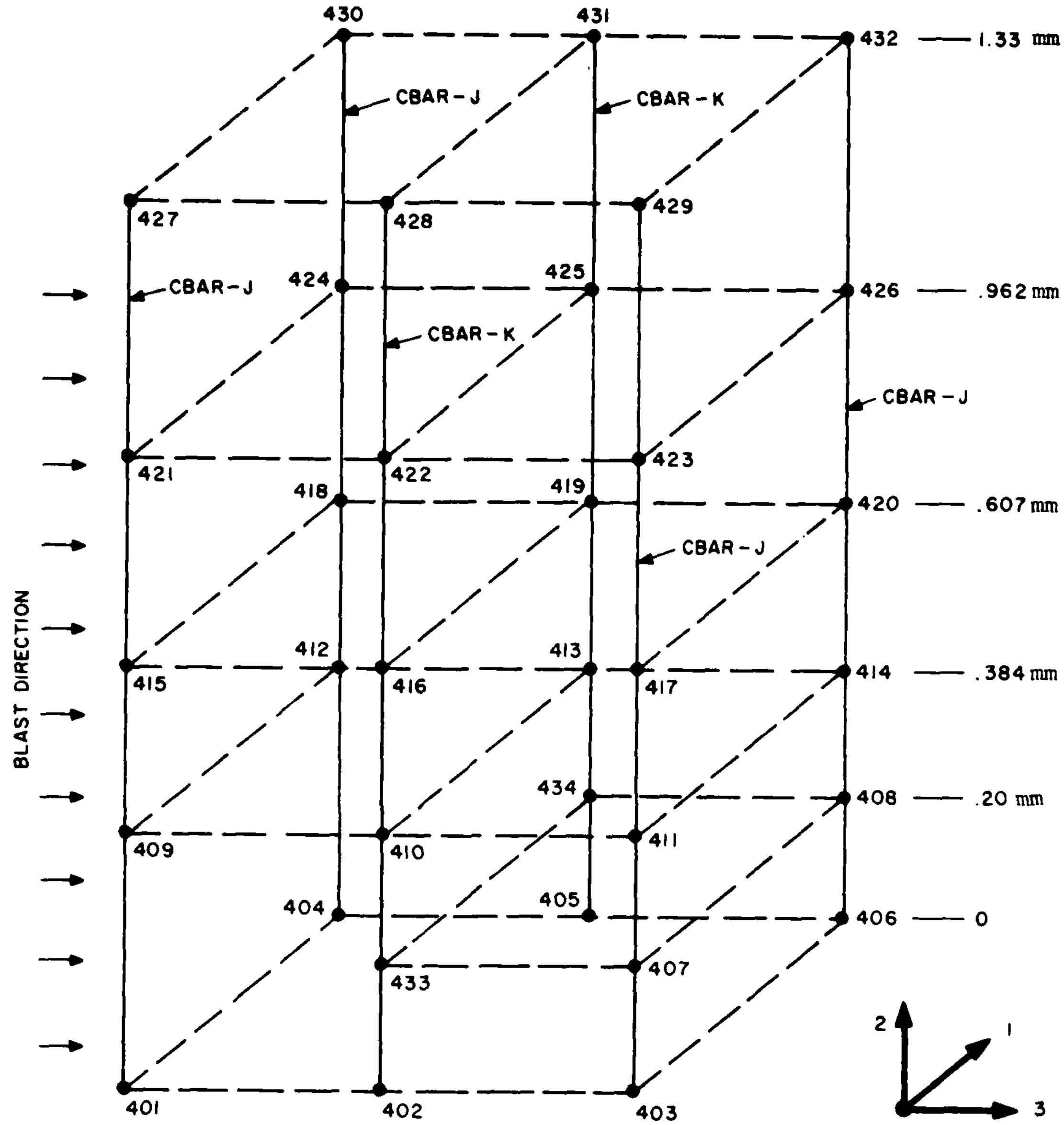

FIGURE 2.14. FRONT END RACKS - AN/TRC-117

Due to the stiffness provided by the rack shelves and the manner in which the equipment housing is bolted to the vertical uprights of the racks, it was assumed that a horizontal cross-section of the rack where equipment was mounted remained rigid and plane. This was accomplished by the use of multipoint constraint equations (MPC) in NASTRAN. Thus, for example, grid points 209-212 in Fig. 2.13 were constrained to translate and rotate as a rigid plane. The vertical rack uprights to which each such rigid plane is connected, however were free to bend and twist. This procedure appears justified by the physical constraints imposed by the equipment mounting arrangement and allows for the structural flexibility of the racks while reducing the degrees-of-freedom at each rack grid point. MPC equations were also used to connect the rear of each rack to the wall. Table 2.4 presents the property data for the rack vertical uprights and for the support brackets used in connecting the racks to the wall. Table 2.5 indicates the grid point connections for the vertical uprights and the support brackets and Table 2.6 gives the grid points that were MPC'd to connect the racks to the walls. The base of each rack was MPC'd to a grid point, GP7777, located at the center of the shelter floor.

The equipment supported by each rack is identified in Table 2.7, along with its mass and the grid points to which this mass was equally apportioned. The mass of the roadside rack complete with equipment is 181 kg and the mass of the front end rack complete with equipment is 371 kg which, when combined with the mass of the shelter and the CN-514/GRC results in a total mass of 1385 kg (see Table 2.8). Additional miscellaneous equipment is housed within the shelter to result in a total mass of 2304 kg for the AN/TRC-117 system (Refs 1 and 2). This additional unspecified equipment has a mass of 919 kg and is supported by the walls, roof and floor of the shelter; however, its actual distribution was not known. Working with photographs of the interior of the AN/TRC-117 system in Ref. 1, a rough estimation was made of the distribution of the 919 kg and it was apportioned as indicated in Table 2.9 with CONM2 mass cards. The mass of 919 kg represents 40% of the total system mass and its distribution constitutes a major uncertainty in the dynamic response. In addition, the manner in which this unspecified mass is attached to the shelter walls could affect local stiffness levels significantly, adding additional uncertainty.

2.1.3 AN/TRC-110 Racks

The AN/TRC-110 system contains a set of three racks located near the front end wall (see Fig. 2.15). Modeling of the racks followed the same procedures described for the AN/TRC-117 system in subsection 2.1.2. Figure 2.16 presents the rack grid system and Tables 2.10-2.13 present data relevant to the rack beam members, their connectivity, wall connections, equipment and system weight. The complete system has a mass of 2336 kg (Refs 1 and 2), of which 1108 kg (47% of the total system mass)

Reference 2. Organizational, DS, GS, and Depot Maintenance Manual For Medium Capacity Tactical Radio Relay system, Department of the Army Technical Manual TM-11-5895-456-15, Headquarters Department of the Army, July 1967.

TABLE 2.4

PROPERTIES OF SUPPORT BRACKETS AND RACK BEAM ELEMENTS
FOR AN/TRC-117, AN/TRC-110 AND AN/TCC-61

CBAR	I_{zz} (cm^4)	I_{yy} (cm^4)	I_{yz} (cm^4)	J (cm^4)	k_y	k_z	A (cm^2)	ECOM DRAWING NO.
H	18.3	7.27	0	.370	.70	.30	491	SC-C-585118 SC-C-585117
I	30.5	2.04	0	.129	.63	.37	383	SC-C-547604 SC-C-547606
J	2.37	2.37	0	3.49	.40	.40	282	1x1x 1/8
K	5.23	111.0	0	.208	.20	.80	615	SC-C-547061
L	10.2	207.0	0	.333	.40	.60	504	SC-C-547078
M	41.8	29.6	$\pm$.6751	.529	.70	.30	701	SC-C-546982
N	14.2	14.2	0	20.8	.50	.021	606	2x2x1/4 Angle
O	27.1	15.4	0	25.0	.40	.0234	690	SC-C-379522

TABLE 2.5

CBAR ELEMENT CONNECTIONS FOR AN/TRC-117 RACKS

CBAR	GRID POINT CONNECTIONS	NUMBER OF ELEMENTS	LOCATION
H	36 → 38	2	ROADSIDE
	28,29	1	WALL
I	40,41	1	ROADSIDE
	24 → 27	3	WALL
	17,18	1	
J	201 → 228	24	ROADSIDE WALL RACKS
	301 → 338	24	FRONT END RACKS
K	402,433,410,416,422,428	5	FRONT END RACKS
	405,434,413,419,425,431	5	

TABLE 2.6

CONSTRAINT CONNECTIONS BETWEEN
RACKS AND SHELTER

AN/TRC-117 SYSTEM

ROADSIDE WALL RACKS		FRONT END RACKS	
RACK GRID POINT	WALL GRID POINT	RACK GRID POINT	WALL GRID POINT
223	38	430	128
224	39	424	138
215	22	412	132
216	23		
207	14	432	126
208	15	426	137
		414	130
323	39		
324	40		
315	23		
316	24		
307	15		
308	16		

TABLE 2.7

RACK-SUPPORTED EQUIPMENT FOR AN/TRC-117 SYSTEM

EQUIPMENT	MASS (kg)	GRID POINT SUPPORTS	LOCATION
CV-1548	24.5	201 → 204; 301 → 304	ROADSIDE WALL RACK
TD-352/ν	46.3	205 → 208; 305 → 308	
TSEC/KG-5	36.3	213 → 216; 313 → 316	
TD-202/U	22.7	217 → 220; 317 → 320	
TD-204/U	25.4	221 → 224; 321 → 324	
R-1331(P)GRC	45.4	421,422,424,425	FRONT END RACK
R-1331(P)GRC	45.4	422,425,423,426	
T-893(P)GRC	47.6	415,418,416,419	
T-893(P)GRC	47.6	416,419,417,420	
PP-2054/GRC	37.6	409,412,410,413	
PP-2054/GRC	37.6	410,413,411,414	
SAFE	45.4(EST)	401,404,402,405	
SPARE PARTS	22.7(EST)	433,434,407,408	
SPARE PARTS	22.7(EST)	402,405,403,406	
CN-514/GRC	40.5	126,128	FRONT END WALL

TOTAL WEIGHT OF EACH RAODSIDE WALL RACK FRAME PLUS SUPPORTED EQUIPMENT = 181 kg

TOTAL WEIGHT OF FRONT END RACK FRAME PLUS SUPPORTED EQUIPMENT = 371 kg

TABLE 2.8

MASS BREAKDOWN OF AN/TRC-117

ITEM	MASS (kg)
SHELTER	613
ROADSIDE RACKS	361
FRONT END RACK	371
CN-514/GRC	40
TOTAL	1385
SYSTEM MASS	2304
UNSPECIFIED MASS	919

TABLE 2.9

ASSUMED DISTRIBUTION OF UNSPECIFIED MASS
FOR AN/TRC-117

ITEM	MASS DISTRIBUTED (kg)
ROADSIDE WALL	136
CURBSIDE WALL	181
ROOF	45
FRONT END	136
DOOR END	91
FLOOR	330
TOTAL	919

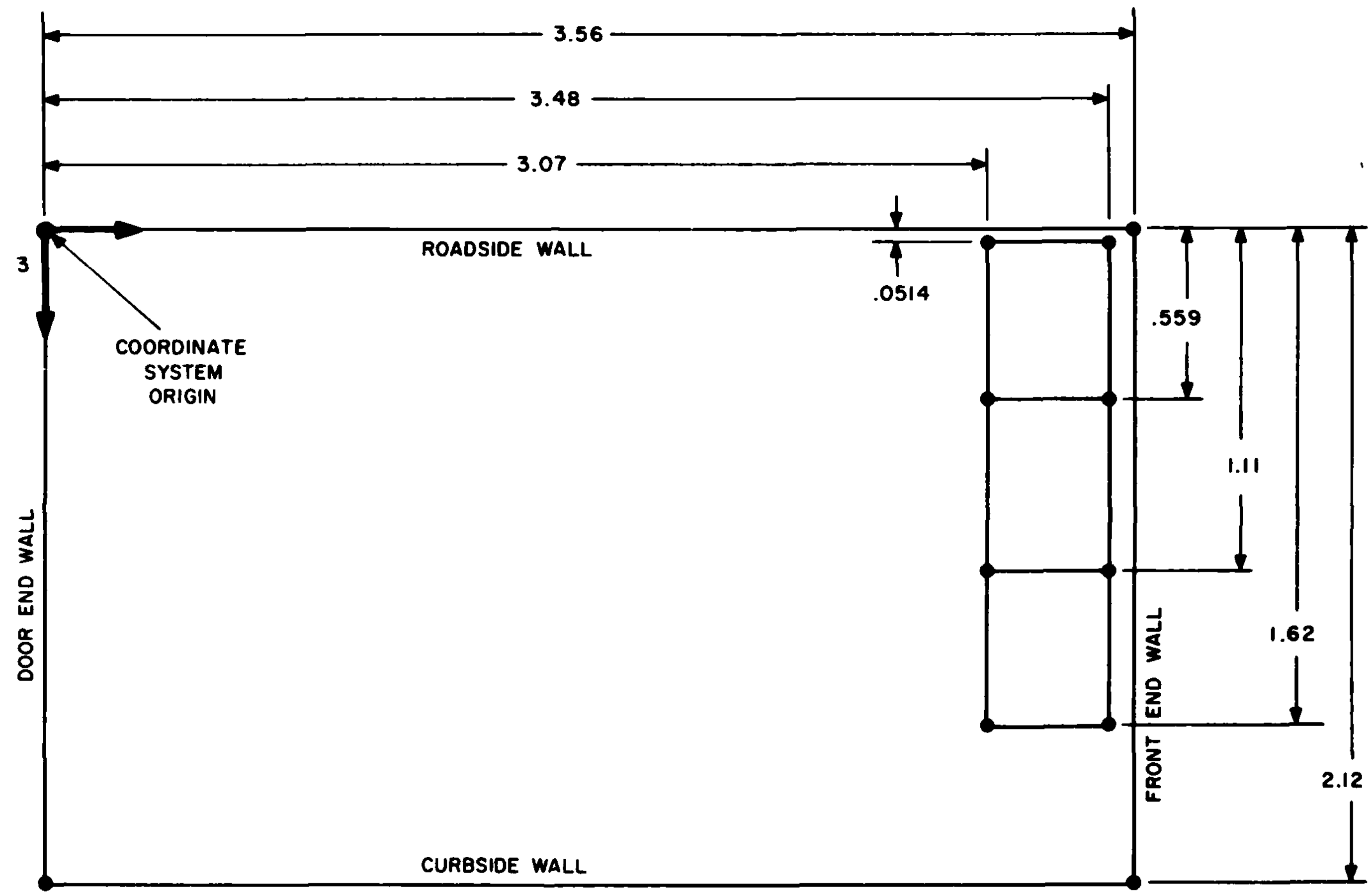

NOTE: ALL DIMENSIONS IN METRES

FIGURE 2.15. LOCATION OF THE AN/TRC-110 RACKS WITHIN THE S-280 SHELTER (TOP VIEW)

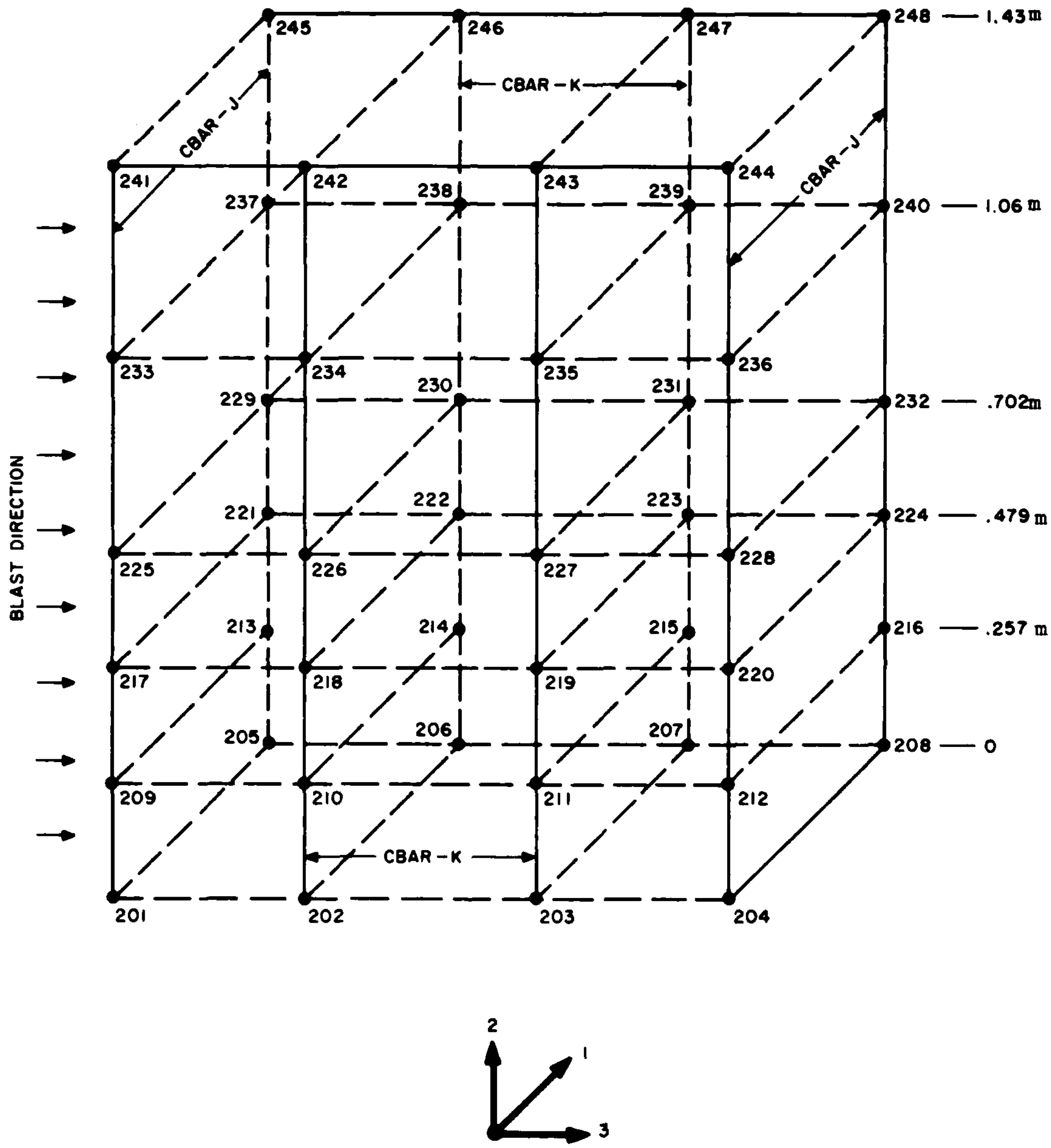

FIGURE 2.16. FRONT END RACK GRID SYSTEM - AN/TRC-110

TABLE 2.10

CBAR ELEMENT CONNECTIONS FOR THE AN/TRC-110 RACKS

CBAR	GRID POINT CONNECTIONS	NUMBER OF ELEMENTS	LOCATION
J	201,209,217,225,233,241	5	EQUIPMENT RACKS
	205,213,221,229,237,245	5	
	204,212,220,228,236,244	5	
	208,216,224,232,240,248	5	
K	202,210,218,226,234,242	5	EQUIPMENT RACKS
	206,214,222,230,238,246	5	
	203,211,219,227,235,243	5	
	207,215,223,231,239,247	5	
L	99,128	1	FRONT END
	107,126	1	
M	130,132,141	2	FRONT END
	137,138,139	2	
	126,128,129	2	
N	132,141	1	FRONT END
O	21,22	1	FRONT END

TABLE 2.11

CONSTRAINT CONNECTIONS BETWEEN RACKS
AND SHELTER WALLS

AN/TRC-110 SYSTEM

RACK GRID POINT	WALL GRID POINT
245	129
237	139
221	141
248	126
240	137
224	130
246	128
238	138
222	132

TABLE 2.12

RACK SUPPORTED EQUIPMENT FOR AN/TRC-110 SYSTEM

EQUIPMENT	MASS (kg)	GRID POINT SUPPORTS	LOCATION
TD-204/U	25.4	201,202,205,206	EQUIPMENT RACKS
TD-204/U	25.4	202,203,206,207	
TD-204/U	25.4	203,204,207,208	
TD-202/U	22.7	209,210,213,214	
TD-202/U	22.7	210,211,214,215	
TD-202/U	22.7	211,212,215,216	
PP-2054/GRC	37.6	217,218,221,222	
PP-2054/GRC	37.6	218,219,222,223	
PP-2054/GRC	37.6	219,220,223,224	
T-893(P)	47.6	225,226,229,230	
T-893(P)	47.6	226,227,230,231	
T-893(P)	47.6	227,228,231,232	
R-1331(P)	45.4	233,234,237,238	
R-1331(P)	45.4	235,236,239,240	
CN/514/GRC	40.5	107,128,126,99	FRONT END WALL
LS-147/F1	4.81	38,39,46,47	CURBSIDE WALL

TOTAL WEIGHT OF RACK FRAME PLUS SUPPORTED EQUIPMENT = 569 kg.

TABLE 2.13

MASS BREAKDOWN OF AN/TRC-110

ITEM	MASS (kg)
SHELTER	613
RACKS	570
CN-514/GRC	40
LS-147/F1	5
TOTAL	1228
SYSTEM MASS	2336
UNSPECIFIED MASS	1108

is due to miscellaneous equipment whose mass distribution was unknown. Table 2.14 presents the assumed distribution of the 1108 kg, using photographs of the shelter interior in Ref. 2 as a guide.

2.1.4 AN/TCC-61

The AN/TCC-61 systems consists of eight individual racks, four of which are located near the roadside wall and four near the curbside wall (see Eig. 2.17). Figures 2.18 and 2.19 show the grid point systems for the racks. Racks 3, 4, 5, 6, and 8 are identical to rack 1, and rack 2 is identical to rack 7, in frame construction. The racks differ somewhat with respect to the supported equipment, except for racks 3 and 6, and racks 4 and 8. The vertical uprights of each rack are made from the standard 1x1x1/8 in. extrusion, CBAR=J(Table 2.4).

As with the racks of the AN/TRC-117 and AN/TRC-110, the rear of each rack is bolted to its adjacent wall. Table 2.15 shows the rack and wall grid points which were connected by MPC equations. The masses supported by each rack are given in Tables 2.16 and 2.17 and the system mass breakdown is given in Table 2.18. For the AN/TCC-61, the distribution of 272 kg, i.e., 11% of the total mass of the system was unknown. Distribution of this mass was assumed using the photographs in Ref. 2 as a guide and allocated as shown in Table 2.19. As with the previous two systems, the bases of the AN/TCC-61 racks were MPC'd to grid point 7777 located in the center of the floor.

2.1.5 Summary of S-280 Shelter Models

A summary of the basic structural and mass elements used to construct each model and the corresponding dynamical degrees-of-freedom are given in Table 2.20. The degree of complexity of the model depends strongly on the rack system. Since the AN/TCC-61 has the greatest number of racks it is the most complex model, requiring the largest number of grid points, elements and dynamical degrees-of-freedom. The AN/TRC-110 is the least complex of the three. In Table 2.20, a single point constraint (SPC) represents constraint of motion in any one of the six possible degrees-of-freedom at a grid point, multipoint constraint represents the dependence of motion at a grid point on the motions of another (independent) grid point and omitted coordinates (OMIT) designate degrees-of-freedom which are allowed elastically but are omitted from the inertia forces. The maximum possible degrees-of-freedom are computed as simply 6 times the number of grid points.

The base grid points of the roadside, curbside, front end and door end walls, as well as the base points of the racks, were multipoint constrained to a grid point located at the center of the floor to form a rigid floor. Since the shelter receives a base excitation in the blast

TABLE 2.14

DISTRIBUTION OF UNSPECIFIED MASS
FOR AN/TRC-110

ITEM	MASS DISTRIBUTED
ROADSIDE WALL	181
CURBSIDE WALL	181
ROOF	45
FRONT END	136
DOOR END	91
FLOOR	474
TOTAL	1108

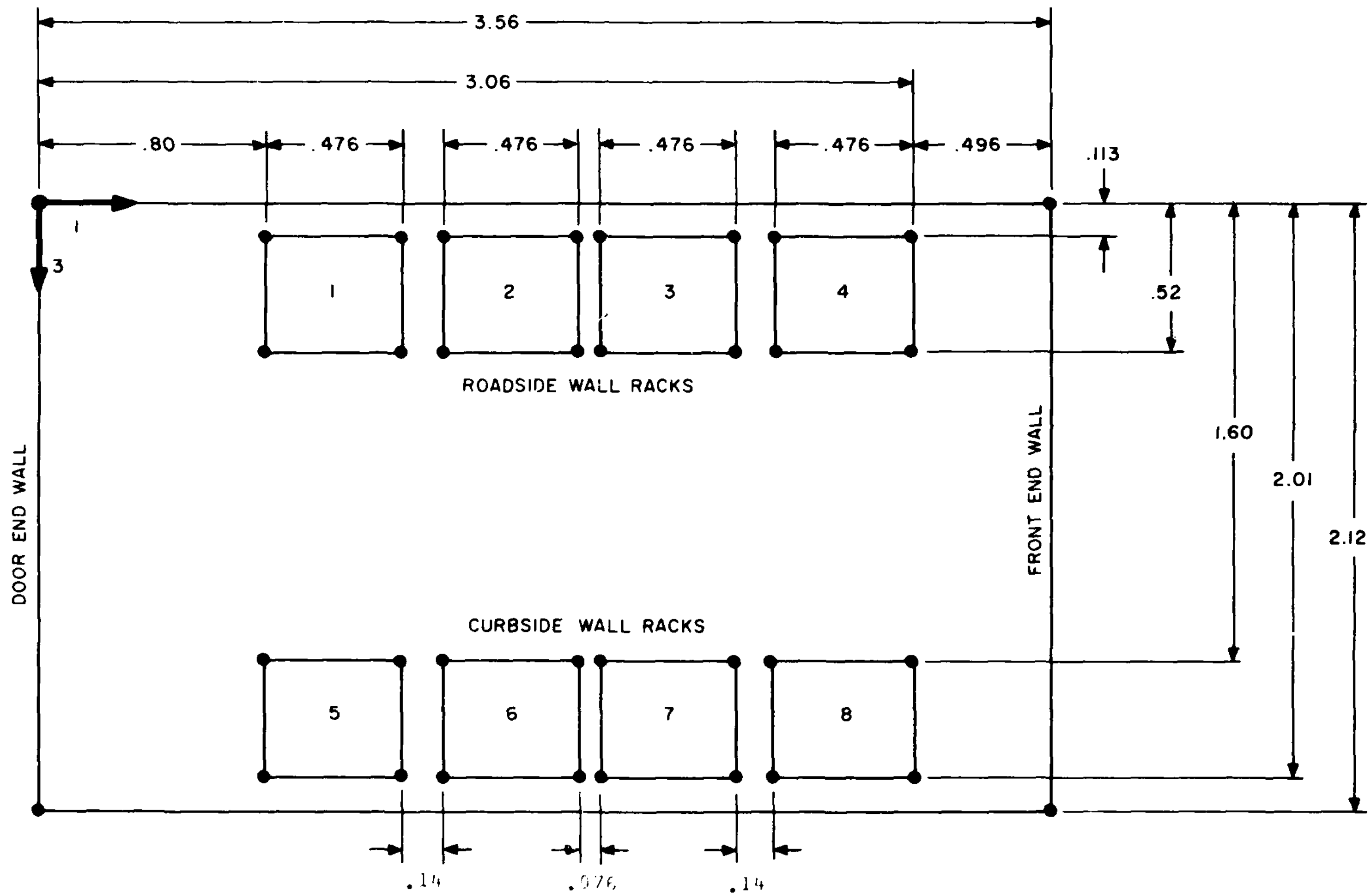

NOTE: DIMENSIONS ARE IN METRES

FIGURE 2.17. LOCATION OF THE AN/TCC-61 RACKS WITHIN THE S-280 SHELTER

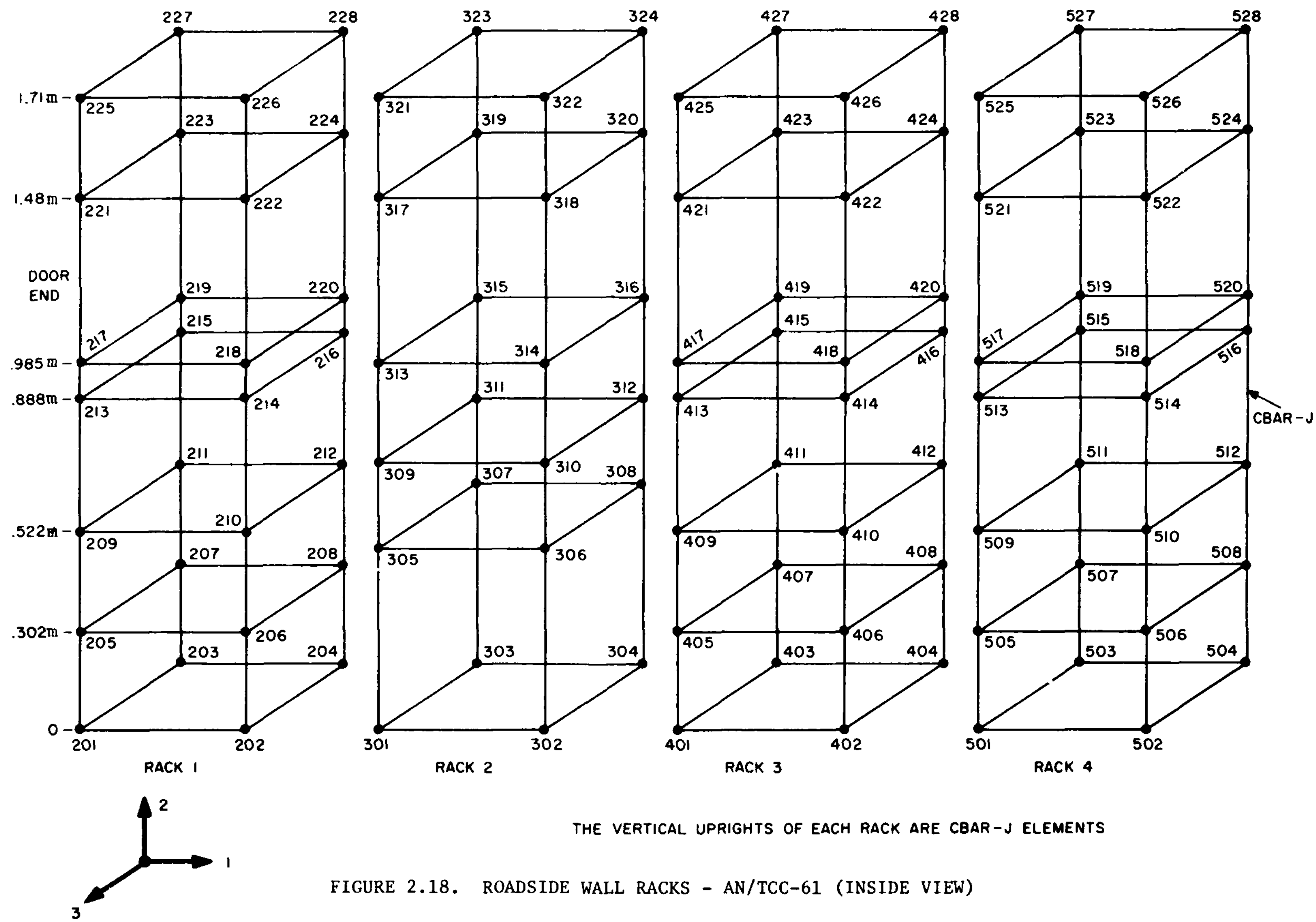

THE VERTICAL UPRIGHTS OF EACH RACK ARE CBAR-J ELEMENTS

FIGURE 2.18. ROADSIDE WALL RACKS - AN/TCC-61 (INSIDE VIEW)

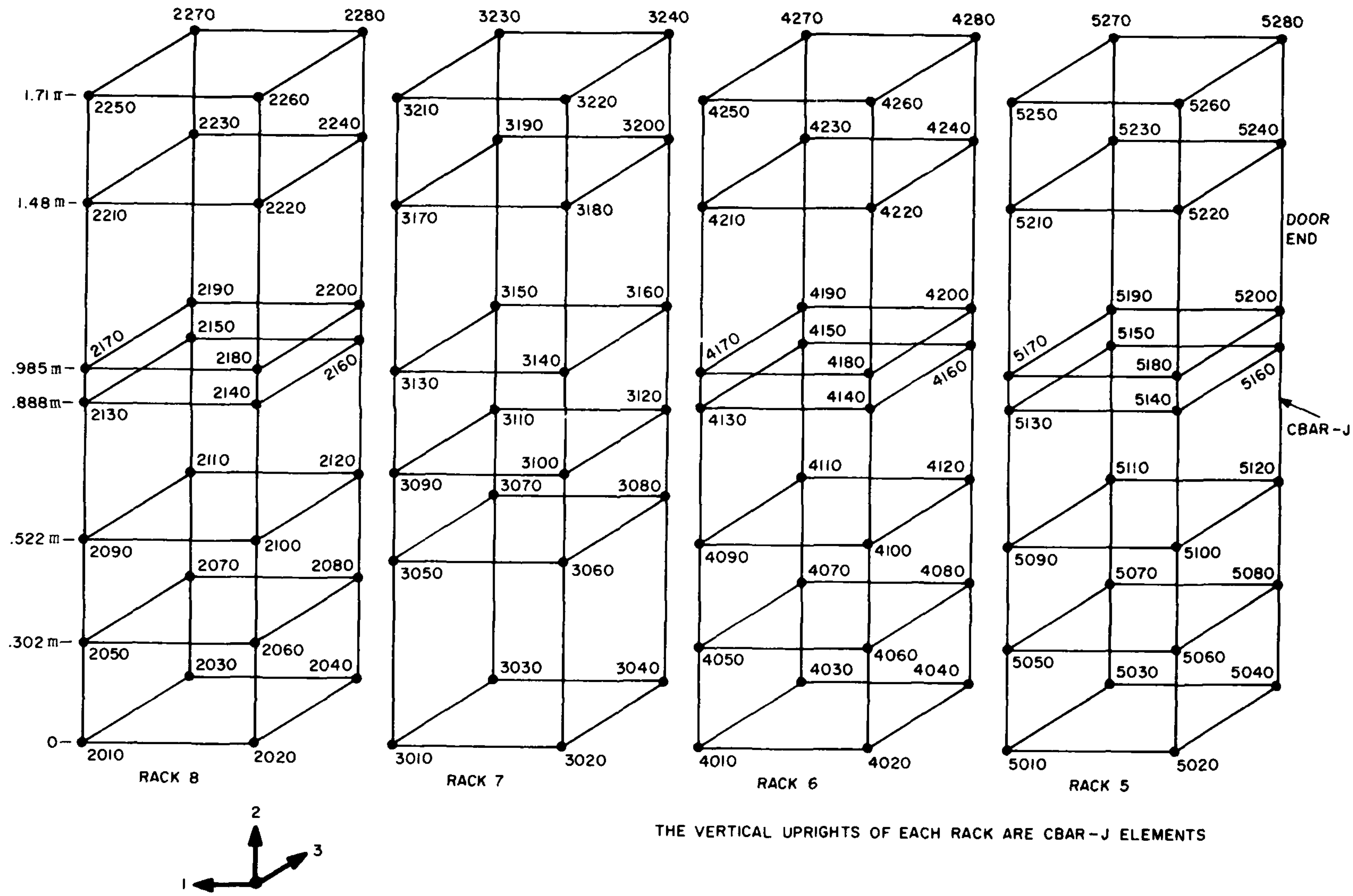

FIGURE 2.19. CURBSIDE WALL RACKS - AN/TCC-61 (INSIDE VIEW)

TABLE 2.15

CONSTRAINT CONNECTIONS BETWEEN RACKS
AND SHELTER WALLS

AN/TCC-61 SYSTEM

	ROADSIDE WALL RACKS		CURBSIDE WALL RACKS	
RACK	RACK GRID POINT	WALL GRID POINT	RACK GRID POINT	WALL GRID POINT
1	223 219 211	38 30 14	224 220 212	39 31 15
2	319 315 307	39 31 15	320 316 306	40 32 16
3	423 419 411	40 32 16	424 420 412	41 33 17
4	523 519 511	41 33 17	524 520 512	42 34 18
5	5150 5230	63 71	62 70	5140 5240
6	4150 4230	64 72	63 71	4140 4240
7	3110 3190	65 73	64 72	3120 3200
8	2150 2230	66 74	65 73	2140 2240

TABLE 2.16

EQUIPMENT MASSES FOR AN/TCC-61 SYSTEM

ROADSIDE WALL RACKS

EQUIPMENT	MASS (kg)	GRID POINT SUPPORTS	LOCATION	TOTAL MASS WITH RACK FRAME (kg)
CN-514/GRC	47.6	201 → 204	RACK 1	232
CV-1548/G	22.7	205 → 208		
TD-352/V	54.4	209 → 212		
TIMING	18.1	213 → 216		
TSEC/KG-5	36.3	217 → 220		
TD-204/U	25.4	221 → 222		
SPARES	27.2	301 → 304	RACK 2	193
CV-1548/G	22.7	305 → 308		
TD-352/U	54.4	309 → 312		
TSEC/KG-5	36.3	313 → 316		
TD-204/U	25.4	317 → 320		
SPARES	18.1	401 → 404	RACK 3	184
CV-1548/G	22.7	405 → 408		
TD-352/U	54.4	409 → 412		
TSEC/KG-5	36.3	417 → 420		
TD-204/U	25.4	421 → 424		
SPARES	18.1	501 → 504	RACK 4	202
CV-1548/G	22.7	505 → 508		
TD-352/U	54.4	509 → 512		
TIMING	18.1	513 → 516		
TSEC/KG-5	36.3	517 → 520		
TD-204/U	25.4	521 → 524		
TOTAL (kg)				811

TALLE 2.17

EQUIPMENT MASSES FOR AN/TCC-61 SYSTEM
CURBSIDE WALL RACKS

EQUIPMENT	MASS (kg)	GRID POINT SUPPORTS	LOCATION	TOTAL MASS WITH RACK FRAME (kg)
SPARES	18.1	5010 → 5040	RACK 5	202
CV-1548/G	22.7	5050 → 5080		
TD-352/U	54.4	5090 → 5120		
TIMING	18.1	5130 → 5160		
TSEC/KG-5	36.3	5170 → 5200		
TD-204/U	25.4	5210 → 5240		
SPARES	18.1	4010 → 4040	RACK 6	184
CV-1548/G	22.7	4050 → 4080		
TD-352/U	54.4	4090 → 4120		
TSEC/KG-5	36.3	4170 → 4200		
TD-204/U	25.4	4210 → 4240		
SAFE	45.4	3010 → 3020	RACK 7	211
CV-1548/G	22.7	3050 → 3080		
TD-352/U	54.4	3090 → 3120		
TSEC/KG-5	36.3	3130 → 3160		
TD-204/U	25.4	3170 → 3200		
SPARES	18.1	2010 → 2040	RACK 8	202
CV-1548/G	22.7	2050 → 2080		
TD-352/U	54.4	2090 → 2120		
TIMING	18.1	2130 → 2160		
TSEC/KG-5	36.3	2170 → 2200		
TD-204/U	25.4	2210 → 2240		
TOTAL (kg)				799

TABLE 2.18

MASS BREAKDOWN OF AN/TCC-61

ITEM	MASS (kg)
SHELTER	613
ROADSIDE RACKS	811
CURBSIDE RACKS	799
TOTAL	2223
SYSTEM MASS	2495
UNSPECIFIED MASS	272

TABLE 2.19

DISTRIBUTION OF UNSPECIFIED MASS FOR AN/TCC-61

ITEM	MASS DISTRIBUTED (kg)
ROADSIDE WALL	21.3
CURBSIDE WALL	22.7
ROOF	45.4
FRONT END	68.0
DOOR END	68.0
FLOOR	46.6
TOTAL	272

TABLE 2.20

MODEL SUMMARY OF S-280 SYSTEMS

ELEMENTS	AN/TRC-117	AN/TRC-110	AN/TCC-61
BEAM	287	237	359
PLATE	133	112	158
MASS (CONM2)	227	191	351
GRID POINTS	224	182	350
SINGLE POINT CONSTRAINTS (SPC)	5	5	5
MULTIPOINT-CONSTRAINTS (MPC)	524	444	1080
OMITTED COORDINATES (OMIT)	581	422	740
MAXIMUM POSSIBLE DEGREES OF FREEDOM	1344	1092	2100
DYNAMICAL DEGREES OF FREEDOM	234	221	275

MAXIMUM POSSIBLE DEGREES OF FREEDOM = 6x No. of GRID POINTS

DYNAMICAL DEGREES OF FREEDOM = MAXIMUM POSSIBLE - SPC - MPC - OMIT

direction (direction 3), the remaining five rigid body degrees-of-freedom of the base were SPC'd. This accounts for the five SPC's in Table 2.20. The base excitation is applied to the centroid grid point of the floor (grid point 7777) and the blast overpressure loads are applied to the wall and roof grid points as functions of time.

As an aid in validating the structural models, mode shapes and frequencies were obtained for each system. The first ten natural frequencies of the complete set, as obtained by the Givens Method in NASTRAN, are given in Table 2.21. Prior to executing the mode shape runs, the BANDIT code was run to resequence the numbering of the grid points for the purpose of minimizing matrix bandwidth.

2.2 S-250 SHELTER SYSTEMS

The AN/TRC-145 and the AN/GRC-142B systems are each housed in the S-250 electronic equipment shelter. A photograph of the S-250 shelter is shown in Fig. 2.20 and the overall dimensions are given in Figs. 2.21-2.23.

The S-250 shelter is shaped like a rectangular box with the two lower longitudinal edges indented to form a narrower base which fits between the wheel wells of a 1° ton truck used to transport it. The shelter sidewalls, roof, and floor are of sandwich construction, with aluminum interior and exterior skins, a urethane foam core, and hat-section internal stiffeners. The stiffeners are mounted vertically within the sidewalls and laterally in the roof and floor. A rear entrance door is provided. Channel extrusions along each edge of the shelter provide the attachment points between the separate panels and add strength and stiffness to the structure. In addition, the shelter sits on two longitudinal skids which form the contact point with the truck bed.

The AN/TRC-145 and the AN/GRC-142B systems differ from each other with respect to the installation of the rack frames mounted within the shelter, and the electronic equipment housed within the shelter on the supporting racks or on the shelter walls, floor, and ceiling. The S-250 shelter structure, however, remains the same for both systems.

2.2.1 Basic Shelter Model

Two variants of a NASTRAN finite element model of the S-250 shelter were developed from engineering drawings provided by ECOM. The two models differed from each other in the treatment of the knee panel and floor modeling detail. In addition, a "hardened" version of the shelter, retrofitted with additional sandwich panels on the walls, was modeled for one of the variants. The shelter walls and roof were modeled as flexible structures using the NASTRAN plate (CQUAD1) and beam (CBAR) elements. The floor and vertical knee-panel regions, forming the narrower U-shaped base to fit between the truck wheel wells, were

TABLE 2.21

NATURAL FREQUENCIES OF S-280 SHELTER SYSTEMS

(Hz)

MODE	AN/TRC-117	AN/TRC-110	AN/TCC-61
1	23.92	25.53	19.30
2	25.77	27.21	23.47
3	27.23	28.95	26.57
4	28.48	30.08	26.92
5	29.73	31.95	31.18
6	31.94	34.22	33.81
7	34.22	35.88	35.23
8	36.64	36.63	35.39
9	38.33	38.46	35.72
10	40.00	40.84	36.34

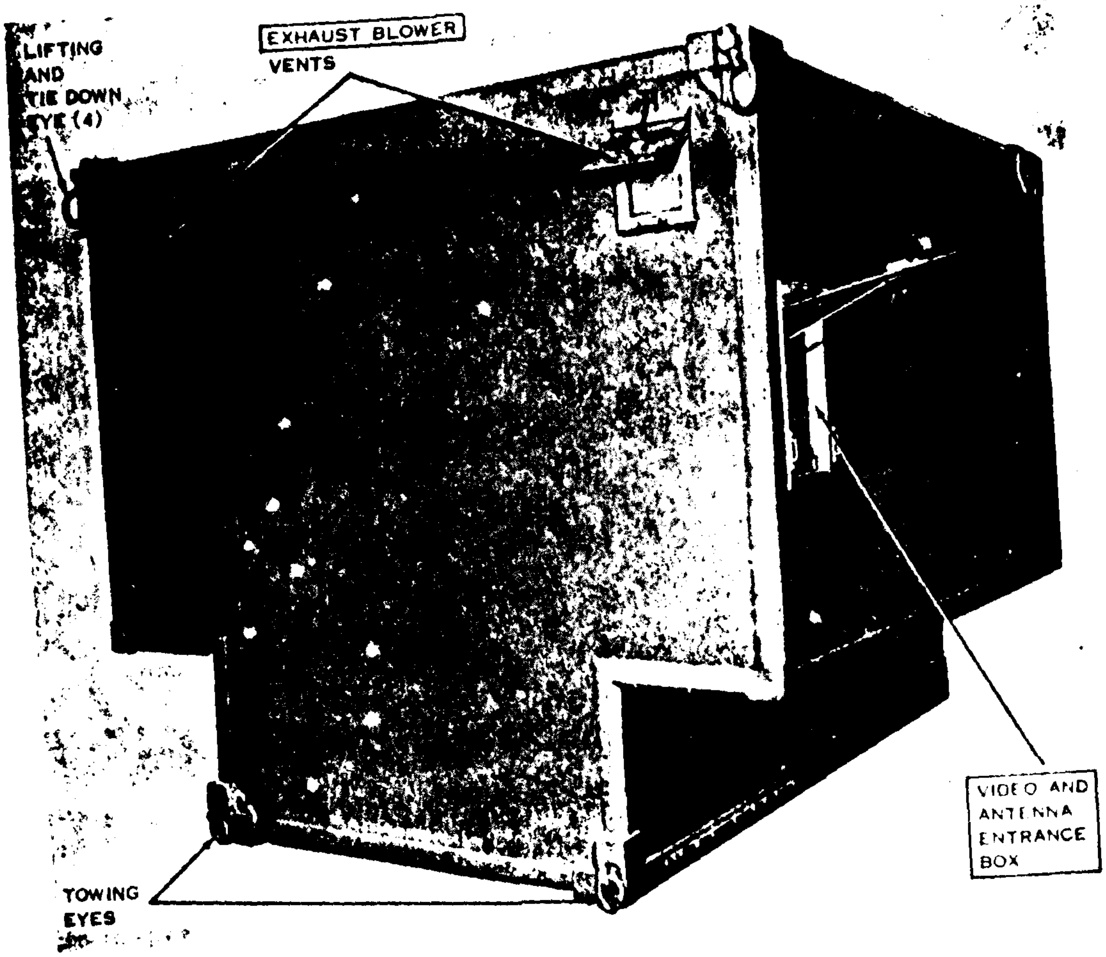

FIGURE 2.20. S-250 SHELTER

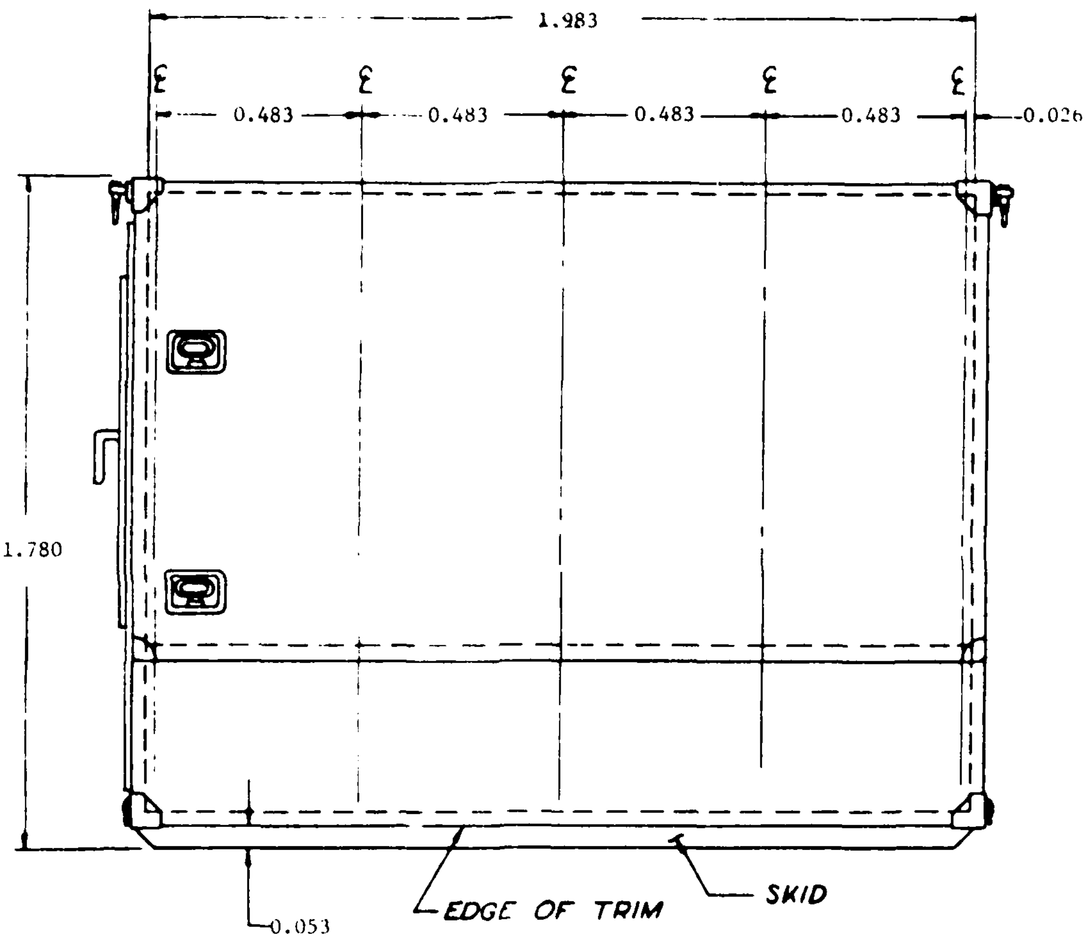

(DIMENSIONS GIVEN IN METRES)

FIGURE 2.21. S-250 ROADSIDE AND CURBSIDE WALL DIMENSIONS

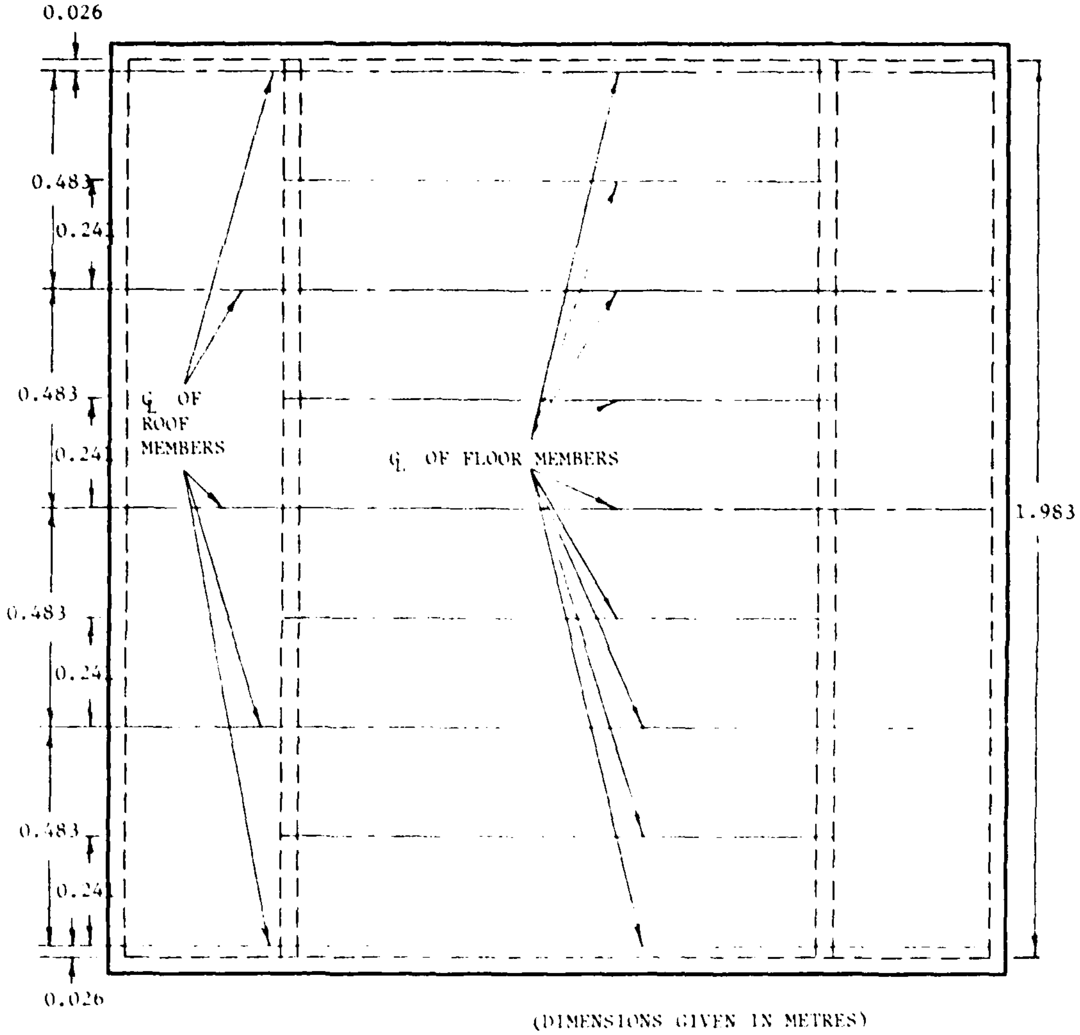

FIGURE 2.22. S-250 FLOOR AND ROOF DIMENSIONS

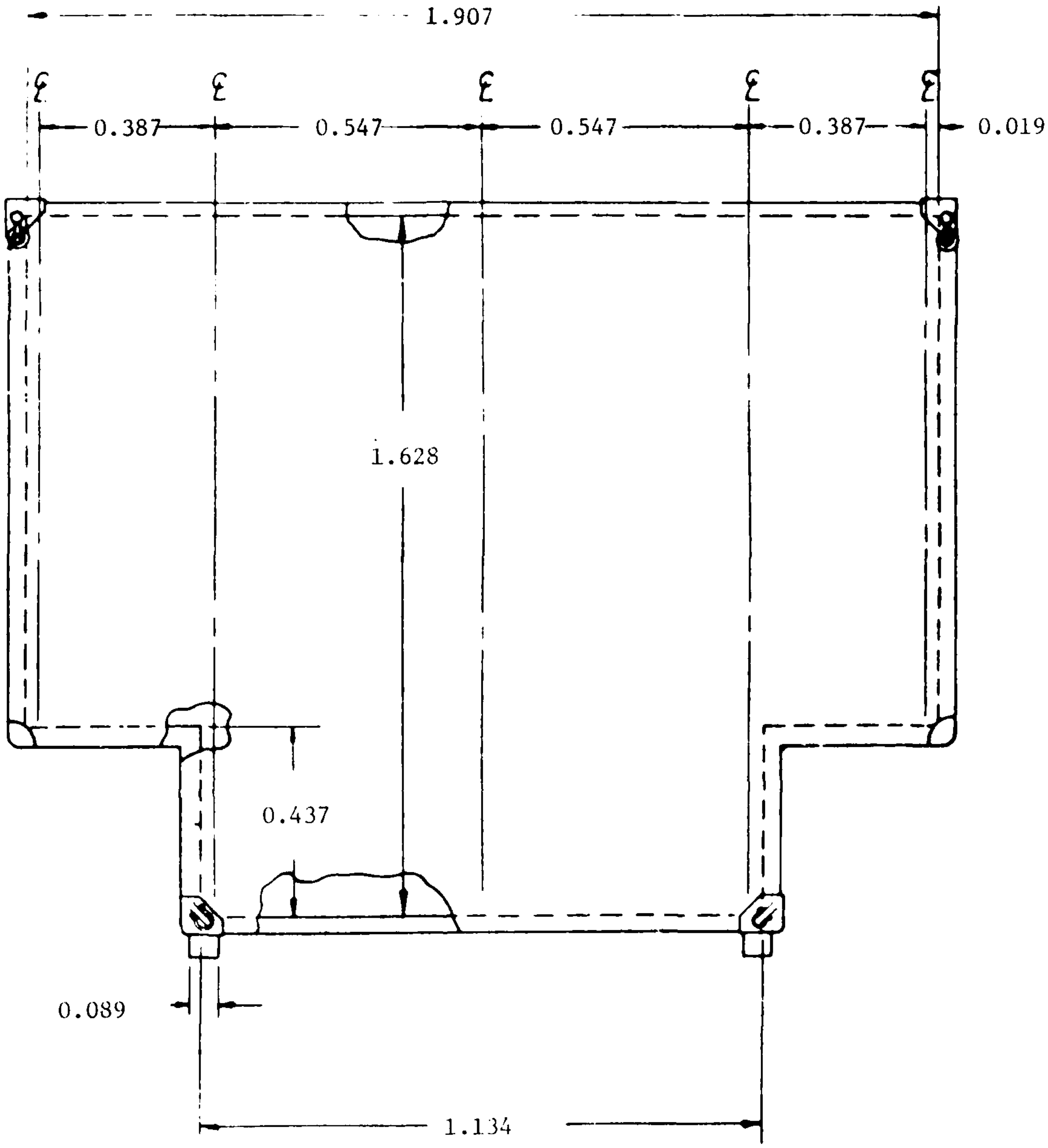

(DIMENSIONS GIVEN IN METRES)

FIGURE 2.23. S-250 END WALL DIMENSIONS

assumed rigid. Although the shelter has approximate symmetry structurally and inertially, the inclusion of the racks and electronic equipment destroys the symmetry of the complete system under consideration, and makes it necessary to model the entire system, eliminating the benefit of reduced dynamic degrees-of-freedom due to symmetry.

The basic coordinate system of the structure was located as shown in Fig. 2.24. It is assumed that the blast wave will be applied in direction 1, impinging on the roadside wall and subsequently engulfing the entire shelter.

The sandwich panels employed for the construction of the shelter are comprised of 0.813-mm thick aluminum facing sheets with a urethane foam core. The density of the urethane core is 32 kg/m^3. A typical cross-section is shown in Fig. 2.25. At certain intervals, the sandwich panels are reinforced with hat-section stiffeners.

The sandwich panels were modeled with the CQUAD1 plate element of NASTRAN, reproducing the bending, extensional, and shear stiffnesses. Table 2.22 lists the panel properties, referring to the dimensions given in Fig. 2.25. The average mass density ρ for the panel is calculated as shown earlier in Eq. 2.1.

The shelter has vertical and horizontal extrusions along its edges and internal stiffeners within the sandwich panels. These elements were modeled with the CBAR beam element of NASTRAN, reproducing the bending, extensional, torsional, and shear stiffnesses. Table 2.23 lists the properties of the CBAR elements having various cross-sections.

The above structural components result in a total structural mass of the shelter which falls short of the actual mass of the S-250 shelter, since miscellaneous items such as hardware, weldments, fasteners, paint, adhesive, and sealant are not accounted for. To make up this deficit in mass, the concentrated mass input card CONM2 of NASTRAN is employed to locate various masses at specified grid points.

The following two subsections present the two variants of the NASTRAN model of the shelter. They differ in the location of some grid points and the modeling detail of the lower section of the shelter. The retrofitted "hardened" version of the first variant is also described.

2.2.1.1 Shelter Model for AN/TRC-145

Inspection of the shelter structure indicates that the floor and vertical knee sections on either side of the shelter are of relatively strong construction, with twice the number of hat-section stiffeners employed in comparison with the sidewalls and roof. The floor is also supported by two longitudinal skids which add further stiffness to the floor. In addition, the racks for the AN/TRC-145 system rest on beams that span the knee-to-knee space above the floor. It was assumed that

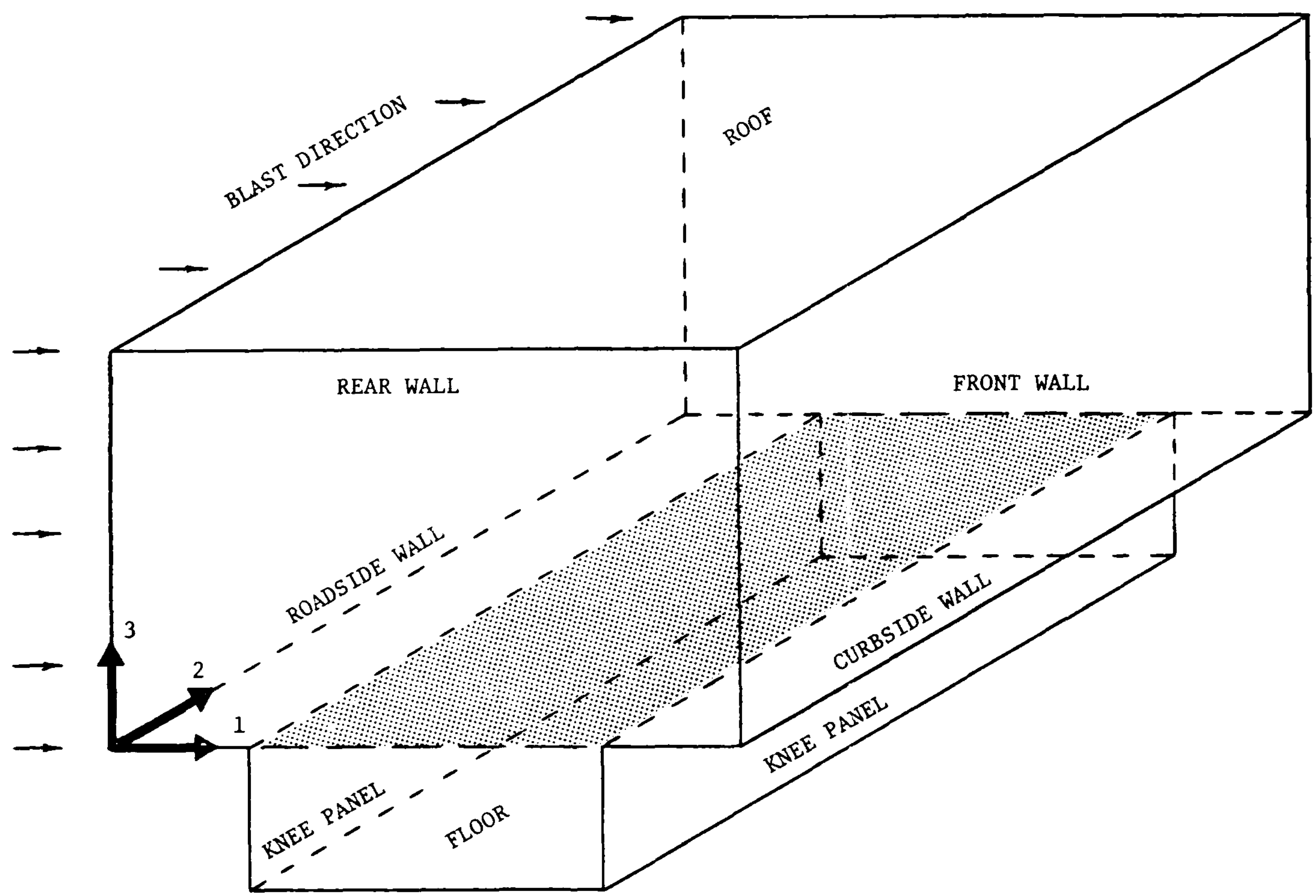

FIGURE 2.24. COORDINATE SYSTEM DEFINITION FOR AN/TRC-145 AND AN/GRC-142B SYSTEMS

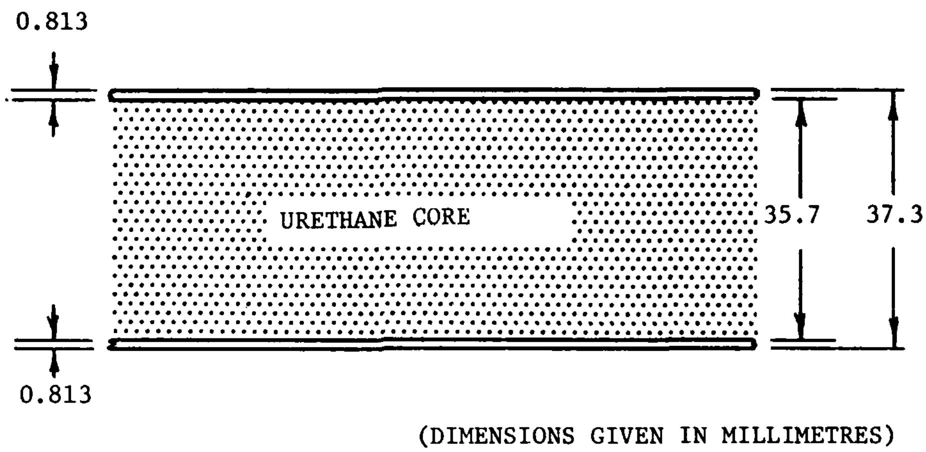

FIGURE 2.25. S-250 SANDWICH PANEL CONSTRUCTION

TABLE 2.22

S-250 PANEL PROPERTIES (CQUAD1)

PROPERTY	VALUE
I $(\frac{cm^4}{cm})$	0.541
T_1 (mm)	1.63
T_3 (mm)	35.7
E (GPa)	68.9
G_F (MPa)	1.38
ν	0.33
ρ $(\frac{Mg}{m^3})$	3.47

TABLE 2.23

PROPERTIES OF S-250 SHELTER BEAM ELEMENTS

CBAR	I_{zz} (cm^4)	I_{yy} (cm^4)	I_{yz} (cm^4)	J (cm^4)	A (mm^2)	ECOM DRAWING NUMBER
a	3.79	9.29	0.00	4.683	242	SM-B-649956
b	2.48	1.43	0.00	0.012	143	SM-B-649980
c	4.83	10.98	0.00	5.444	299	SM-B-649955
d	35.92	344.18	0.00	0.291	907	SC-D-693748
e	4.59	37.88	0.00	0.154	464	SC-D-693942
f	5.44	29.84	0.00	0.150	444	SC-D-693721
g	89.78	189.34	0.00	0.312	932	SC-D-693775
h	18.25	13.99	-61.52	0.104	565	COMPOSITE: SM-B-639957 SM-B-649958 SM-C-650117
i (mirror image of h)	18.25	13.99	61.52	0.104	565	
j	47.55	77.46	-24.77	10.822	997	COMPOSITE: SM-B-649957 SM-B-649955 SM-B-650106 SM-C-650117
k (mirror image of j)	47.55	77.46	24.77	10.822	997	
l	3.92	63.18	0.00	5.411	257	SM-B-650106
m —					943	COMPOSITE: H+L+1/2A
n —					1118	COMPOSITE: J+1/2 A
o —					483	COMPOSITE: 2A
p —					565	COMPOSITE: H,I

the combined effects of the above would result in a very stiff structure for the base section of the shelter, and it would be justified to treat this section as a rigid plane in the NASTRAN structural model. Referring to Fig. 2.24, the shaded planar region is considered as a rigid body, and all masses below that plane are lumped into that plane for the inertial model.

Figure 2.26 shows the grid point system for the rear and curbside walls and the roof of the shelter, and Figure 2.27 shows the grid point system for the front and roadside wall and the base of the shelter for the same viewing angle as in Fig. 2.24. The dimensions are shown to the midplanes of the walls, roof and base, and to the centerlines of the stiffeners. The grid point numbering system for the GRID input of NASTRAN is shown. The roadside wall is modeled with more detail than the curbside wall as it faces the blast. The positioning of grid points on the walls is selected to provide the attachment points for the racks. Solid lines represent CBAR beam elements connecting the grid points, and the dashed lines, in addition to the solid lines, represent the boundaries of the CQUAD1 plate elements. Table 2.23 may be referred to for CBAR element cross-section identification and properties. Table 2.24 presents the CBAR element grid point connections for the identified cross-sections. CQUAD1 plate elements were connected between the grid points of each surface in Figures 2.26 and 2.27, resulting in 17 elements for the roadside wall, 8 elements for the curbside wall, 12 elements for the roof, 8 elements for the front wall, 6 elements for the rear wall, and 8 elements for the two horizontal knee panels.

2.2.1.2 Hardened Shelter Model for AN/TRC-145

A hardening concept of the AN/TRC-145 system was also investigated in the current study. The hardening consisted of the addition of 19.1 mm aluminum honeycomb with a face sheet of 2.29 mm of Kevlar 49 epoxy composite material, with filaments running in both perpendicular directions, bonded to the exterior surfaces of the S-250 shelter (excluding the knee section). Figure 2.28 shows the cross-section of a typical S-250 shelter wall panel with the retrofit addition. The retrofit alters the stiffness and mass properties of the CQUAD1 plate elements which make up the wall panels. Table 2.25 presents the properties of the plate elements which were used for the hardened shelter walls. No other modifications were made to the previously described AN/TRC-145 structure to obtain the hardened configuration.

2.2.1.3 Shelter Model for AN/GRC-142B

For the same reasons enumerated in the discussion in subsection 2.2.1.1, it was assumed that the base section of the shelter could justifiably be treated as a rigid region. Unlike the previous modeling variant for the AN/TRC-145 system where the base region was lumped into a rigid plane, additional modeling detail was observed for the AN/GRC-142B system shelter model. This was partly necessitated by the fact

TABLE 2.24

CBAR ELEMENT CONNECTIONS FOR THE
AN/TRC-145 S-250 SHELTER

CBAR	GRID POINT CONNECTIONS	NUMBER OF ELEMENTS	LOCATION
a	2,7,12,17,26,22	5	ROADSIDE WALL
	3,8,13,18,27,23	5	
	4,9,14,19,24	4	
	57,60,63	2	CURBSIDE WALL
	56,59,62	2	
	55,58,61	2	
	22,67,64,63	3	ROOF
	23,68,65,62	3	
	24,69,66,61	3	
	2,80,76	2	KNEE PANELS
	3,81,77	2	
	4,92,78	2	
	72,57	1	
	73,56	1	
	74,82,55	2	
b	48,51,54	2	CURBSIDE WALL
c	28,33,42	2	FRONT WALL
	29,36,43	2	
	30,39,44	2	
	46,49,52	2	REAR WALL
	47,50,53	2	
	11,49,50,51	3	
d	15,32,33,34,35,36, 37,38,39,40,41	10	FRONT WALL
e	71,93,79	2	KNEE PANELS
	75,83,70	2	

TABLE 2.24 (CONCL'D)

CBAR	GRID POINT CONNECTIONS	NUMBER OF ELEMENTS	LOCATION
f	80,81	1	KNEE PANEL
g	26,27	1	ROADSIDE WALL
h	1,2,3,4,71,5	5	ROADSIDE WALL
	54,63,62,61,45	4	CURBSIDE WALL
	21,52,53,54	3	ROOF
	5,28	1	KNEE PANEL
	30,31	1	
i	21,22,23,24,25	4	ROADSIDE WALL
	48,57,56,55,70,31	5	CURBSIDE WALL
	25,42,43,44,45	4	ROOF
	1,46	1	KNEE PANEL
	47,48	1	
j	1,6,11,16,21	4	ROADSIDE WALL
	31,41,45	2	CURBSIDE WALL
k	5,10,15,20,25	4	ROADSIDE WALL
	48,51,54	2	CURBSIDE WALL
l	21,52,53,54	3	ROOF
	25,42,43,44,45	4	
	1,46	1	KNEE PANELS
	47,48	1	
	5,28	1	
	30,31	1	

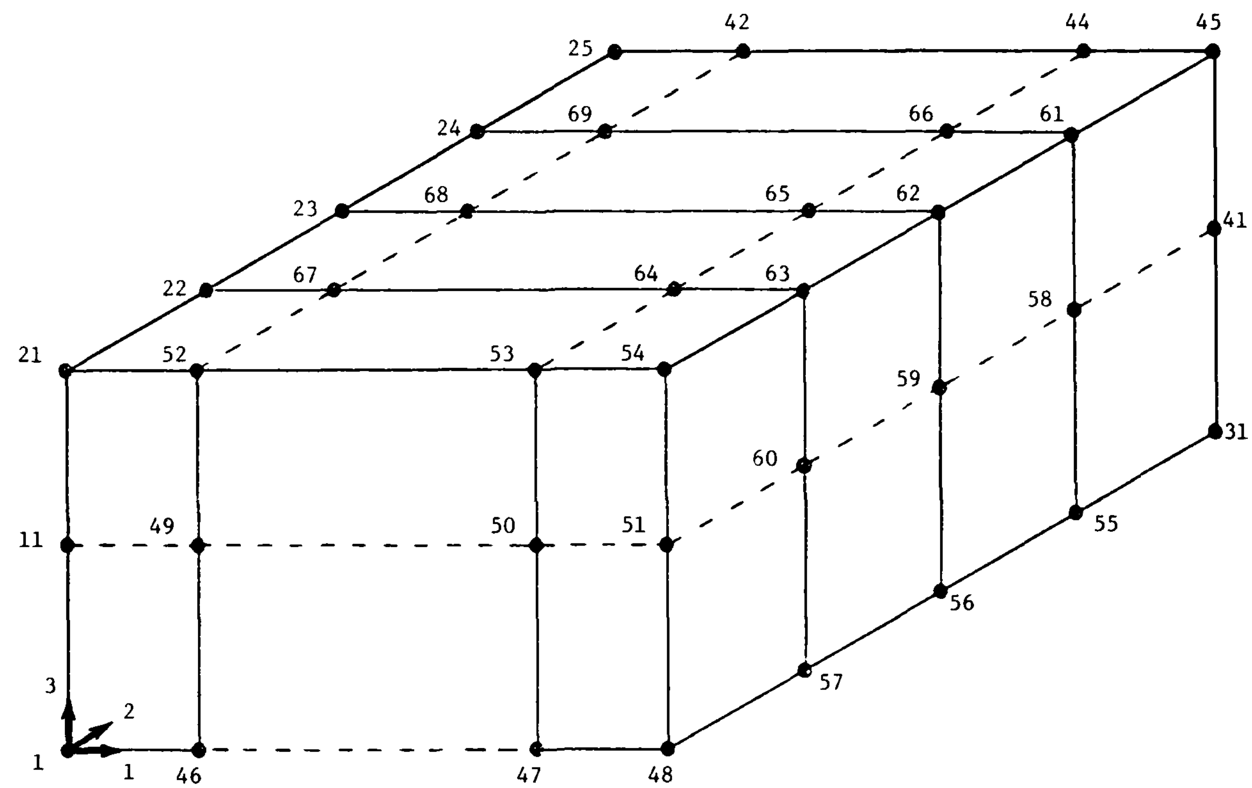

FIGURE 2.26. GRID POINT SYSTEM FOR AN/TRC-145 REAR AND CURBSIDE WALLS AND ROOF

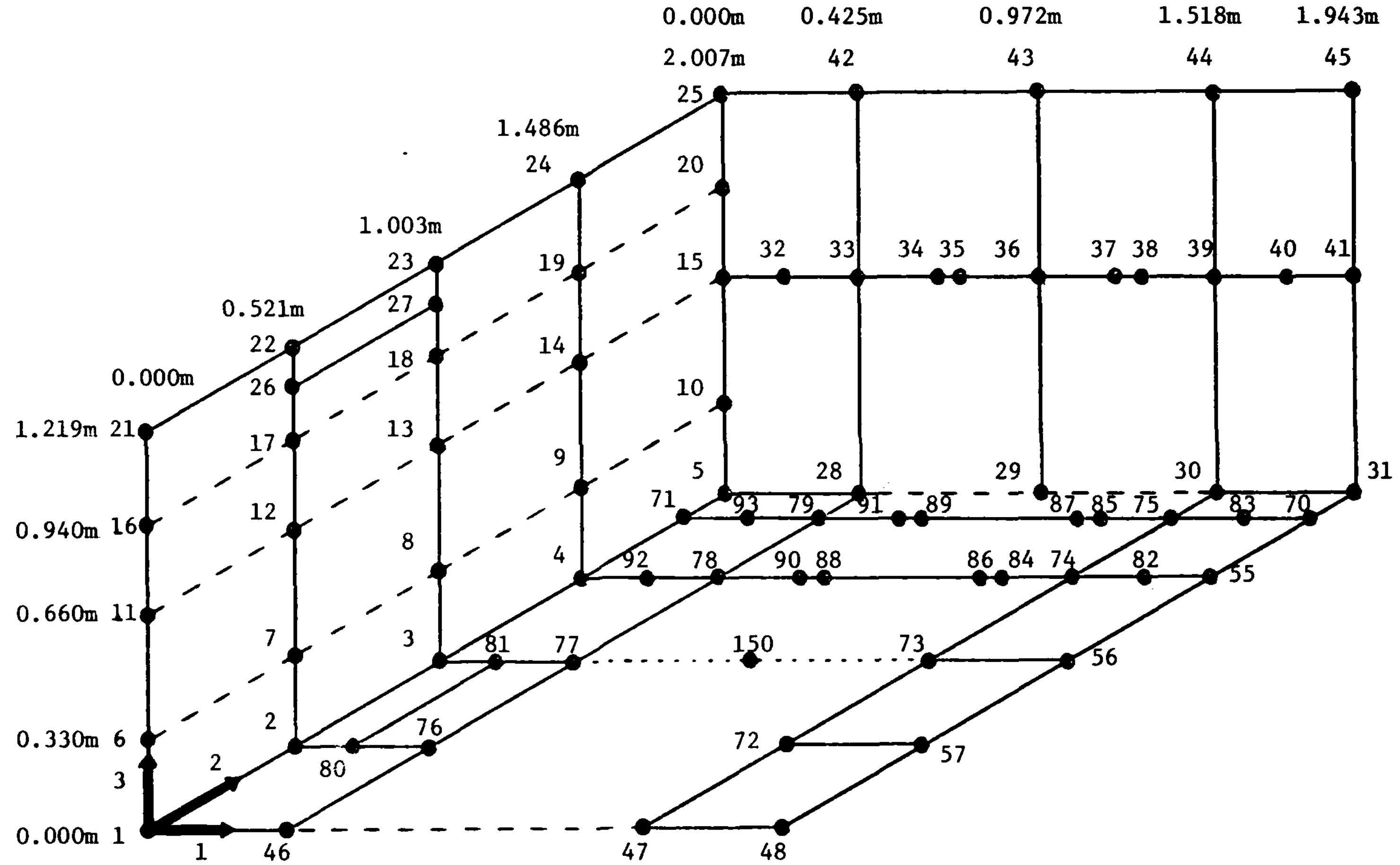

FIGURE 2.27. GRID POINT SYSTEM FOR AN/TRC-145
FRONT AND ROADSIDE WALLS AND BASE

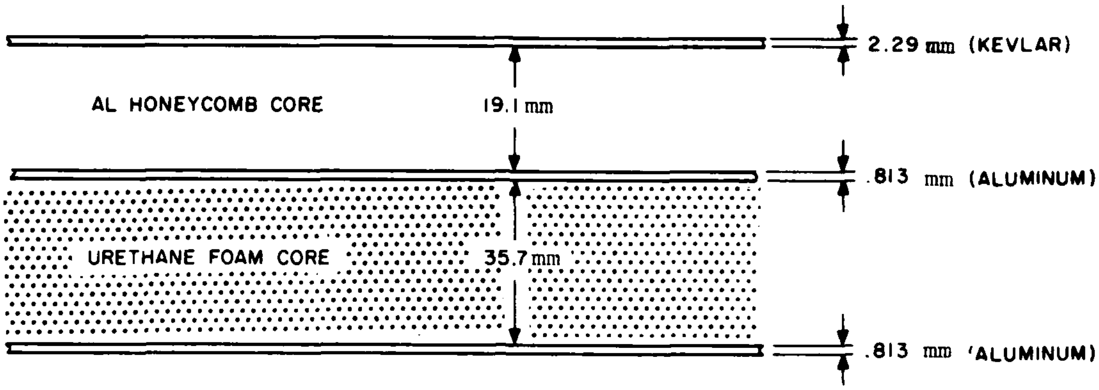

$$\left.\begin{aligned} \rho_F &= 32\ \mathrm{kg/m^3} \\ G_F &= 1.38\ \mathrm{MPa} \end{aligned}\right\}\ \text{URETHANE FOAM}$$

$$\left.\begin{aligned} \rho_{HC} &= 130\ \mathrm{kg/m^3} \\ G_{HC} &= 345\ \mathrm{MPa} \end{aligned}\right\}\ \text{HONEYCOMB (5056 AL ALLOY)}$$

$$\left.\begin{aligned} \rho_K &= 1.38\ \mathrm{Mg/m^3} \\ E_K &= 23.7\ \mathrm{GPa} \end{aligned}\right\}\ \text{KEVLAR 49 COMPOSITE}$$

FIGURE 2.28. RETROFIT CONCEPT OF S-250 SHELTER WALLS

TABLE 2.25

S-250 HARDENED PANEL PROPERTIES (CQUAD1)

PROPERTY	VALUE
I $(\frac{cm^4}{cm})$	3.41
T_1 (mm)	2.41
T_3 (mm)	19.2
E (GPa)	68.9
G (MPa)	345
ν	.33
ρ $(\frac{Mg}{m^3})$	4.68

that the racks for this system have vertical columns that rest directly on channels on the floor of the shelter (the 145 system racks had no connections to the floor) and a desire to have an improved definition of the mass distribution in the base region of the shelter for future dynamic response analyses. Thus, the overall shape of the S-250 shelter base region was retained in this modeling variant, with the addition of grid points to define the vertical knee panels and floor of the shelter. In addition, the vertical positioning of grid points on the shelter walls was altered to accommodate the attachment points for the different racks in the AN/GRC-142B system.

Figure 2.29 shows the grid point system for the rear and curbside walls and the roof of the shelter, and Figure 2.30 shows the grid point system for the front and roadside wall and the base of the shelter for the same viewing angle as in Fig. 2.24. Again, the dimensions are shown to the midplanes of the walls, roof, and base sections, and to the centerlines of the stiffeners. It should be noted that the additional stiffeners in the U-shaped base region of the shelter (vertical knee panels and floor) have been accounted for by lumping their mass contribution into their adjacent CBAR elements. The grid point numbering system for the GRID input of NASTRAN is shown. As before, the solid lines represent CBAR beam elements connecting the grid points, and the dashed lines, in addition to the solid lines, represent the boundaries of the CQUAD1 plate elements. Table 2.23 may be referred to for CBAR element cross-section identification and properties. Table 2.26 presents the CBAR element grid point connections for the identified cross-sections. CQUAD1 plate elements were connected between the grid points of each surface in Figs. 2.29 and 2.30, resulting in 16 elements for the roadside wall, 12 elements for the curbside wall, 12 elements for the roof, 10 elements for the front wall, 7 elements for the rear wall, and 22 elements for the knee panels and floor.

2.2.2 AN/TRC-145 Racks

The AN/TRC-145 electronic equipment system employs three equipment racks located against the front wall and one rack located against the roadside wall near the rear of the S-250 shelter. The three racks are bolted at their rear to the front wall, and their bases rest on two beams laterally spanning the space between the knee panels. The single roadside rack is attached to the roadside wall and horizontal knee panel via elastic supports. A schematic of the rack arrangement is shown in Fig. 2.31, with dimensions shown to the neutral axes of structural member cross sections. Figures 2.32 and 2.33 show the grid points and numbering system for the racks.

As described in earlier discussions of equipment rack systems, the equipment support shelves and the equipment attached to the shelves combine to give a reasonably stiff horizontal plane, which may be assumed to translate and rotate as a rigid plane. Multipoint constraint relations (MPC) in NASTRAN are employed to impose the rigidity assumption

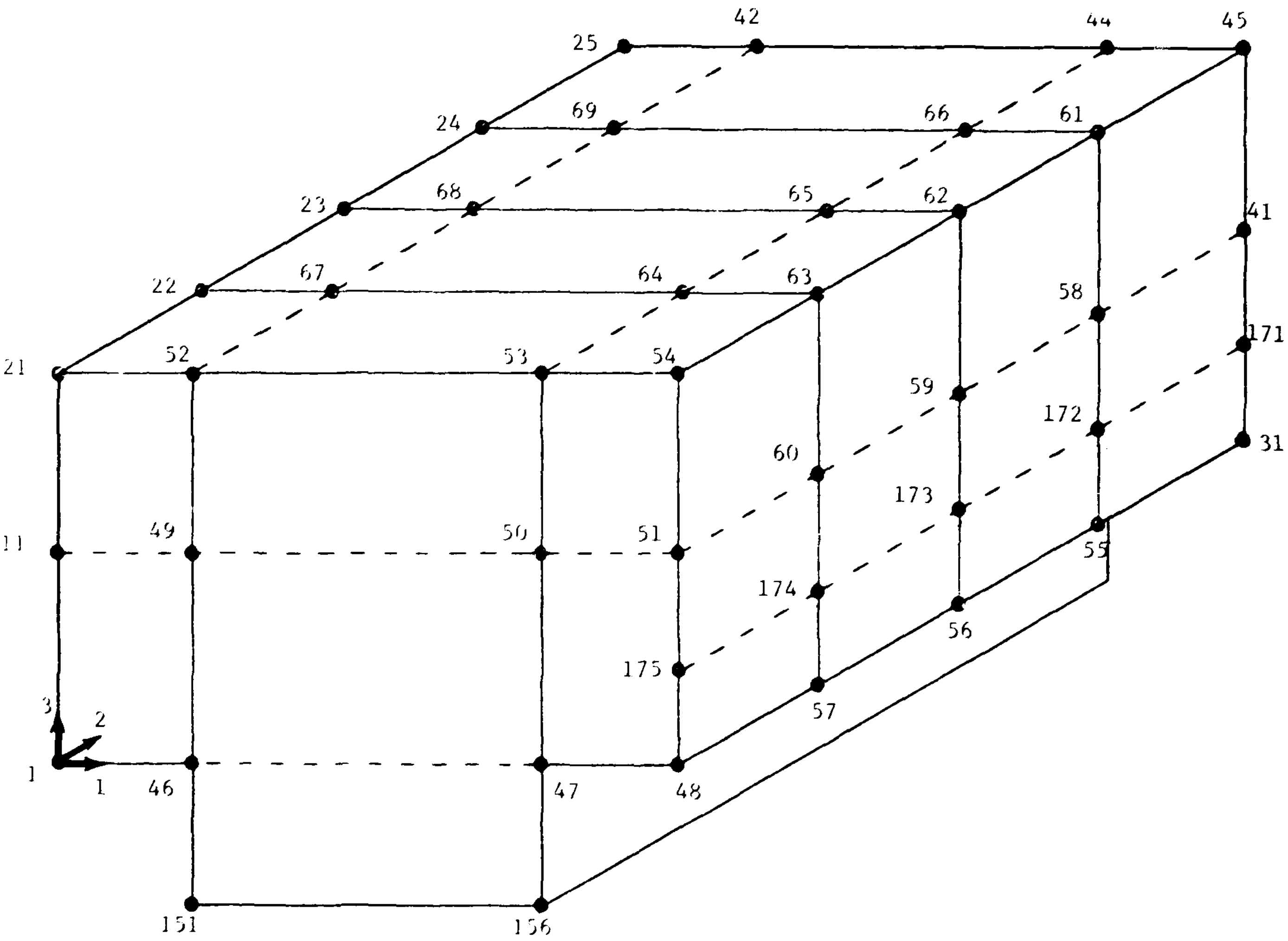

FIGURE 2.29. GRID POINT SYSTEM FOR AN/GRC-142B
REAR AND CURBSIDE WALLS AND ROOF

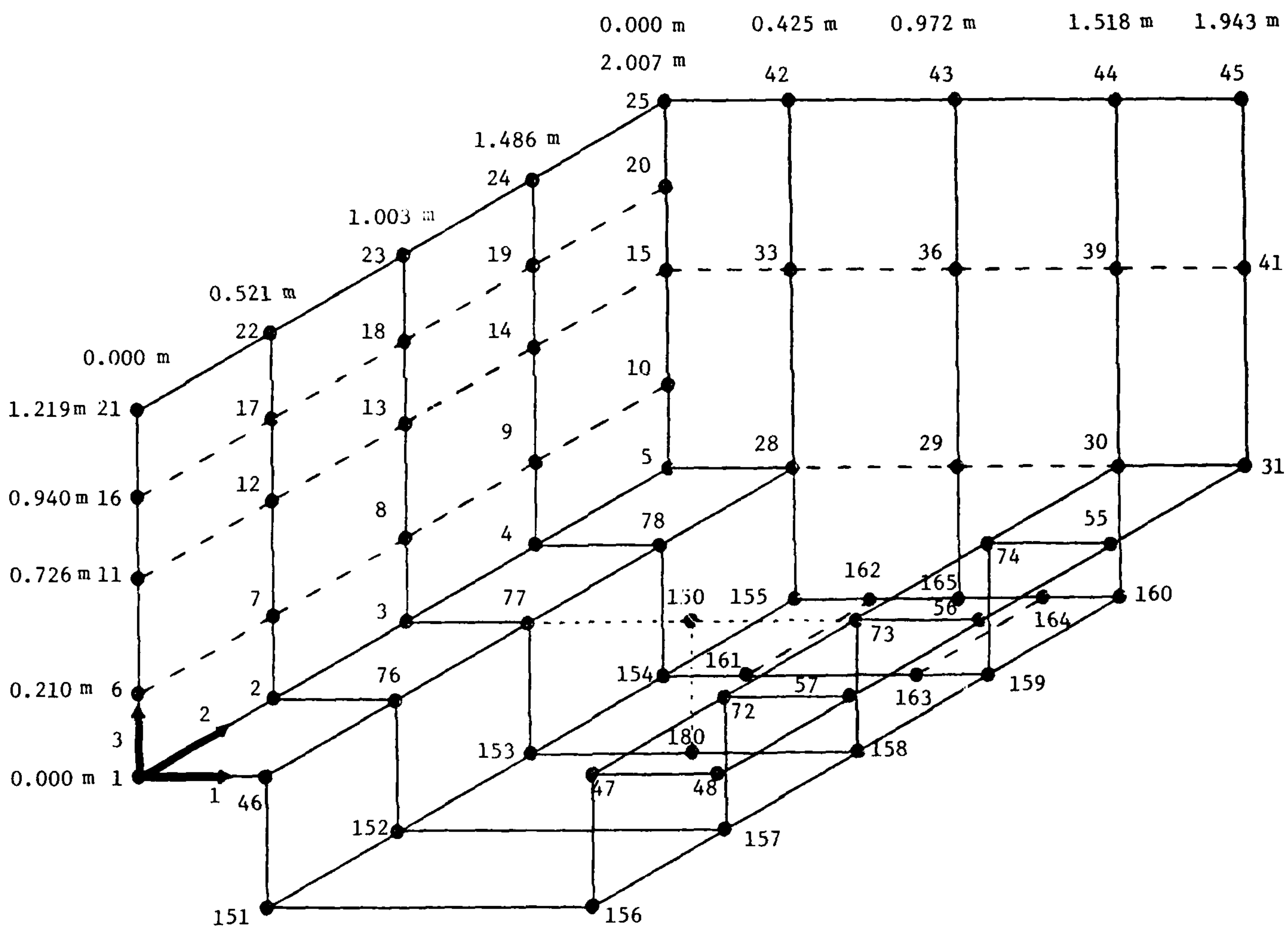

FIGURE 2.30. GRID POINT SYSTEM FOR AN/GRC-142B

TABLE 2.26

CBAR ELEMENT CONNECTIONS FOR THE
AN/GRC-142B S-250 SHELTER

CBAR	GRID POINT CONNECTIONS	NUMBER OF ELEMENTS	LOCATION
a	2,7,12,17,26,22	5	ROADSIDE WALL
	3,8,13,18,27,23	5	
	4,9,14,19,24	4	
	57,174,60,63	3	CURBSIDE WALL
	56,173,59,62	3	
	55,172,58,61	3	
	22,67,64,63	3	ROOF
	23,68,65,62	3	
	24,69,66,61	3	
	2,80,76	2	KNEE PANELS
	3,81,77	2	
	4,92,78	2	
	72,57	1	
	73,56	1	
	74,82,55	2	
b	48,51,54	2	CURBSIDE WALL
c	28,33,42	2	FRONT WALL
	165,29,36,43	3	
	30,39,44	2	
	46,49,52	2	REAR WALL
	47,50,53	2	
	11,49,50,51	3	

TABLE 2.26 (CONT'D)

CBAR	GRID POINT CONNECTIONS	NUMBER OF ELEMENTS	LOCATION
h	1,2,3,4,71,5	5	ROADSIDE WALL
	54,63,62,61,45	4	CURBSIDE WALL
	21,52,53,54	3	ROOF
	5,28	1	KNEE PANEL
	30,31	1	
i	21,22,23,24,25	4	ROADSIDE WALL
	48,57,56,55,70,31	5	CURBSIDE WALL
	25,42,43,44,45	4	ROOF
	1,46	1	KNEE PANEL
	47,48	1	
j	1,6,11,16,21	4	ROADSIDE WALL
	31,171,41,45	3	CURBSIDE WALL
k	5,10,15,20,25	4	ROADSIDE WALL
	48,175,51,54	3	CURBSIDE WALL
l	21,52,53,54	3	ROOF
	25,42,43,44,45	4	
	1,46	1	KNEE PANELS
	47,48	1	
	5,28	1	
	30,31	1	

TABLE 2.26 (CONCL'D)

CBAR	GRID POINT CONNECTIONS	NUMBER OF ELEMENTS	LOCATION
m	151,156	1	FLOOR
	155,162,165,164,160	4	
n	151,46	1	KNEE PANELS
	155,28	1	
	156,47	1	
	160,30	1	
o	152,76	1	KNEE PANELS
	153,77	1	
	154,78	1	
	157,72	1	
	158,73	1	
	159,74	1	
	152,157	1	FLOOR
	153,180,158	2	
	154,161,163,159	3	
p	151,152,153,154,155	4	FLOOR
	156,157,158,159,160	4	
	46,76,77,78,28	4	KNEE PANELS
	47,72,73,74,30		

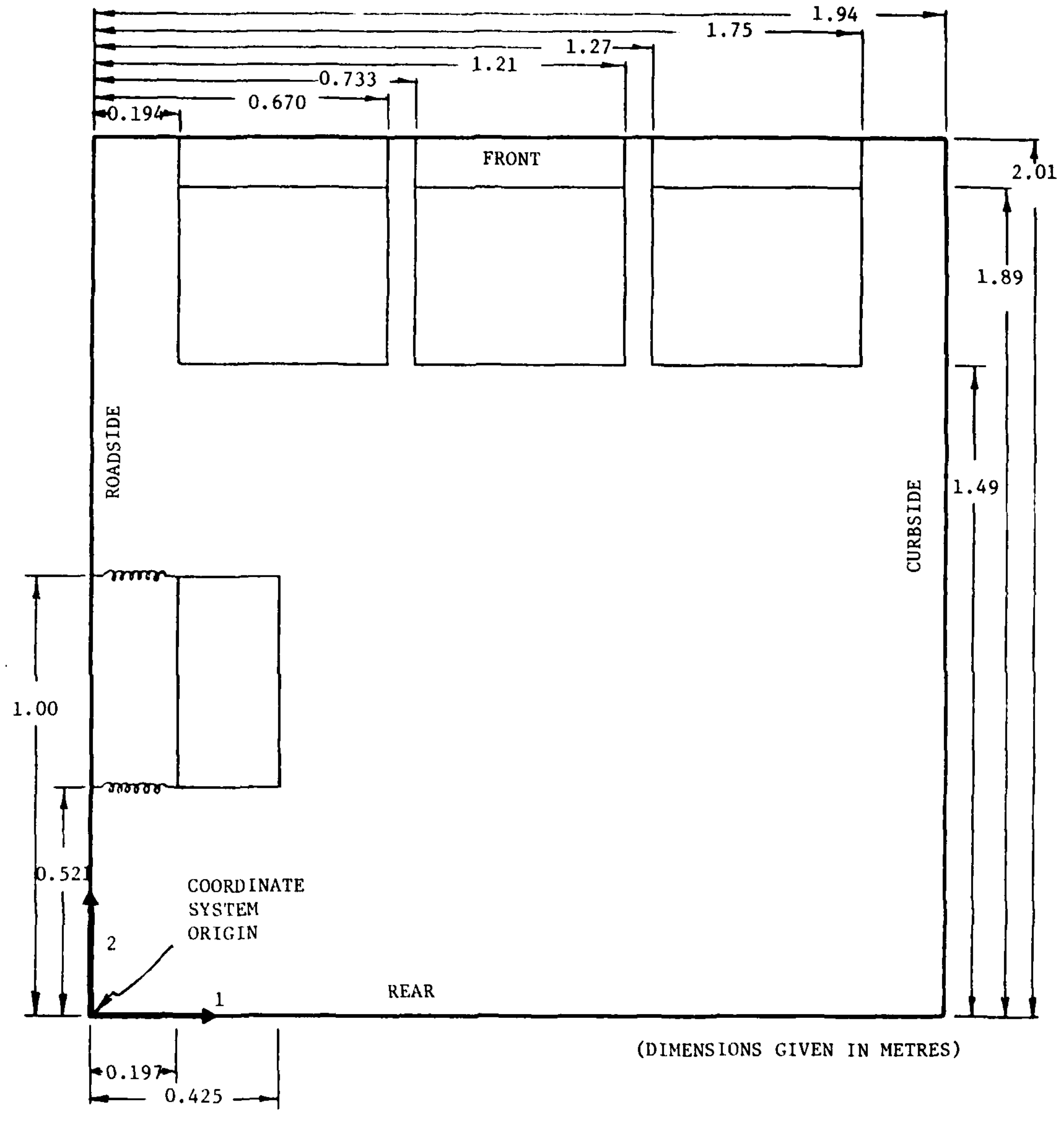

FIGURE 2.31. LOCATION OF THE AN/TRC-145 RACKS WITHIN THE S-250 SHELTER (TOP VIEW)

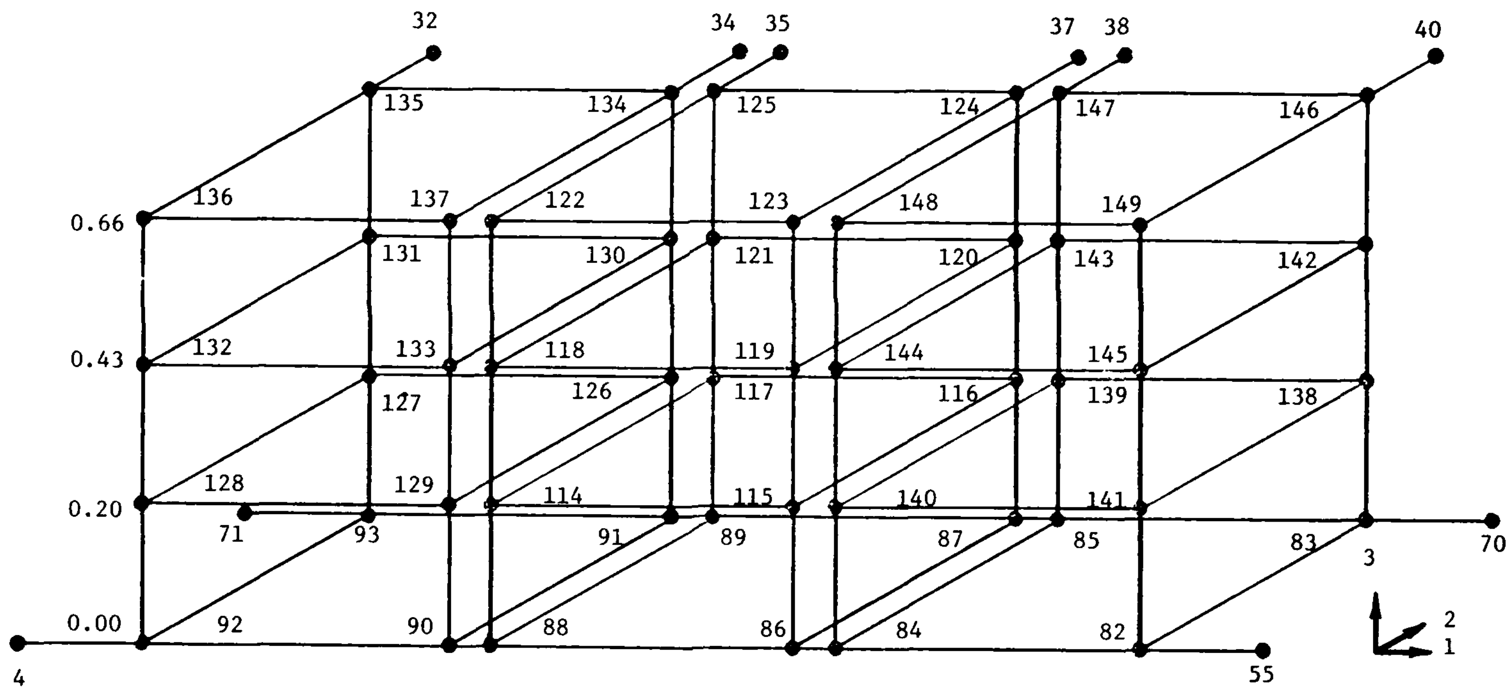

FIGURE 2.32. AN/TRC-145 RACKS AGAINST FRONT WALL

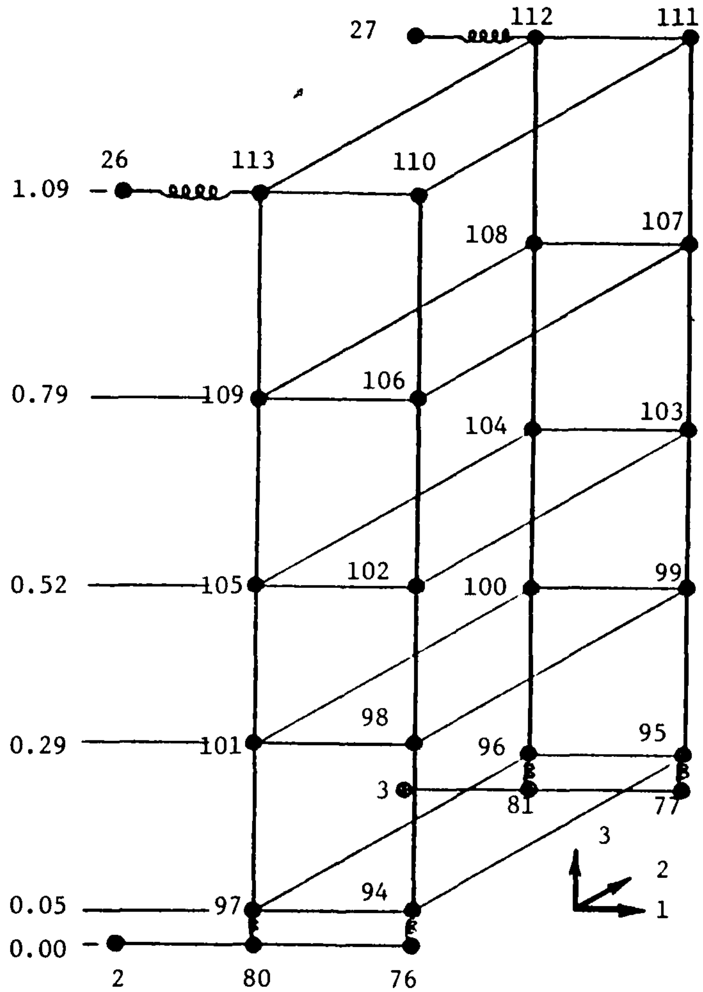

FIGURE 2.33. AN/TRC-145 RACK AGAINST ROADSIDE WALL

for each shelf. The vertical structural members are assumed to be flexible. Table 2.27 lists the properties of the CBAR beam elements employed in modeling the racks. Table 2.28 presents the CBAR element grid point connections for the identified cross-sections, and Table 2.29 shows the grid point pairs that were connected with MPC relations to model the rack-to-wall attachments.

The pieces of equipment supported by the racks are listed in Table 2.30 along with their masses and the grid points to which the masses are equally apportioned. Table 2.31 presents the mass breakdown of the AN/TRC-145 system. Additional miscellaneous equipment is housed within the shelter to result in a total mass of 975 kg for the entire AN/TRC-145 system (Ref. 2). This additional unspecified equipment mass of 257 kg, representing 26% of the total, was distributed as concentrated masses via CONM2 cards onto the walls, roof, and floor of the shelter, based on estimates of weight and distribution of equipment by inspection of photographs of the interior of the shelter given in Ref. 3. Table 2.32 shows the apportionment of masses to account for this weight deficiency. This arbitrary mass distribution may result in uncertainties in dynamic response analyses. In addition, the presence of pieces of equipment and the method of attachment to the structure may introduce changes in the structural stiffness levels, adding further uncertainties.

2.2.3 AN/GRC-142B Racks

The AN/GRC-142 electronic equipment system employs a set of equipment racks located against the front wall of the S-250 shelter. The rack assembly is bolted at both sides to the roadside and curbside walls, and the base rests on the floor of the shelter. A schematic of the rack arrangement is shown in Fig. 2.34, with dimensions shown to the neutral axes of structural member cross sections. Figure 2.35 shows the grid points and numbering system for the rack assembly.

As the rack structure is composed of upright columns supporting horizontal beam elements which in turn support the equipment mounted on them, the assumption of rigid shelves (employed for the earlier models) is not valid. However, each piece of equipment bolted to the beam elements consists of a relatively rigid rectangular construction. Thus, it is assumed that the base of each piece of equipment provides a rigid plane between the attachment points, which are modeled to translate and rotate as a rigid plane by using the multipoint constraint relations (MPC) in NASTRAN. The structural members are assumed to be flexible. Table 2.33 lists the properties of the CBAR beam elements employed in modeling the racks. Table 2.34 presents the CBAR element grid point connections for the identified cross sections, and Table 2.35 shows the grid point pairs that were connected with MPC relations to model the rack-to-wall or rack-to-floor attachments.

Reference 3. Radio Terminal Sets AN/TRC-145(V) 1, AN/TRC-145(V)2, AN/TRC-145(V)3, AN/TRC-145A(V)2, AN/TRC-145A(V)2, and AN/TRC-145A(V)3 (FSN 5895-791-3365), Department of the Army Technical Manual TM 11-5895-453-14, January 1973.

TABLE 2.27

PROPERTIES OF AN/TRC-145 RACK BEAM ELEMENT

CBAR	I_{zz} (cm^4)	I_{yy} (cm^4)	I_{yz} (cm^4)	J (cm^4)	A (mm^2)	COMMENT
AA 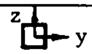	2.37	2.37	0.00	3.49	282	(1x1x 1/8 TUBE)

TABLE 2.28

CBAR ELEMENT CONNECTIONS FOR AN/TRC-145 RACKS

CBAR	GRID POINT CONNECTIONS	NUMBER OF ELEMENTS	LOCATION
AA	95,99,103,107,111	4	ROADSIDE RACK
	96,100,104,108,112	4	
	97,101,105,109,113	4	
	94,98,102,106,110	4	
	87,116,120,124	4	FRONT/CENTER RACK
	89,117,121,125	4	
	88,114,118,122	4	
	86,115,119,123	4	
	91,126,130,134	4	FRONT/ROADSIDE RACK
	93,127,131,135	4	
	92,128,132,136	4	
	90,129,133,137	4	
	83,138,142,146	4	FRONT/CURBSIDE RACK
	85,139,143,147	4	
	84,140,144,148	4	
	82,141,145,149	4	

TABLE 2.29

CONSTRAINT CONNECTIONS BETWEEN
AN/TRC-145 RACKS AND S-250 SHELTER

RACK GRID POINT	SHELTER GRID POINT	RACK GRID POINT	SHELTER GRID POINT
113*	26	135	32
112*	27	134	34
97**	80	125	35
96**	81	124	37
95**	77	147	38
94**	76	146	40
		82, 83, 84, 85	150
		86, 87, 88, 89	150
		90, 91, 92, 93	150

*CONSTRAINED IN DIRECTIONS 2 AND 3 ONLY. ELASTIC CONNECTION IN DIRECTION 1.

**CONSTRAINED IN DIRECTIONS 1 AND 2 ONLY. ELASTIC CONNECTION IN DIRECTION 3.

TABLE 2.30

EQUIPMENT MASSES FOR AN/TRC-145 SYSTEM

EQUIPMENT	MASS (kg)	GRID POINT SUPPORTS	LOCATION
CV-1548/G	24.49	94,95,96,97	ROADSIDE RACK
CV-1548/G	24.49	98,99,100,101	
TD-660A/G	22.23	102,103,104,105	
TD-660A/G	22.23	106,107,108,109	
TD-204	25.40	86,87,88,89	FRONT/CENTER RACK
TD-204	25.40	114,115,116,117	
CARD STORAGE	9.07(EST)	118,119,120,121	
PATCH PANEL	9.07(EST)	122,123,124,125	
T-983(P)	19.28	126,127,128,129	FRONT/ROADSIDE RACK
AM-4320	9.43		
R-1329(P)	16.33	130,131,132,133	
AM-4316	12.70		
RT-773	3.45	134,135,136,137	
DA-437/GRC-103(V)	9.07(EST)	134,135,136,137	
T-983(P)	19.28	138,139,140,141	FRONT/CURBSIDE RACK
AM-4320	9.43		
R-1329(P)	16.33	142,143,144,145	
AM-4316	12.70		
RT-773	3.45	146,147,148,149	
DA-437/GRC-103(V)	9.07(EST)	146,147,148,149	
TOTAL	303		

TOTAL MASS OF RAODSIDE RACK FRAME AND SUPPORTED EQUIPMENT = 109 kg

TOTAL MASS OF FRONT RACK FRAMES AND SUPPORTED EQUIPMENT = 264 kg

TABLE 2.31

MASS BREAKDOWN OF AN/TRC-145 SYSTEM

ITEM	MASS (Kg)
SHELTER	345
ROADSIDE RACK	109
FRONT RACKS	264
TOTAL	718
SYSTEM MASS	975
UNSPECIFIED MASS	257

TABLE 2.32

ASSUMED DISTRIBUTION OF UNSPECIFIED MASSES
FOR AN/TRC-145 SYSTEM

ITEM	MASS DISTRIBUTION (kg)
ROADSIDE WALL	27
CURBSIDE WALL	35
ROOF	23
FRONT WALL	23
REAR WALL	36
FLOOR	113
TOTAL	257

AD-A085 759 KAMAN AVIDYNE BURLINGTON MA F/G 17/2
STRUCTURAL MODELING AND RESPONSE OF COMMAND, CONTROL AND COMMUN--ETC(U)
MAR 80 J M CALLIGEROS, J P WALSH DAAD05-74-C-0744
UNCLASSIFIED KA-TR-151 ARBRL-CR-00421 NL

2 of 3

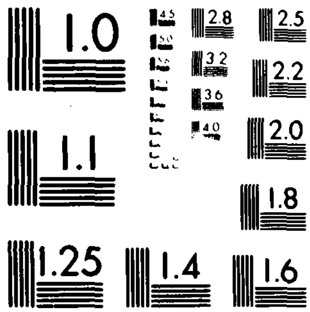

MICROCOPY RESOLUTION TEST CHART
NATIONAL BUREAU OF STANDARDS 1963 A

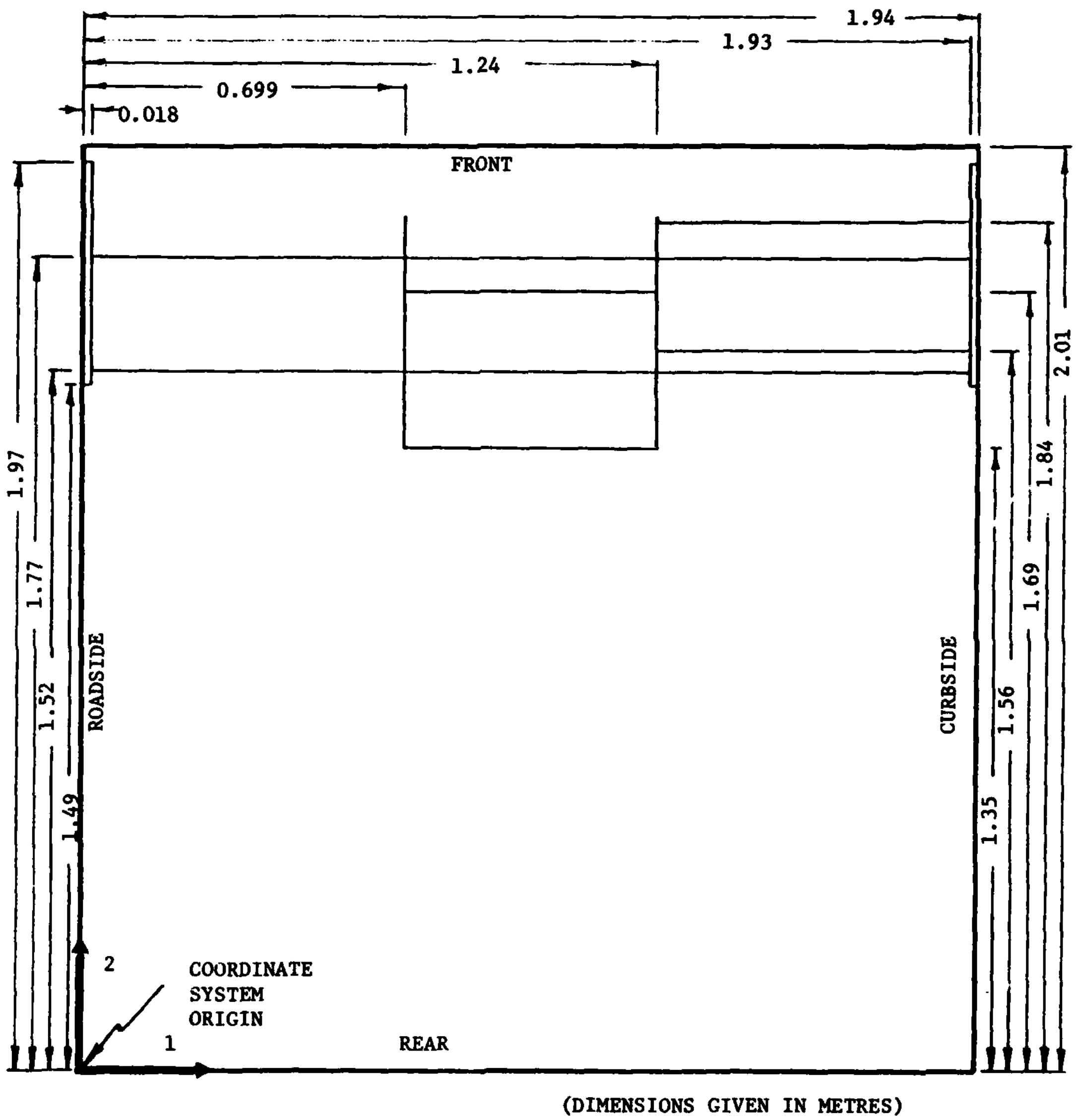

FIGURE 2.34. LOCATION OF THE AN/GRC-142B RACKS WITHIN THE S-250 SHELTER (TOP VIEW)

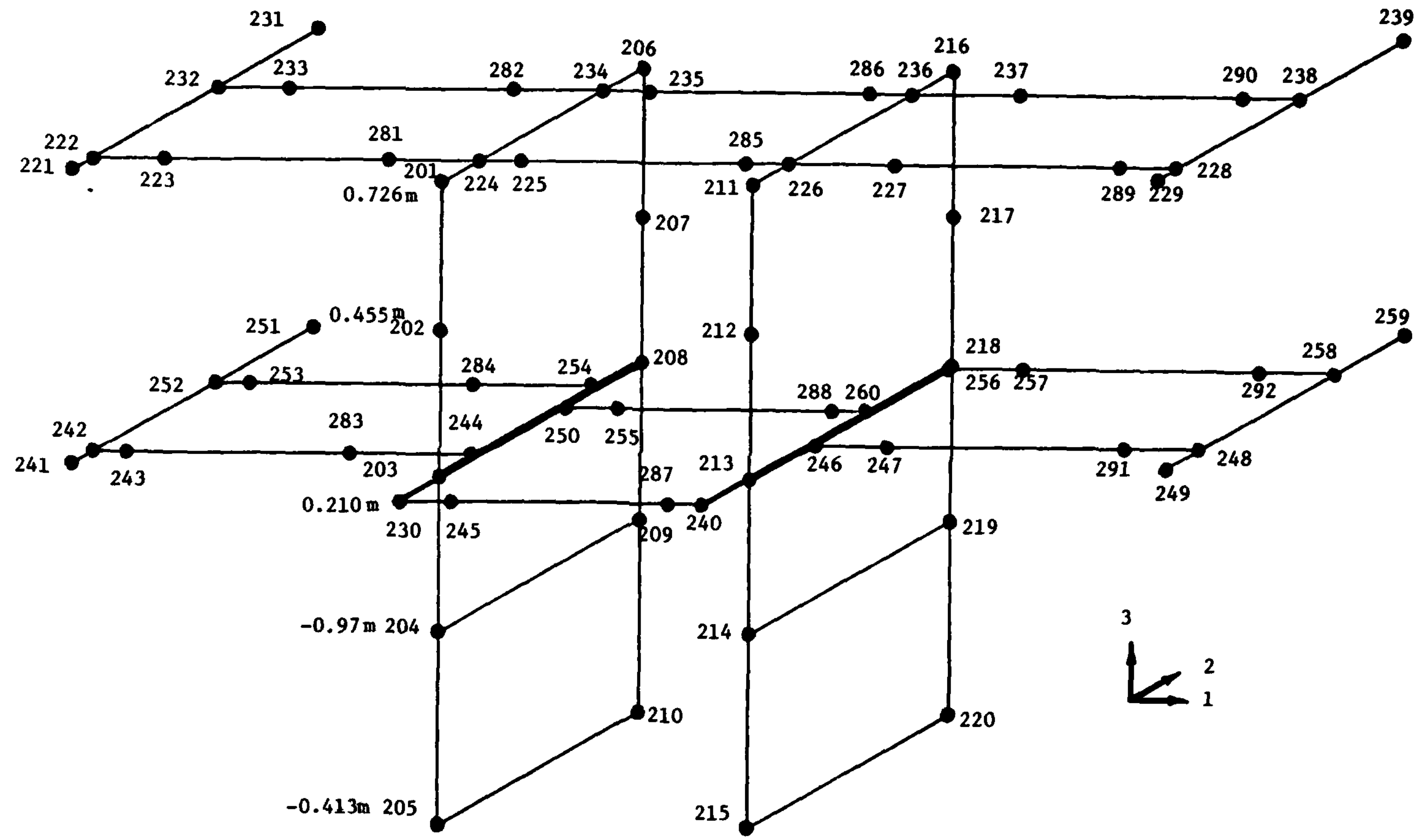

FIGURE 2.35. GRID POINT SYSTEM FOR AN/GRC-142B RACKS

TABLE 2.33

PROPERTIES OF AN/GRC-142B RACK BEAM ELEMENT

CBAR		I_{zz} (cm^4)	I_{yy} (cm^4)	I_{yz} (cm^4)	J (cm^4)	K_z	K_y	A (mm^2)	ECOM DRAWING NUMBER
A	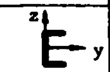	17.69	26.54	0.00	0.512	0.719	0.281	674.8	SM-B-603201
B	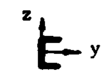	5.10	8.25	0.00	0.112	0.706	0.294	342.6	SM-D-613209
C	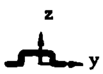	88.72	6.20	0.00	0.554	0.530	0.470	685.8	SM-C-613203
D	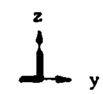	56.42	115.29	47.71	1.465	0.408	0.592	1089.0	SM-C-685242
E	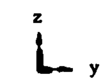	56.42	115.29	-47.71	1.465	0.408	0.592	1089.0	SM-C-685242
F	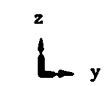	37.33	59.14	-27.61	2.185	0.422	0.578	1044.5	SM-C-685228
G	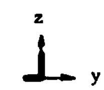	37.33	59.14	27.61	2.185	0.422	0.578	1044.5	SM-C-685228
H		5.01	10.34	-4.22	0.304	0.396	0.604	401.9	SM-D-613191
I	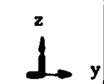	5.01	10.34	4.22	0.304	0.396	0.604	401.9	SM-D-613191

TABLE 2.34

CBAR ELEMENT CONNECTIONS FOR AN/GRC-142B RACKS

CBAR	GRID POINT CONNECTIONS	NUMBER OF ELEMENTS	LOCATION
A	201,224,234,206	3	RACK BASE
	211,226,236,216	3	AND TOP
	205,210	1	CHANNELS
	215,220	1	
B	201 - 205	4	RACK VERTICAL
	206 - 210	4	CHANNELS
	211 - 220	4	
	216 - 220	4	
C	222,223,281,224,225,	9	RACK SHELF
	285,226,227,289,228,		BEAMS
	232,233,282,234,235	9	
	286,236,237,290,238		
	242,243,283,244	3	
	230,245,287,240	3	
	246,247,291,248	3	
	252,253,284,254	3	
	250,255,288,260	3	
	256,257,292,258	3	
D	204,209	1	LOWER SUPPORT
E	214,219		ANGLE
F	221,222,232,231	3	RACK WALL
	241,242,252,251	3	SUPPORT
G	229,228,238,239	3	
	249,248,258,259	3	
H	203,244,254,208	3	RACK SHELF
	240,213,260,218	3	SUPPORT
I	230,203,250,208	3	ANGLE
	213,246,256,218	3	

TABLE 2.35

CONSTRAINT CONNECTIONS BETWEEN
AN/GRC-142B RACKS AND S-250 SHELTER

RACK GRID POINT	SHELTER GRID POINT
205	161
210	162
215	163
220	164
221	14
229	58
231	15
239	41
241	9
249	172
251	10
259	171

The weight of the structural model totals 197 kg, a shortfall of 148 kg from the known 345 kg total weight of the shelter. To account for the weight of the door hardware, skids, trim angles, castings, fasteners, sealant, etc., the 148 lb weight was appropriately distributed with CONM2 concentrated mass cards onto adjacent grid points.

The equipment supported by the racks are listed in Table 2.36 along with their masses and the grid points to which the weights are equally apportioned, resulting in a total mass of 179 kg including the rack structural mass. Table 2.37 presents the mass breakdown of the AN/GRC-142B system. Additional miscellaneous equipment is housed within the shelter to result in a total mass of 862 kg for the entire AN/GRC-142B system (Ref. 4). This additional unspecified equipment mass of 308 kg, representing 36% of the total, was distributed as concentrated masses via CONM2 cards onto the walls, knee panels, and floor of the shelter, based on estimates of weight and distribution of equipment by inspection of photographs of the interior of the shelter. Table 2.38 shows the apportionment of masses to account for this equipment mass deficiency. Again, the arbitrary distribution of the shelter and equipment mass deficiencies may result in uncertainties in dynamic response analyses with its effect on the inertial and stiffness properties of the model.

2.2.4 Summary of S-250 Shelter Models

A summary of the basic structural and mass elements used to construct each model, the constraint relations employed, and the resulting degrees-of-freedom are presented in Table 2.39. The degree of complexity depends on the detail in modeling the shelter and electronic equipment for the two systems, and the number of constraint relations employed to reduce the total degrees of freedom.

All grid points common with the assumed rigid base region of the shelter were related to a central point on the base via MPC cards to model the rigid body motion of the base, as in the S-280 models. Thus the base motion is described with the maximum possible six degree-of-freedom motion of the central point. For the mode shape and frequency analysis, that point is constrained from motion in six degrees-of-freedom with an SPC card. For the blast loading dynamic analysis runs, a base motion may be imposed on that central point, with appropriate changes in the single point constraints.

The mode shapes and frequencies were obtained for each system as an aid in validating the structural models. The first ten natural frequencies of the complete set, as obtained by the Givens Method in NASTRAN, are presented in Table 2.40.

Reference 4. Radio Teletypewriter Sets AN/GRC-142, AN/GRC-142A, AN/GRC-142B, AN/GRC-122, AN/GRC-122A and AN/GRC-122B, Department of the Army Technical Manual TM 11-5815-334-12, May 1970.

TABLE 2.36

EQUIPMENT MASSES FOR AN/TRC-145 SYSTEM

EQUIPMENT	MASS (kg)	GRID POINT SUPPORTS	LOCATION
AN/GRC 106	34.02	223,233,281,282	RACK
MD-522A/GRC	16.33	225,235,285,286	RACK
SA-1650/GRC	4.54	225,235,285,286	RACK
J-2728/GRC-142	1.81	227,237,289,290	RACK
SB-3358/GRC	4.54	227,237,289,290	RACK
J-2728/GRC-142	1.81	243,253,283,284	RACK
TT-98/FG	24.49	245,255,287,288	RACK
PP-4763*/GRC	56.70	247,257,291,292	RACK
C-434/GRC	2.72	202	RACK
TOTAL	147.0		

TOTAL WEIGHT OF RACK FRAME AND SUPPORTED EQUIPMENT = 179 kg.

TABLE 2.37

MASS BREAKDOWN OF AN/GRC-142B SYSTEM

ITEM	MASS (kg)
SHELTER	345
RACKS	179
TT-76A/GGC	21
FSN 4520-912-3502	7
TA-312/PT	2
TOTAL	554
SYSTEM MASS	862
UNSPECIFIED MASS	308

TABLE 2.38

ASSUMED DISTRIBUTION OF UNSPECIFIED MASSES
FOR AN/GRC-142B EQUIPMENT

EQUIPMENT	ASSUMED MASS (kg)	GRID POINT SUPPORTS	LOCATION
SHELTER HEATER	36.29	1,2,46,76	KNEE PANEL
STANDING WAVE METER	13.61	16,17	ROADSIDE WALL
TAPE ROLLS AND INVERTER	13.61	28,78,154,155,161,162	KNEE PANEL AND FLOOR
POWER/SIGNAL ENTRANCE BOX	9.07	39,41,44,45	FRONT WALL
LIGHTS & VENTILATOR	4.54	58,59,61,62	CURBSIDE WALL
CLOCK	3.63	18,19	ROADSIDE WALL
LOCKERS AND CONTENTS	136.07	1-5;46,76,77,78,28; 47,72,73,74,30;48,57, 56,55,31	KNEE PANELS
EQUIPMENT ON FLOOR	90.72	151-160	FLOOR
TOTAL	307.5		

TABLE 2.39

SUMMARY OF AN/TRC-145 AND AN/GRC-142B SYSTEM MODELS

ELEMENTS	AN/TRC-145	AN/GRC-142B
SPRING (CELAS2)	6	
BEAM (CBAR)	174	225
PLATE (CQUAD1)	59	79
MASS (CONM2)	138	126
GRID POINTS (GRID)	150	161
SINGLE POINT CONSTRAINTS (SPC)	6	6
MULTIPOINT CONSTRAINTS (MPC)	443	327
OMITTED COORDINATES (OMIT)	304	425
MAXIMUM POSSIBLE DEGREES OF FREEDOM	900	966
DYNAMIC DEGREES OF FREEDOM	147	208

MAXIMUM POSSIBLE DEGREES OF FREEDOM:

= 6 X NO. OF GRID POINTS

DYNAMIC DEGREES OF FREEDOM:

= MAXIMUM POSSIBLE D.O.F. - SPC - MPC - OMIT

TABLE 2.40

NATURAL FREQUENCIES OF AN/TRC-145 AND AN/GRC-142B SYSTEMS

MODE	AN/TRC-145	AN/GRC-142B
1	33.82	54.12
2	37.70	57.86
3	40.44	60.15
4	43.51	65.37
5	44.73	68.26
6	45.08	69.94
7	45.87	71.63
8	50.48	75.03
9	50.86	78.27
10	55.56	78.90

2.3 TRUCK DATA

The AN/TRC-117, AN/TRC-110 and the AN/TCC-61 systems are mounted on the M35A2 2½ ton truck (Fig. 2.36) and the AN/TRC-145 and the AN/GRC-142 systems are mounted on the M715 1¼ ton truck (Fig. 2.37). The base motion excitation experienced by each truck-mounted shelter was found by exercising the TRUCK code. The TRUCK code calculates the nonlinear gross motions (accelerations and displacements) and possible overturning of a truck-shelter-rack system in response to a blast loading (see Ref. 5). The truck, shelter and racks may be treated as rigid masses in the code interconnected by springs and dampers representing their respective suspension systems. The S-280 and S-250 systems which were modeled however, do not have spring and damper connections between the racks, the shelter and the truck bed. Therefore, the racks and shelter were rigidly connected to the truck chassis in the truck model. However, the truck suspension system and the tire flexibility were modeled.

Table 2.41 presents the mass and inertia data for each truck and Table 2.42 presents similar data for the shelter systems. Data for Tables 2.41 and 2.42 were obtained from information furnished by BRL. Figure 2.38 presents a schematic of a typical truck model. The M35A2 has a double-axle bogey in the rear whereas the M715 has a single rear axle. In exercising the TRUCK code, the blast direction was taken as pointing into the x-axis (-x direction) of Fig. 2.38.

Data listings of the TRUCK code for the AN/TRC-117, AN/TRC-110, AN/TCC-61 and the AN/TRC-145 are given in Appendix A. These listings also include the spring-damper data for the truck suspensions. Ref. 5 should be consulted for identifying the various input quantities in the data listings.

Reference 5. Hobbs, N. P., et al, TRUCK - A Digital Computer Program for Calculating the Response of Army Vehicles to Blast Waves, Kaman AviDyne TR-136, March 1977.

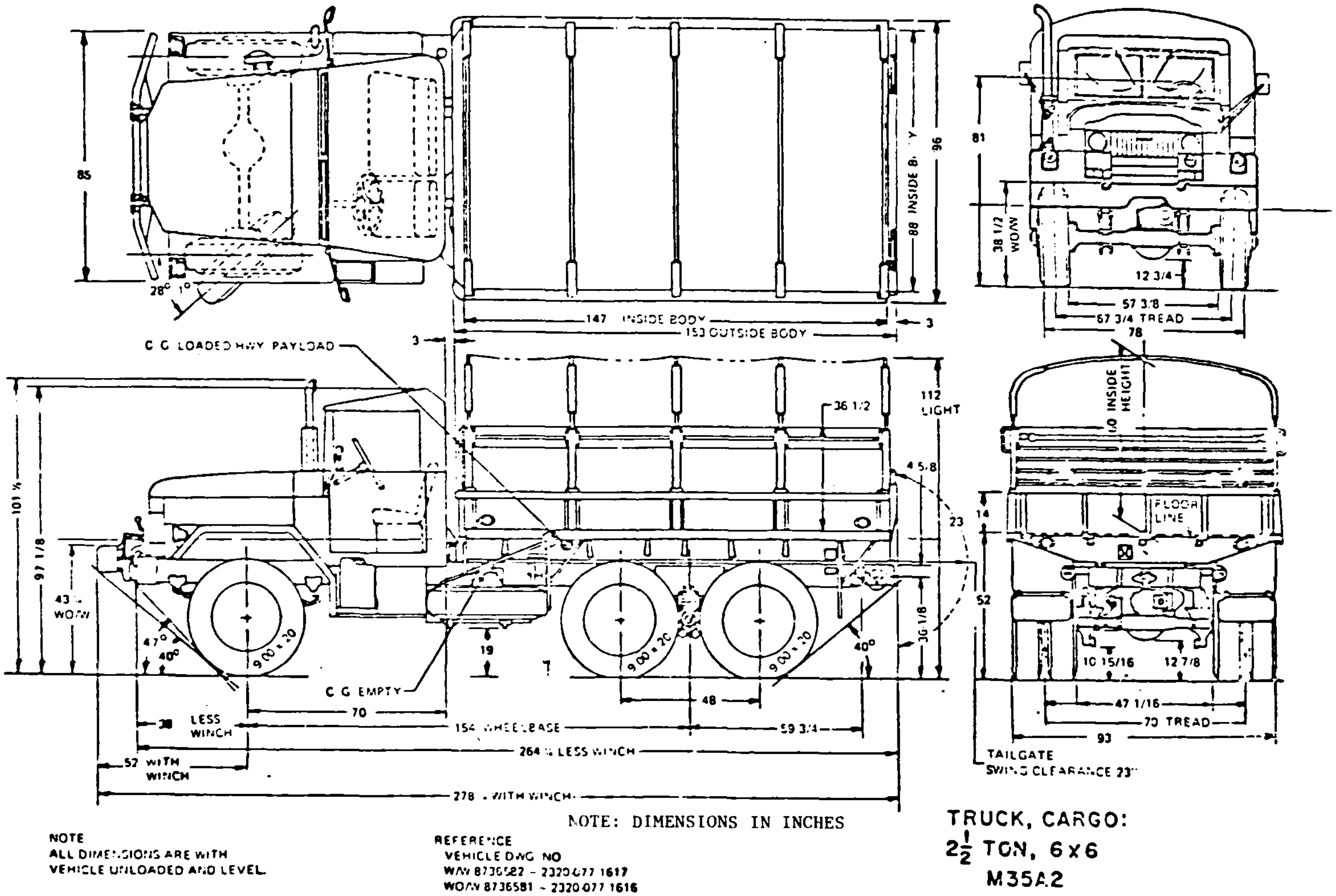

FIGURE 2.36. M35A2 2 1/2 TON TRUCK

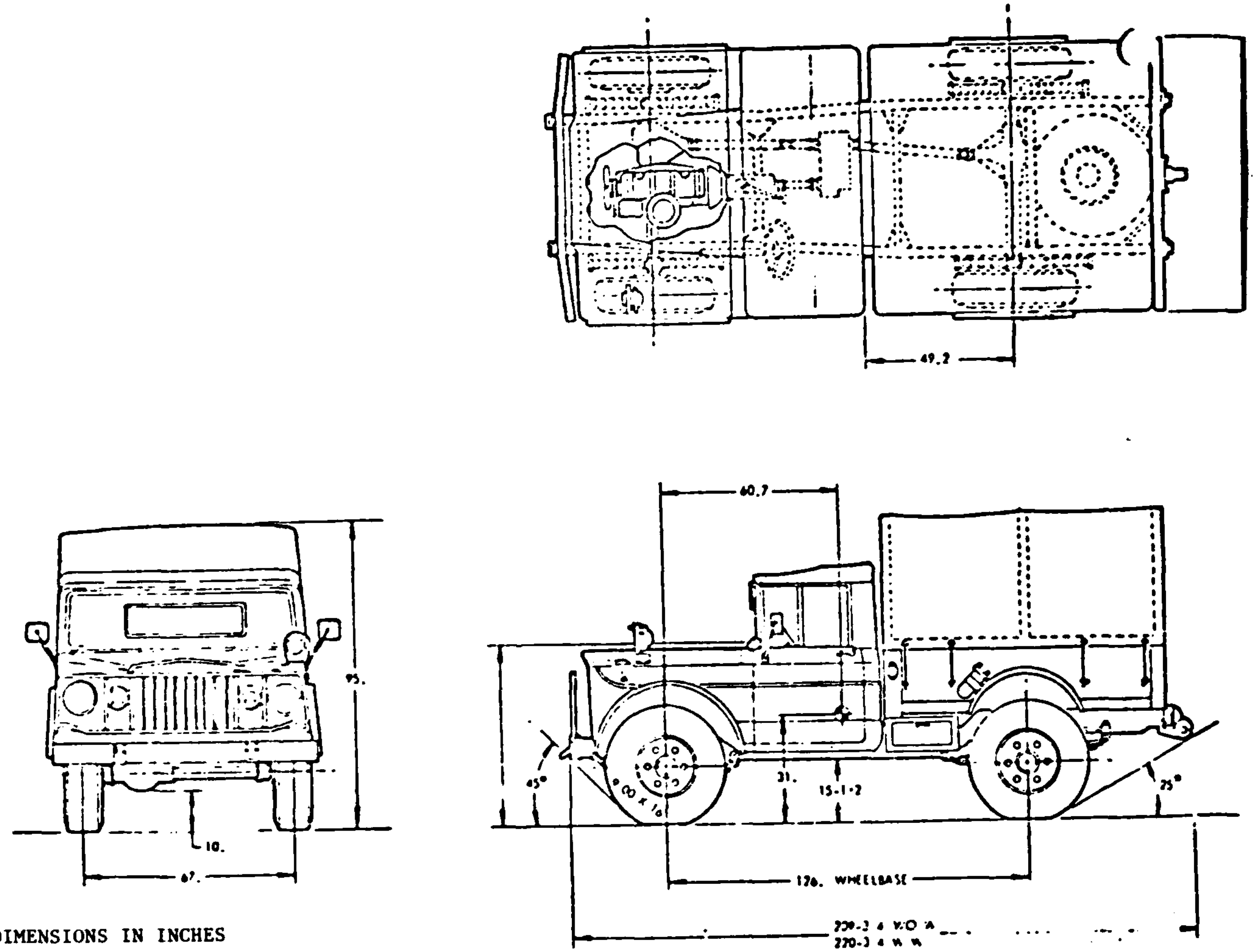

NOTE: DIMENSIONS IN INCHES

FIGURE 2.37. M715 CARGO TRUCK, 1 1/4 TON

TABLE 2.41

TRUCK MASS AND INERTIA DATA

TRUCK	M35A2 2 1/2 TON	M715 1 1/4 TON
CHASSIS MASS (kg)	3406	1826
x_{cg} (m)	0.0	0.0
y_{cg} (m)	.475	.394
z_{cg} (m)	-1.65	-1.40
I_{xx} (Mg-m^2)	13.0	1.84
I_{yy} (Mg-m^2)	13.5	1.84
I_{zz} (Mg-m^2)	1.40	.570
I_{yz} (Mg-m^2)	.171	.028
FRONT AXLE MASS (kg)	649	334
x_{cg} (m)	0.0	0.0
y_{cg} (m)	.025	0.0
z_{cg} (m)	0.0	0.0
I_{xx} (Mg-m^2)	.035	0
I_{yy} (Mg-m^2)	.333	.293
I_{zz} (Mg-m^2)	.321	.293

TABLE 2.41 (CONT'D)

TRUCK MASS AND INERTIA DATA

TRUCK	M35A2 2 1/2 TON	M715 1 1/4 TON
FORWARD REAR AXLE MASS (kg)	785	334
x_{cg} (m)	0.0	0.0
y_{cg} (m)	0.0	0.0
z_{cg} (m)	-3.30	-3.2
I_{xx} ($Mg\text{-}m^2$)	.011	0
I_{yy} ($Mg\text{-}m^2$)	.382	.312
I_{zz} ($Mg\text{-}m^2$)	.447	.312
AFT REAR AXLE MASS ($Mg\text{-}m^2$)	785	
x_{cg} (m)	0.0	
y_{cg} (m)	0.0	
z_{cg} (m)	-4.52	
I_{xx} ($Mg\text{-}m^2$)	.011	
I_{yy} ($Mg\text{-}m^2$)	.382	
I_{zz} ($Mg\text{-}m^2$)	.447	

NOTE: 1. Centroidal distances are given with respect to an axis system located at the center of the front axle.

2. Inertias are referred to local centroidal axes.

TABLE 2.42

SHELTER-RACK MASS AND INERTIA DATA

SYSTEM	AN/TRC-117	AN/TRC-110	AN/TCC-61	AN/TCC-145
MASS (kg)	2304	2336	2495	5.44
x_{cg}*(m)	0.0	0.0	0.0	0.0
y_{cg} (m)	.889	.889	.889	.937
z_{cg} (m)	0.0	.152	0.0	4.94
I_{xy}** ($Mg-m^2$)	3.73	3.73	4.02	.737
I_{yy} ($Mg-m^2$)	4.52	4.52	4.87	.880
I_{zz} ($Mg-m^2$)	2.37	2.37	2.58	.634

*Measured from center of shelter floor at truck bed height.

**With respect to centroidal axes of system.

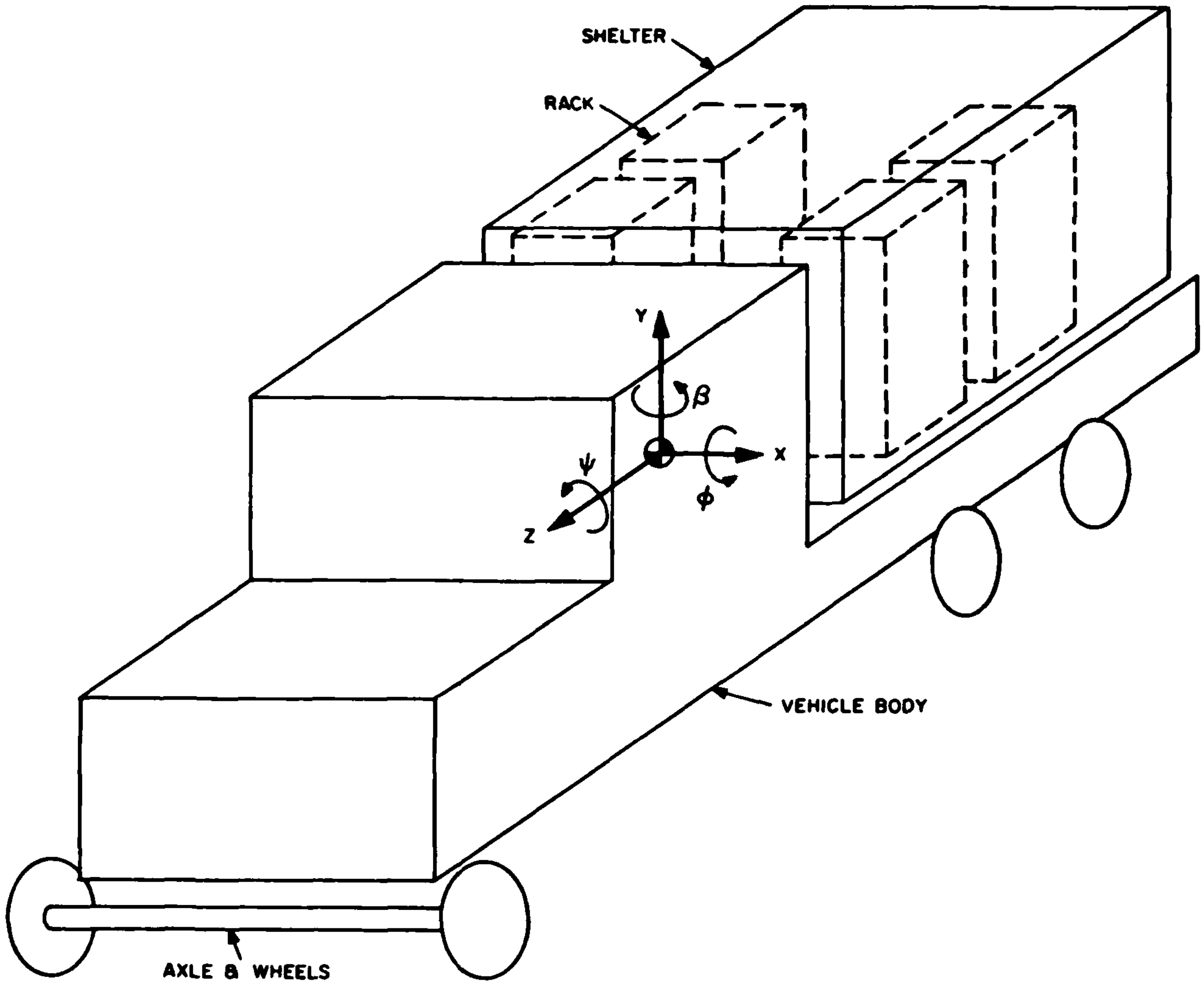

FIGURE 2.38. MASS MODEL LAYOUT

SECTION 3

TRANSIENT RESPONSE

3.1 INTRODUCTION

The acceleration time history responses of the S-280 and S-250 systems modeled in Section 2, with the exception of the AN/GRC-142B, were obtained for several overpressure levels experienced in the DICE THROW field test. A summary of the overpressure levels for each system is given in Table 3.1. Each system was subjected to the overpressure loading of the blast wave acting on the shelter and to the simultaneous effect of the base motion of the supporting truck. The yield of the DICE THROW charge was 600 tons of ANFO, corresponding to approximately a 4.2 TJ (1KT) nuclear yield.

Section 3.2 presents the responses of the S-280 systems, using the BAAL hydrodynamic code to predict the overpressure loading (Ref. 6). The responses of the S-250 systems are given in Section 3.3, using the SHELTR code to determine the overpressure loading. No comparisons are made between the predicted and measured responses in Sections 3.2 and 3.3 Instead, comparisons are made for two of these systems, the AN/TRC-117 and the AN/TRC-145, in Section 3.4, each at an overpressure level of 6.0 psi (41.4 kPa). For these comparisons, the overpressure model used in the TRUCK code was used for consistency to determine the blast loading.

3.2 S-280 Systems

Acceleration time histories of the S-280 systems subjected simultaneously to the overpressure loading and to the corresponding base motion of the truck were obtained for the overpressure levels indicated in Table 3.1. The BAAL code, which was used to determine the overpressure models for this section of the report, is a three-dimensional transient hydrodynamic code developed by the Los Alamos Scientific Laboratory.

The overpressure time histories for the various overpressure levels indicated in Table 3.1 were obtained by scaling the output of a reference 5.0 psi (34.5 kPa) case of the BAAL code provided by BRL. Following BRL's recommendation for scaling, the estimated values for the overpressure-time history for an incident overpressure Δp_i in Table 3.1 were calculated by multiplying the corresponding overpressures of the 34.5 kPa reference case by the ratio

$$\frac{(\Delta p_r)_i}{(\Delta p_r)_{34.5}} \qquad (3.1)$$

Reference 6. Lottero, R.E., Computational Predictions of Shock Diffraction Loading on an S-280 Electrical Equipment Shelter, BRL MR 2599, March 1976. (AD#A022804).

TABLE 3.1

OVERPRESSURE LEVELS

SYSTEM	INCIDENT OVERPRESSURE Δp_i		OVERPRESSURE MODEL
	kPa	psi	
AN/TRC-117 (S-280)	41.4	6.0	BAAL, TRUCK
AN/TRC-110 (S-280)	17.9	2.6	BAAL
	27.6	4.0	BAAL
AN/TCC-61 (S-280)	19.3	2.8	BAAL
	32.4	4.7	BAAL
AN/TRC-145 (S-250)	50.3	7.3	SHELTR
	41.4	6.0	TRUCK
	34.5	5.0	SHELTR
	20.7	3.0	SHELTR

Note: Reference 34.5 kPa (5.0 psi) case of the BAAL code is used, and its output is appropriately scaled to obtain overpressure time histories for the indicated Δp_i.

where $(\Delta p_r)_i$ and $(\Delta p_r)_{34.5}$ are the theoretical one-dimensional reflected overpressures corresponding to the incident overpressure levels Δp_i and 34.5 kPa, respectively. Similarly, the estimated values for time for an incident overpressure Δp_i were calculated by multiplying the time for the 34.5 kPa case by

$$\frac{(V_s)_{34.5}}{(V_s)_i} \tag{3.2}$$

where $(V_s)_{34.5}$ and $(V_s)_i$ are the shock wave velocities corresponding to the incident overpressures of 34.5 kPa and $(\Delta p)_i$, respectively. The incident wave in the BAAL model consisted of a step profile. However, since the structural accelerations are of interest for a relatively short time period of approximately 30 msec or less, the use of a step wave instead of a decaying incident wave will have a very minor effect on the early-time structural response.

Some representative overpressure-time history plots obtained by scaling the reference 34.5 kPa case in the manner described above are shown in Figs. 3.1-3.10 for the S-280 shelter at 6.0 psi (41.3 kPa). Similar results would be obtained for the other (lower) overpressure levels in Table 3.1.

A loading preprocessor called NALO was developed to convert overpressure-time history data into force data at the loaded grid points of the exposed shelter surfaces in the form required by NASTRAN. The NALO program was used to first convert the overpressure output of the reference 34.5 kPa case from the original BAAL mesh system to the NASTRAN grid system for each loaded surface. The program then performed the overpressure and time scaling indicated in Eqs. 3.1 and 3.2 above, accounting for flow shielding provided by the truck (such as the sidegates, tailgates and cab), and automatically punched out the TLOAD1, TABLED1 and DAREA cards required by NASTRAN, all in one continuous mode. The end product was a set of loading (force) tables as a function of time for each loaded shelter grid point.

The base motion excitation was obtained by exercising the TRUCK code for each overpressure level indicated in Table 3.1 and printing out the accelerations at the center of the shelter floor. Since NASTRAN does not accept an acceleration input directly, the base motion was introduced by locating a large mass (many times greater than the total system mass) at the floor centroid in the NASTRAN model. A base-motion force was then determined by multiplying the base acceleration output from the TRUCK program by this large mass. This base-motion force (as a function of time) was then applied to the large mass located at the floor centroid in NASTRAN. Some typical base accelerations for the AN/TRC-117 system, and also the AN/TRC-145 system, obtained by the TRUCK code (using the data in Tables 2.41 and 2.42) are shown in Figs. 3.11-3.14. Since the gross mass data of the AN/TRC-110 and the AN/TCC-61 are

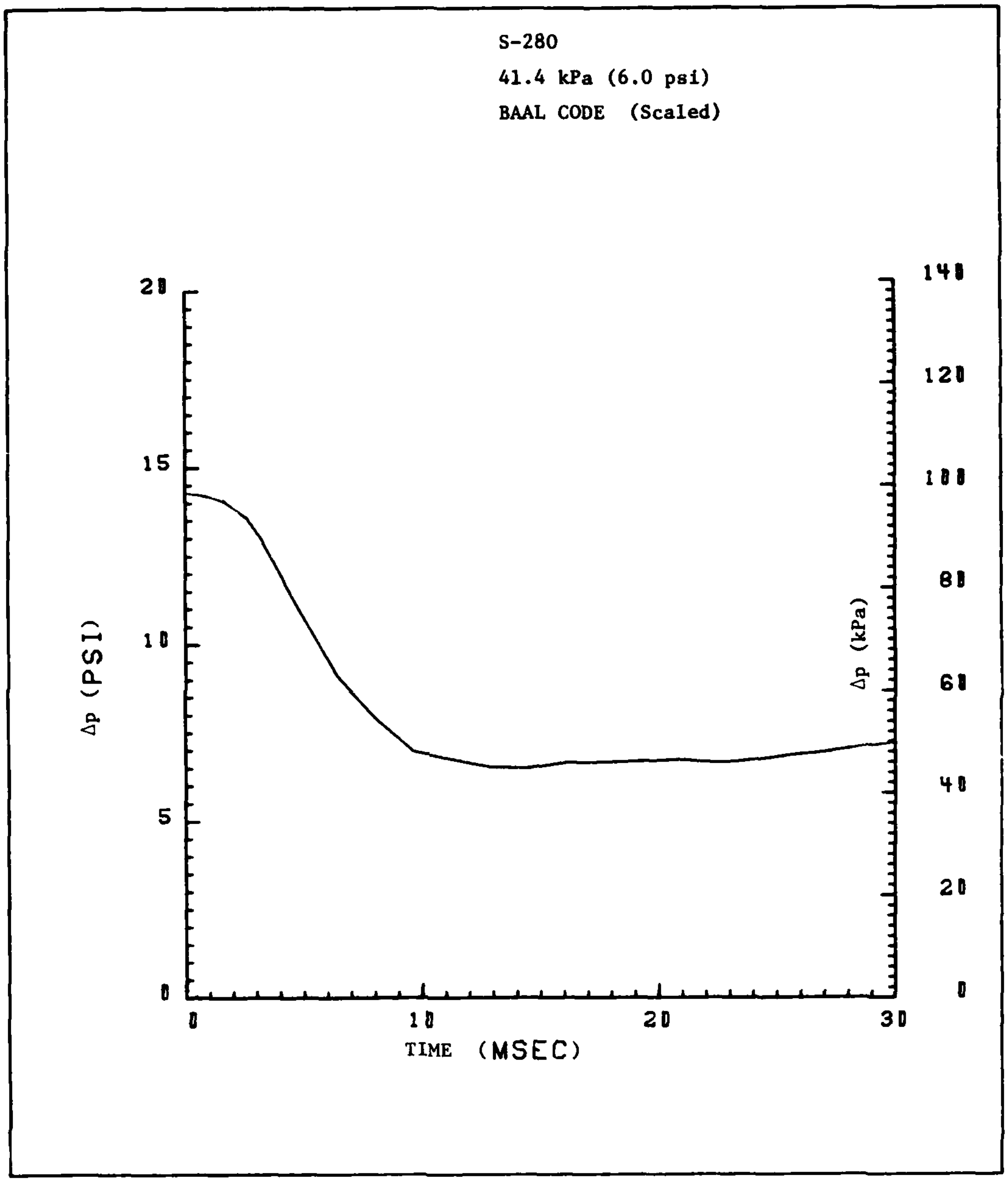

Figure 3.1. Overpressure Near Center of S-280 Roadside Wall

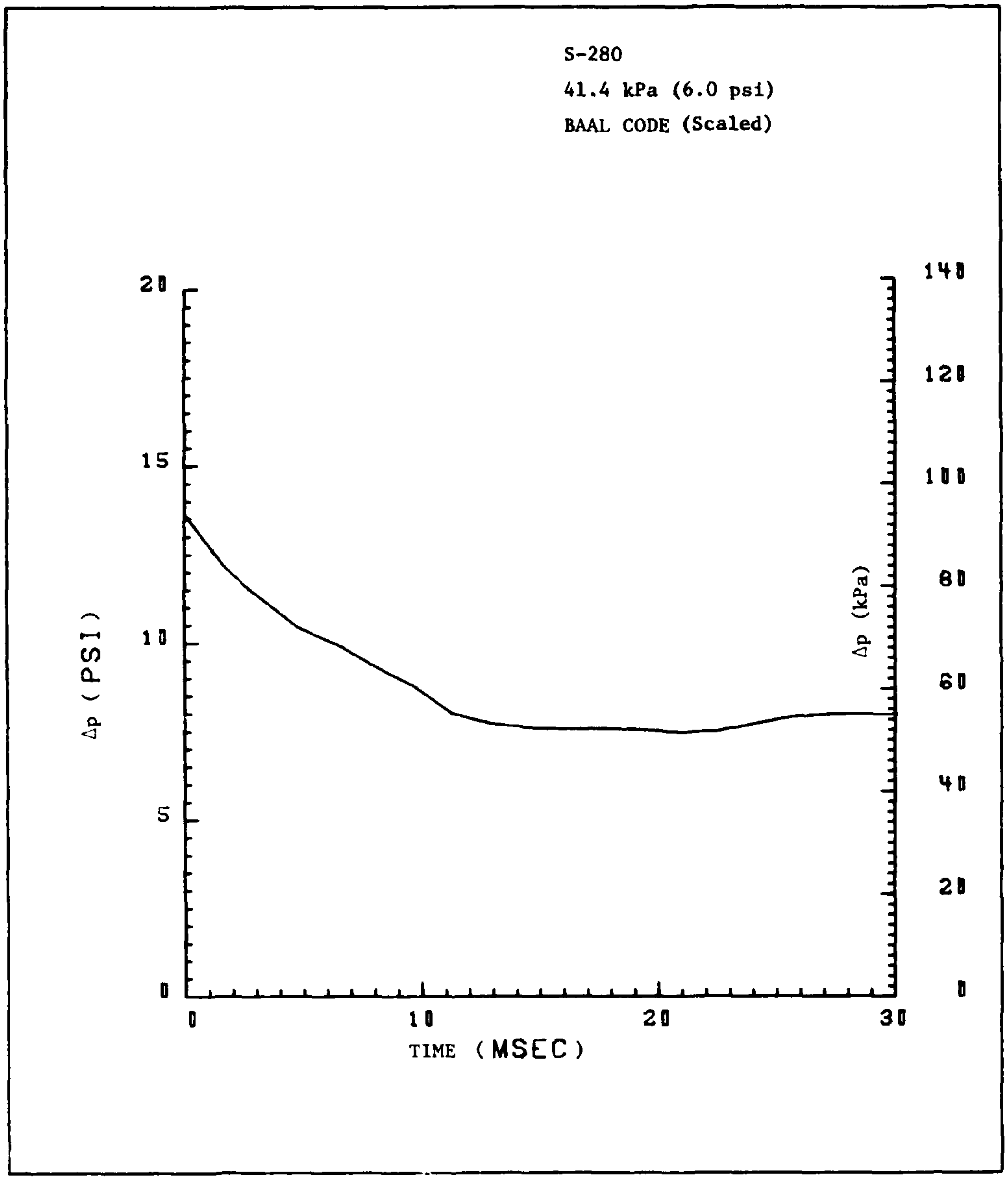

Figure 3.2. Overpressure on S-280 Roadside Wall
Near Center of Vertical Edge

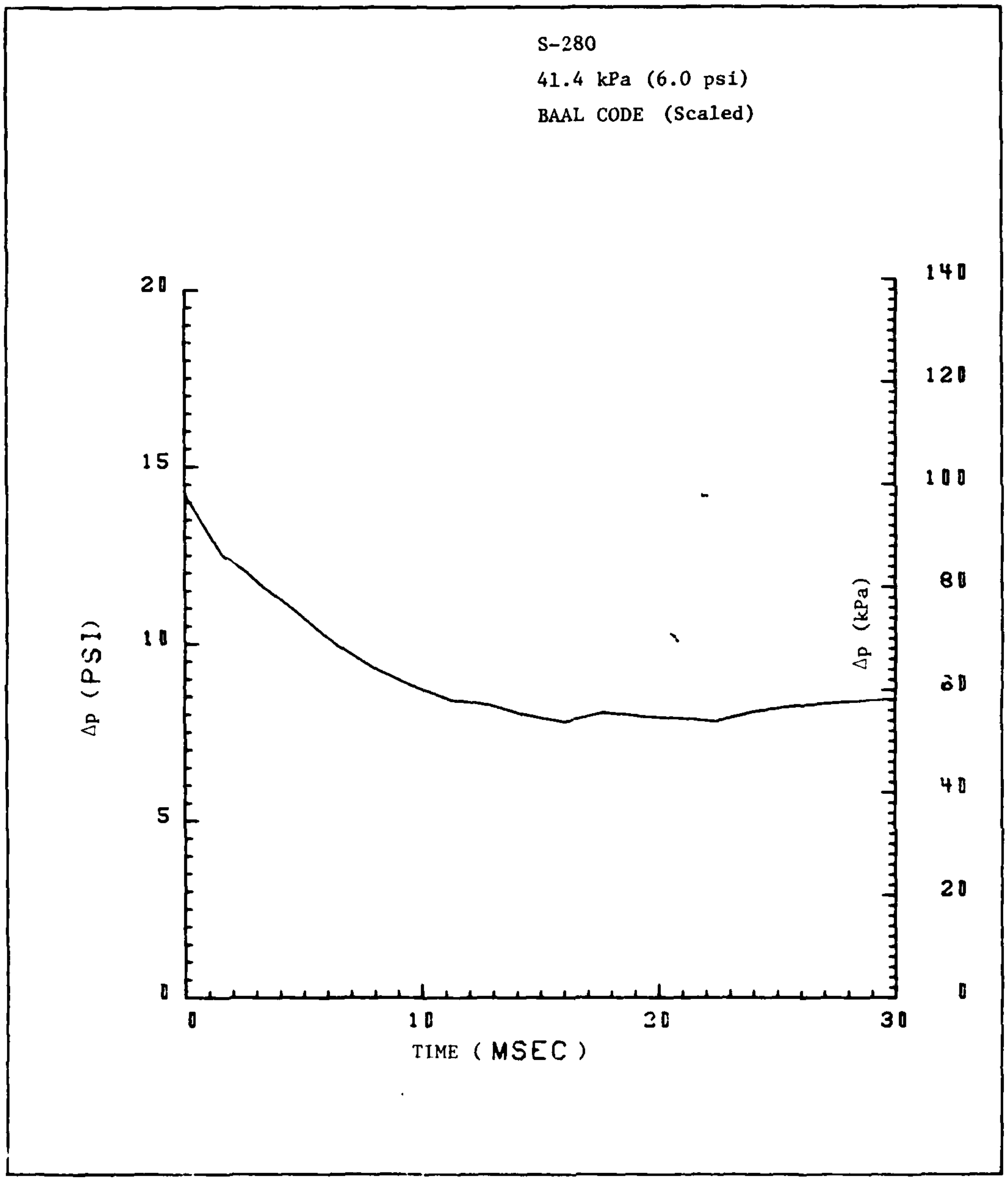

Figure 3.3. Overpressure on S-280 Roadside Wall
Near Center of Roof Edge

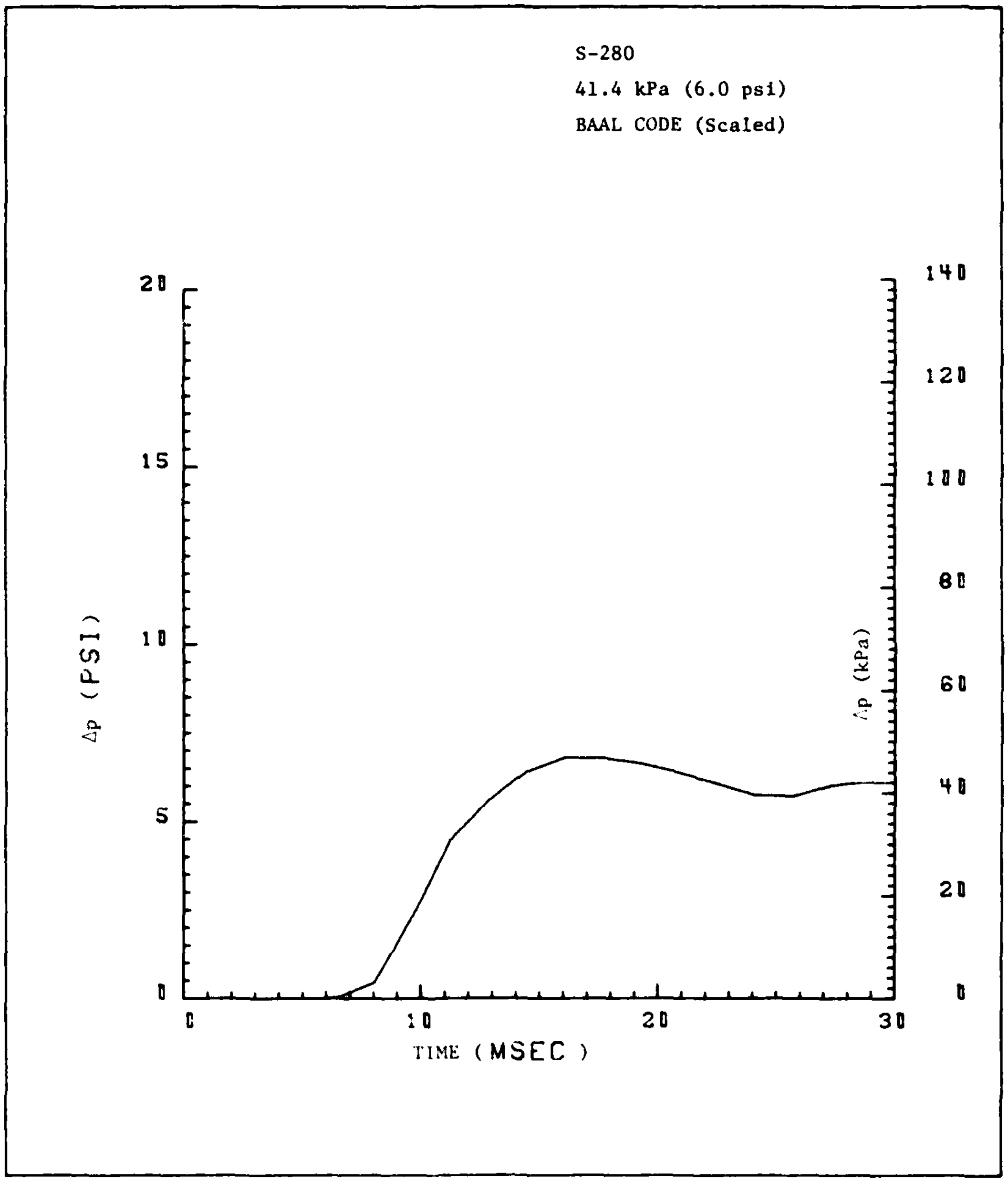

FIGURE 3.4. OVERPRESSURE NEAR CENTER OF S-280 CURBSIDE WALL

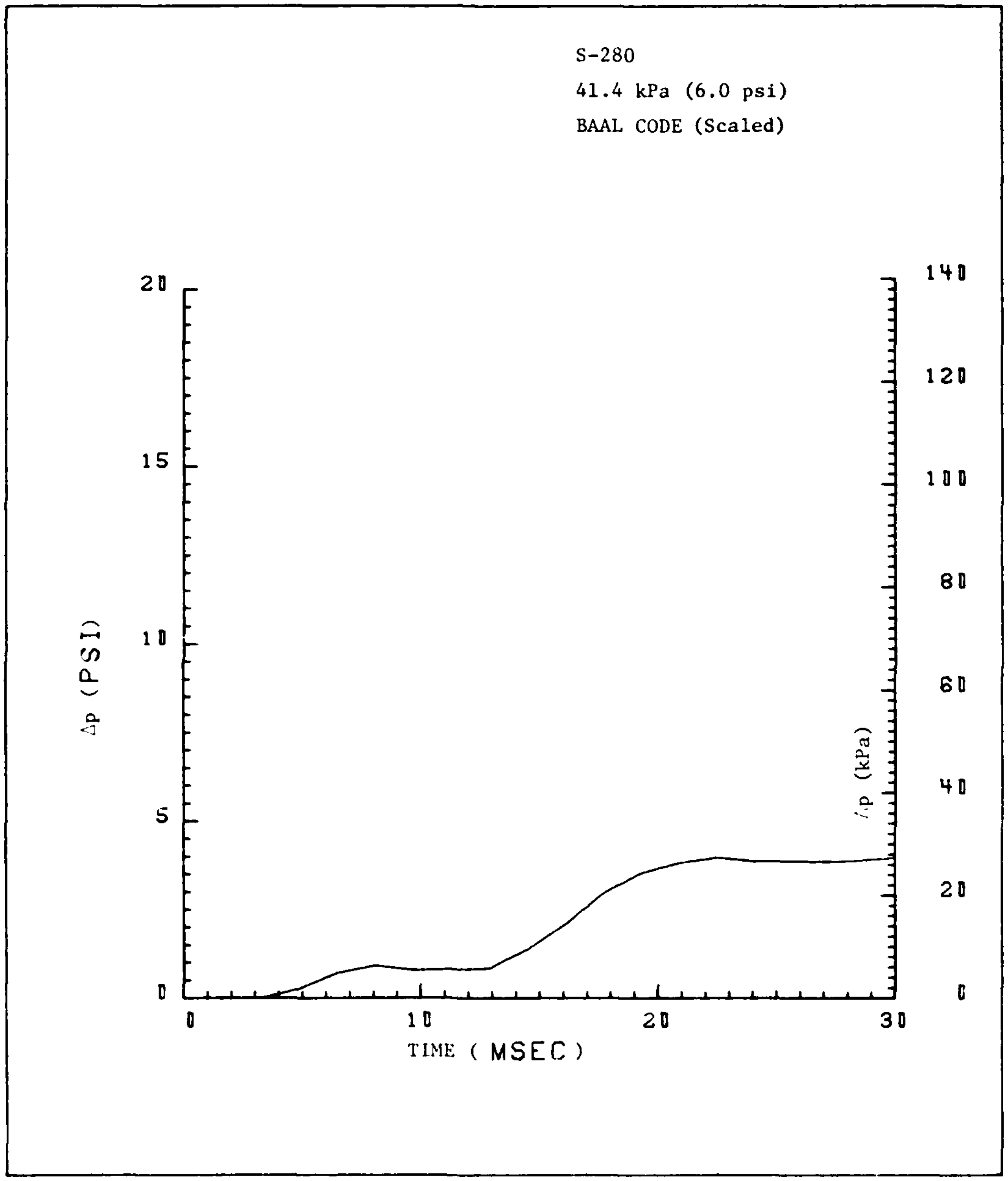

FIGURE 3.5. OVERPRESSURE ON S-280 CURBSIDE WALL
NEAR CENTER OF VERTICAL EDGE

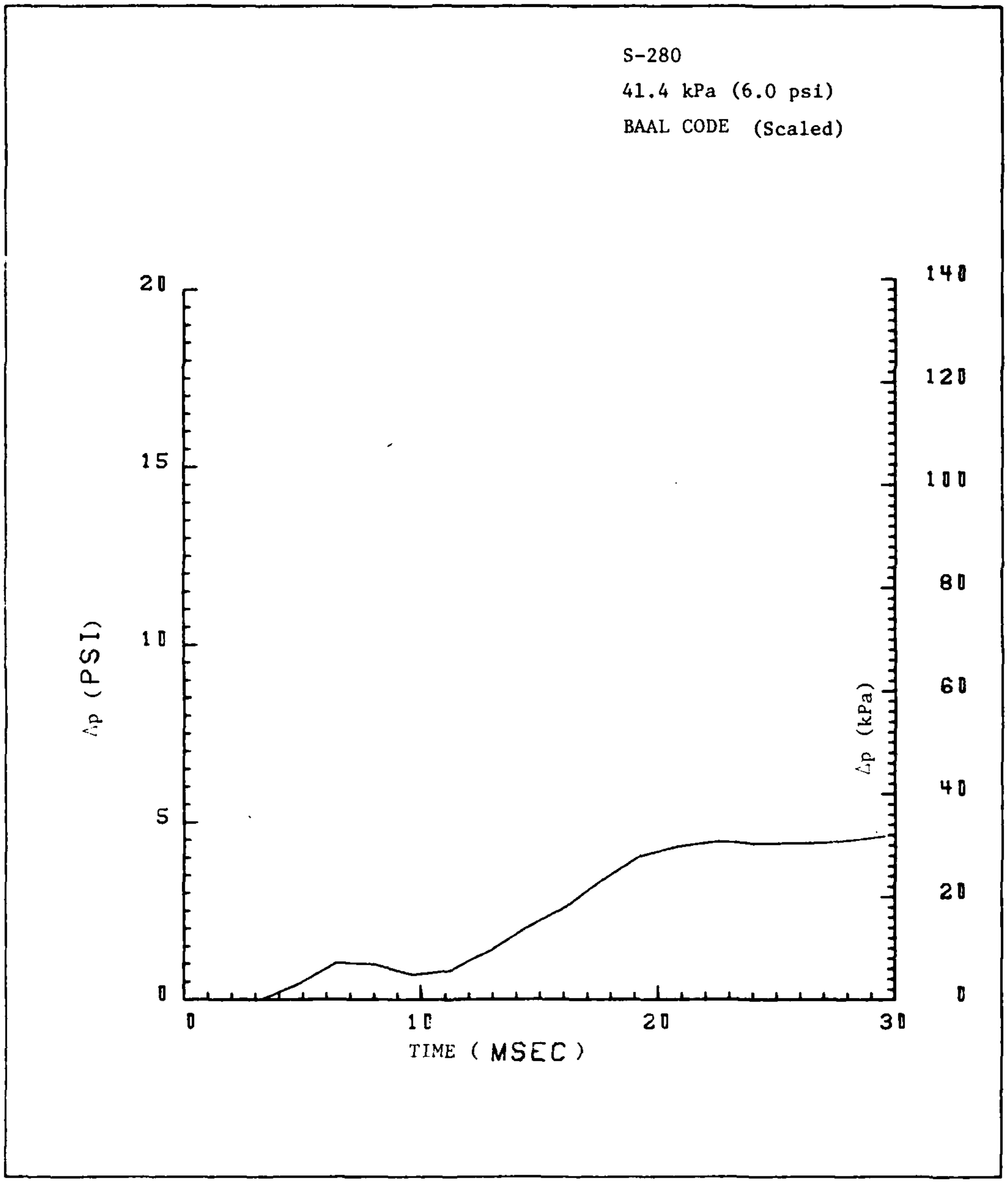

FIGURE 3.6. OVERPPESSURE ON S-280 CURBSIDE WALL NEAR CENTER OF ROOF EDGE

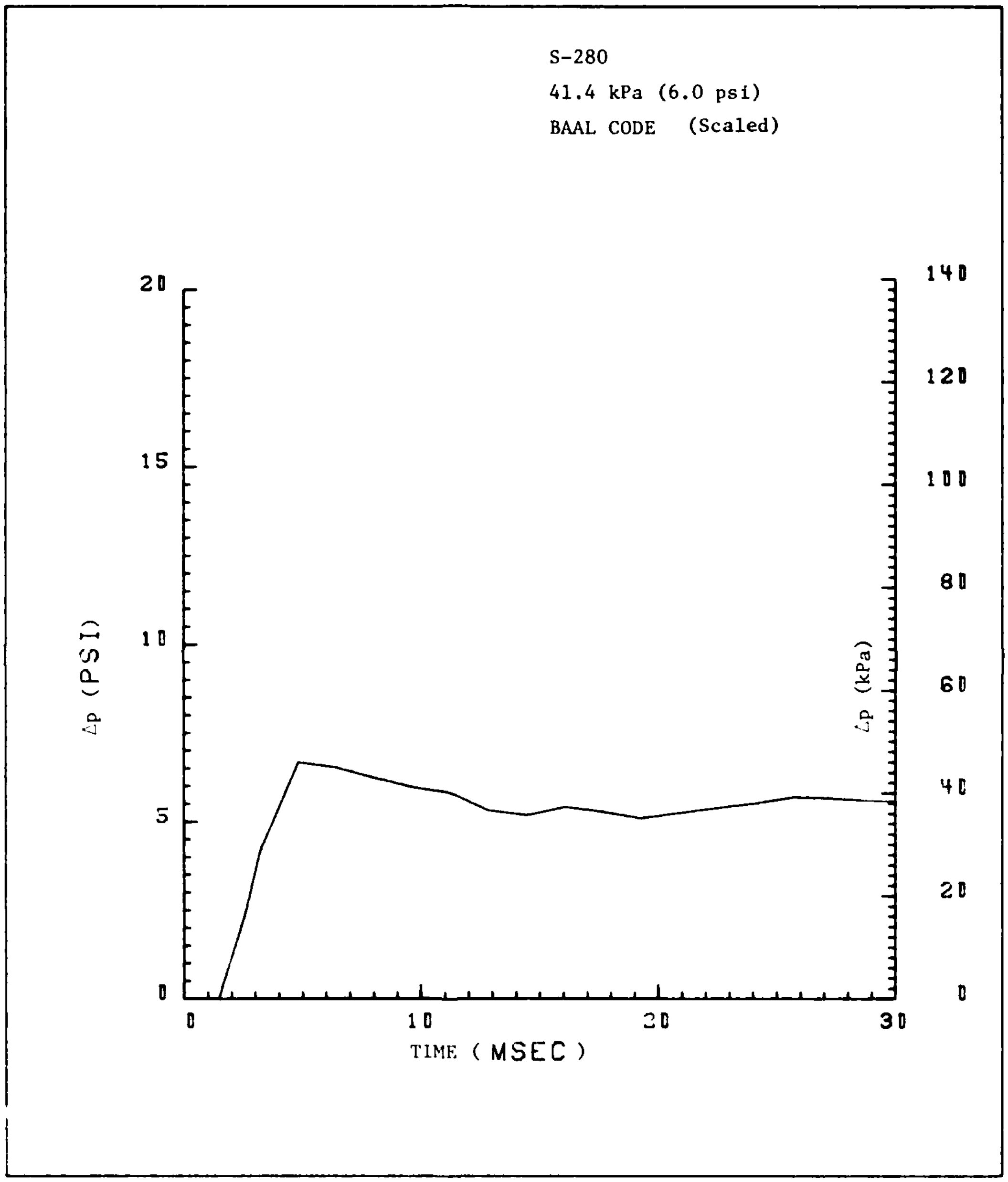

FIGURE 3.7 OVERPRESSURE NEAR CENTER OF S-280 ROOF

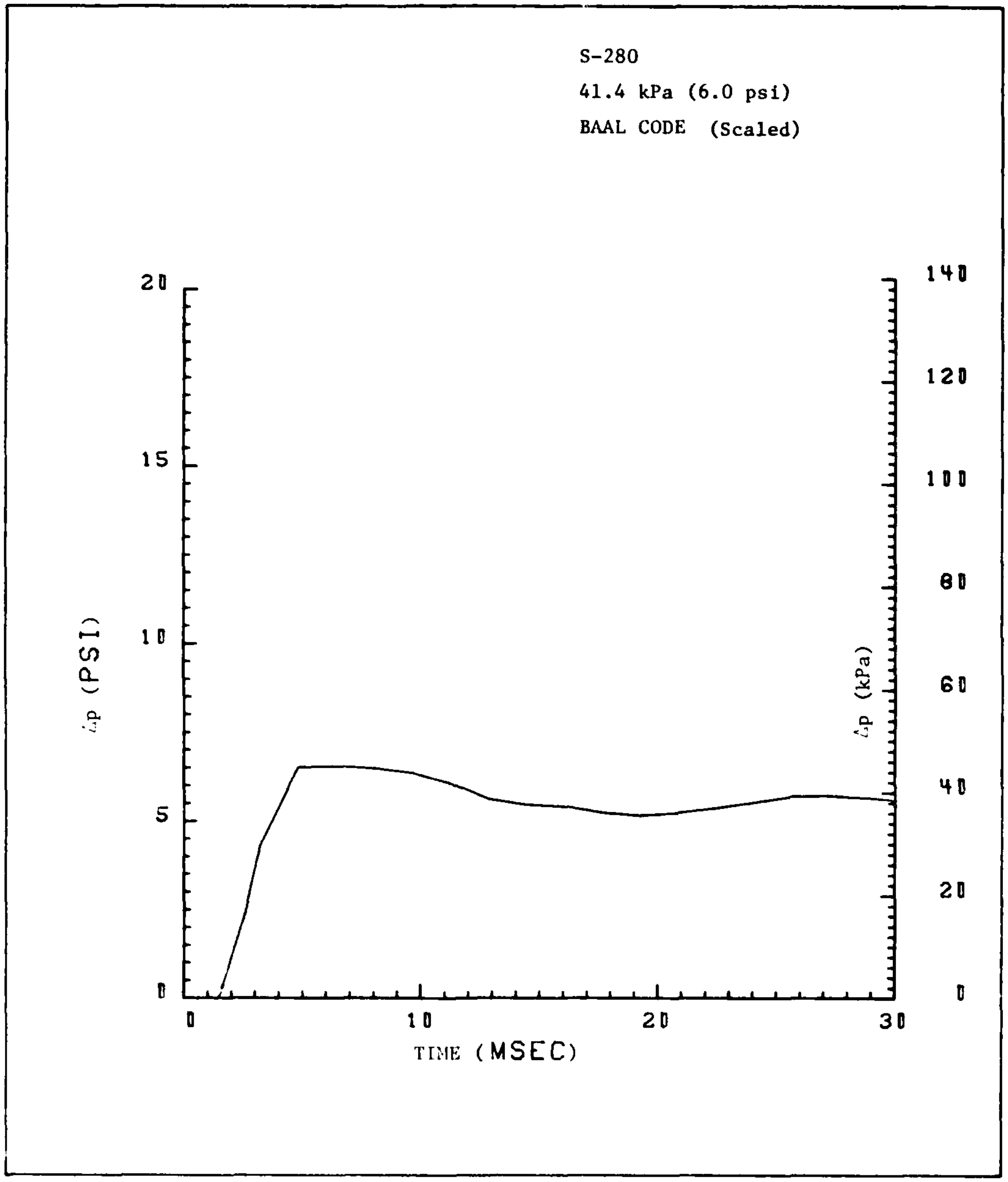

FIGURE 3.8. OVERPRESSURE ON S-280 ROOF NEAR CENTER OF INTERSECTION WITH FRONT END WALL

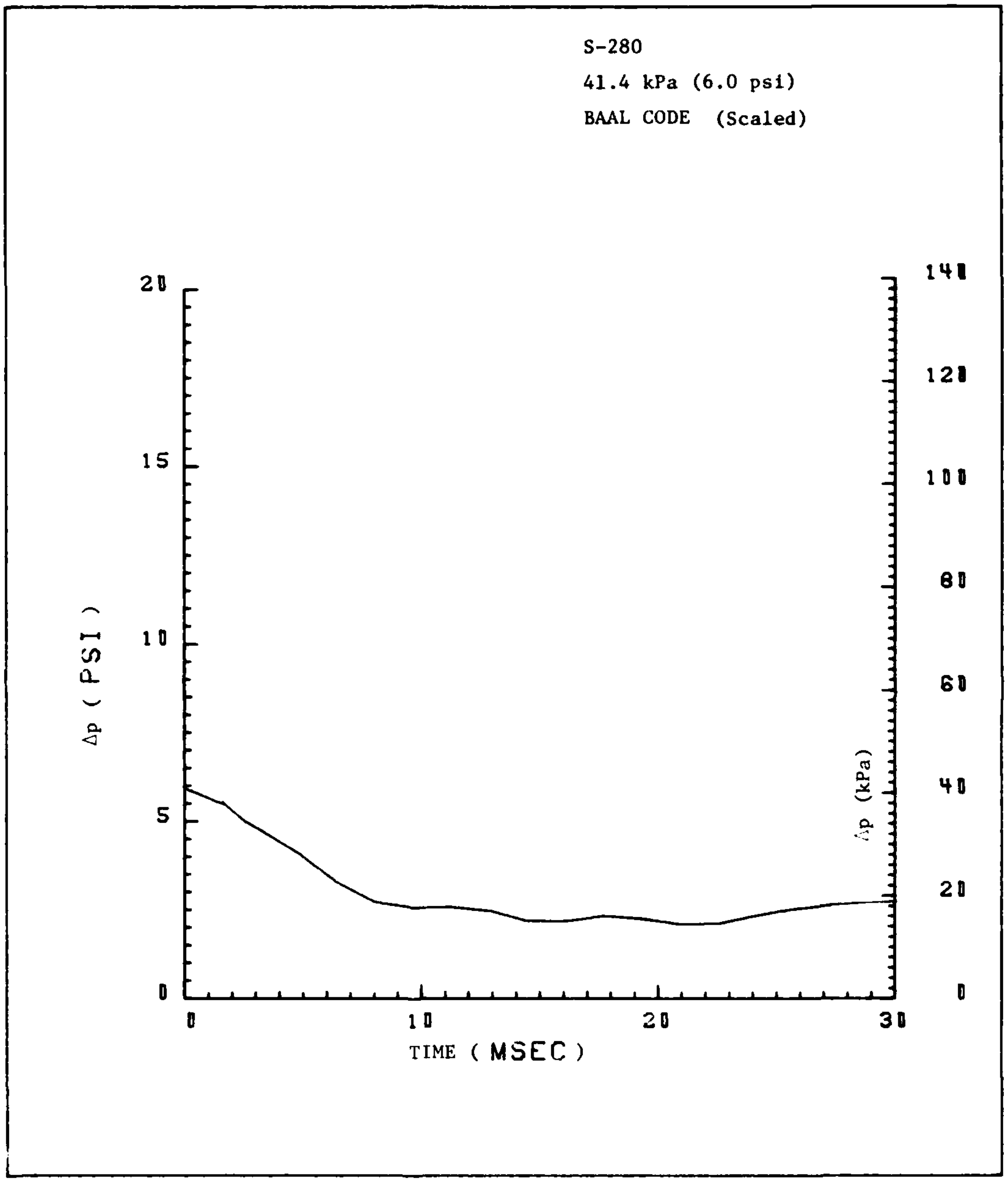

FIGURE 3.9. OVERPRESSURE ON S-280 ROOF NEAR CENTER OF ROADSIDE EDGE

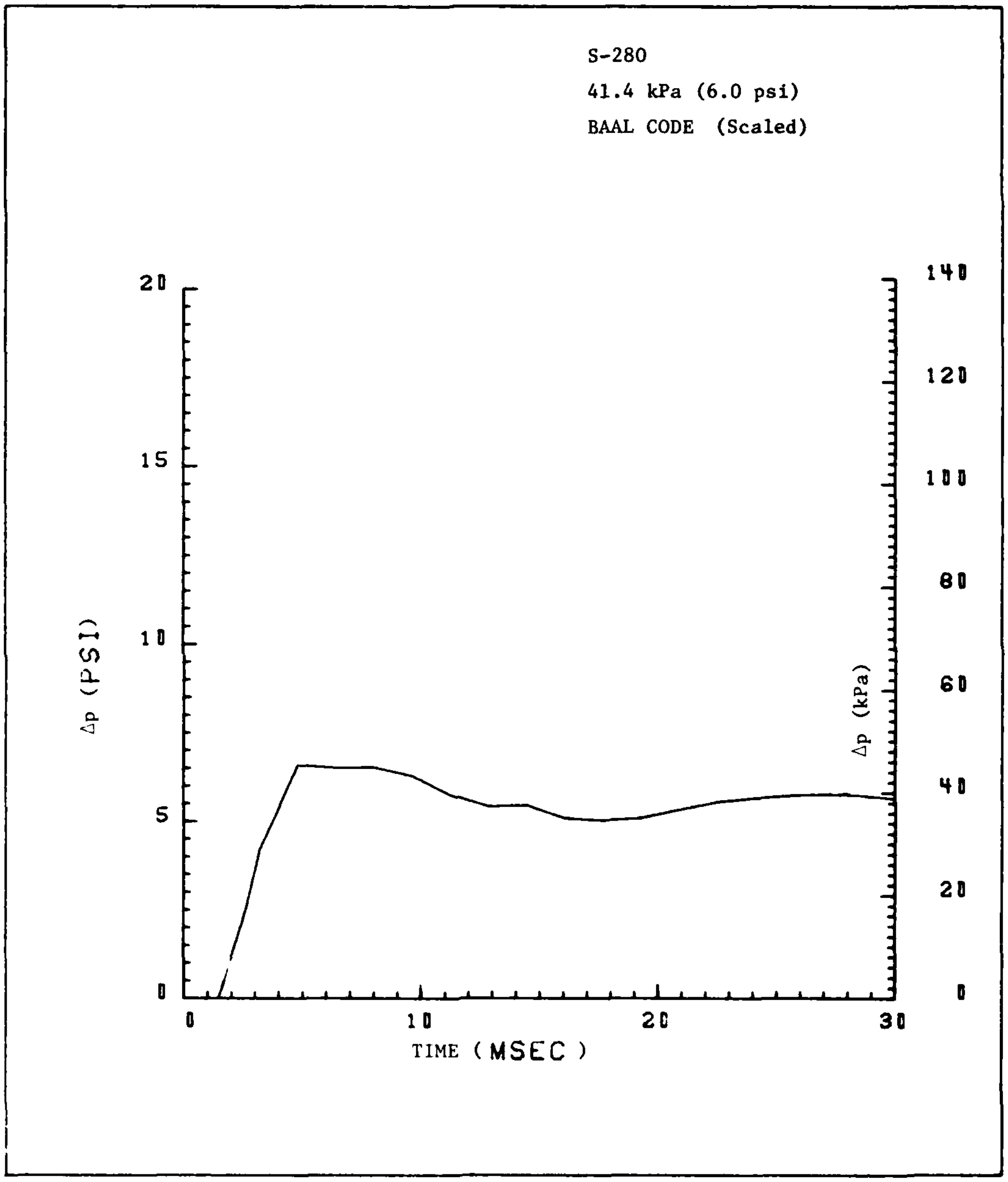

FIGURE 3.10. OVERPRESSURE NEAR CENTER OF S-280
FRONT END WALL

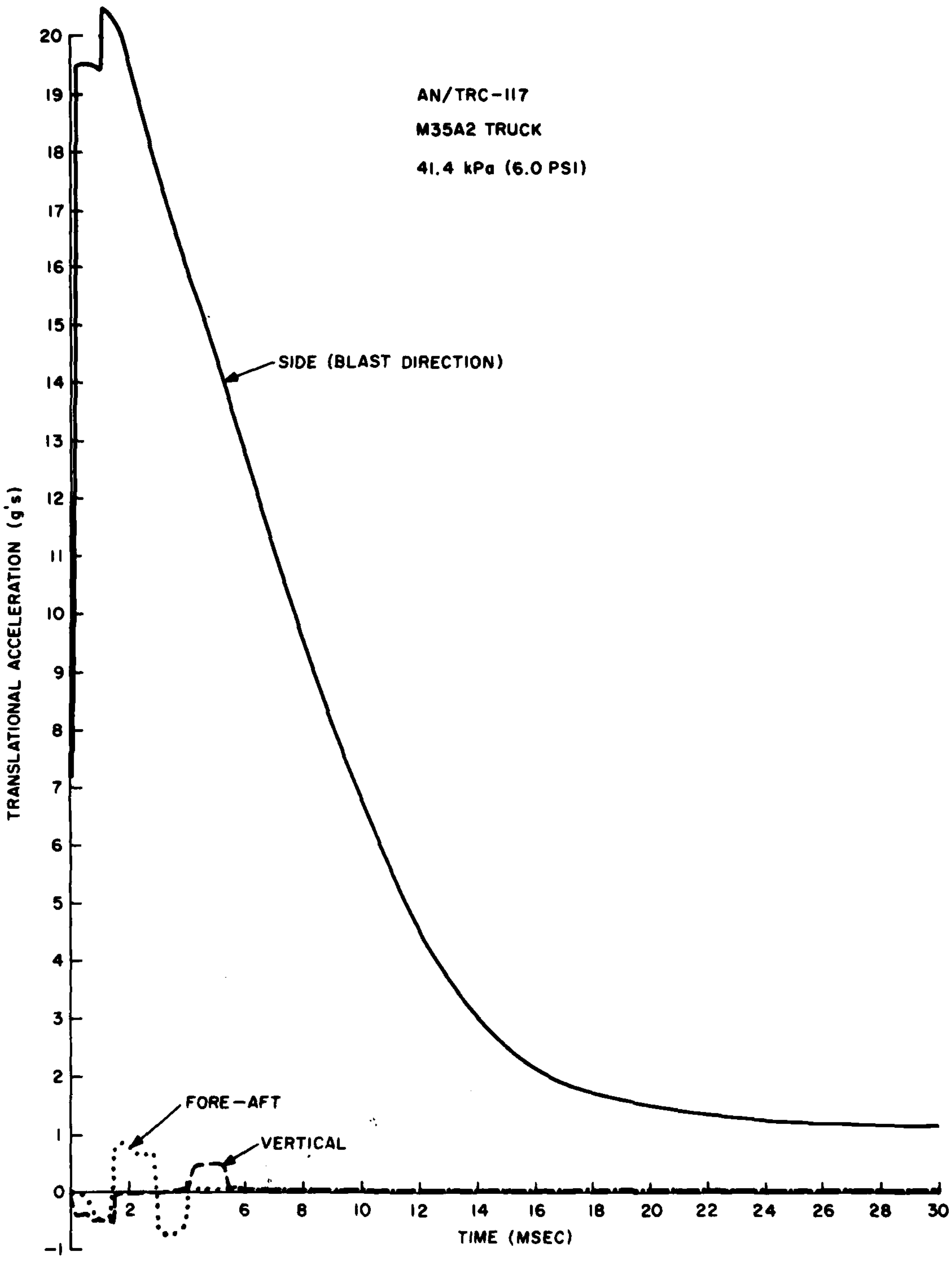

FIGURE 3.11. TRANSLATIONAL ACCELERATIONS OF AN/TRC-117 SYSTEM AT FLOOR CENTER (BASE MOTIONS)

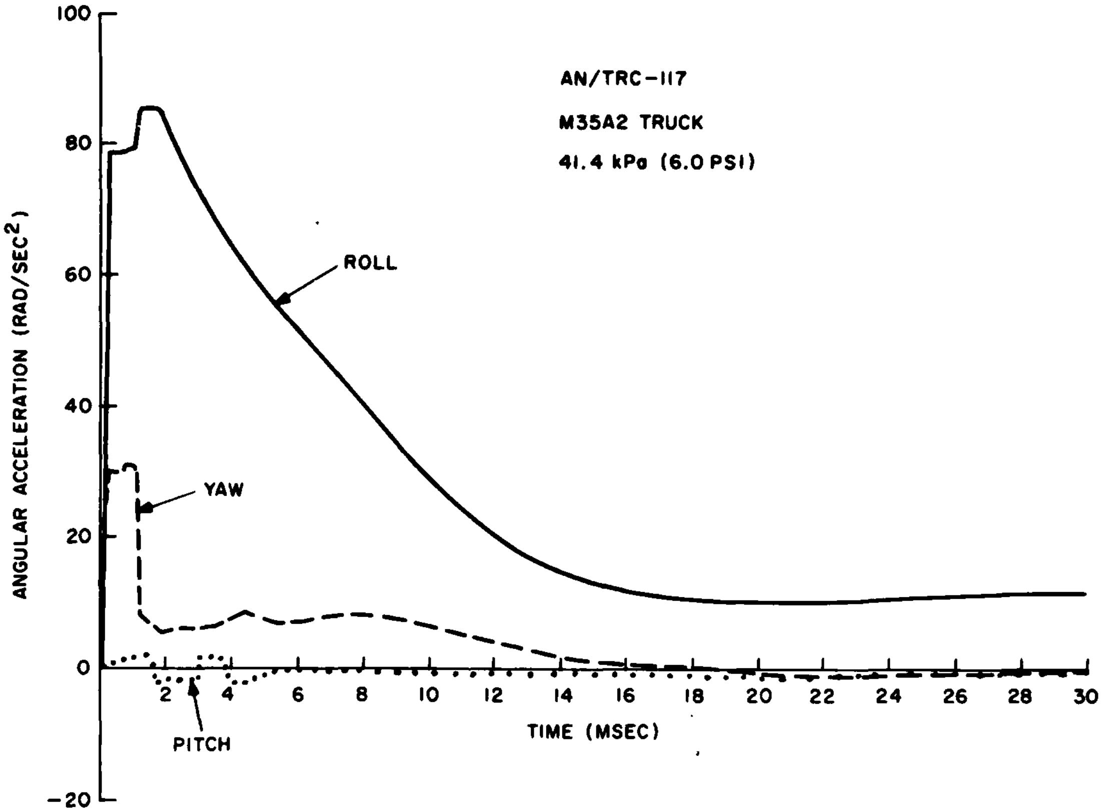

FIGURE 3.12. ANGULAR ACCELERATIONS OF AN/TRC-117 SYSTEM
(BASE MOTIONS)

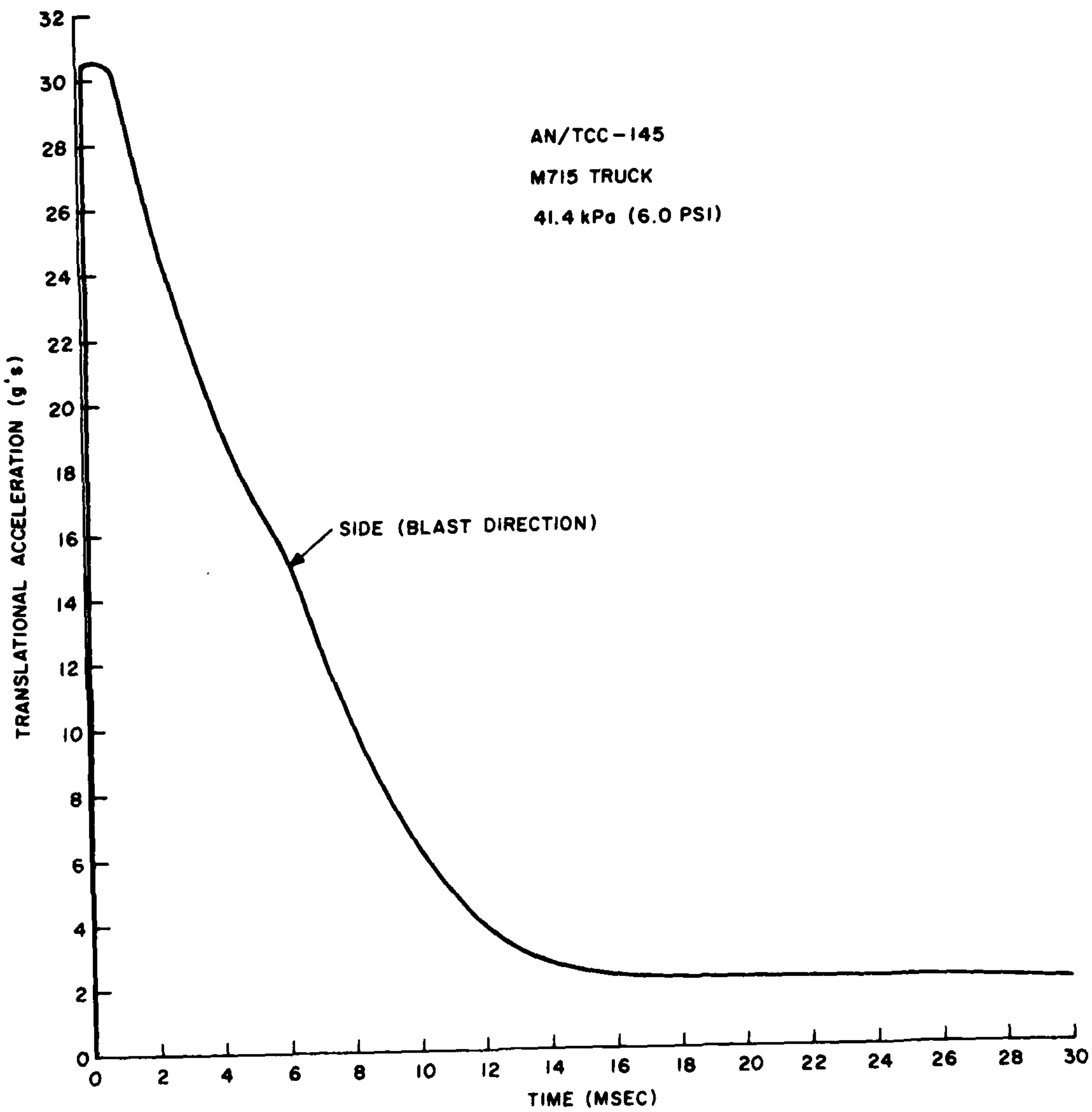

FIGURE 3.13. TRANSLATIONAL ACCELERATION OF AN/TRC-145 SYSTEM AT FLOOR CENTER (BASE MOTIONS)

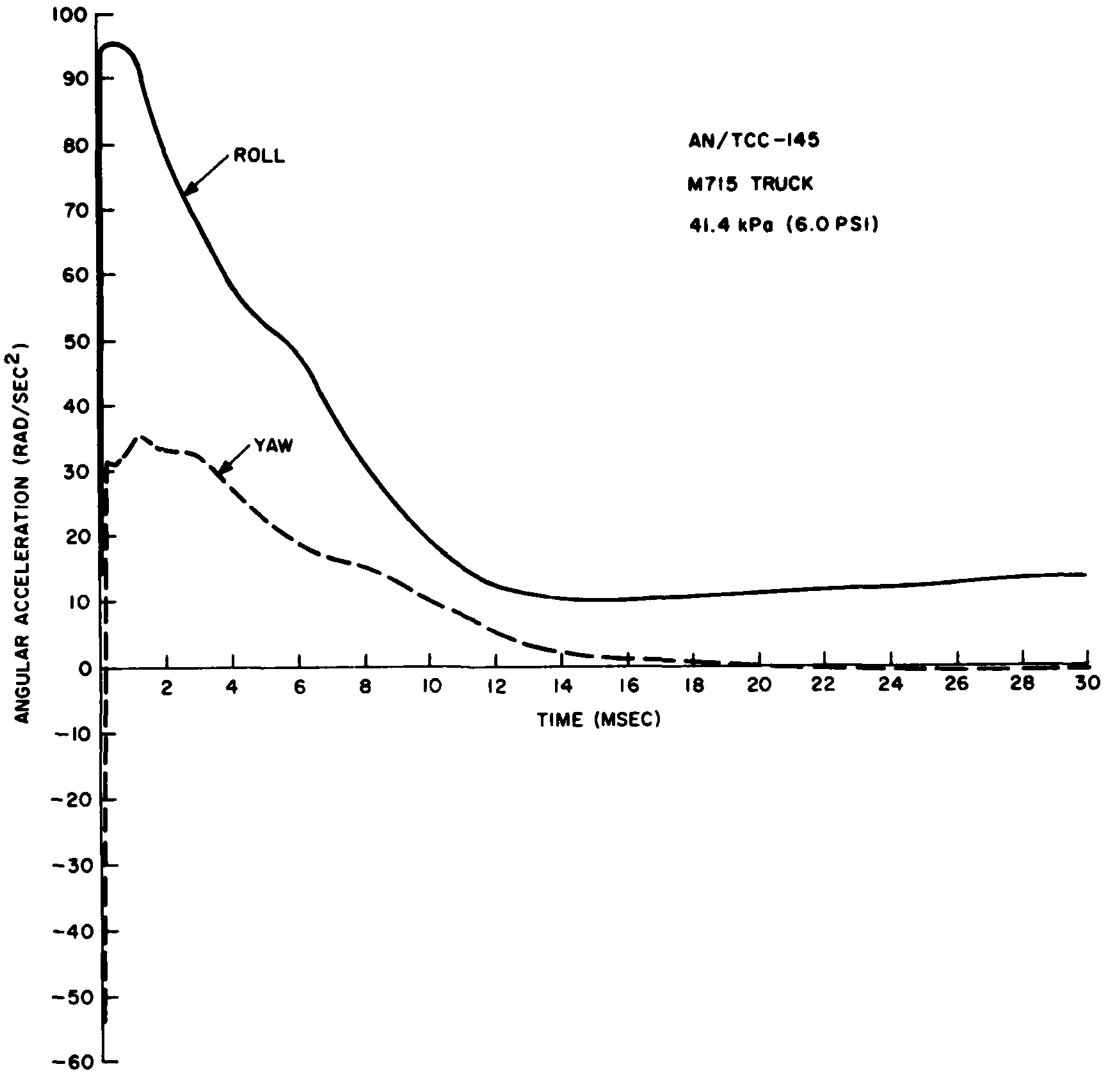

FIGURE 3.14. ANGULAR ACCELERATIONS OF AN/TRC SYSTEM
(BASE MOTIONS)

similar to the AN/TRC-117 system, their base responses will also be similar to the responses shown in Figs. 3.11 and 3.12. Only the base excitation in the blast direction was input to the NASTRAN models for each system since it was felt that it was the most important base motion response, possibly along with the roll acceleration, during the early-time structural response period of 30 msec.

The acceleration time histories of the three S-280 systems as obtained by NASTRAN are shown in Figs. 3.15-3.47 at several selected grid points on each shelter wall and also at grid points on the racks nearest the locations where accelerometers were mounted for the DICE THROW test. The corresponding base acceleration in the blast direction is given in Figs. 3.25, 3.36 and 3.47. Tables 3.2 and 3.3 may be referred to for gage designations and the approximate grid-point correspondence. In Figures 3.15-3.25, the responses for the AN/TRC-117 are also presented for the case where no base motion was applied to the system, i.e., the shelter base was constrained against all motion. It is seen that the inclusion of the base motion is generally unimportant during the early-time structural response of the system. If the roll acceleration were as important as the acceleration in the blast direction, the combined effect if both base accelerations were included would still be minor in Figs. 3.15-3.25.

3.3 S-250 SYSTEMS

Overpressure-time histories from the BAAL code were not available for use with the S-250 shelter as they were for the S-280 systems. Therefore, the S-250 shelter loading was determined with the overpressure code SHELTR (option Method 1), which is described in Section 5 of Ref. 6. The preprocessor NALO was used with the SHELTR code to provide NASTRAN loading tables for the AN/TRC-145 in a manner similar to that used for the BAAL code. Figures 3.48-3.54 show the structural acceleration time histories for the AN/TRC-145 and also for the hardened AN/TRC-145 at an overpressure of 7.3 psi (50.3kPa). Appendix B presents additional response plots for the AN/TRC-145 at overpressure levels of 34.5 kPa and 20.7 kPa.

3.4 COMPARISONS WITH TEST MEASUREMENTS

Two cases from Table 3.1 were selected for comparison with measured acceleration data from the DICE THROW test. These were the AN/TRC-117 and the AN/TRC-145, each at an overpressure level of 6.0 psi (41.4 kPa). For consistency, each system used the blast loading as determined by the overpressure model programmed in the TRUCK code. As with the other overpressure models, BAAL and SHELTR mentioned earlier, the preprocessor NALO was used with the TRUCK overpressure model to determine the NASTRAN grid-point loading tables for each system. Each system was also subjected to the base motion in the blast direction as determined by the TRUCK

Reference 7. Calligeros, John M., and Walsh, John P., Finite Element Modeling of Army Electronic Equipment Shelters Subjected to Blast Loading, BRL CR 281, Dec. 1975. (AD#B008904L)

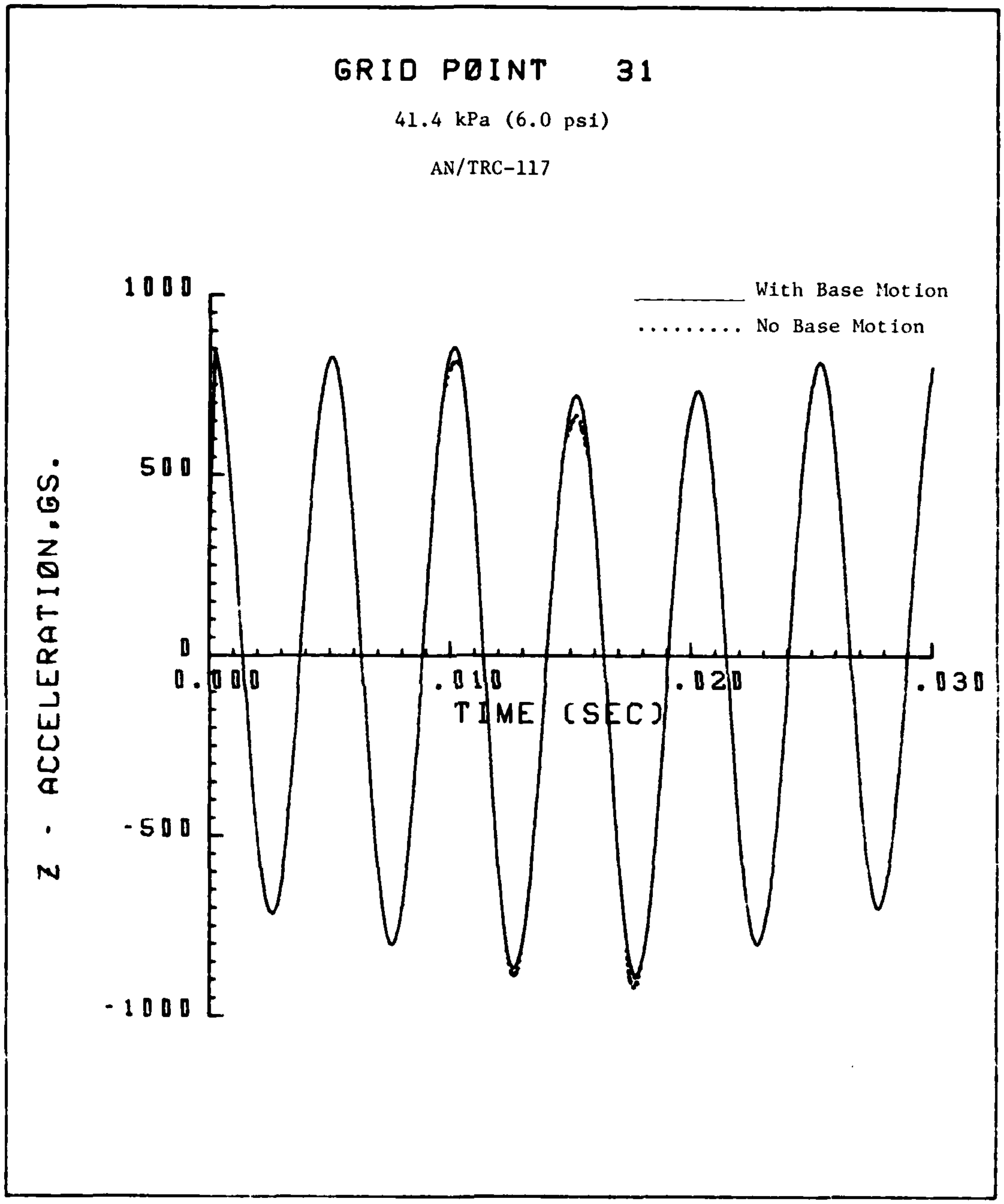

FIGURE 3.15. ACCELERATION TIME HISTORY IN BLAST DIRECTION, NEAR CENTER OF ROADSIDE WALL (NASTRAN)

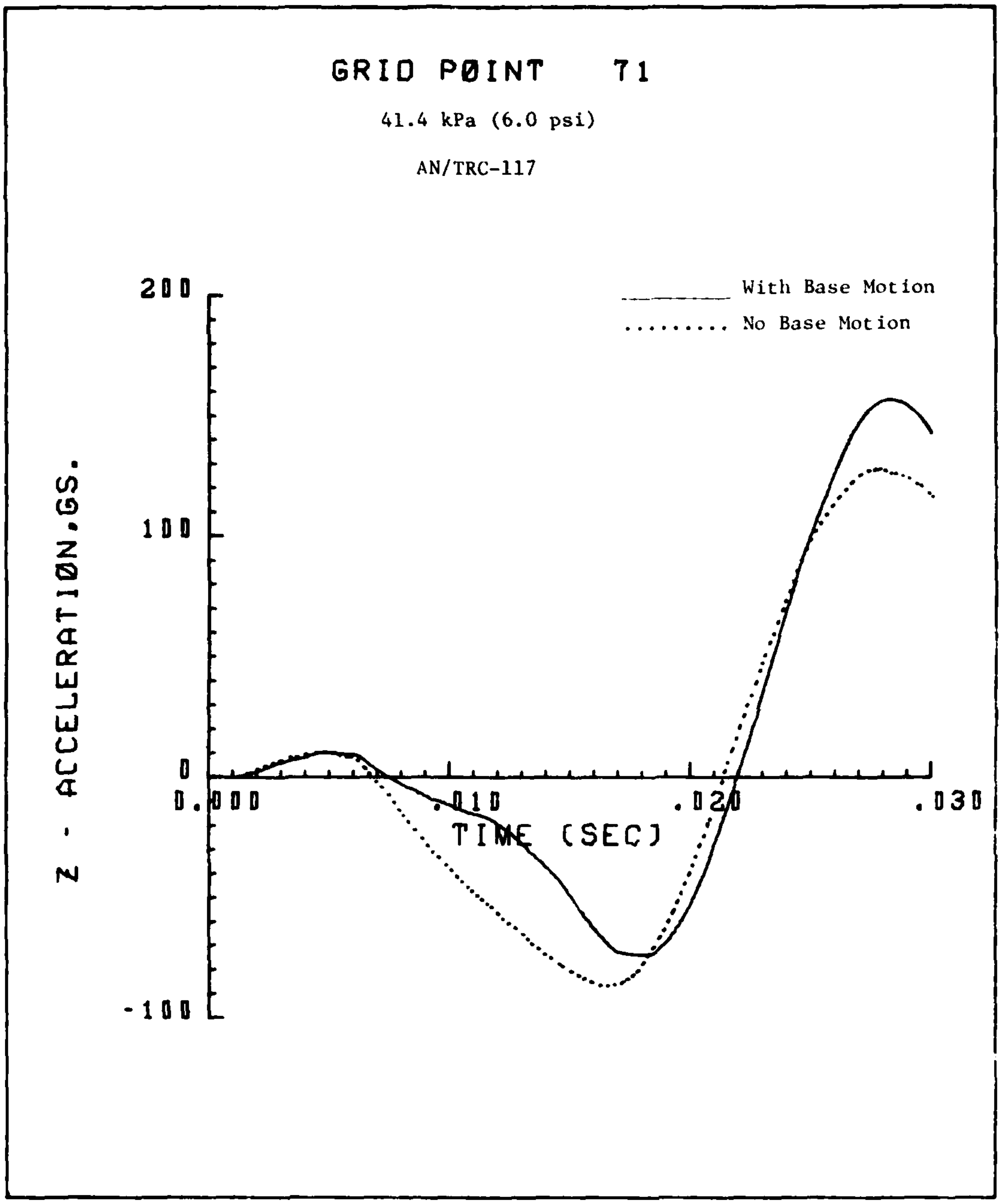

FIGURE 3.16. ACCELERATION TIME HISTORY, IN BLAST DIRECTION, NEAR CENTER OF CURBSIDE WALL (NASTRAN)

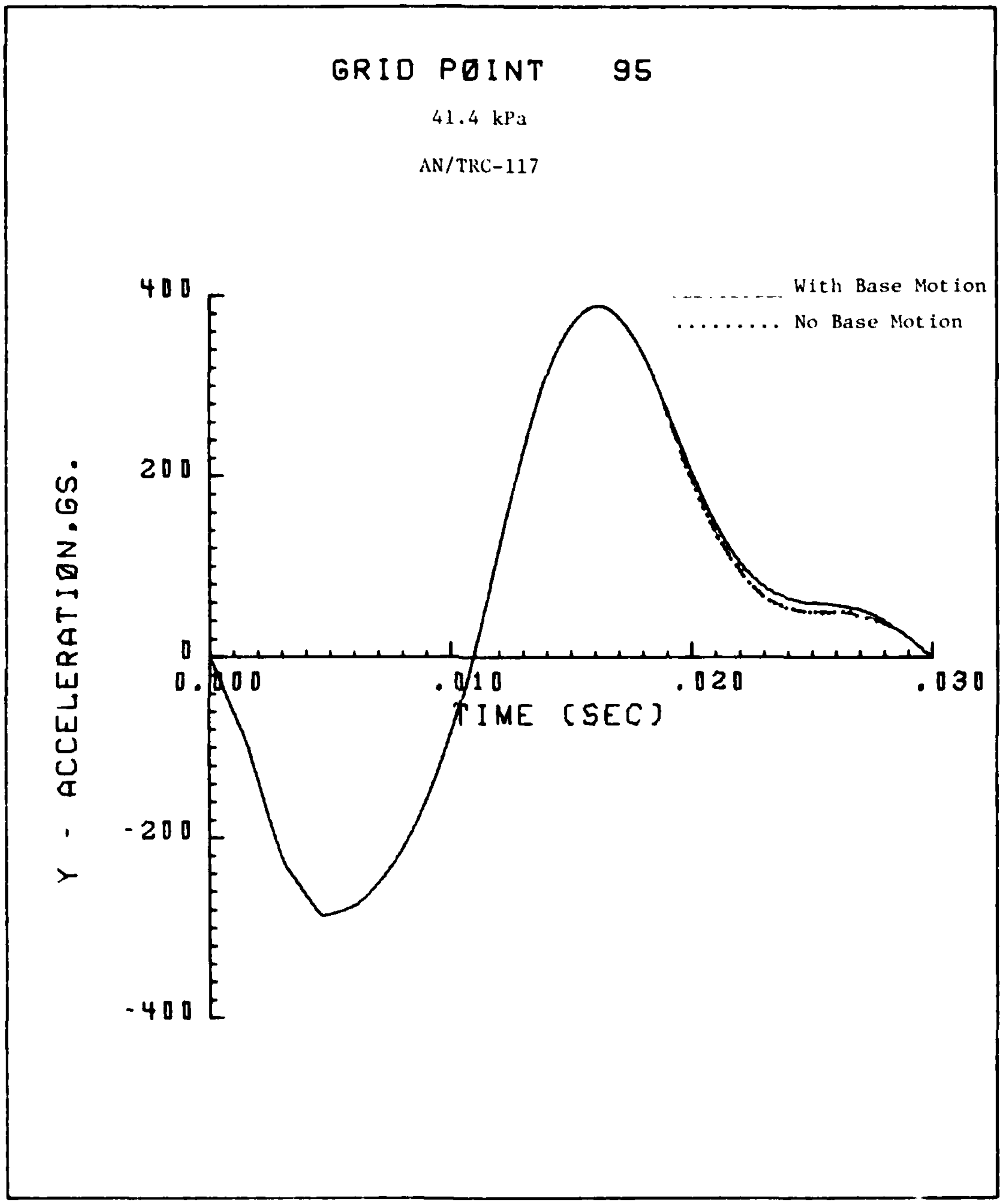

FIGURE 3.17. VERTICAL ACCELERATION TIME HISTORY, NEAR CENTER OF ROOF (NASTRAN)

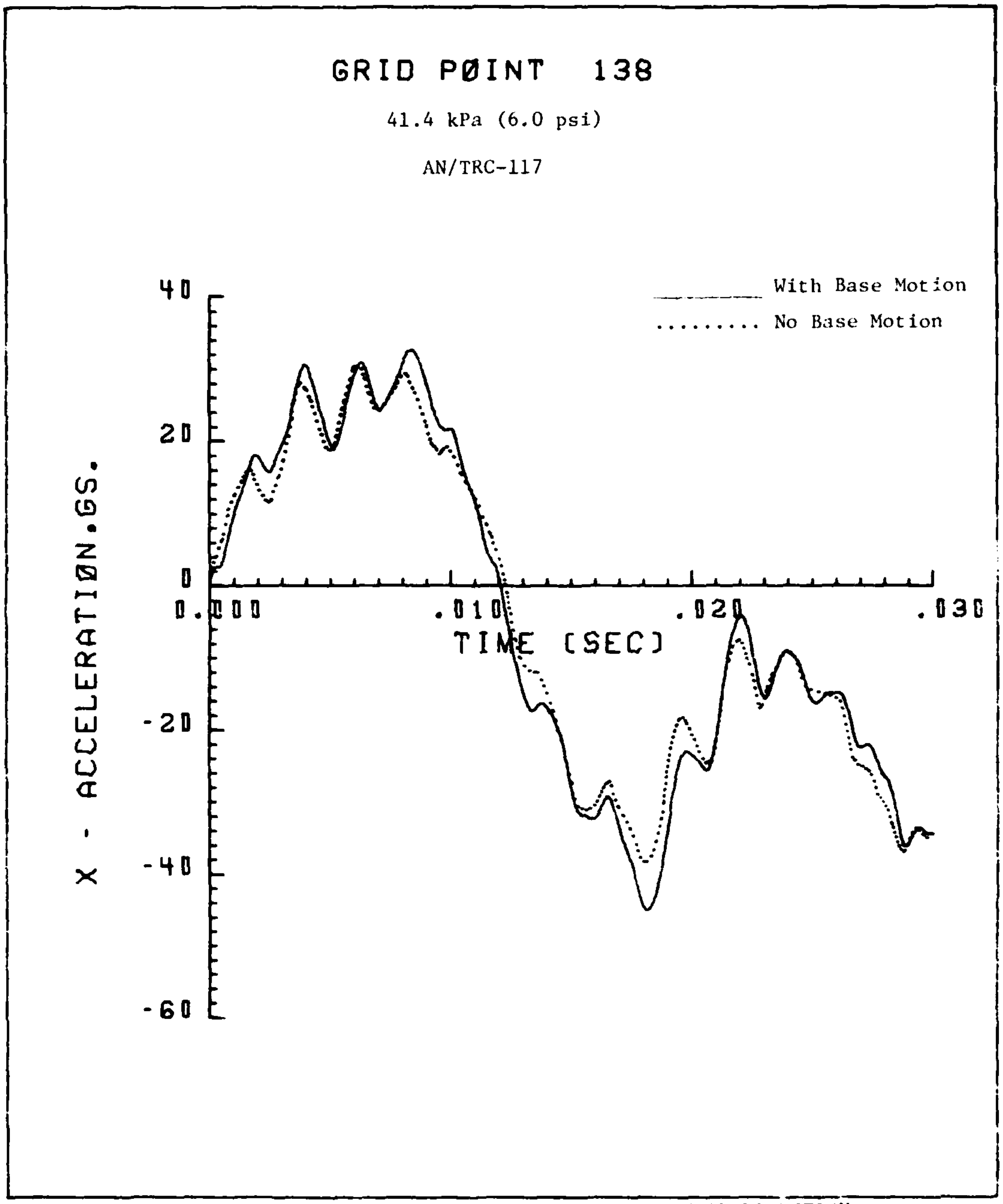

FIGURE 3.18 ACCELERATION TIME HISTORY IN HORIZONTAL DIRECTION, END WALL (NASTRAN)

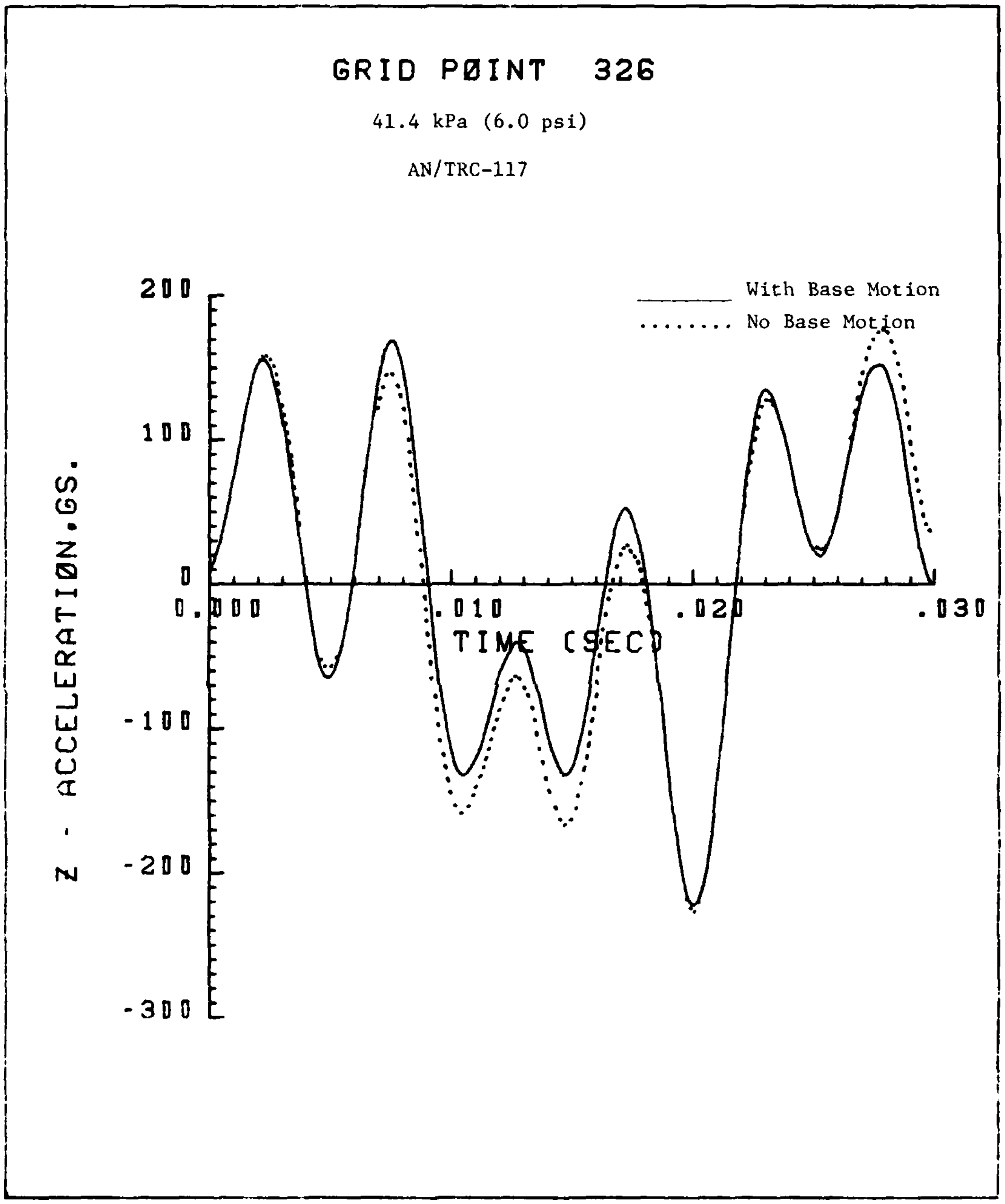

FIGURE 3.19. ACCELERATION TIME HISTORY IN BLAST DIRECTION, ROADSIDE RACK (NASTRAN)

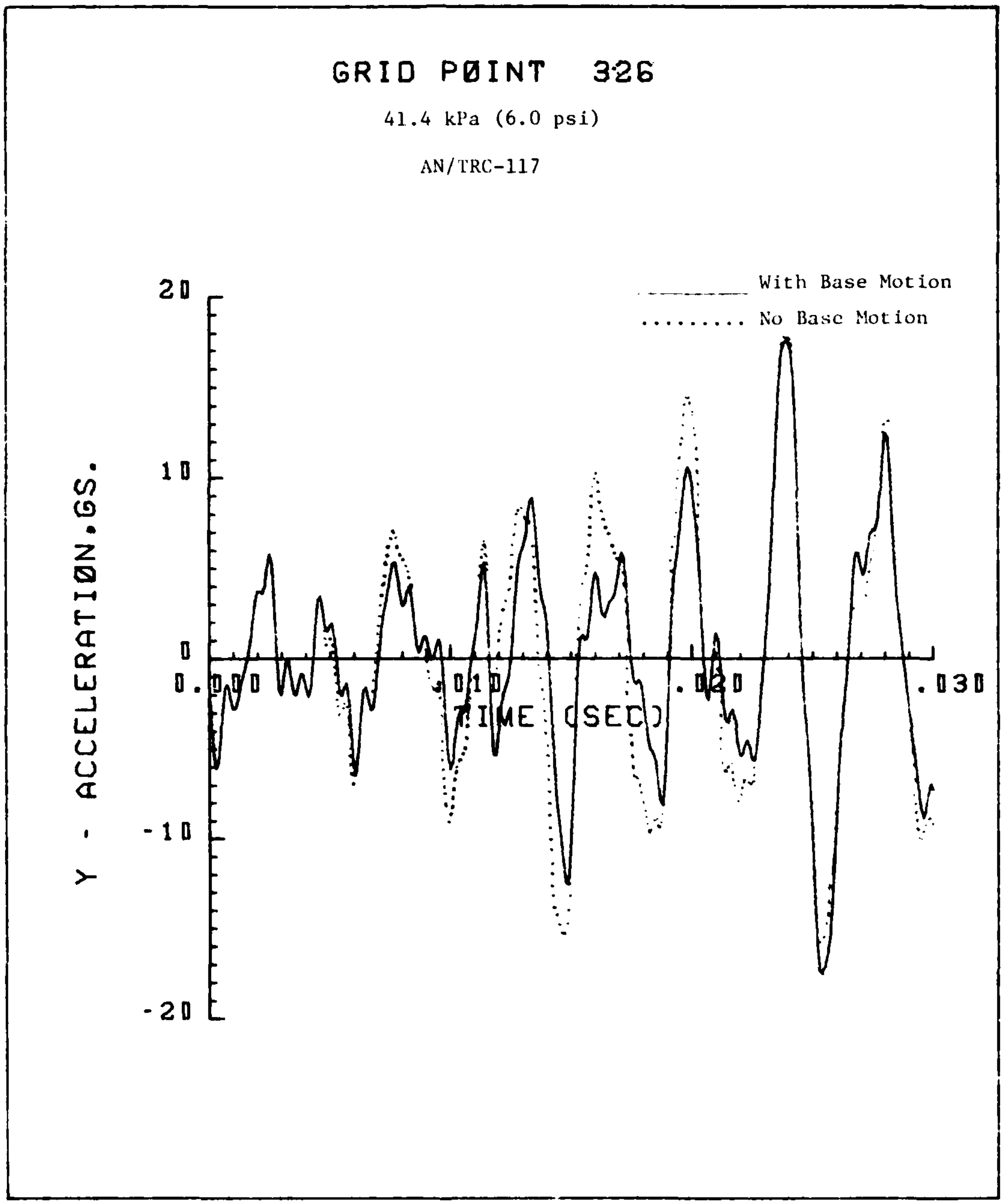

FIGURE 3.20. VERTICAL ACCELERATION TIME HISTORY, ROADSIDE RACK (NASTRAN)

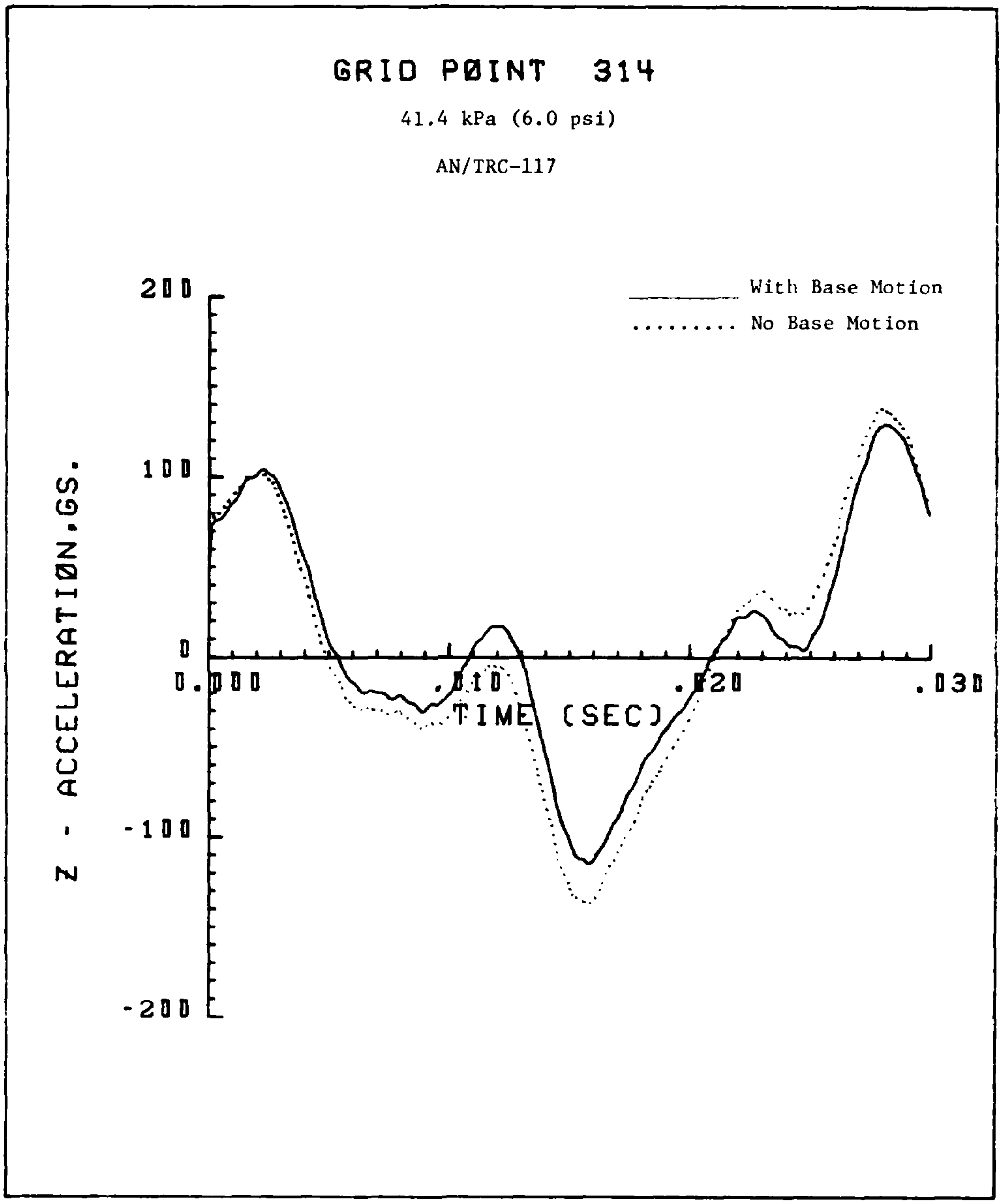

FIGURE 3.21. ACCELERATION TIME HISTORY IN BLAST DIRECTION, ROADSIDE RACK (NASTRAN)

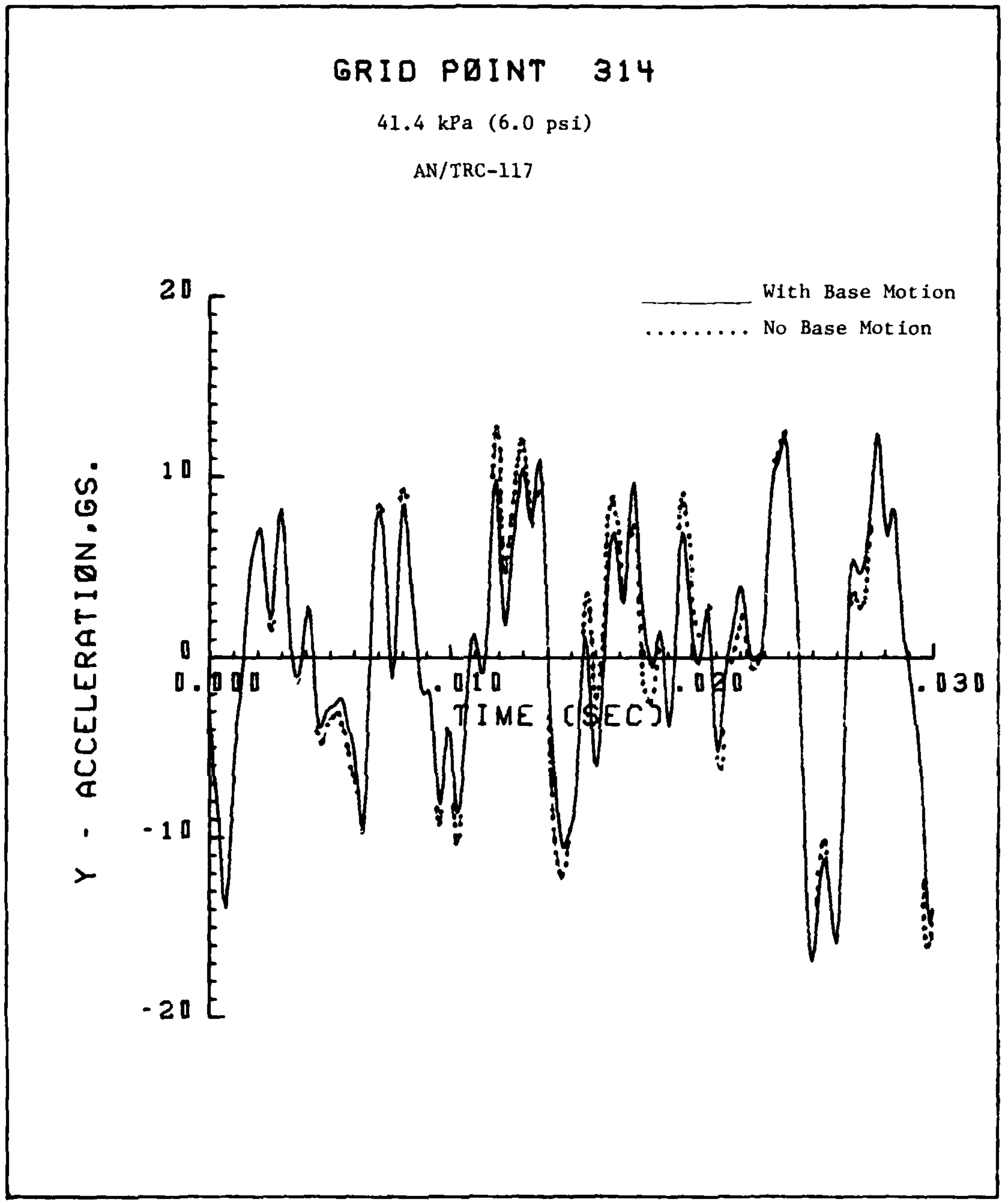

FIGURE 3.22. VERTICAL ACCELERATION TIME HISTORY
ROADSIDE RACK (NASTRAN)

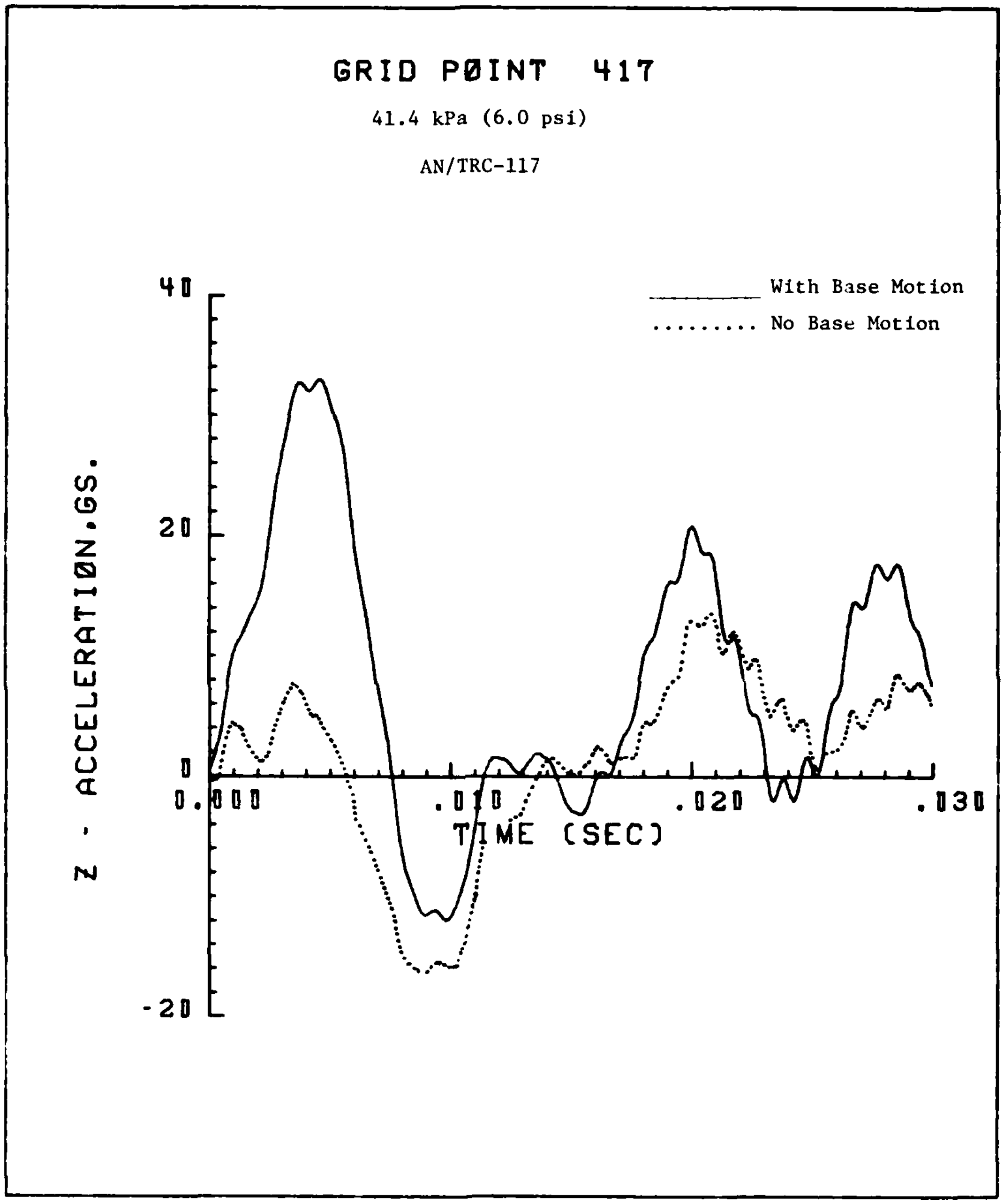

FIGURE 3.23. ACCELERATION TIME HISTORY IN BLAST DIRECTION, FRONT END RACK (NASTRAN)

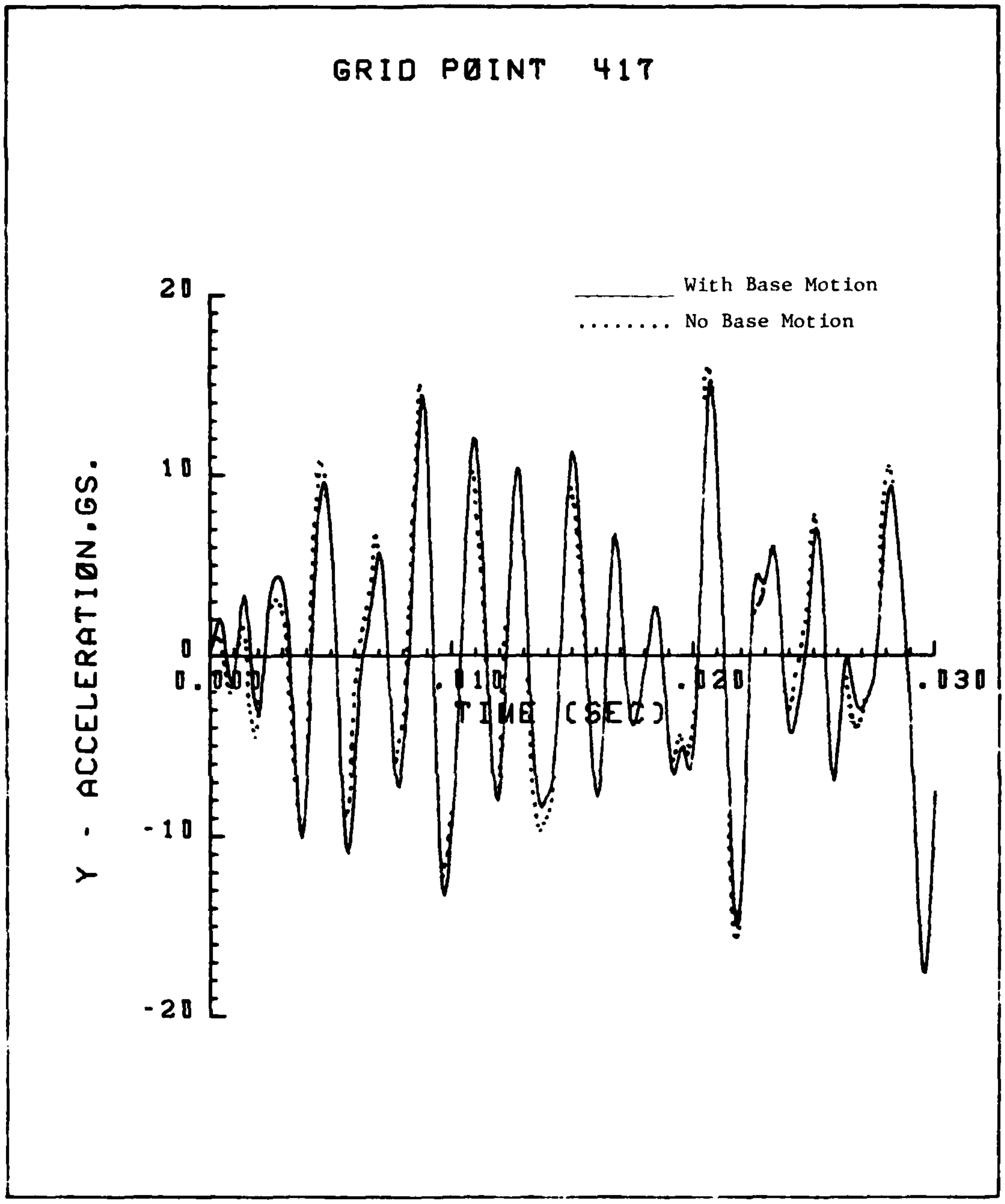

FIGURE 3.24. VERTICAL ACCELERATION TIME HISTORY, FRONT END RACK (NASTRAN)

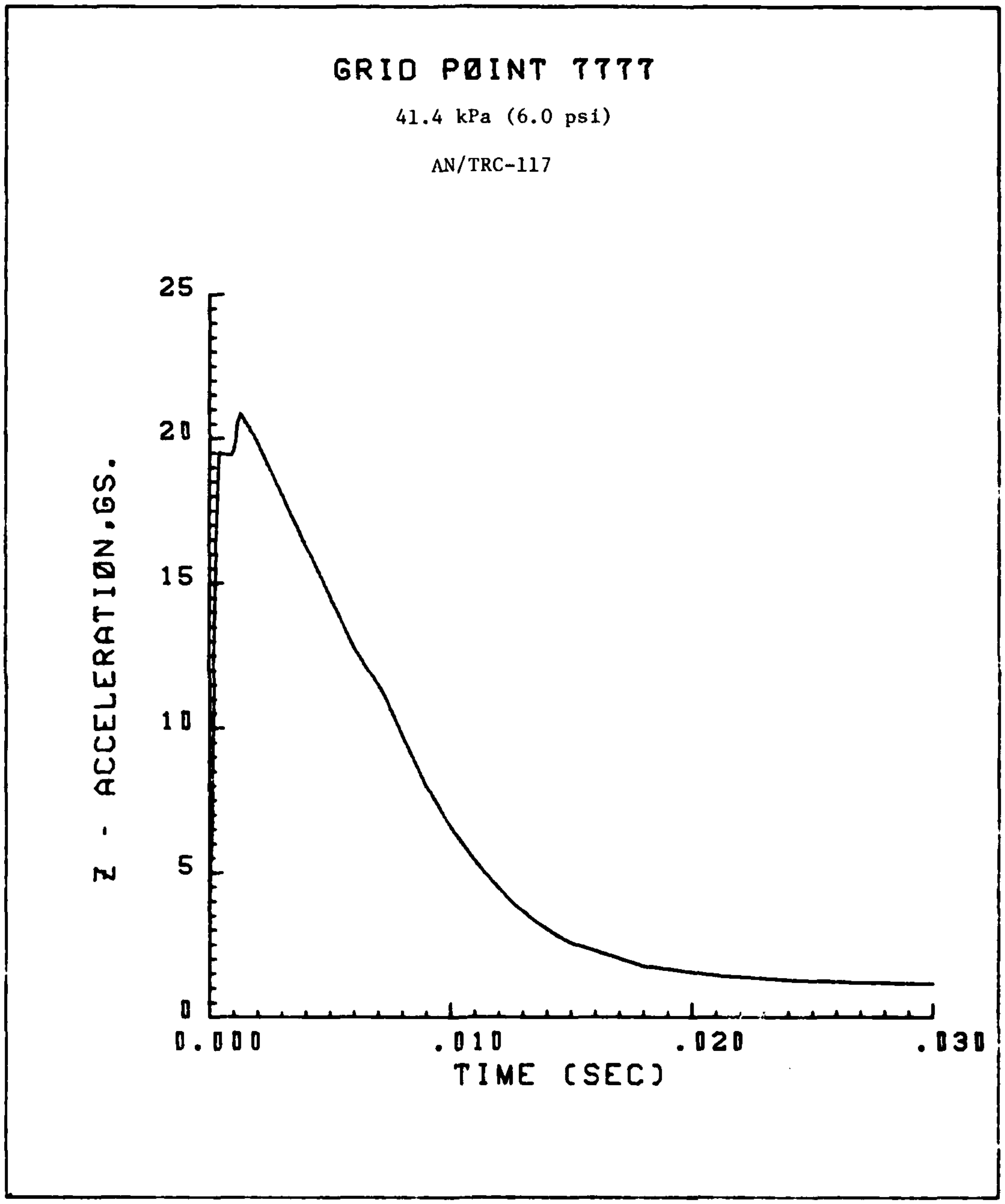

FIGURE 3.25. RIGID BODY ACCELERATION TIME HISTORY IN BLAST DIRECTION, CENTER OF FLOOR (NASTRAN)

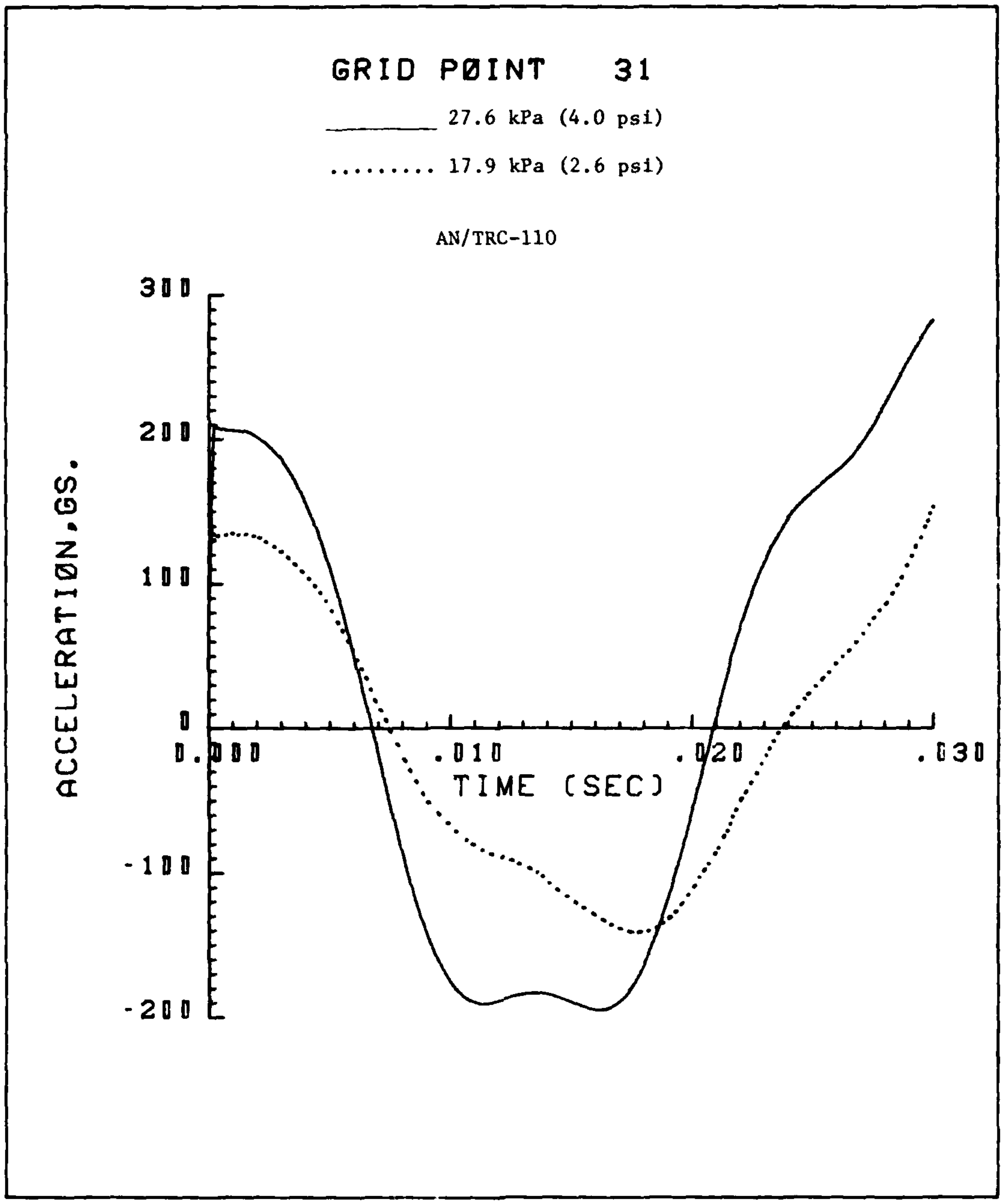

FIGURE 3.26. ACCELERATION TIME HISTORY IN BLAST DIRECTION, NEAR CENTER OF ROADSIDE WALL (NASTRAN)

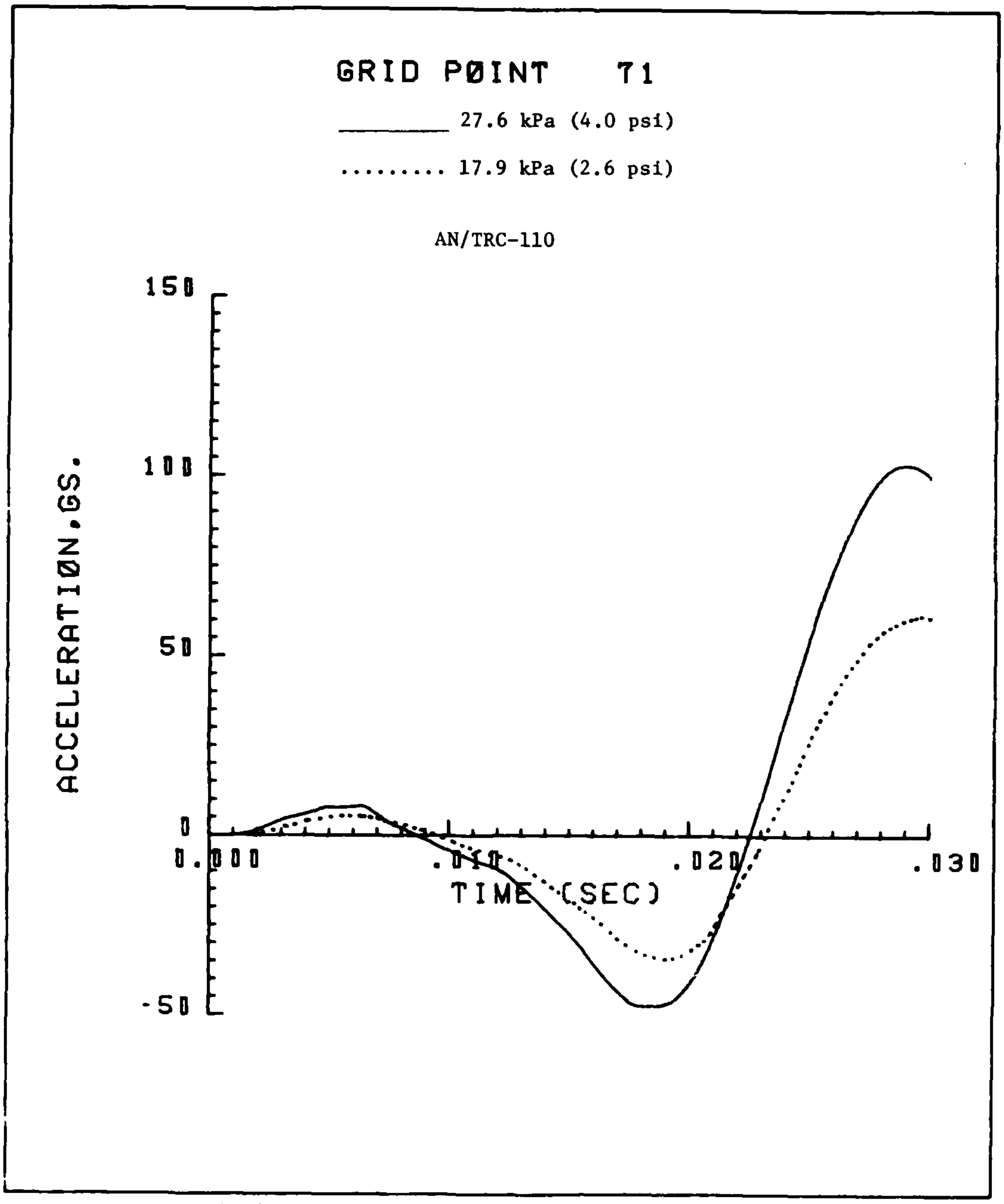

FIGURE 3.27 ACCELERATION TIME HISTORY IN BLAST DIRECTION, NEAR CENTER OF CURBSIDE WALL (NASTRAN)

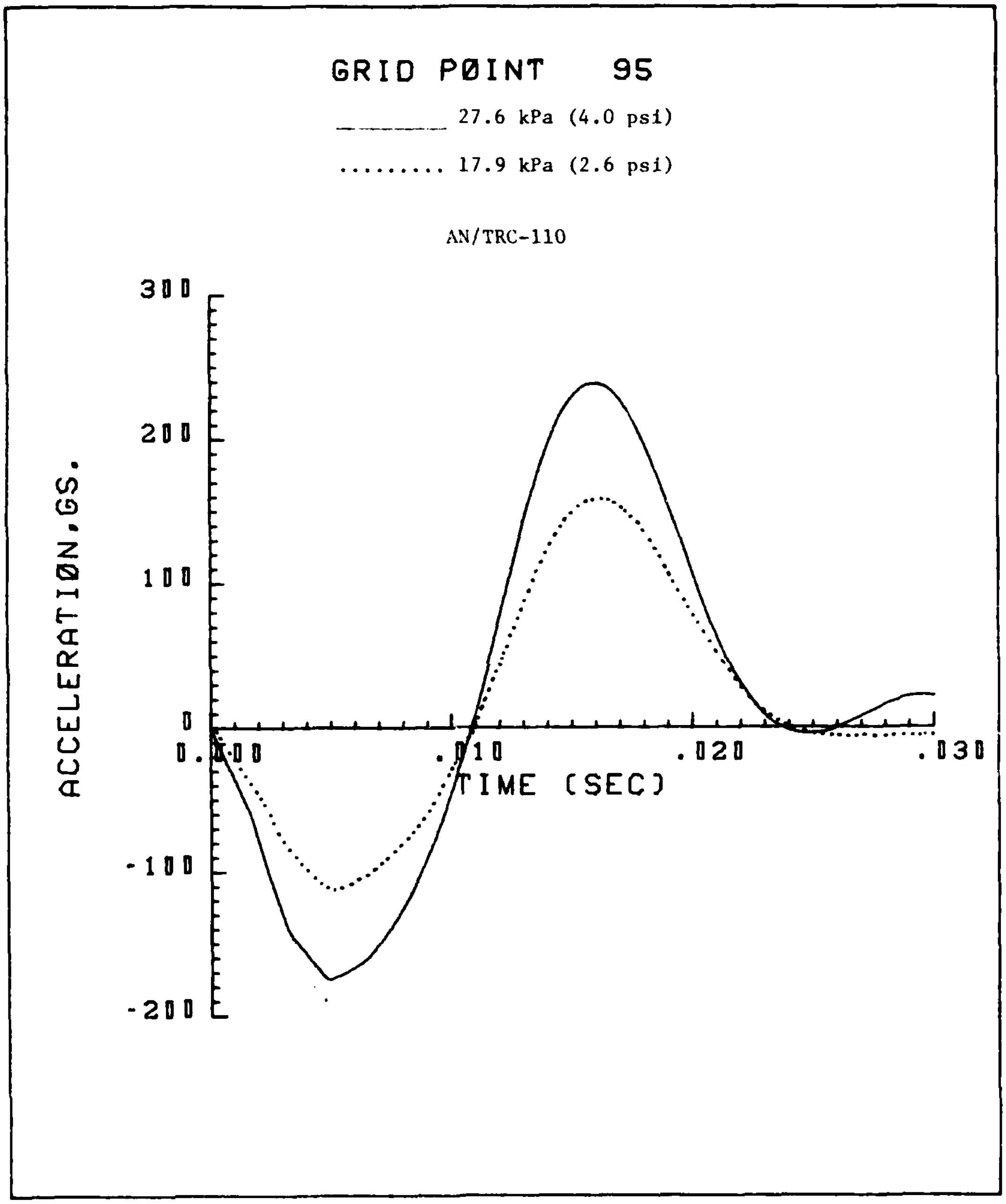

FIGURE 3.28 VERTICAL ACCELERATION TIME HISTORY, NEAR CENTER OF ROOF (NASTRAN)

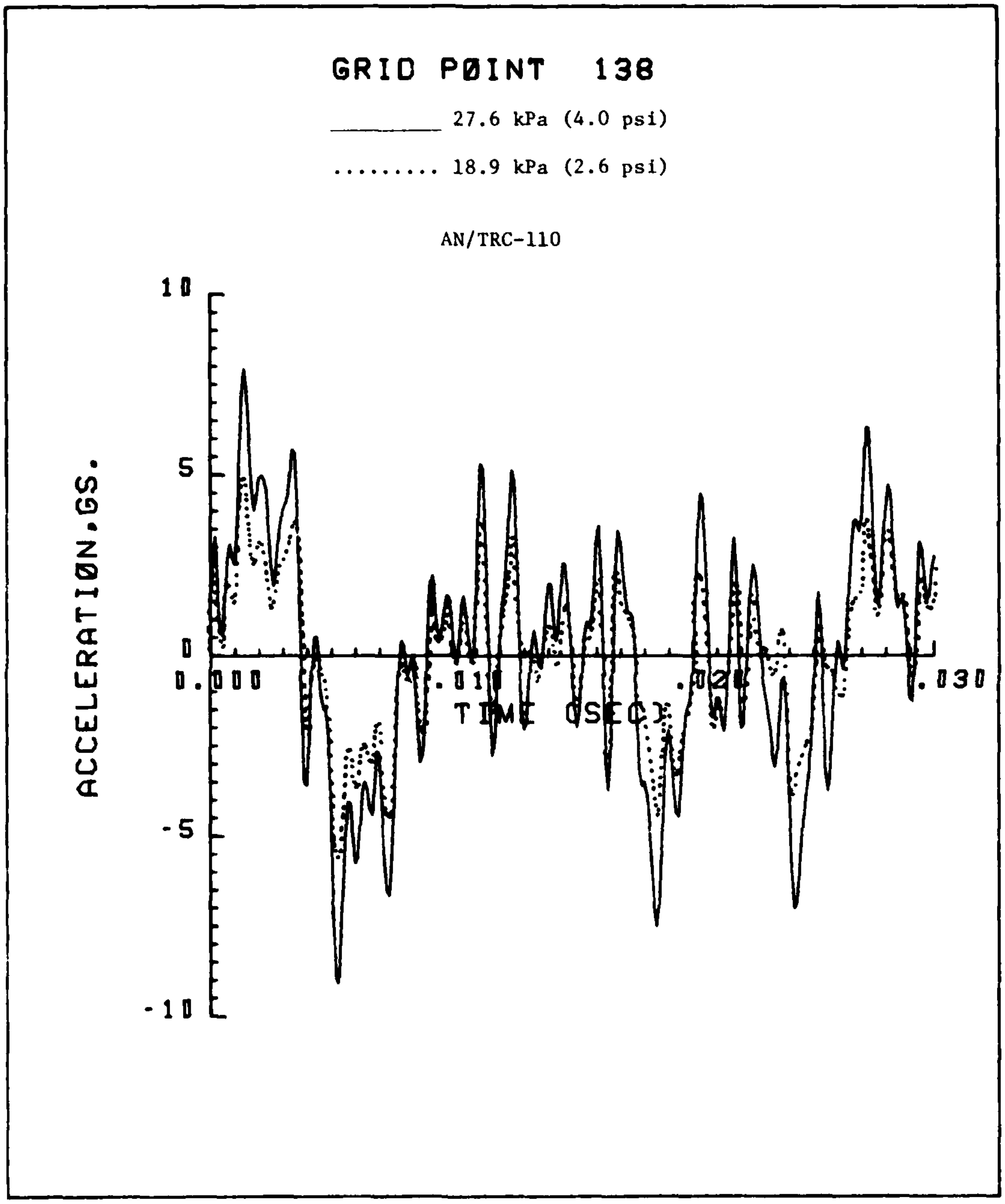

FIGURE 3.29 ACCELERATION TIME HISTORY IN HORIZONTAL DIRECTION, END WALL (NASTRAN)

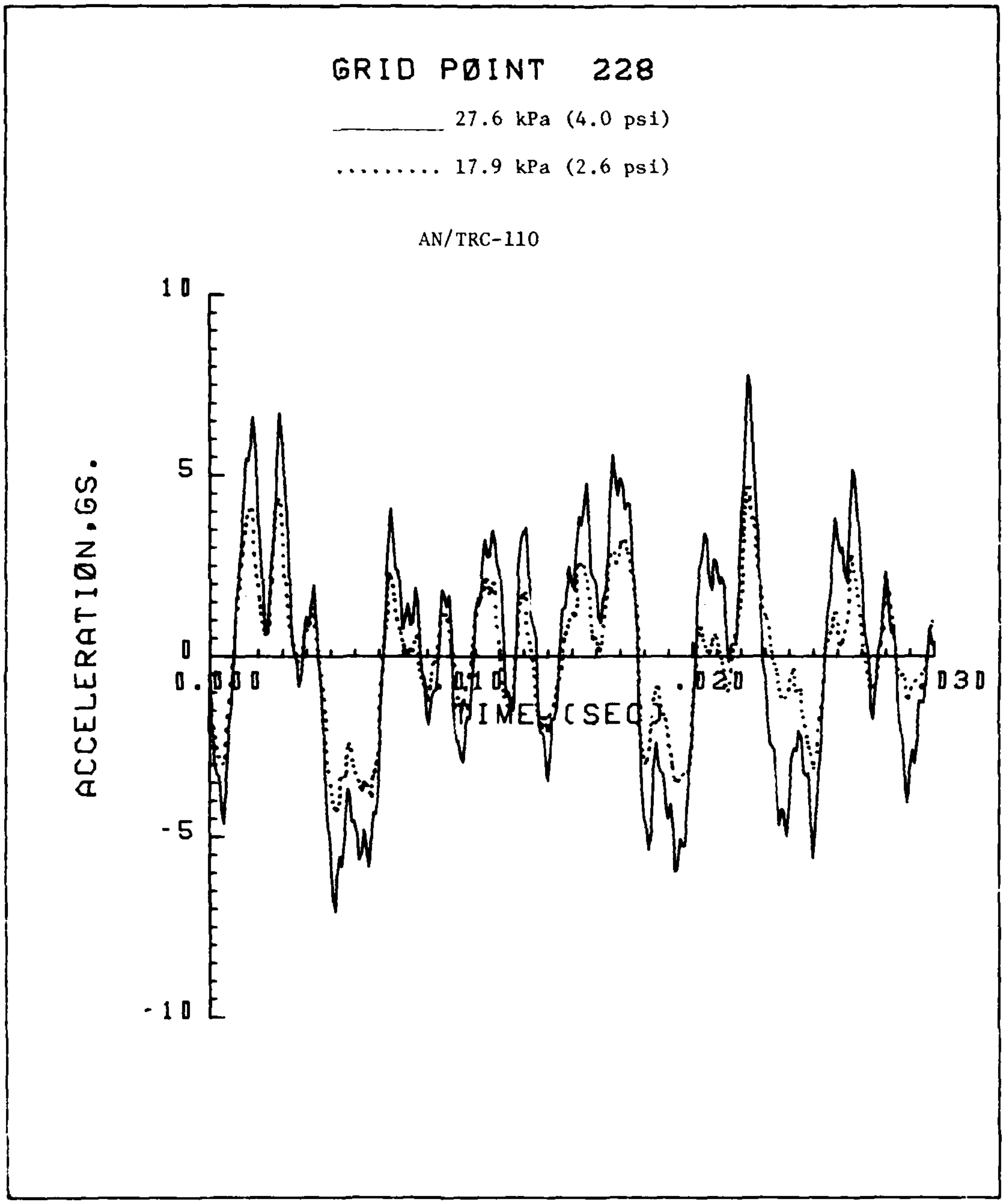

FIGURE 3.30 ACCELERATION TIME HISTORY IN BLAST DIRECTION, FRONT END RACK (NASTRAN)

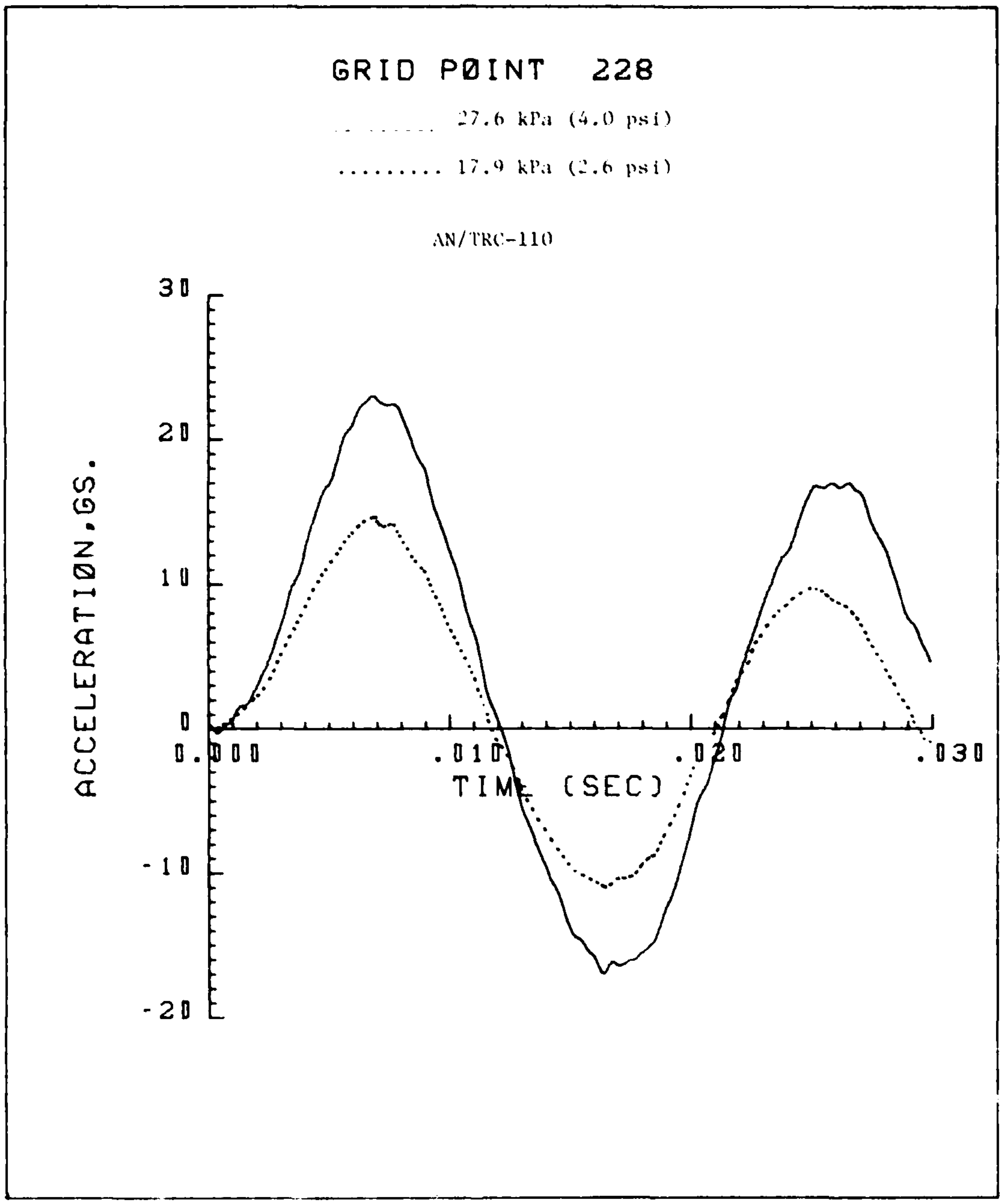

FIGURE 3.31. VERTICAL ACCELERATION TIME HISTORY, FRONT END RACKS (NASTRAN)

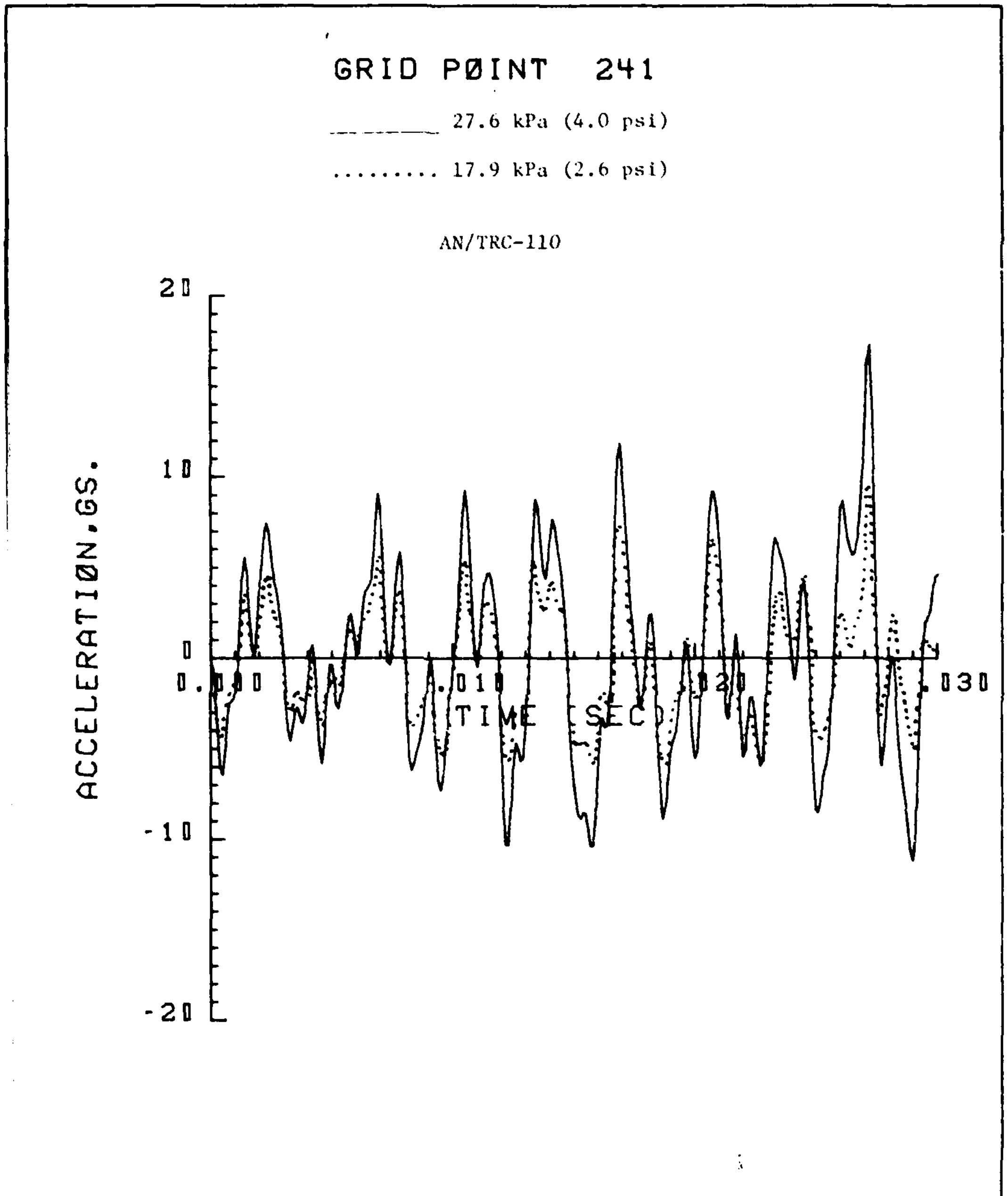

FIGURE 3.32. ACCELERATION TIME HISTORY IN BLAST DIRECTION, FRONT END RACK (NASTRAN)

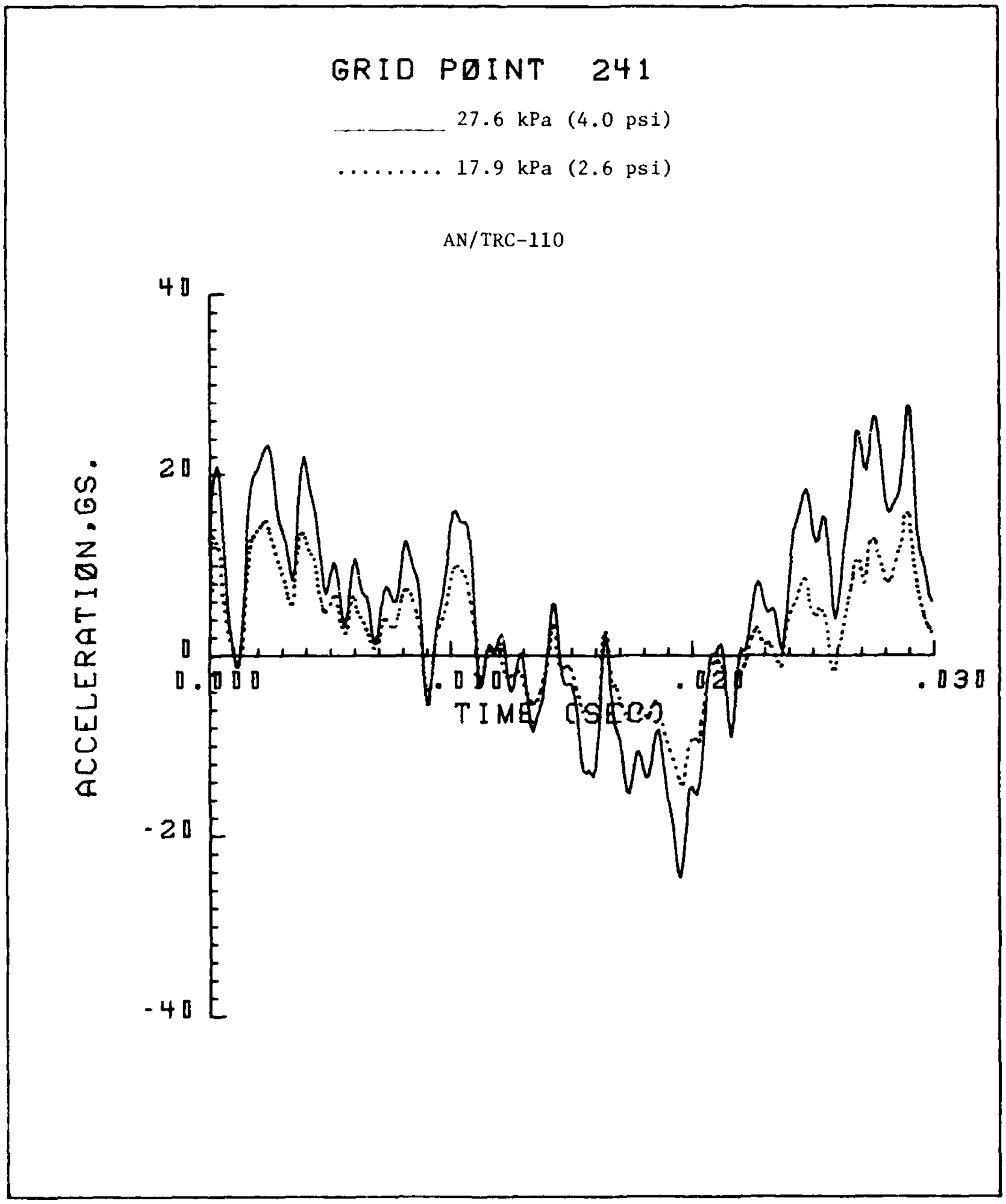

FIGURE 3.33. VERTICAL ACCELERATION TIME HISTORY, FRONT END RACK (NASTRAN)

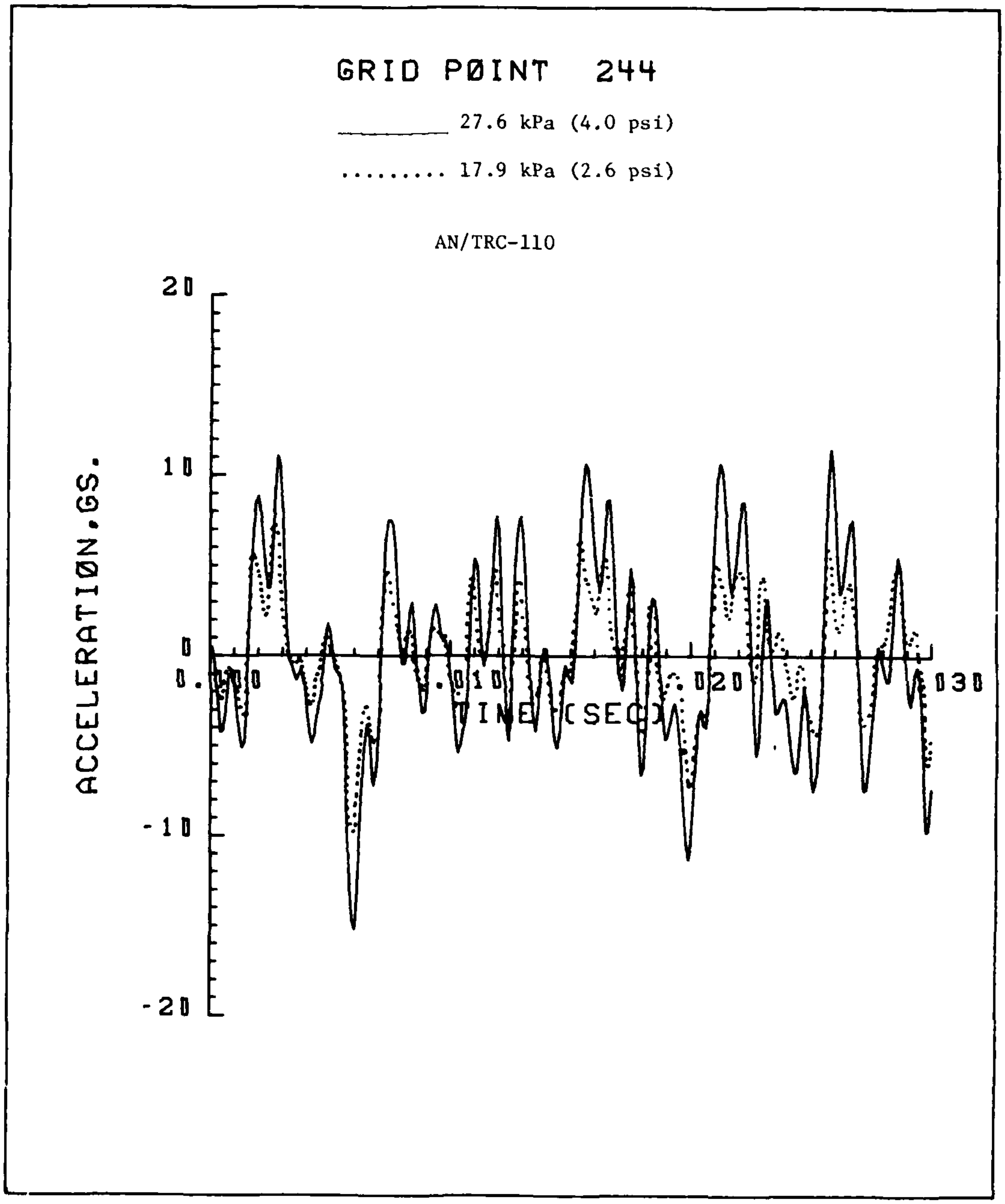

FIGURE 3.34. ACCELERATION TIME HISTORY IN BLAST DIRECTION, FRONT END RACK (NASTRAN)

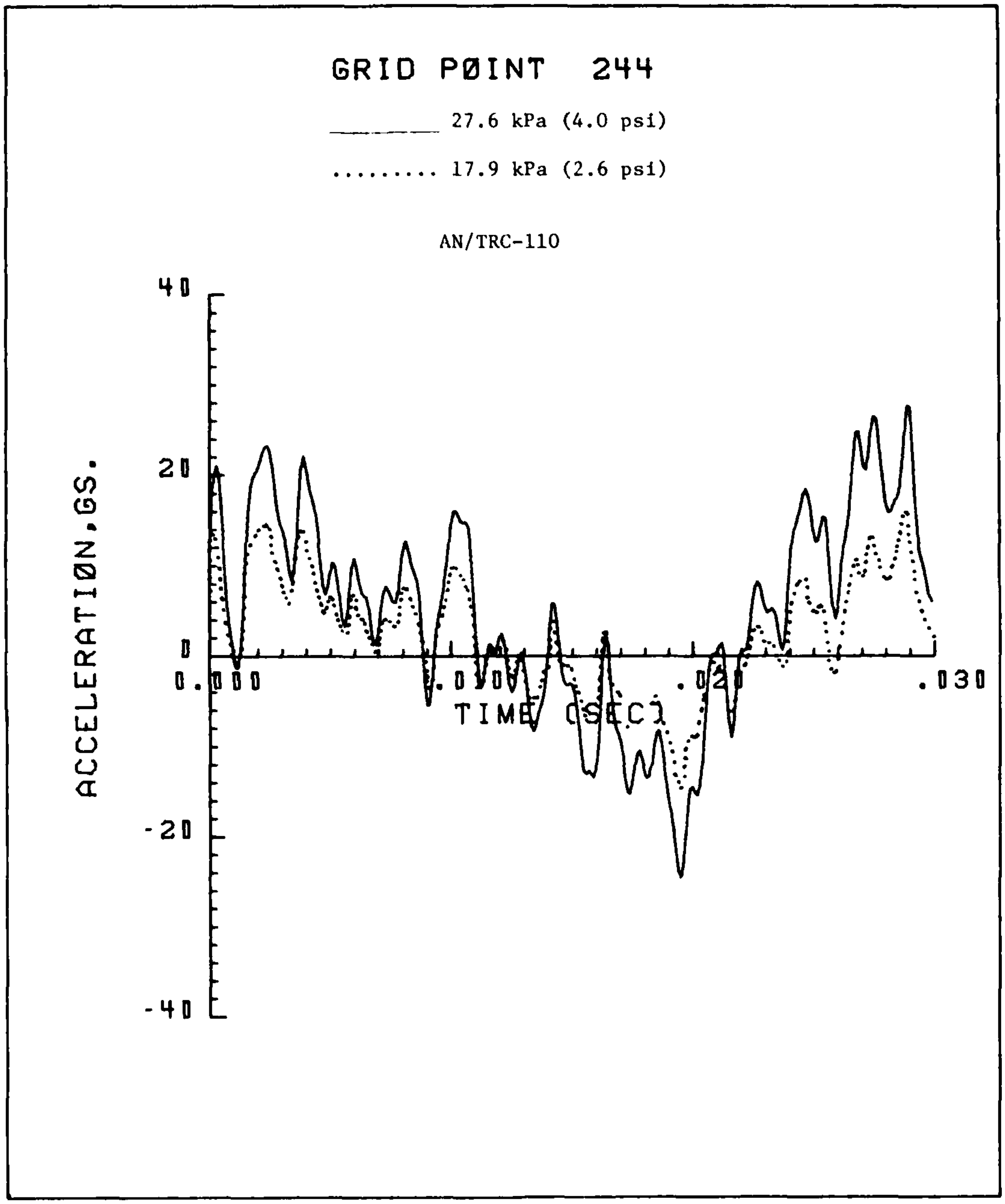

FIGURE 3.35. VERTICAL ACCELERATION TIME HISTORY,
FRONT END RACK (NASTRAN)

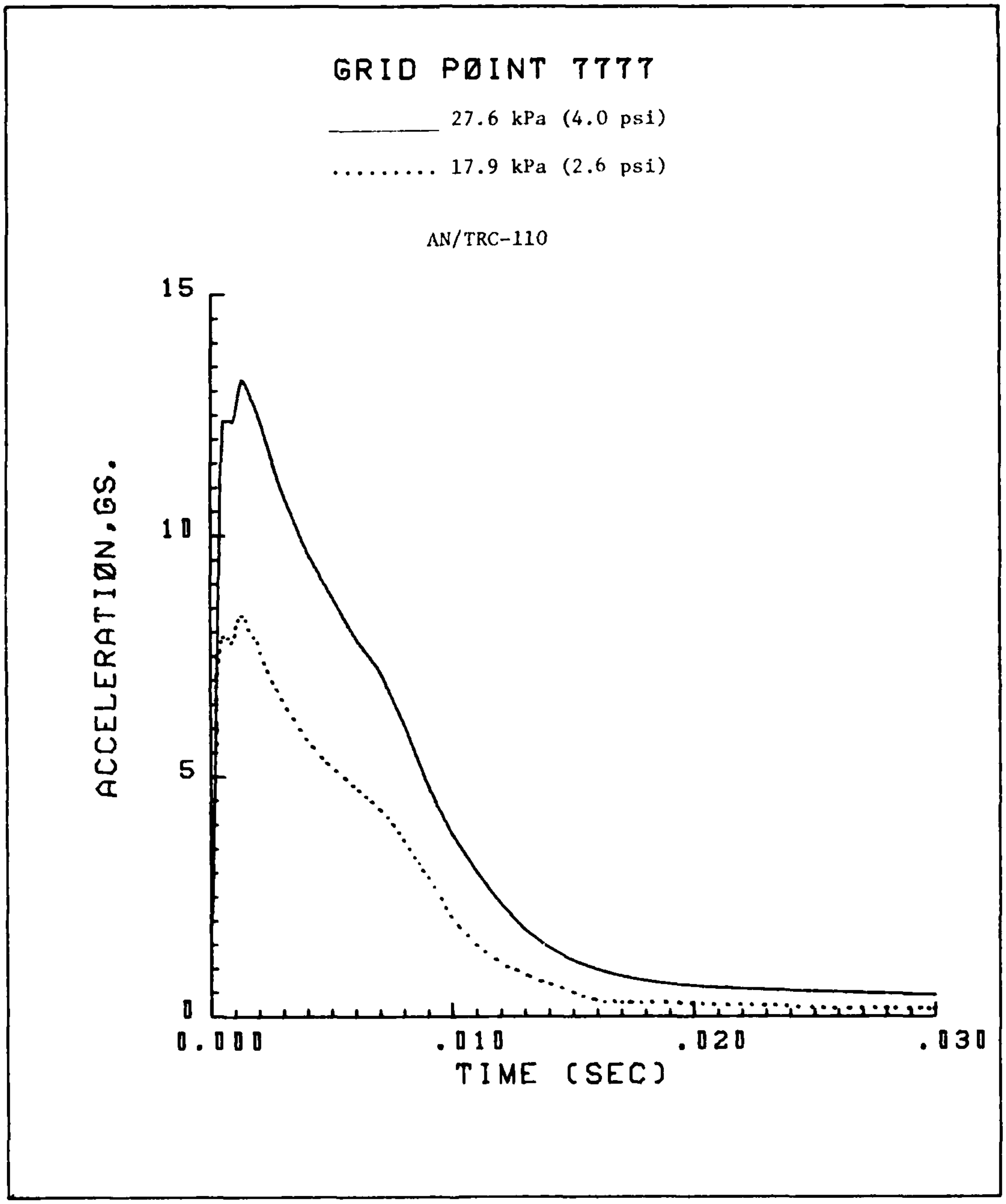

FIGURE 3.36 RIGID BODY ACCELERATION TIME HISTORY IN BLAST DIRECTION, CENTER OF FLOOR (NASTRAN)

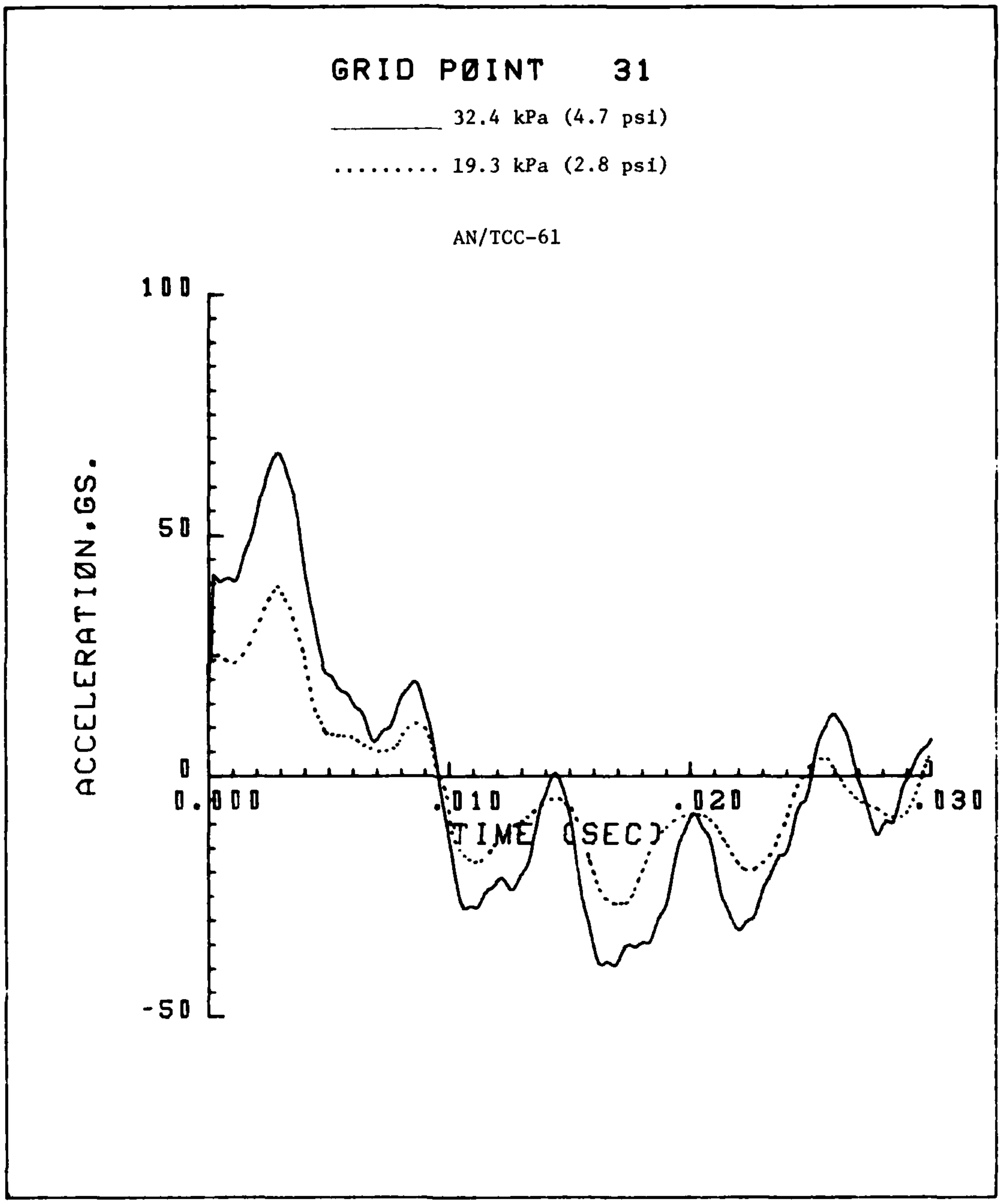

FIGURE 3.37. ACCELERATION TIME HISTORY IN BLAST DIRECTION, NEAR CENTER OF ROADSIDE WALL (NASTRAN)

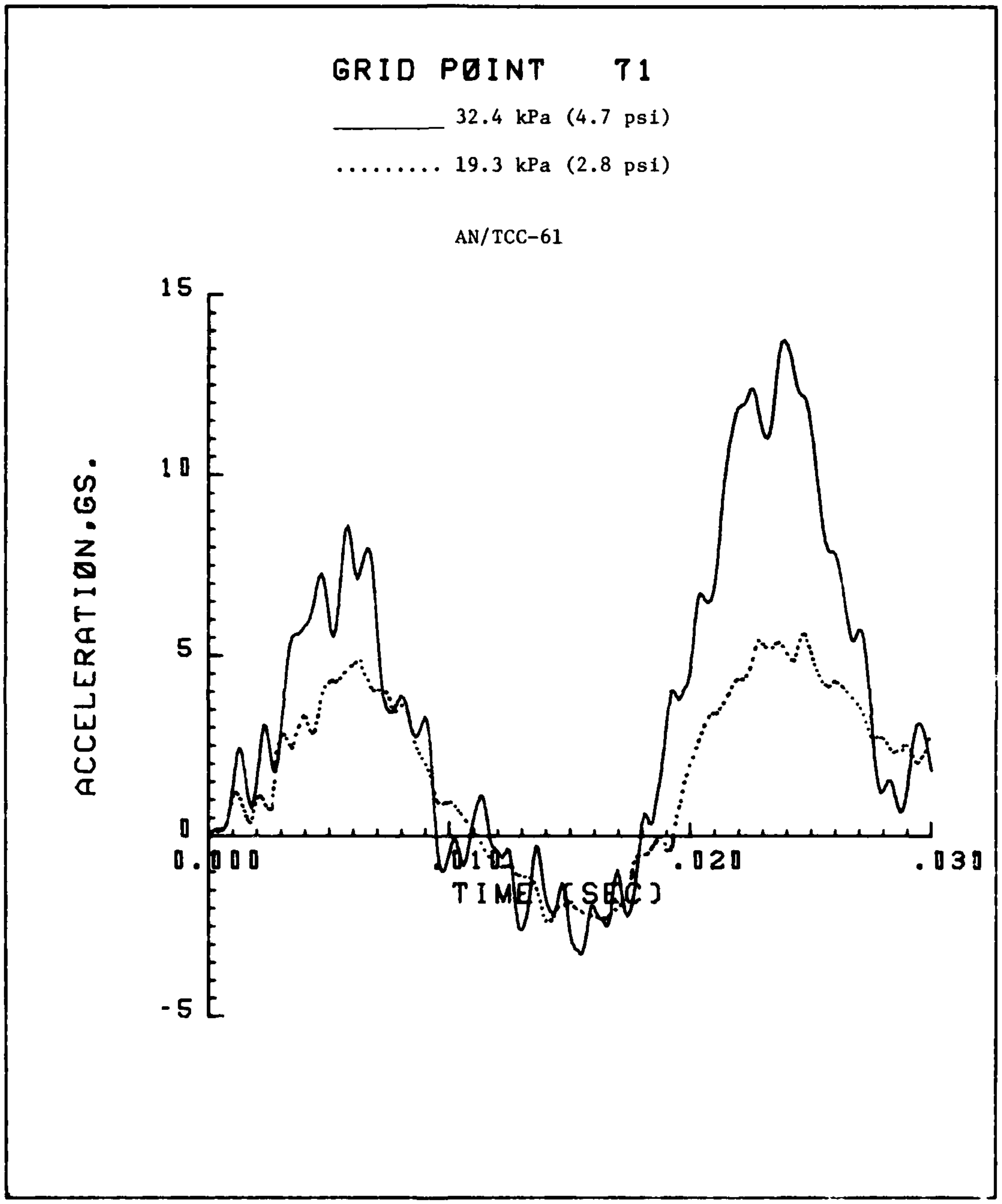

FIGURE 3.38 VERTICAL ACCELERATION TIME HISTORY, NEAR CENTER OF CURBSIDE WALL (NASTRAN)

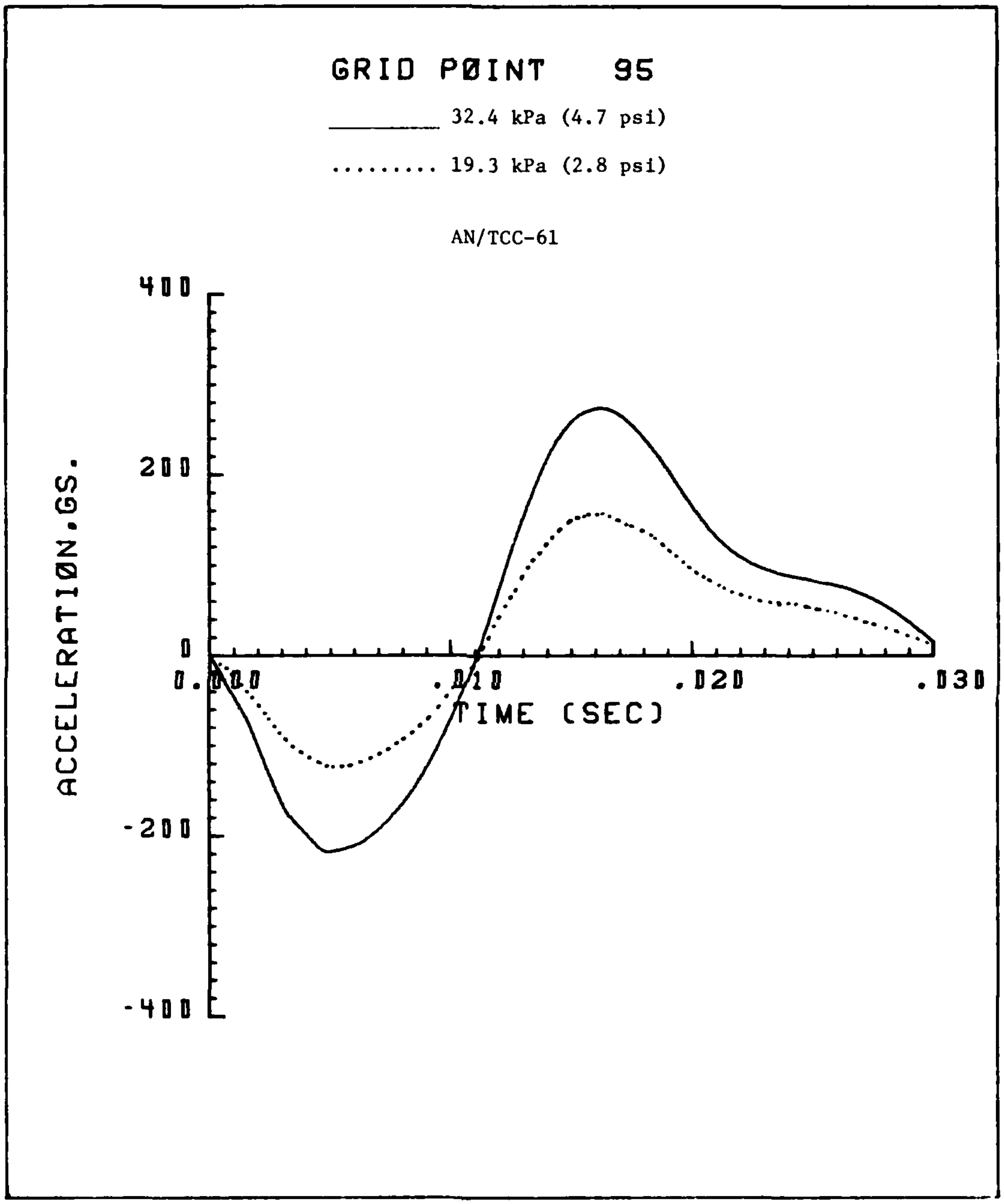

FIGURE 3.39. VERTICAL ACCELERATION TIME HISTORY, NEAR CENTER OF ROOF (NASTRAN)

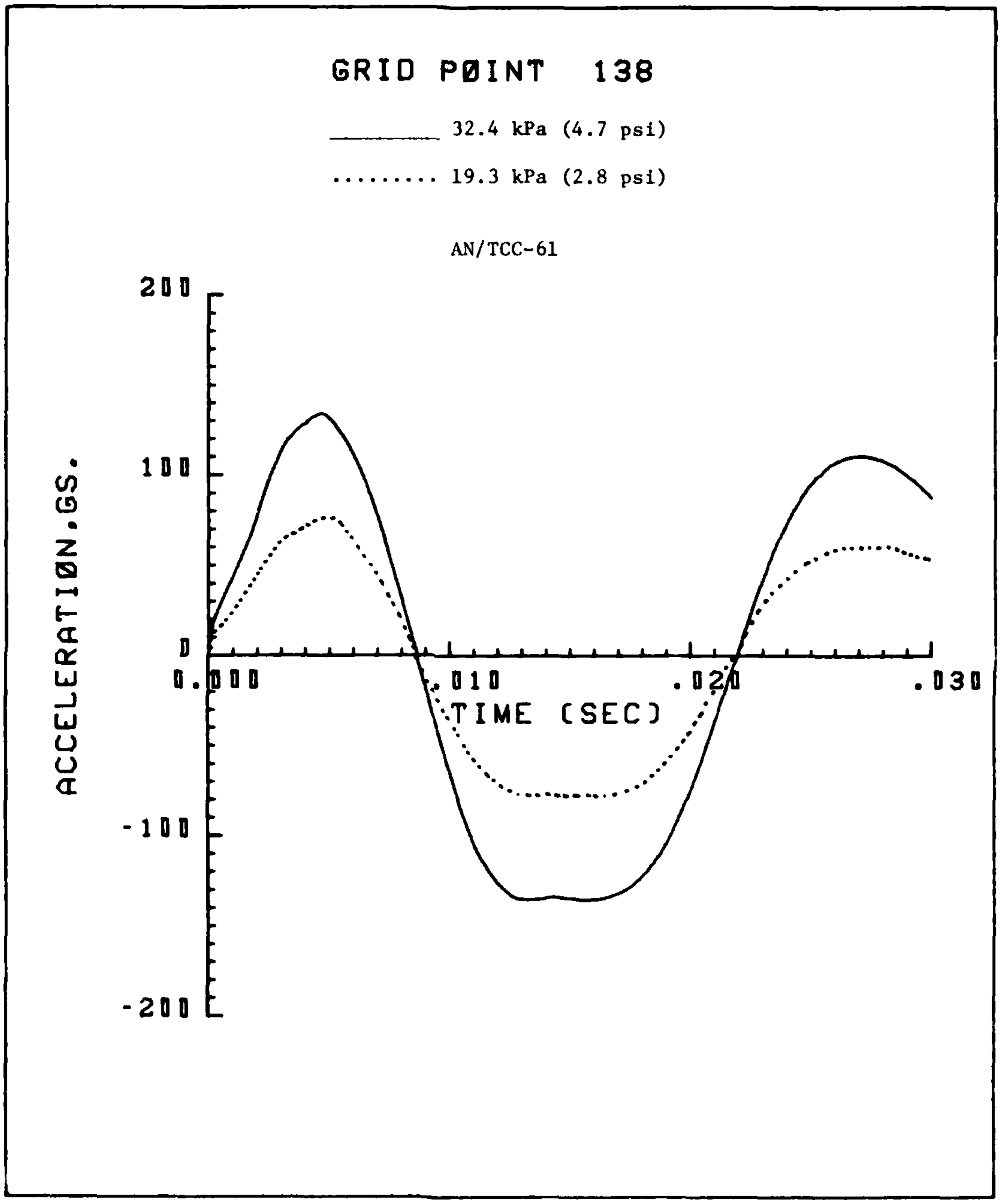

FIGURE 3.40. ACCELERATION TIME HISTORY IN HORIZONTAL DIRECTION, END WALL (NASTRAN)

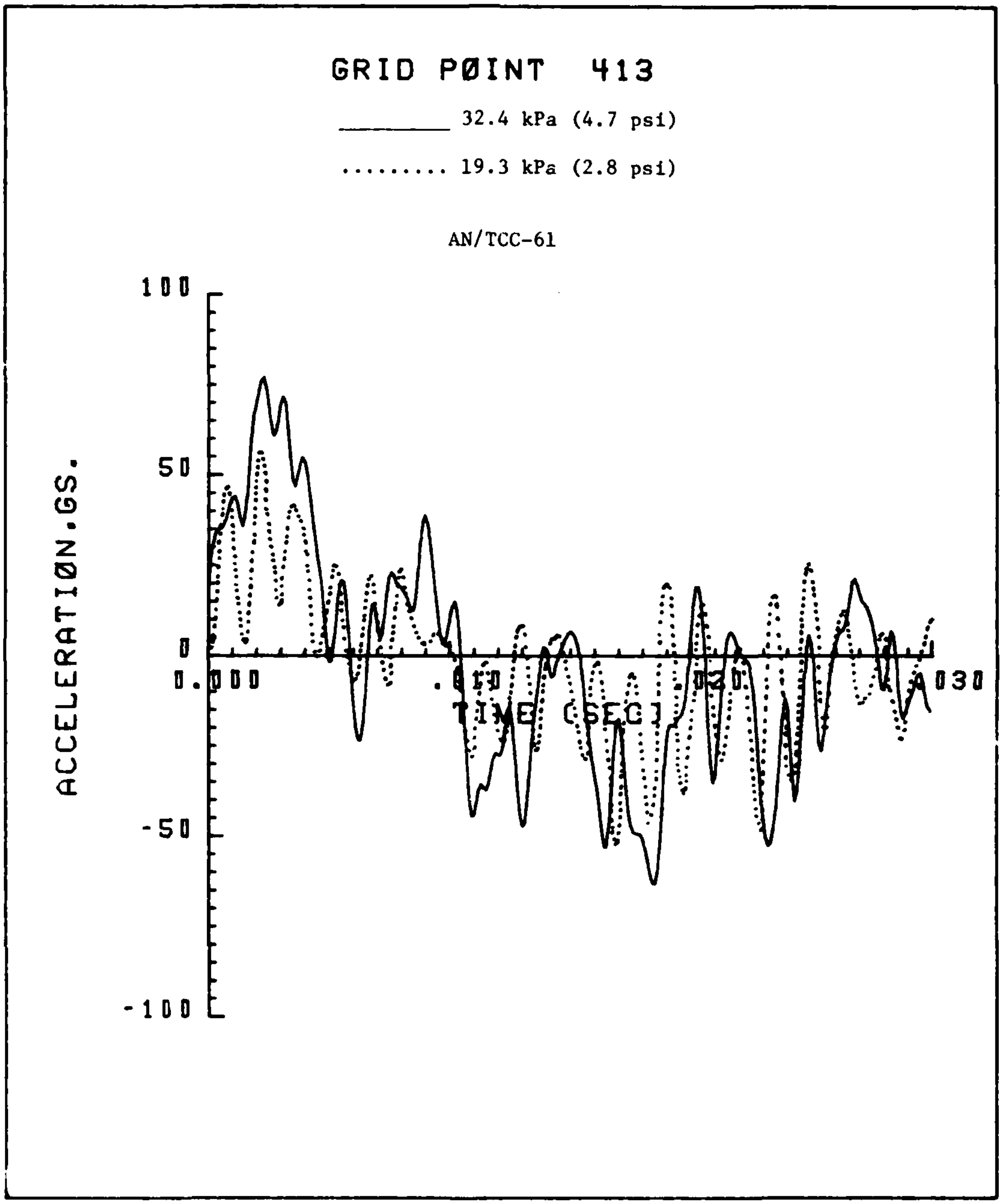

FIGURE 3.41. ACCELERATION TIME HISTORY IN BLAST DIRECTION, ROADSIDE RACK (NASTRAN)

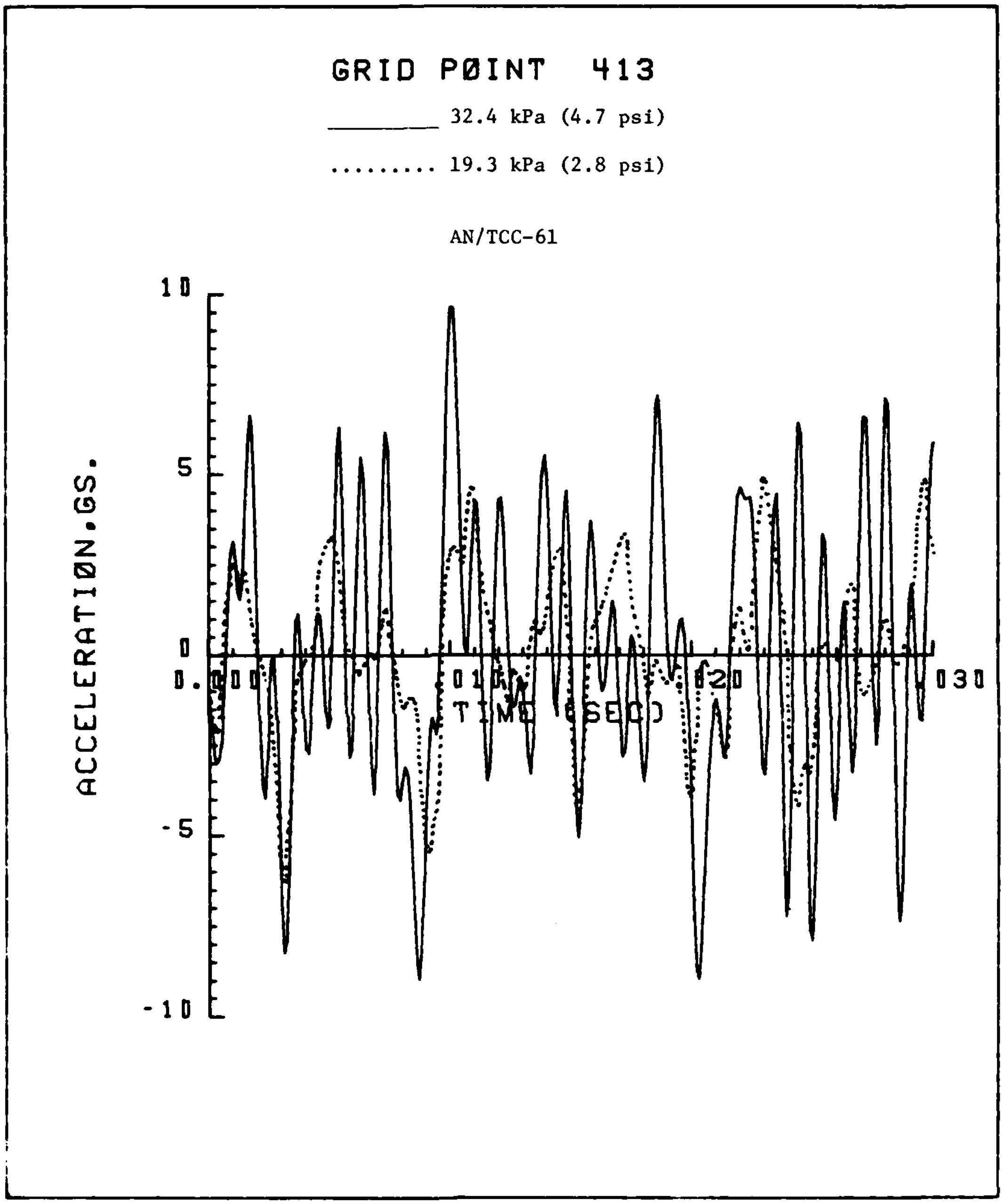

FIGURE 3.42. VERTICAL ACCELERATION TIME HISTORY, ROADSIDE RACK (NASTRAN)

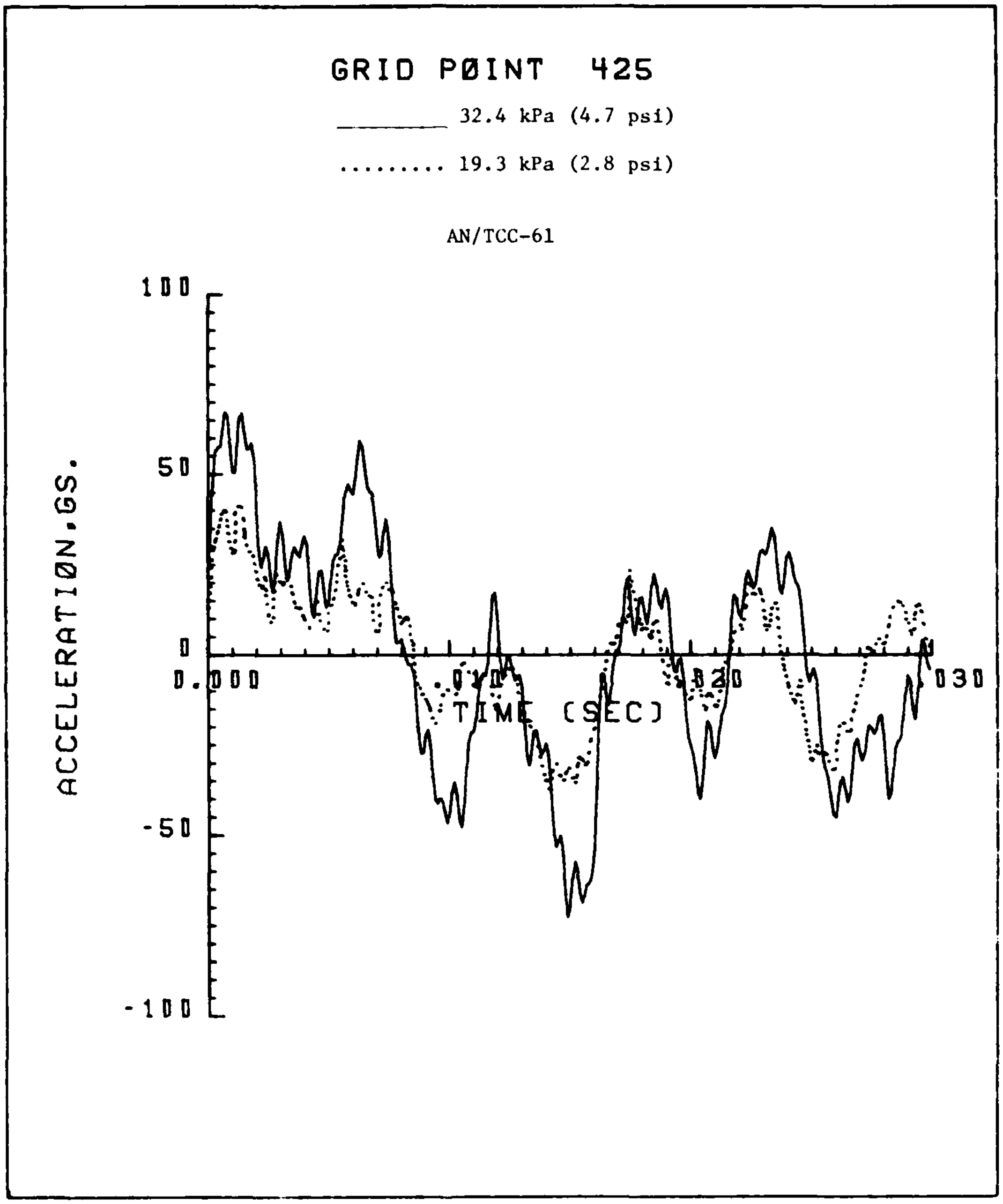

FIGURE 3.43. ACCELERATION TIME HISTORY IN BLAST DIRECTION, ROADSIDE RACK (NASTRAN)

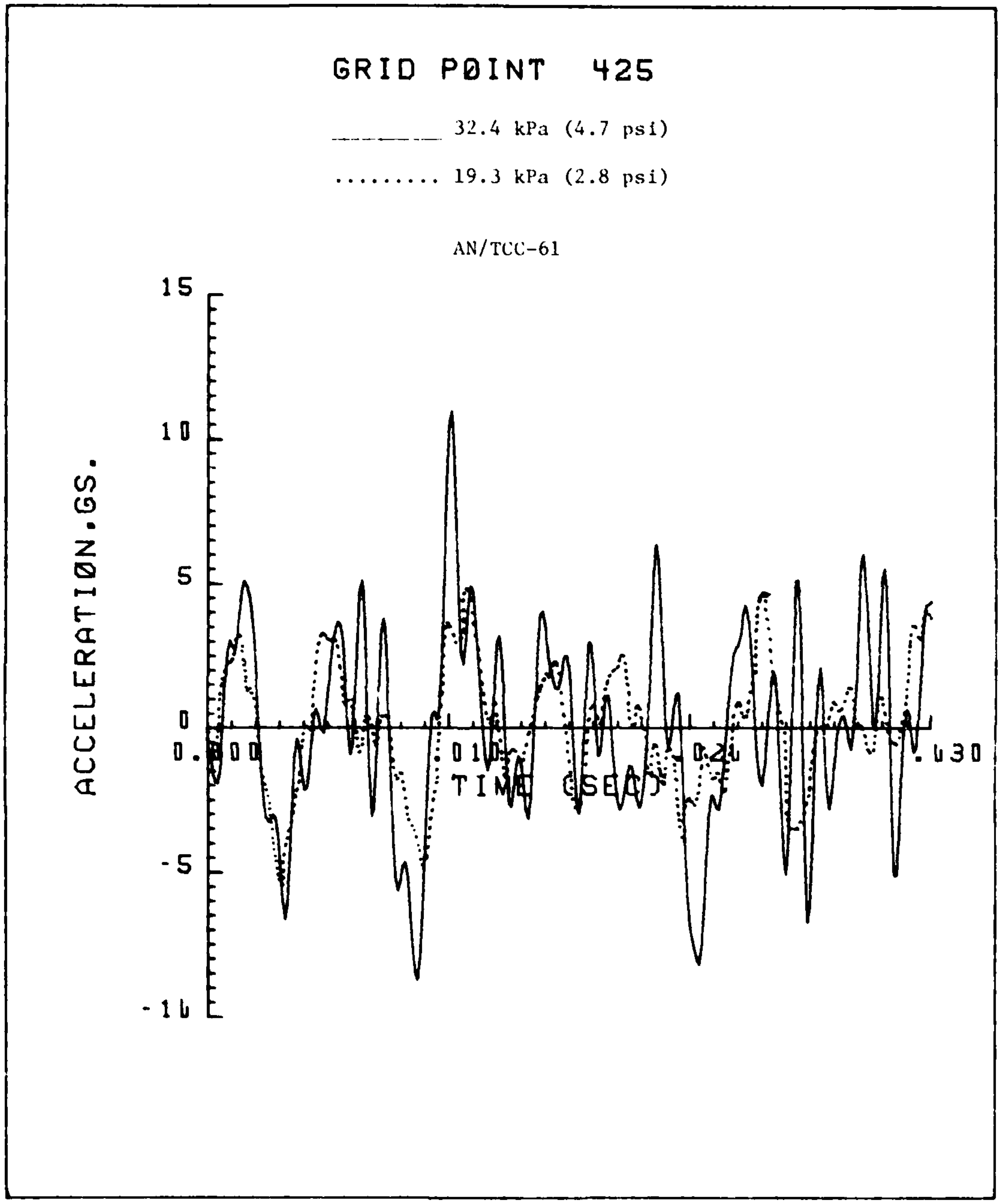

FIGURE 3.44. VERTICAL ACCELERATION TIME HISTORY, ROADSIDE RACK (NASTRAN)

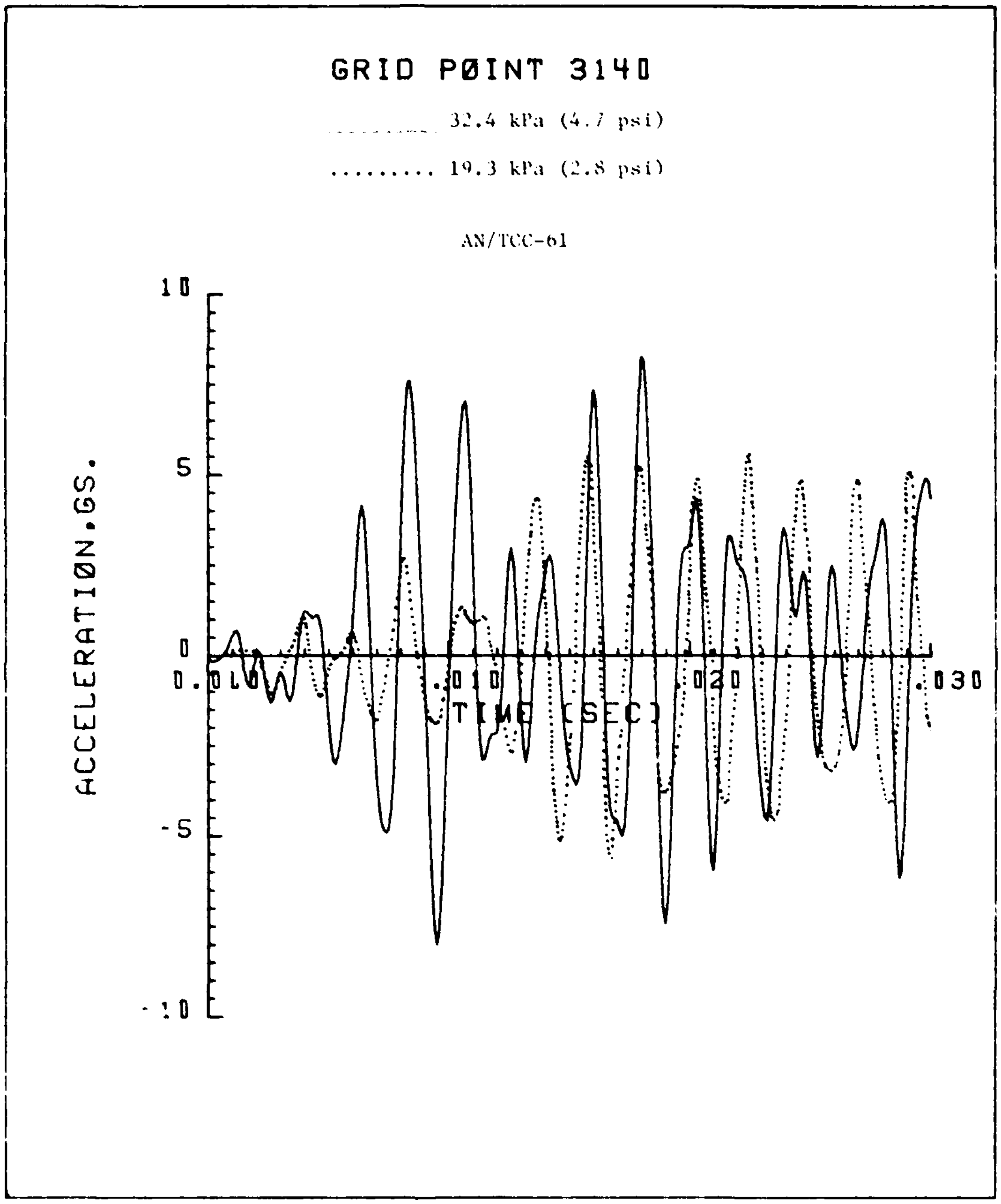

FIGURE 3.55. VERTICAL ACCELERATION TIME HISTORY, CURBSIDE RACK (NASTRAN)

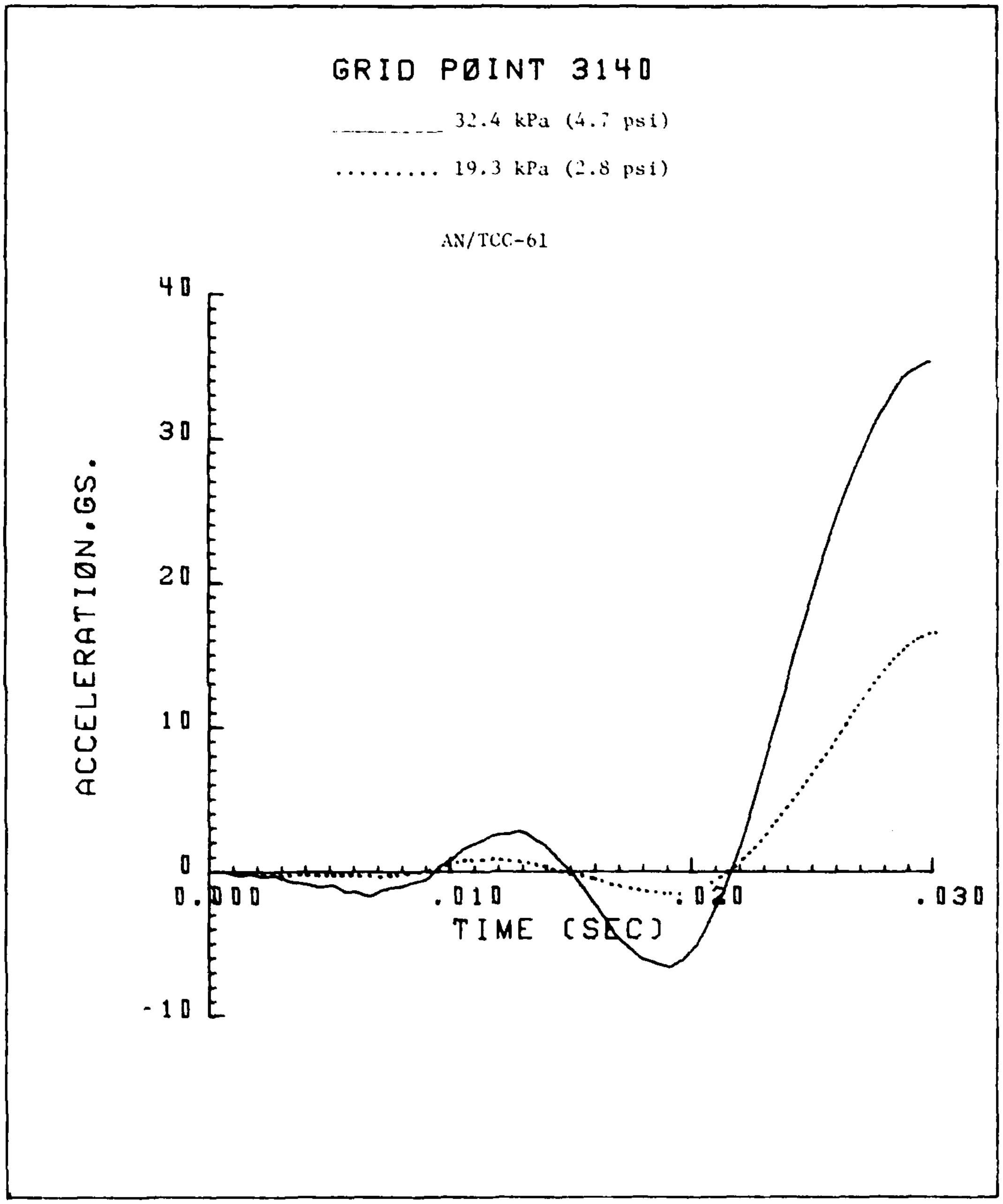

FIGURE 3.46. ACCELERATION TIME HISTORY IN BLAST DIRECTION, CURBSIDE RACK (NASTRAN)

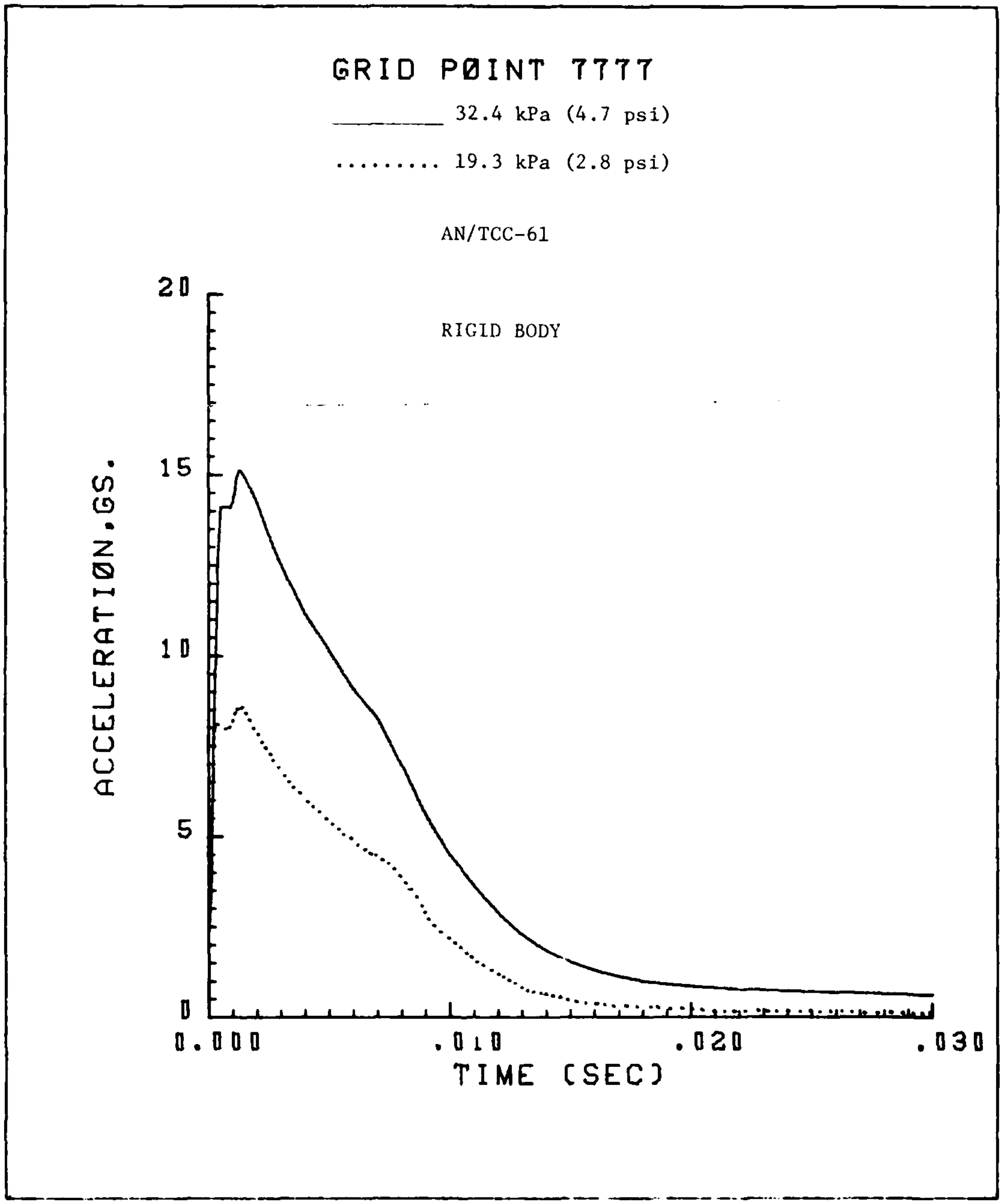

FIGURE 3.47 ACCELERATION TIME HISTORY IN BLAST DIRECTION, CENTER OF FLOOR (NASTRAN)

TABLE 3.2

ACCELEROMETER LOCATIONS FOR S-280 SHELTER SYSTEMS

SYSTEM	NEAREST GRID POINT	GAGE DESIGNATION	LOCATION
AN/TRC-117	326	02/1H* 02/1V	Roadside Racks
	314	02/2H 02/2V	Roadside Racks
	417	02/4H 02/4V	Front End Racks
	7777	02/3H 02/3V	Floor
AN/TRC-110	228	04/4H 04/4V	Front End Racks
	241	04/1H 04/1V	Front End Racks
	244	04/2V 04/2H	Front End Racks
	7777	04/3V 04/3H	Floor
AN/TCC-61	413	08/1H 08/1V	Roadside Rack
	425	08/2H 08/2V	Roadside Rack
	3140	08/4H 08/4V	Curbside Rack
	7777	08/3H 08/3V	Floor

* H denotes blast direction
V denotes vertical direction

TABLE 3.3

ACCELEROMETER LOCATIONS

FOR S-250 SHELTER SYSTEM

SYSTEM	NEAREST GRID POINT	GAGE DESIGNATION	LOCATION
AN/TRC-145	111	01/1H* 01/1V	Roadside Rack
	103	01/2H 01/2V	Roadside Rack
	122	01/4H (NA) 01/4V	Front End Rack
	150	01/3H 01/3V	Floor

*H denotes blast direction
V denotes vertical direction

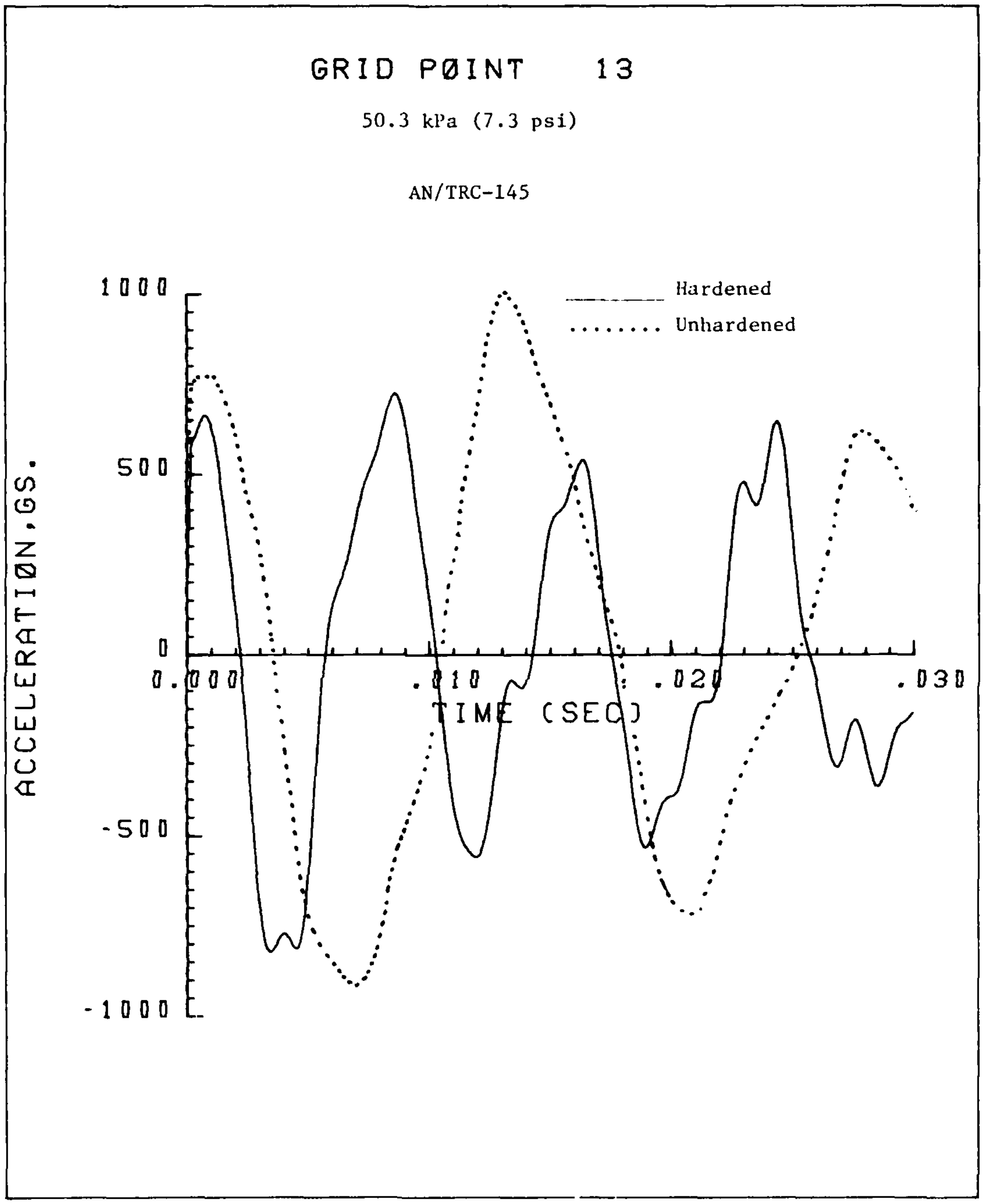

FIGURE 3.48. ACCELERATION TIME HISTORY IN BLAST DIRECTION, NEAR CENTER OF ROADSIDE WALL (NASTRAN)

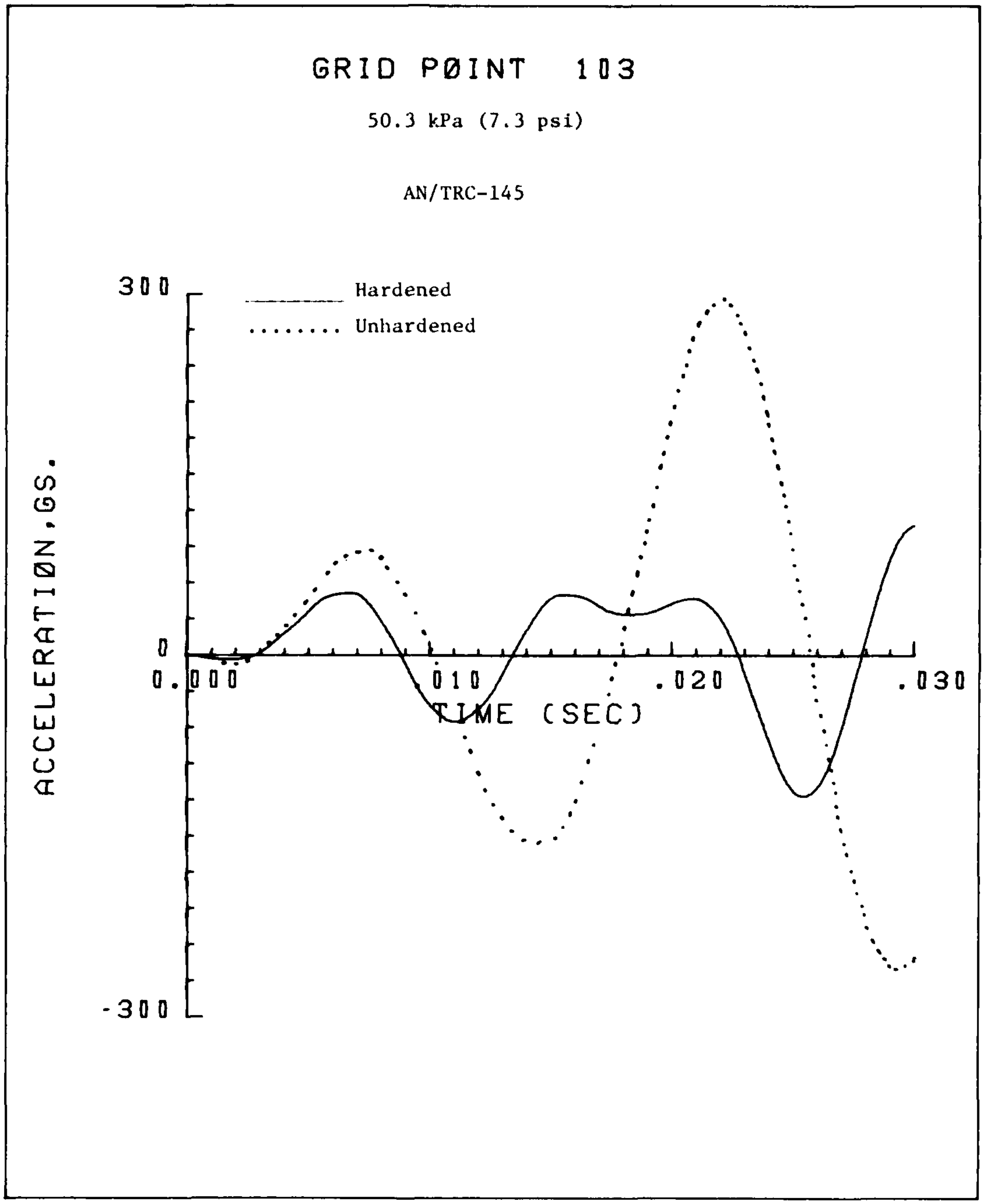

FIGURE 3.49. ACCELERATION TIME HISTORY IN BLAST DIRECTION, ROADSIDE RACK (NASTRAN)

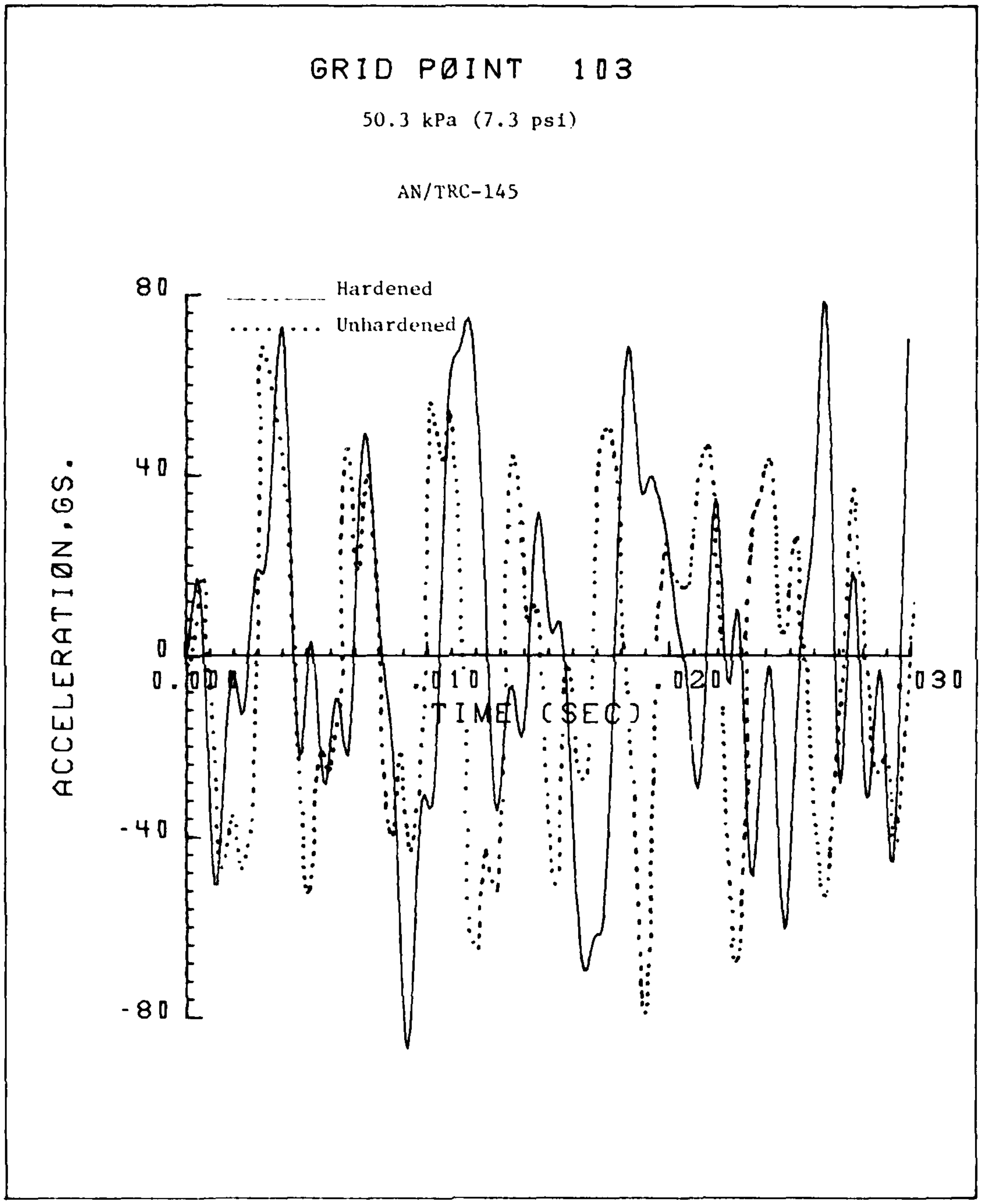

FIGURE 3.50. VERTICAL ACCELERATION TIME HISTORY, ROADSIDE RACK (NASTRAN)

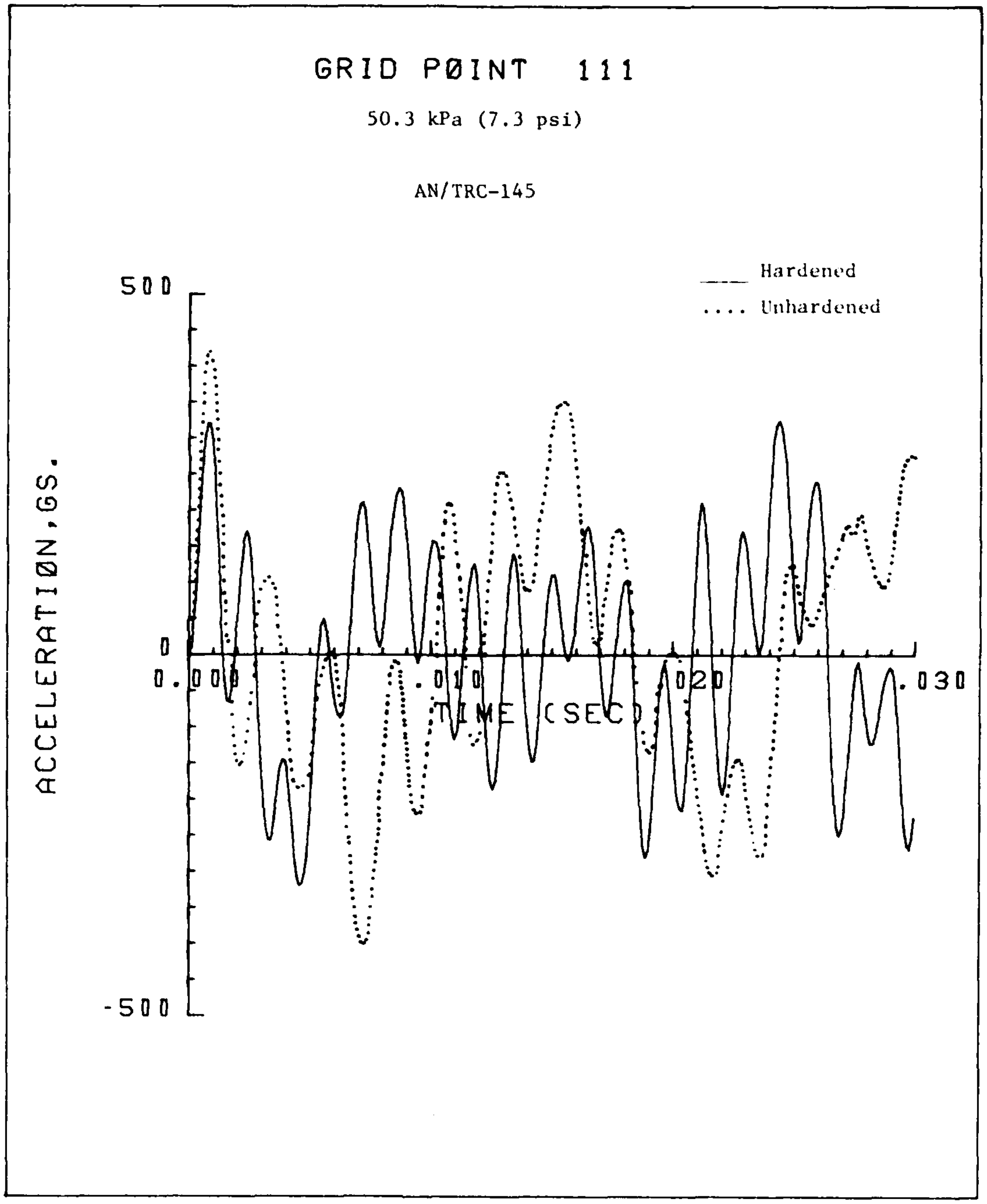

FIGURE 3.51. ACCELERATION TIME HISTORY IN BLAST DIRECTION, ROADSIDE RACK (NASTRAN)

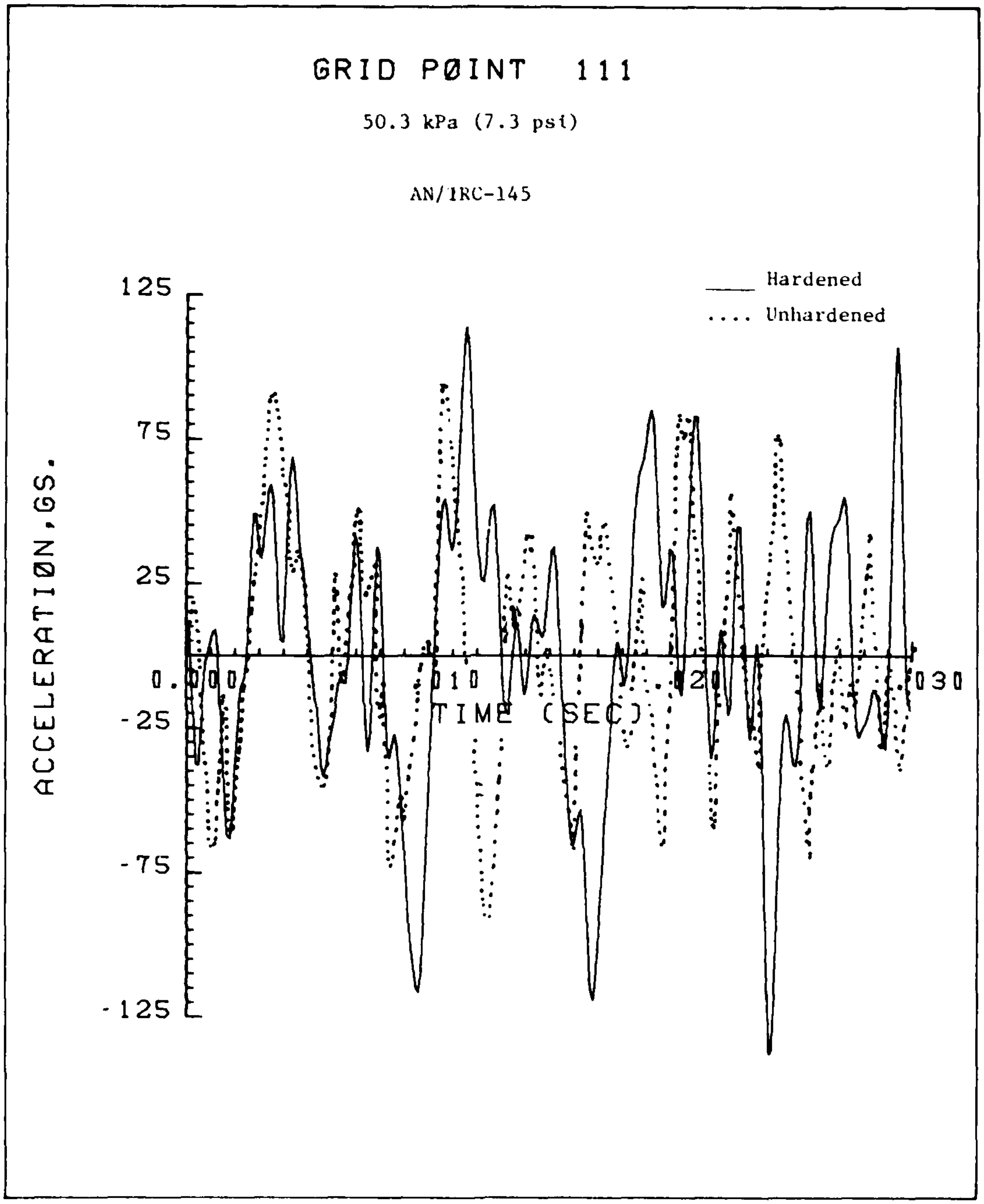

FIGURE 3.52. VERTICAL ACCELERATION TIME HISTORY, ROADSIDE RACK (NASTRAN)

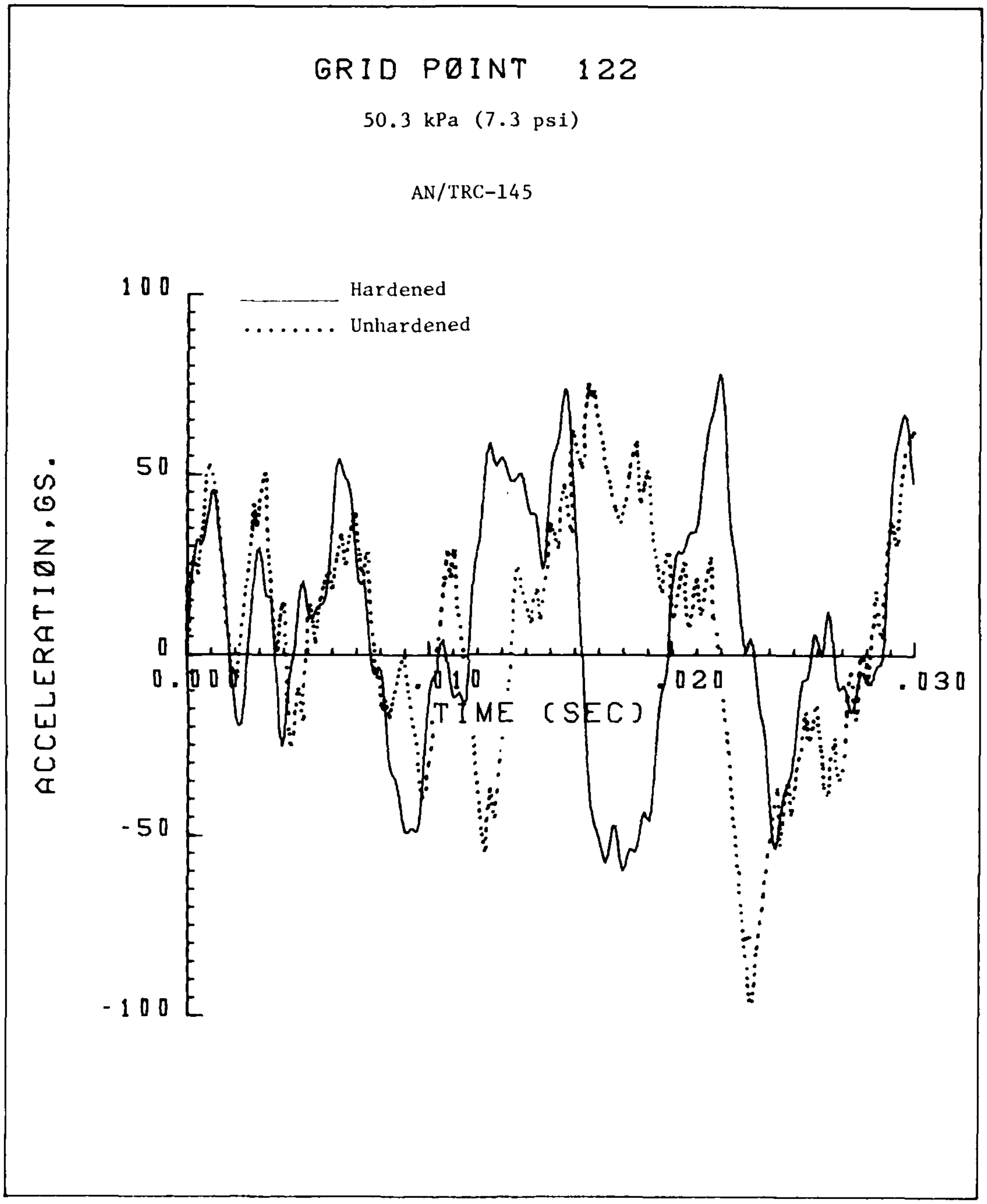

FIGURE 3.53. ACCELERATION TIME HISTORY IN BLAST DIRECTION, FRONT WALL RACK (NASTRAN)

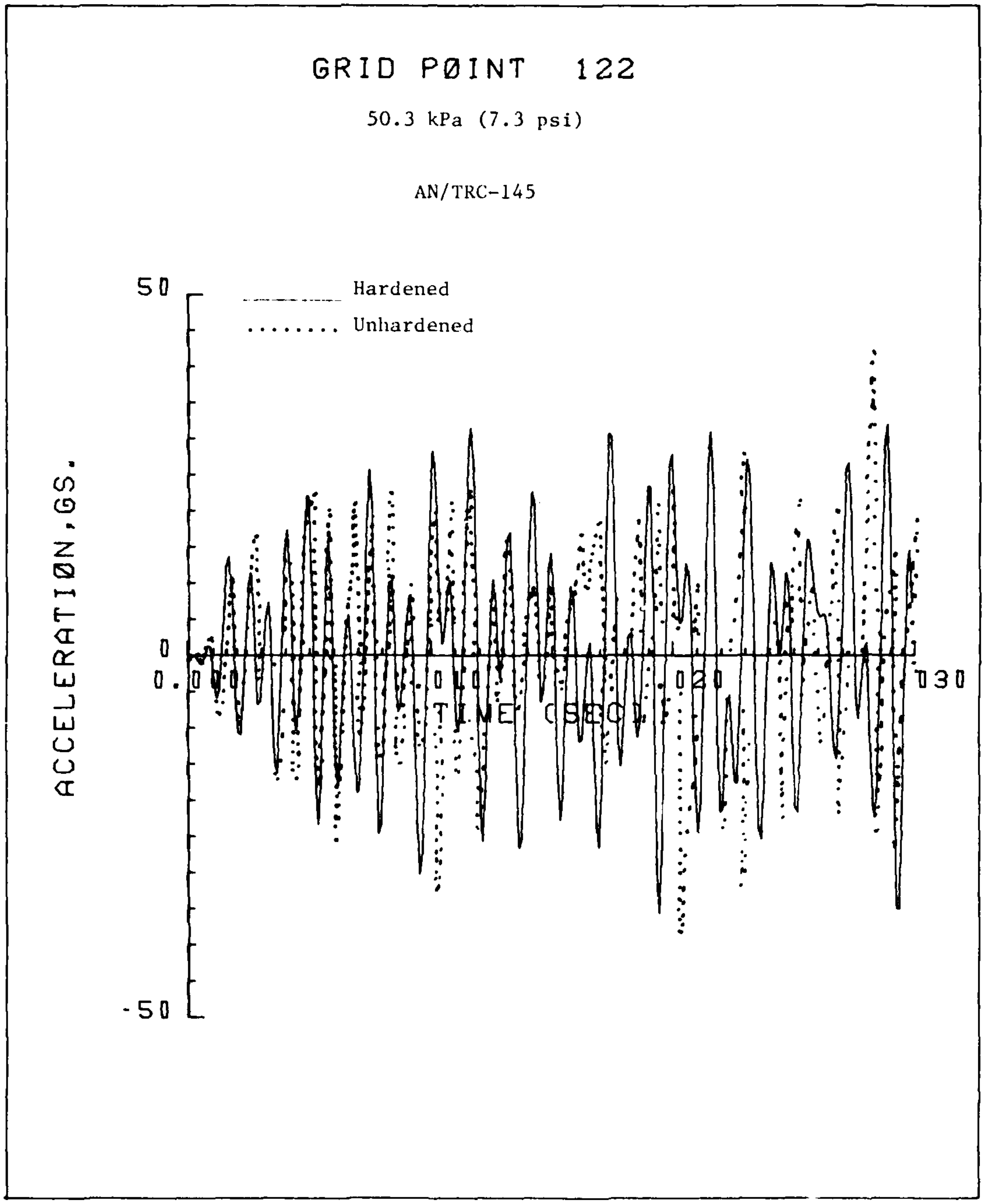

FIGURE 3.54. VERTICAL ACCELERATION TIME HISTORY, FRONT WALL RACK (NASTRAN)

code, i.e., the force in the blast direction shown in Fig. 3.11 for the AN/TRC-117 and in Fig. 3.13 for the AN/TRC-145.

Representative overpressure time histories at the overpressure level of 41.4 kPa are given for the S-280 shelter in Figs. 3.55-3.58, and for the S-250 shelter in Figs. 3.59-3.62 using the TRUCK code overpressure model. The overpressure plots for the S-250 shelter also include predictions from the SHELTR code for comparison.

Biaxial accelerometers were located at three points on the rack frames and also at the center of the floor for each system (see Tables 3.2 and 3.3 for gage locations). Generally, the available measured data extended out to a duration between 60 and 100 msecs. These data were reprocessed to obtain shorter duration plots ranging from 8 to 10 msec. No data were available for gages 02/2V and01/4H, and short duration plots were not available for gages 02/2H, 02/4H, 01/2H, 01/4V and 01/3H. In addition to acceleration time histories, maxi-max shock spectra* of the measured acceleration time histories were available for a limited number of gages, i.e., 01/1H, 01/1V, 01/2H, 01/2V, 02/1H, 02/3H, and 02/4V.

The comparisons between the NASTRAN predictions and the measured data are given in Figures 3.63-3.86 for the AN/TRC-117 and in Figures 3.89-3.109 for the ANTRC-145. The order of presentation consists of first comparing the time histories for the shorter time duration, followed by a plot of the long duration experimental response and then by a 30 msec plot of the NASTRAN response for each gage. In several cases it was not possible to overlap the analytical and test responses because of significant differences in the amplitude scale, and the plots were kept separate. The final set of plots for each system consists of an overlayed comparison of the limited experimental shock spectra data. A complete set of NASTRAN shock spectra is presented, however.

Figures 3.63-3.71 show the accelerations at the two gages located on one of the roadside racks of the AN/TRC-117, and Figures 3.72-3.76 show the accelerations at the gage located on the front end rack. Generally, the peak measured accelerations at these stations are significantly greater than the corresponding analytical responses. In addition, the frequency content of the measured responses is higher than the frequency of the analytical responses. Table 3.4 presents the approximate dominant frequency, as can best be determined from the response plots, and the ratio of the measured peak acceleration to the predicted peak acceleration for each gage. It may be noted that except for gage 02/1V, the frequencies of the measured rack responses are 1500 Hz or greater, whereas the frequencies of the prediced responses are generally less than 500 Hz, except for gage 02/2V. The best comparison on peak accelerations is at gage 02/1H where the measured response is twice as big as the predicted response. The worst comparison is at gage 02/1V (same location but in the vertical direction) where the measured response is 30 times greater than the predicted response.

*The Maxi-Max shock spectrum is the maximum absolute acceleration experienced by a single degree of freedom oscillator as a function of its own natural frequency in response to a shock or vibration input.

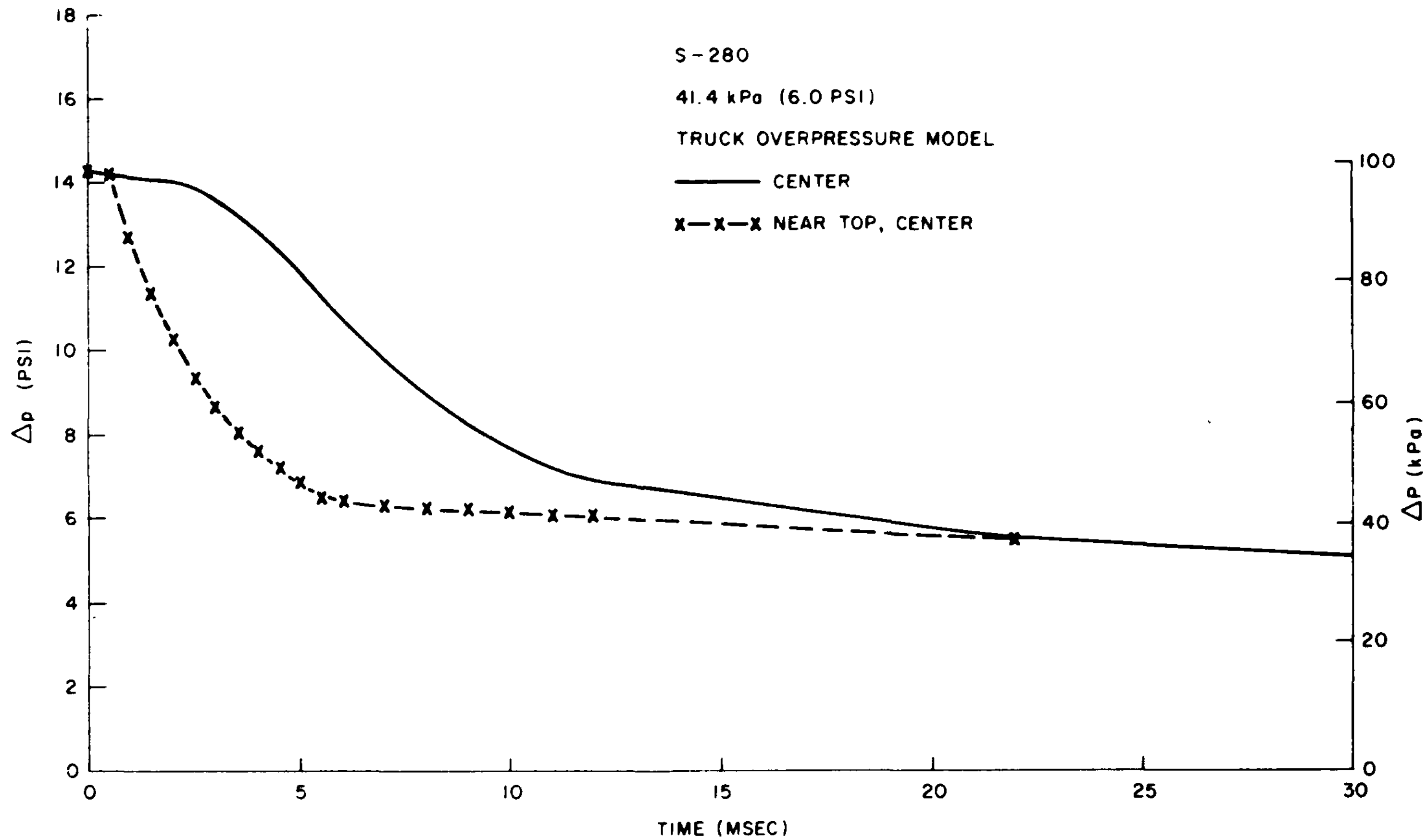

FIGURE 3.55. OVERPRESSURE ON S-280 ROADSIDE WALL

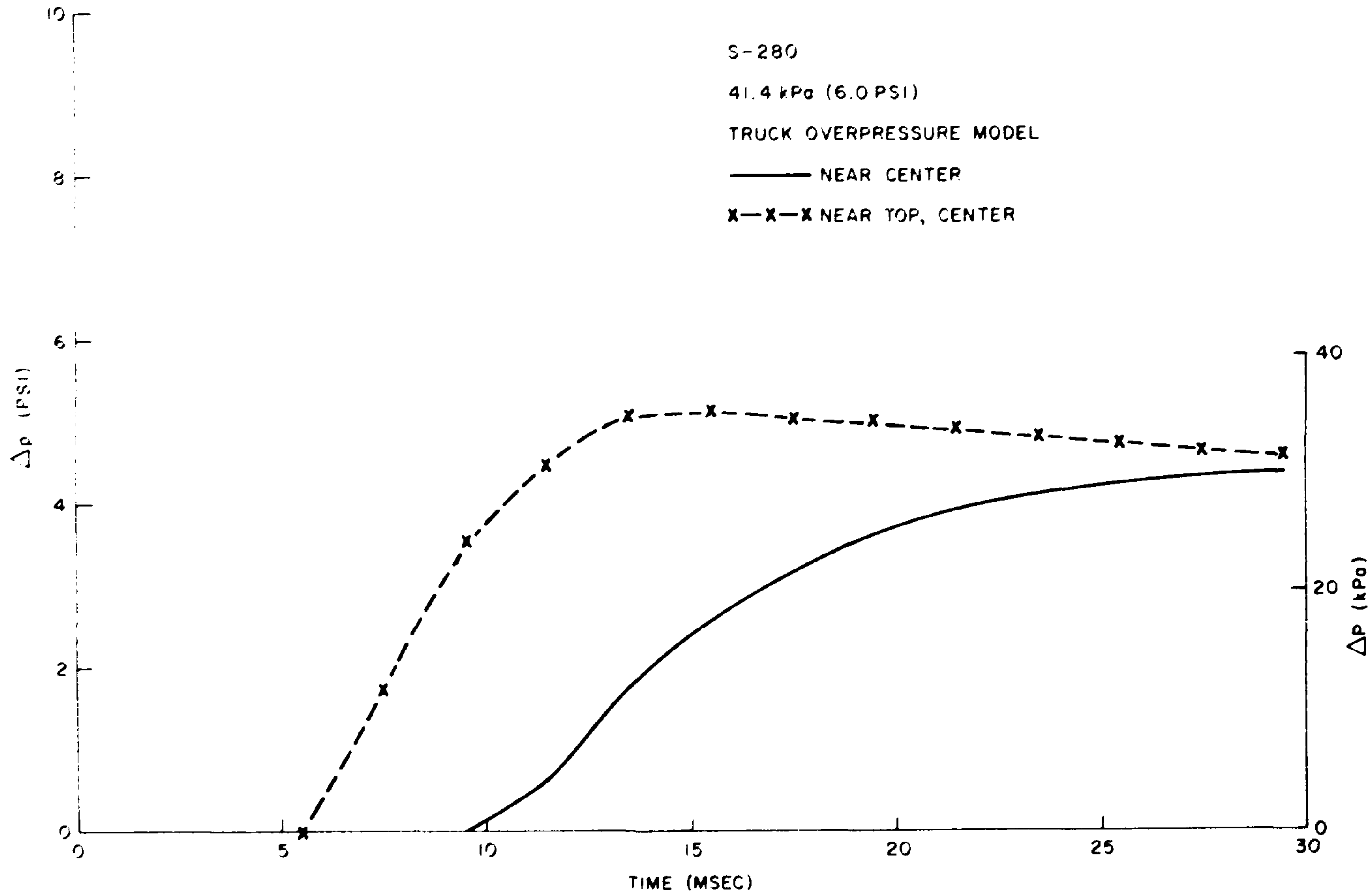

FIGURE 3.56. OVERPRESSURE ON S-280 CURBSIDE WALL

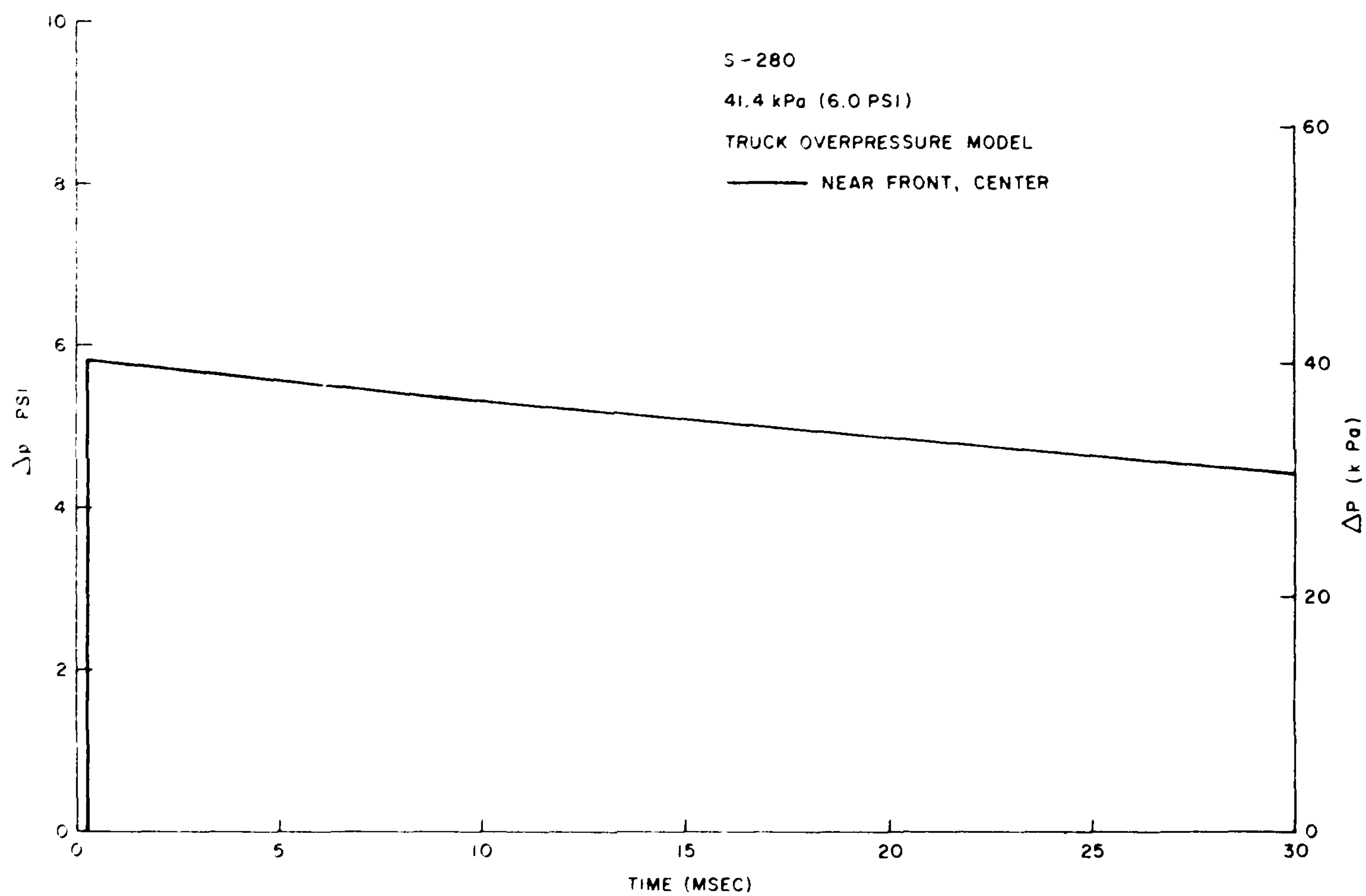

FIGURE 3.57. OVERPRESSURE ON S-280 ROOF

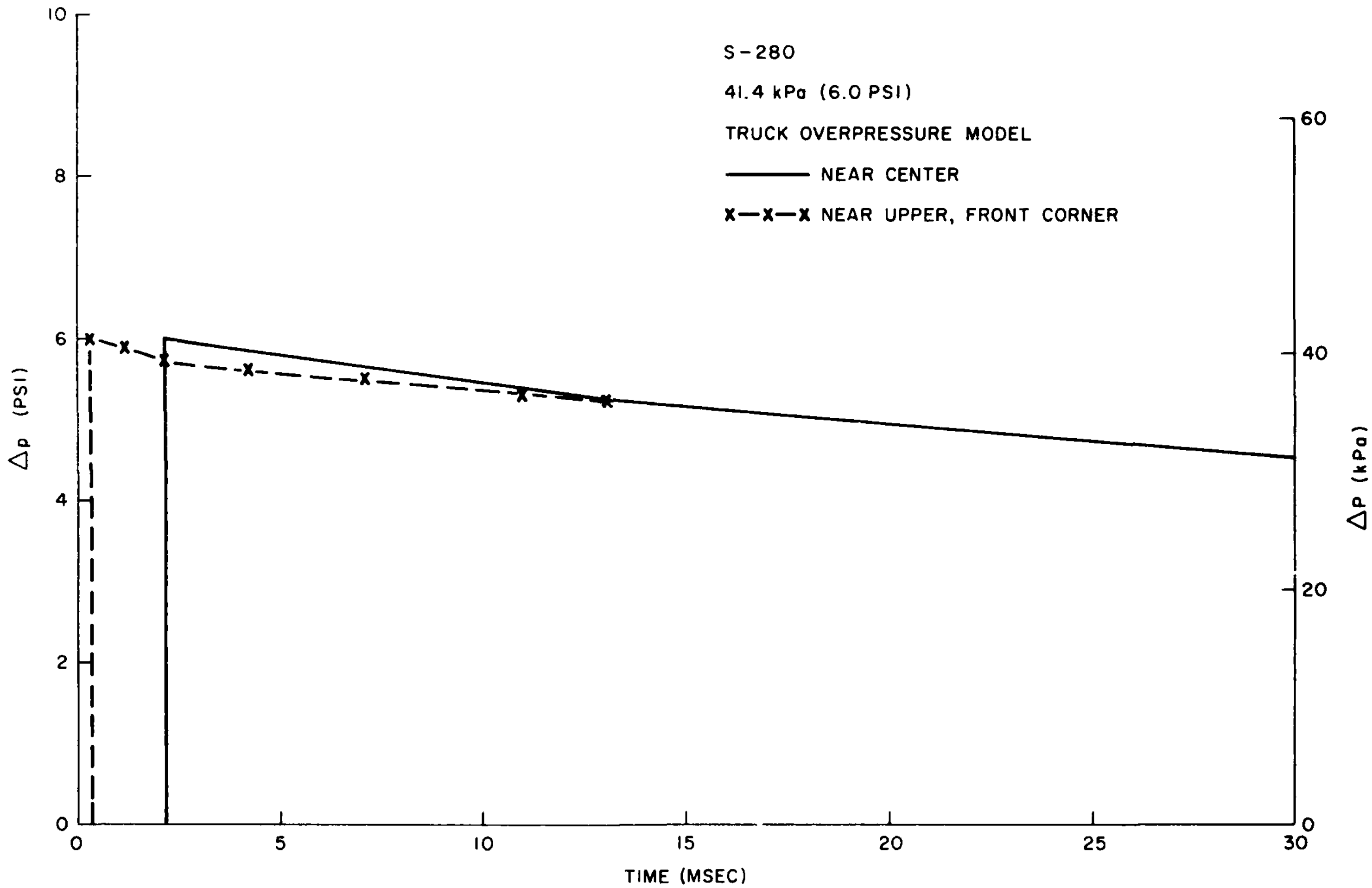

FIGURE 3.58. OVERPRESSURE ON S-280 FRONT END WALL

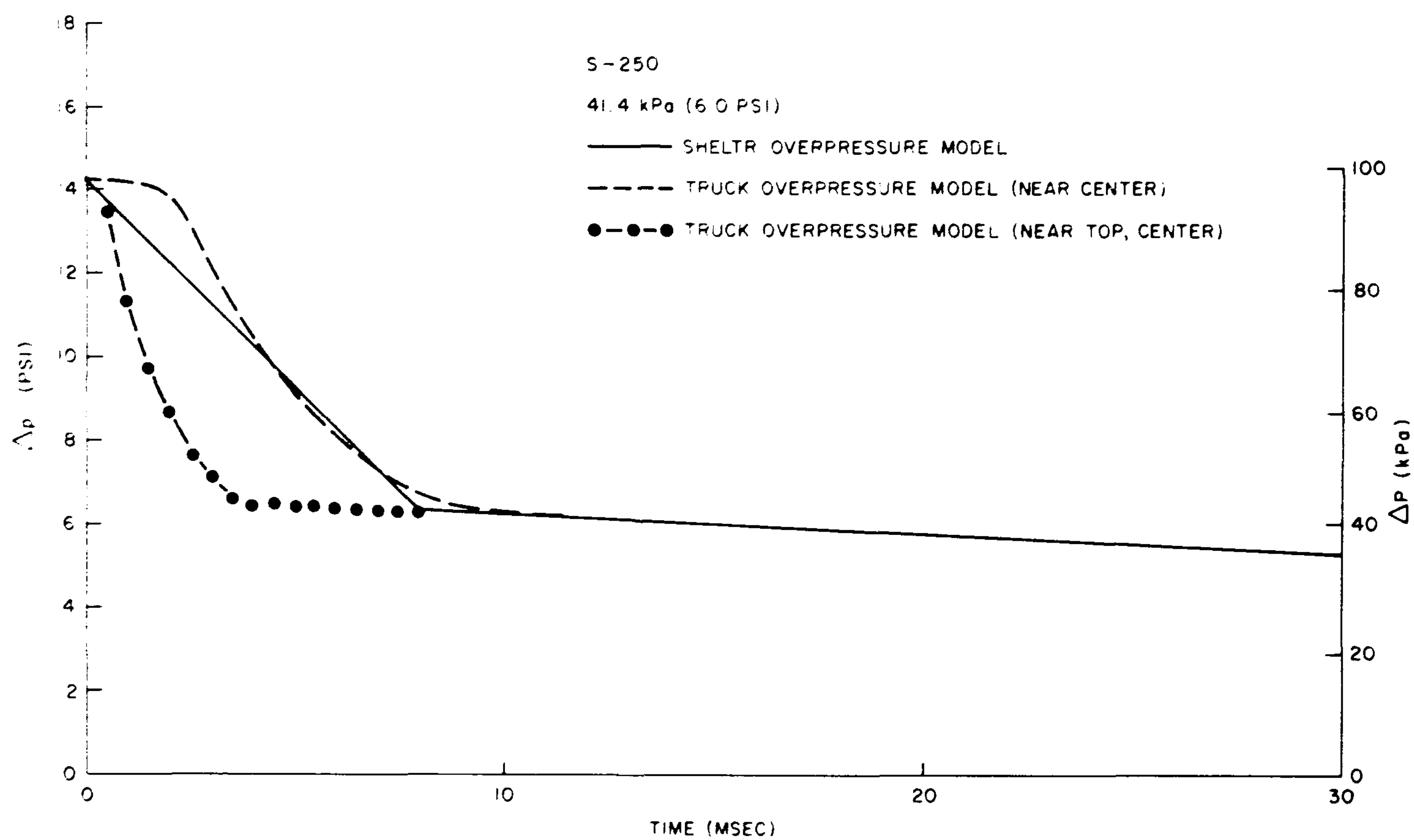

FIGURE 3.59. OVERPRESSURE ON S-250 ROADSIDE WALL

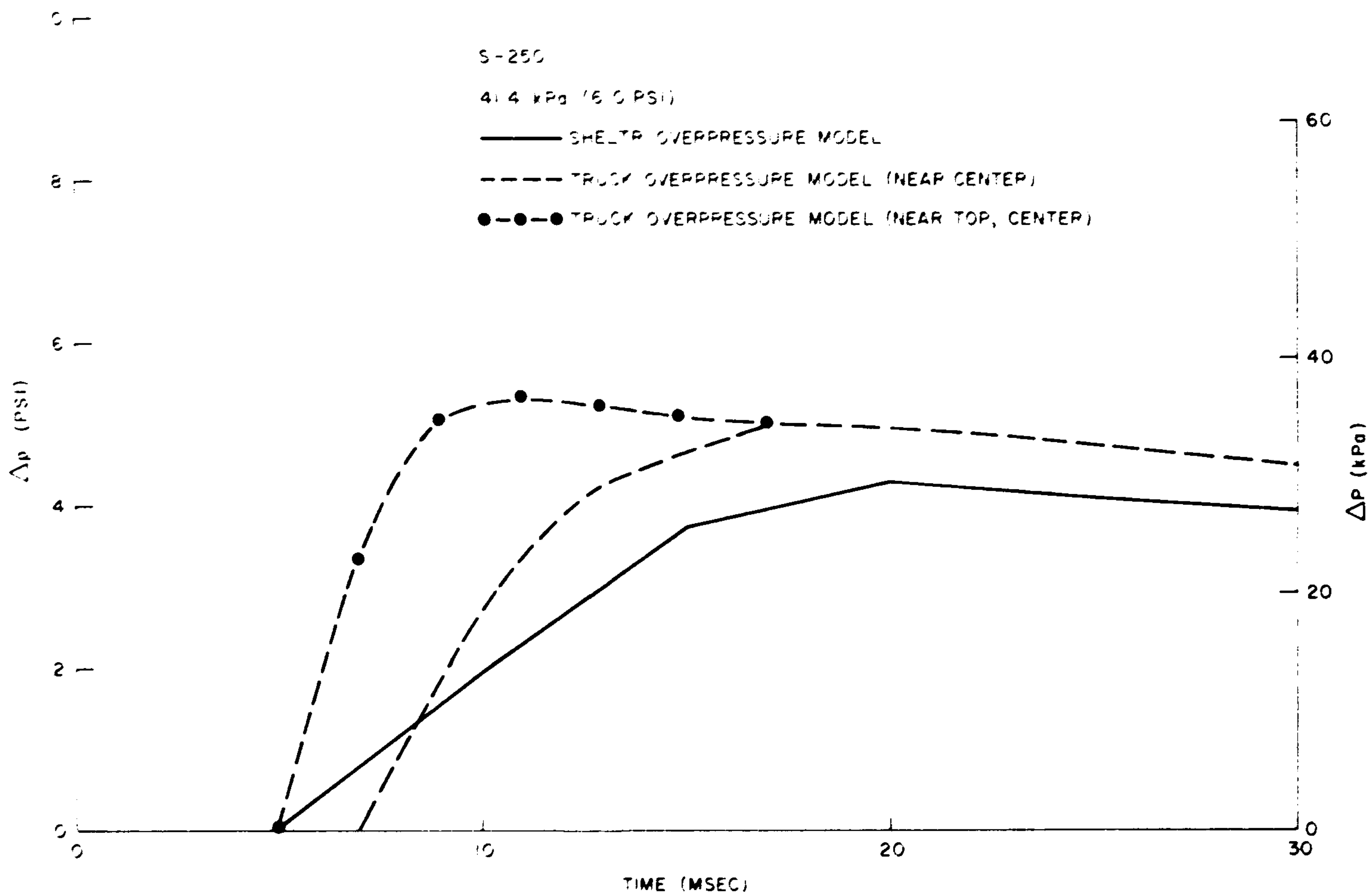

FIGURE 3.60. OVERPRESSURE ON S-250 CURBSIDE WALL

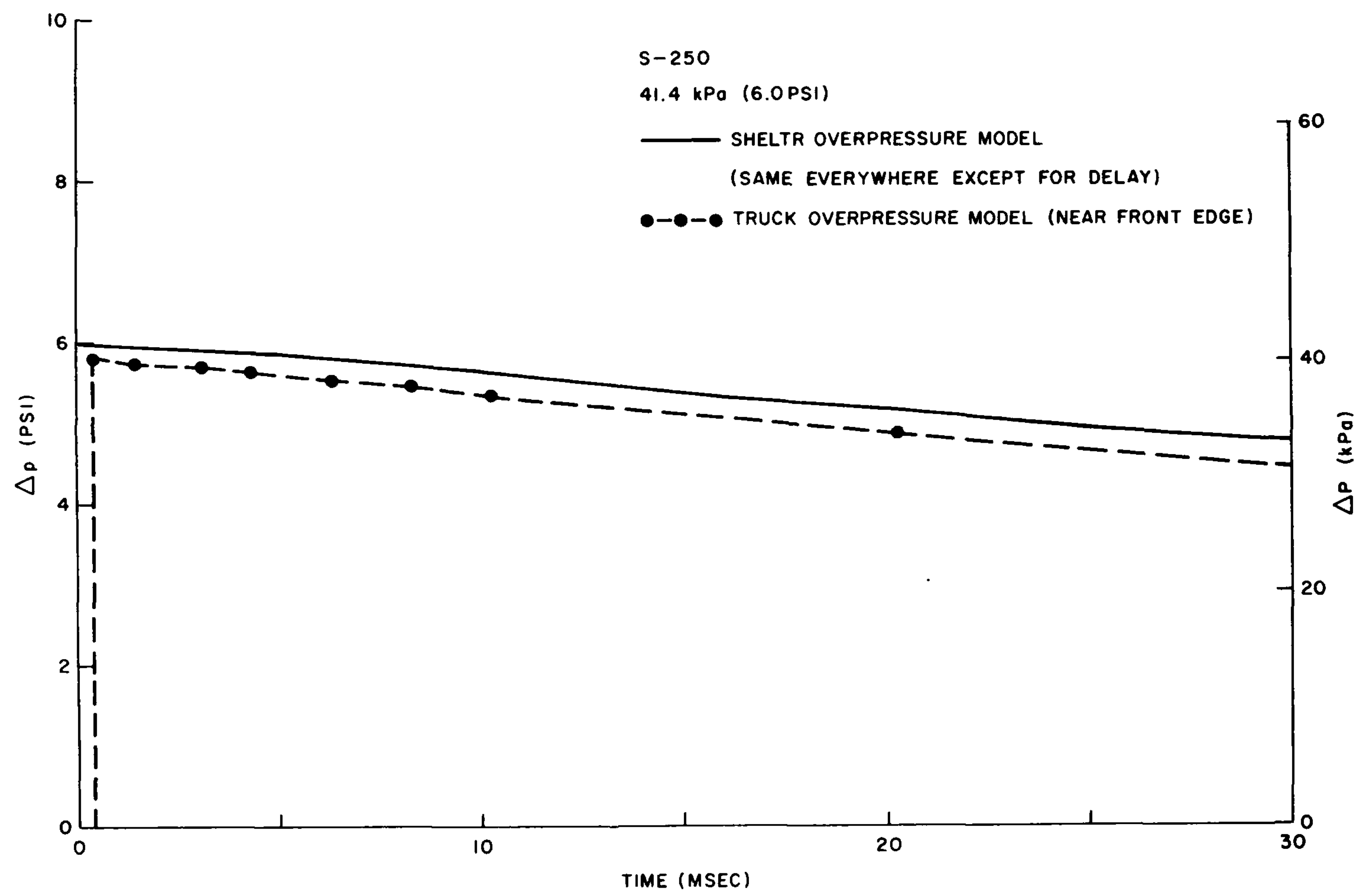

FIGURE 3.61. OVERPRESSURE ON S-250 ROOF

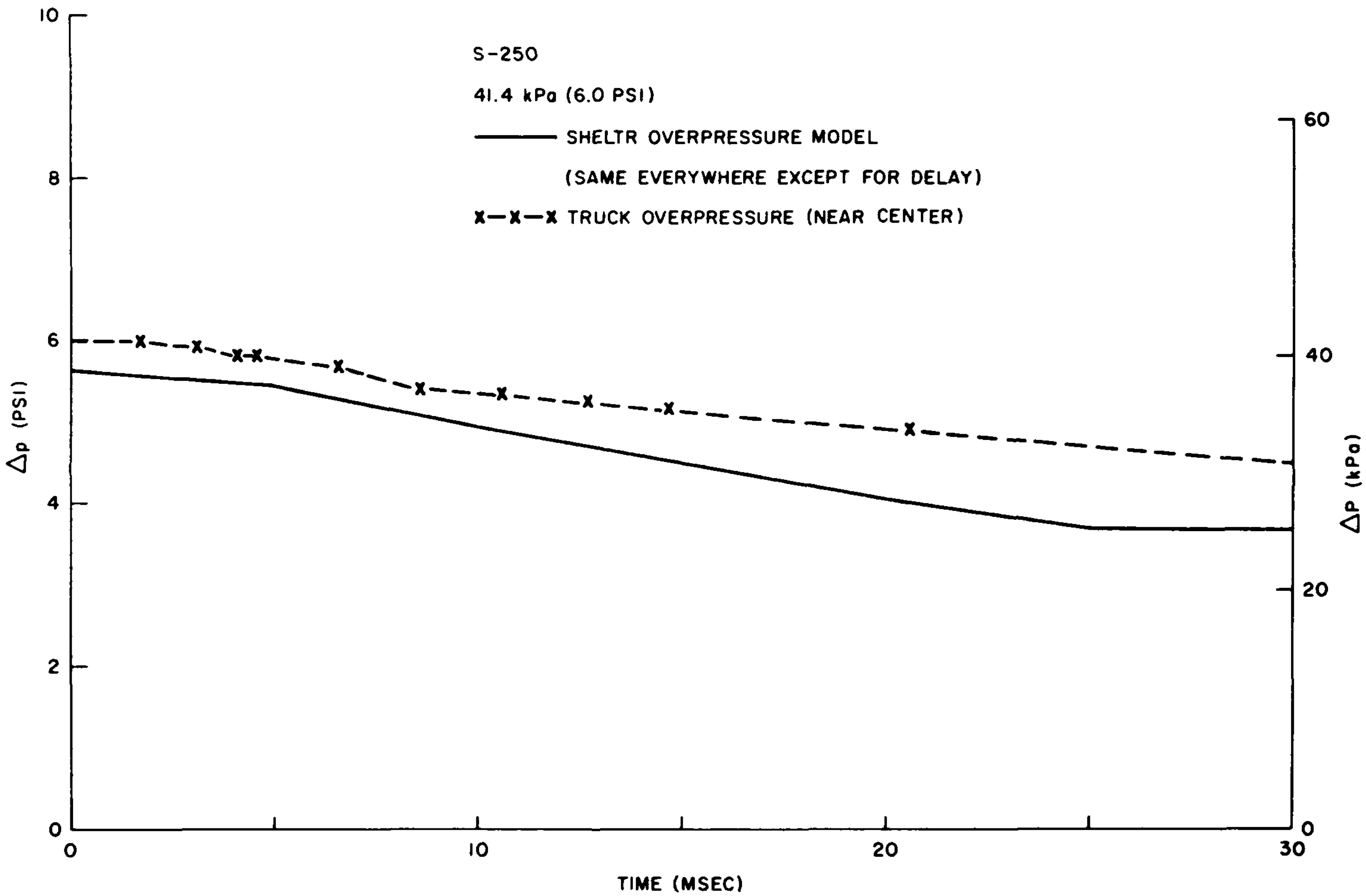

FIGURE 3.62. OVERPRESSURE ON S-250 END WALL

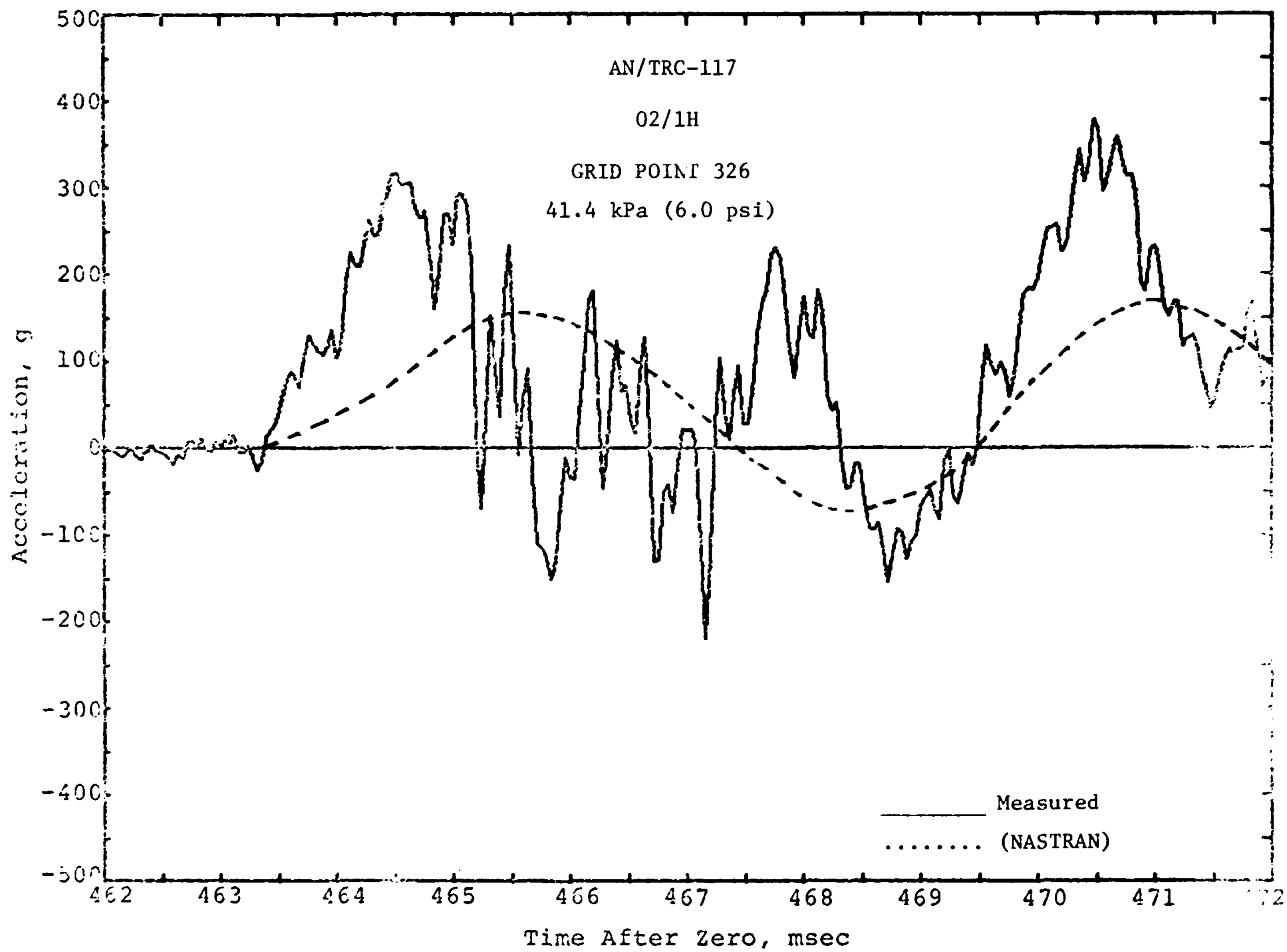

FIGURE 3.63. COMPARISON OF ACCELERATION TIME HISTORIES IN BLAST DIRECTION, ROADSIDE RACK

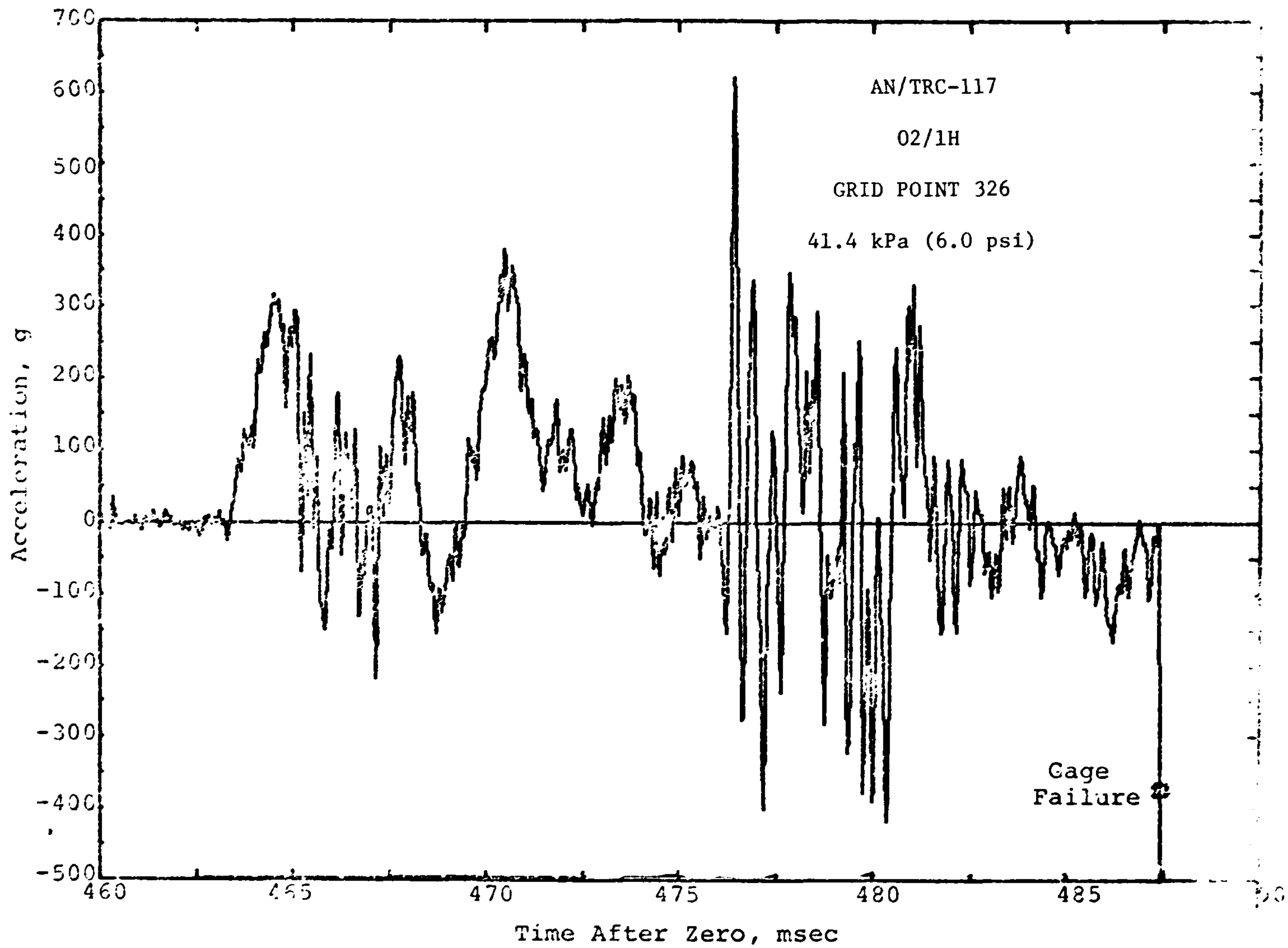

FIGURE 3.64. MEASURED ACCELERATION TIME HISTORY IN HORIZONTAL DIRECTION, ROADSIDE RACK

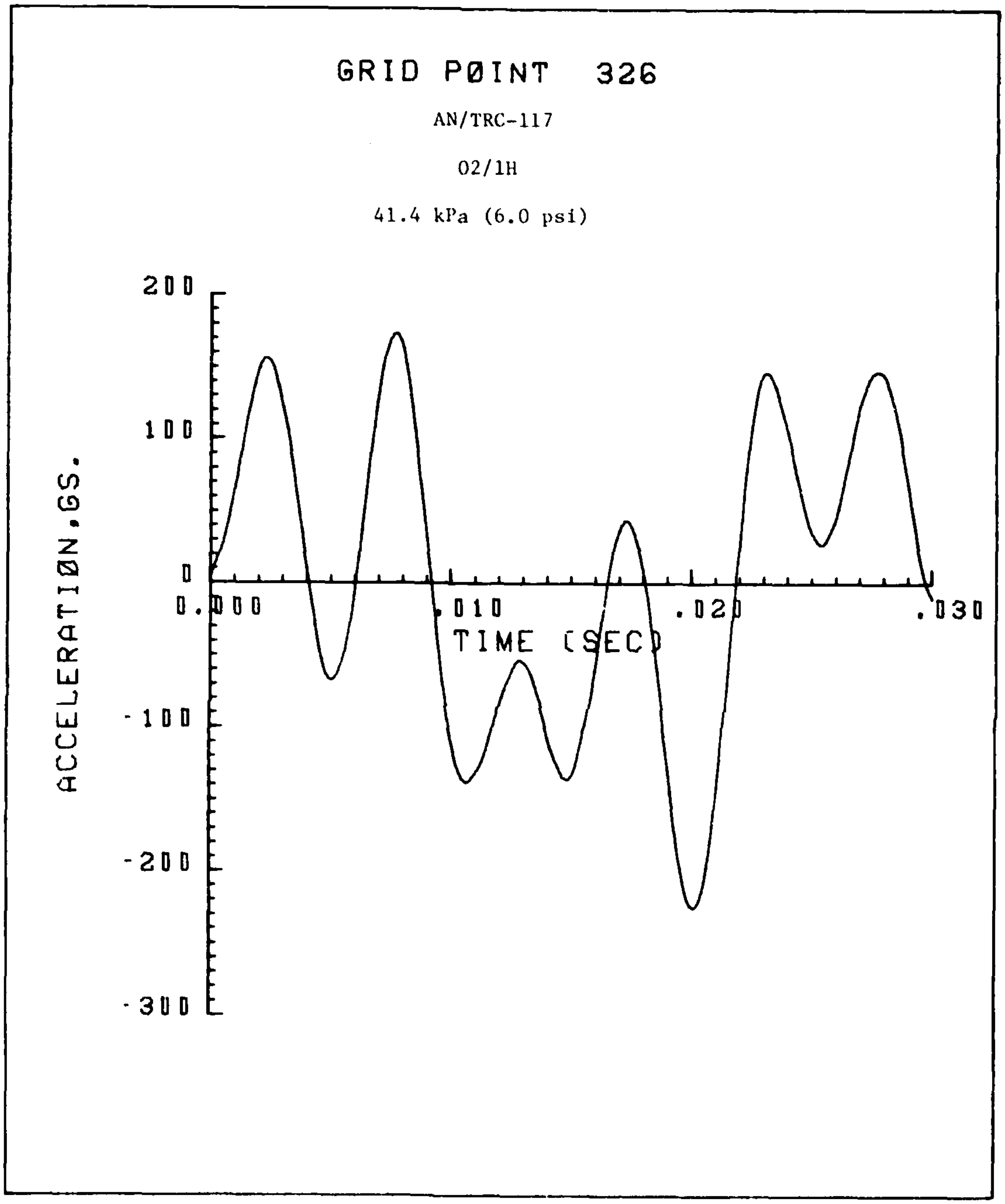

FIGURE 3.65. ACCELERATION TIME HISTORY IN BLAST DIRECTION, ROADSIDE RACK (NASTRAN)

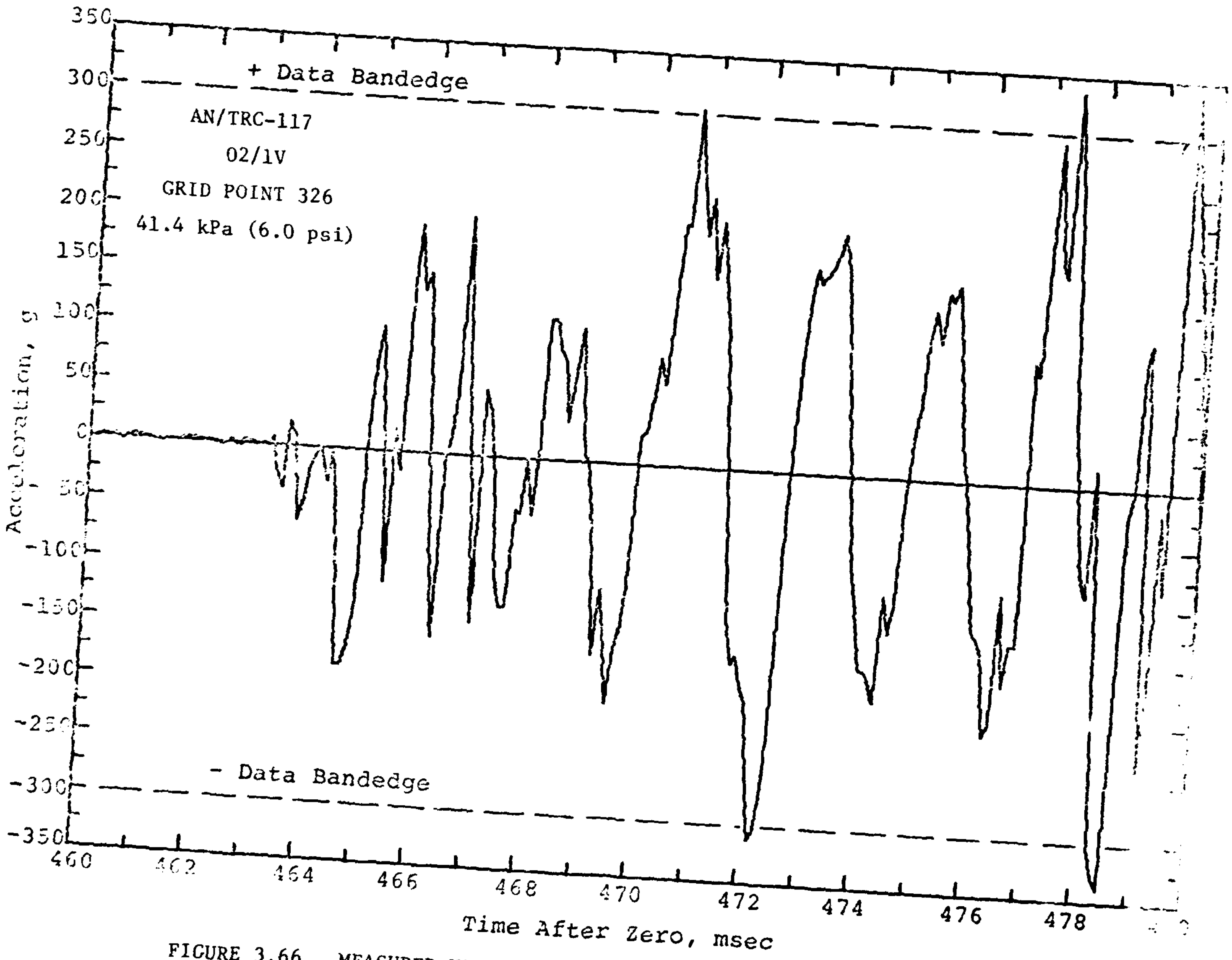

FIGURE 3.66. MEASURED VERTICAL ACCELERATION TIME HISTORY, ROADSIDE RACK

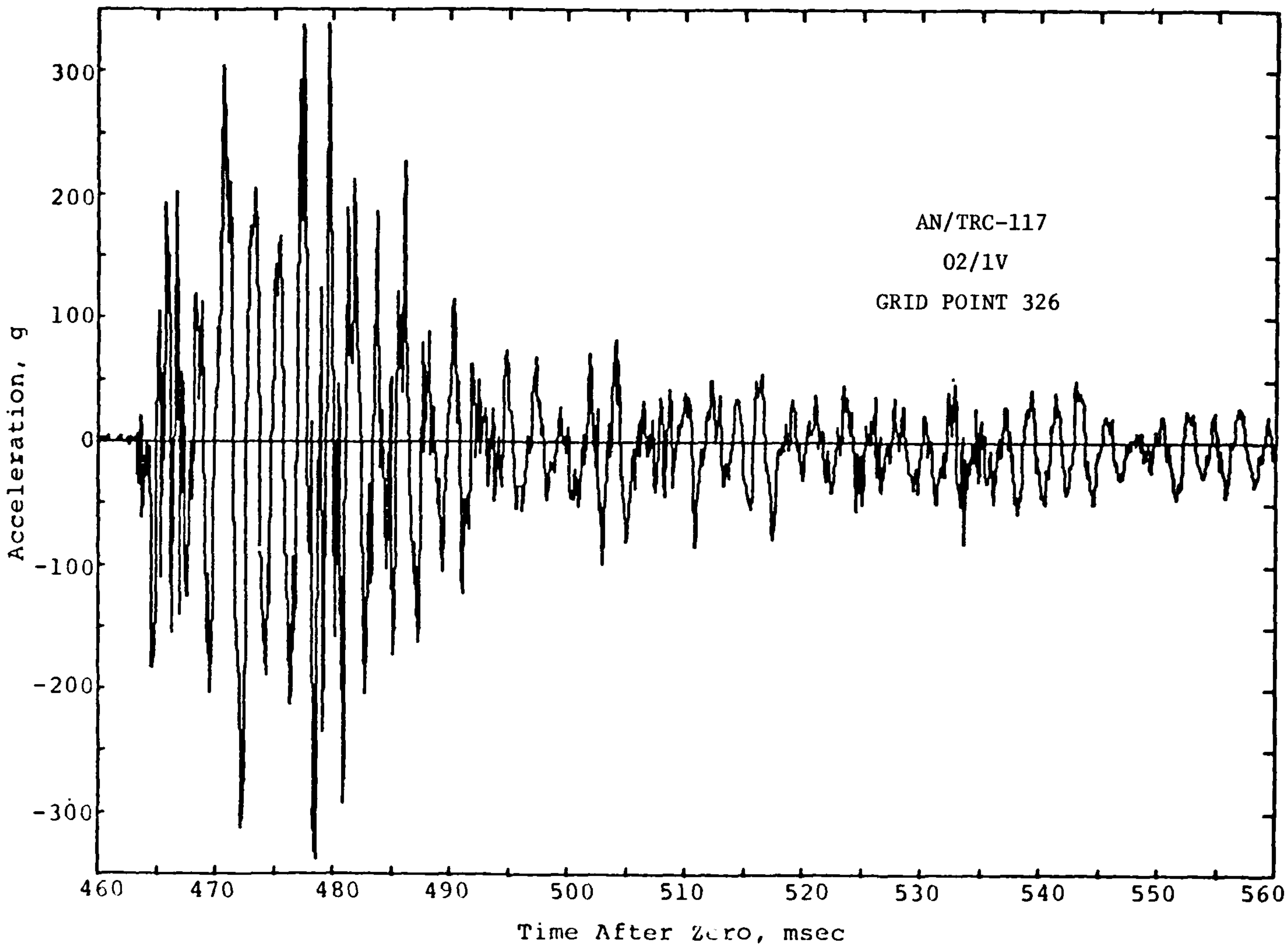

FIGURE 3.67. MEASURED VERTICAL ACCELERATION TIME HISTORY, ROADSIDE RACK

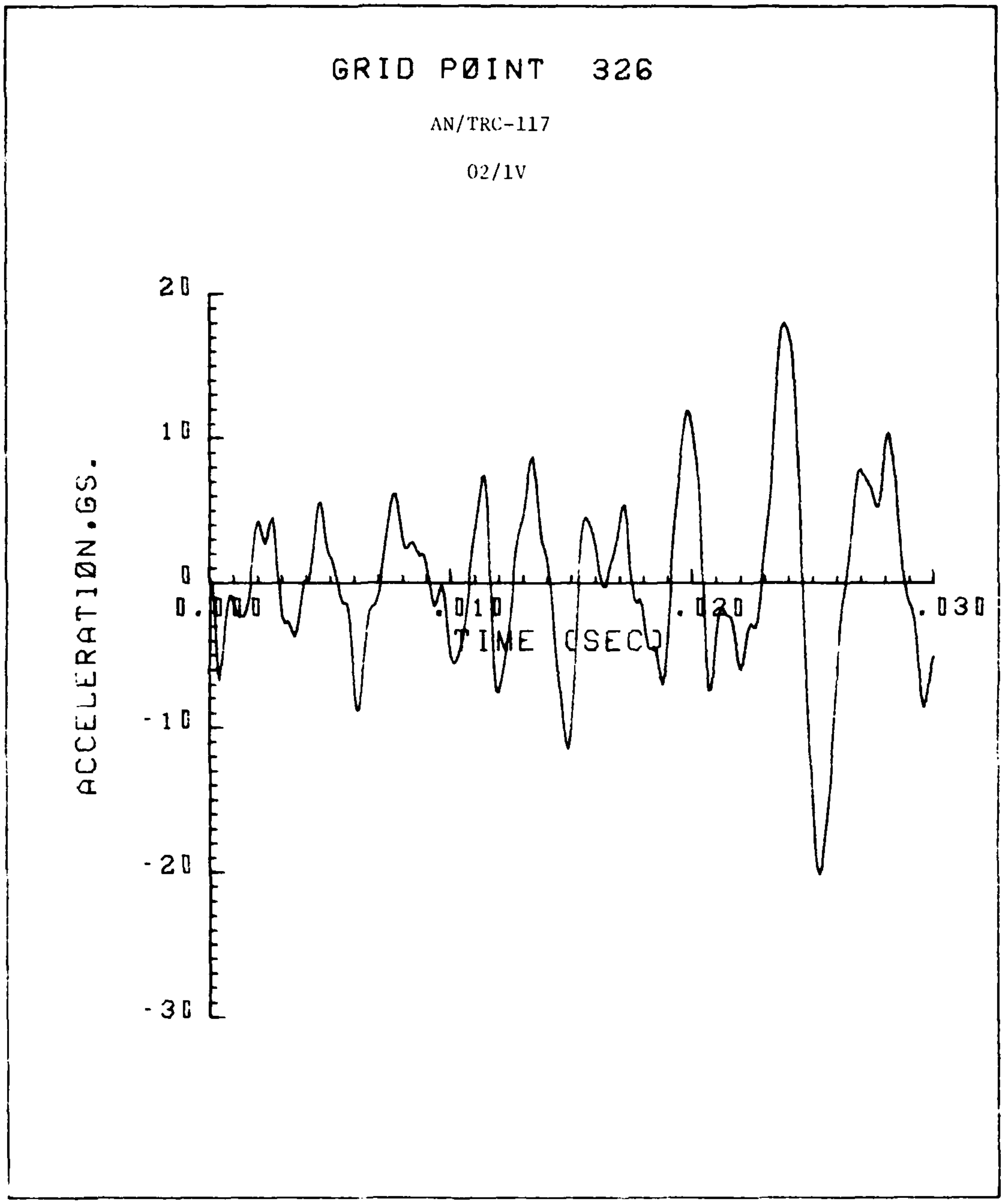

FIGURE 3.68. VERTICAL ACCELERATION TIME HISTORY, ROADSIDE RACK (NASTRAN)

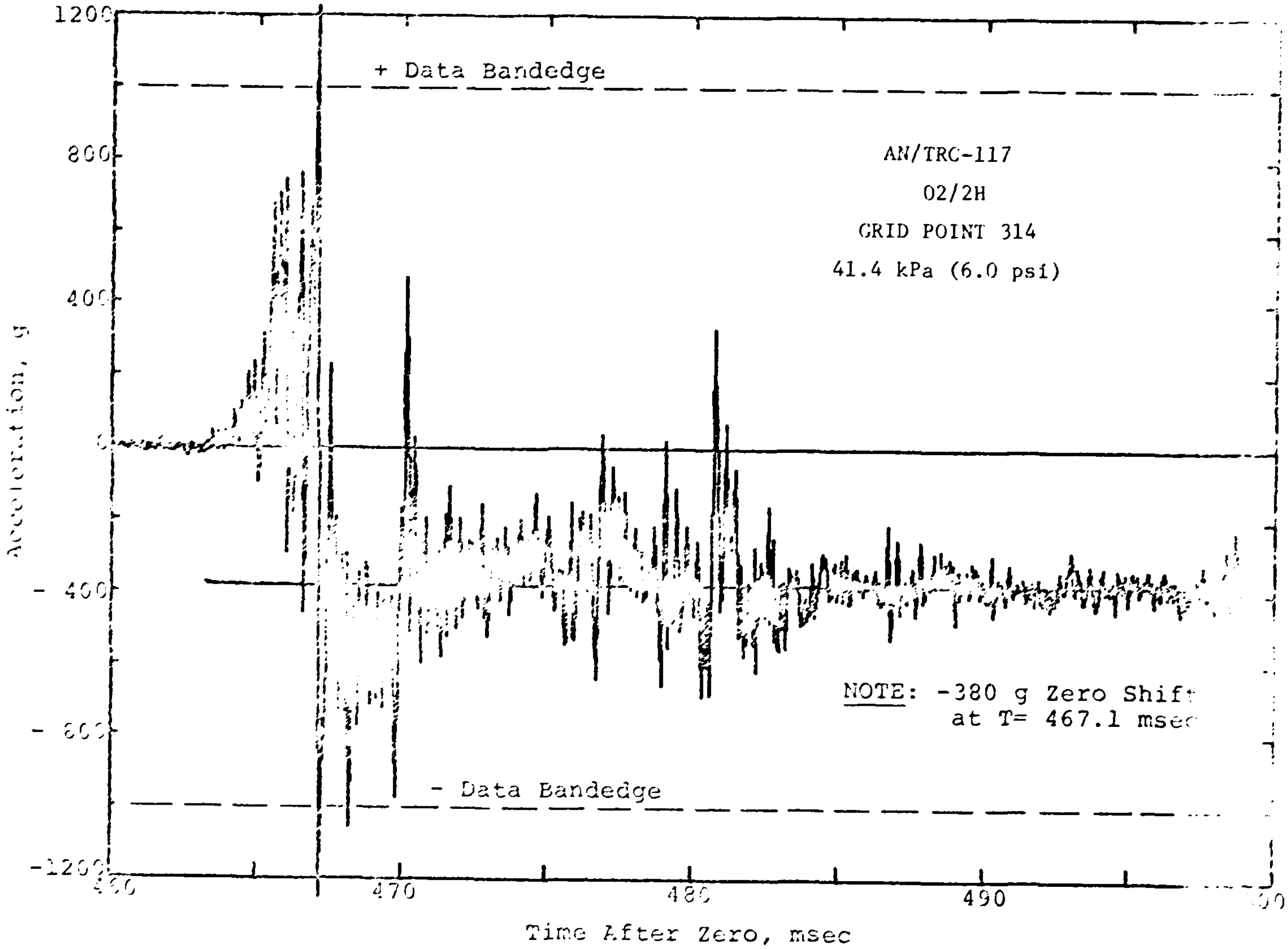

FIGURE 3.69. MEASURED ACCELERATION TIME HISTORY IN BLAST DIRECTION, ROADSIDE RACK

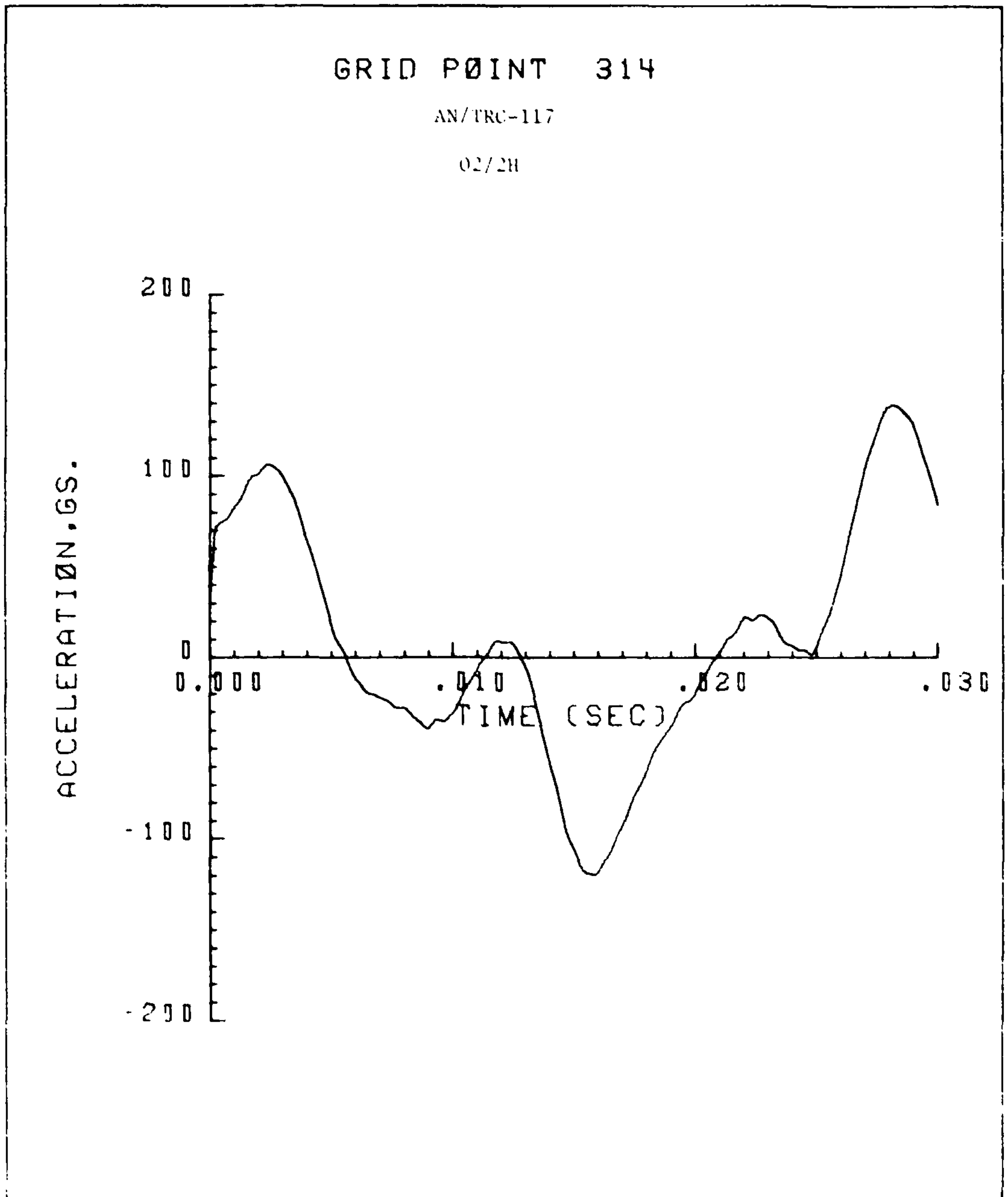

FIGURE 3.70. ACCELERATION TIME HISTORY IN BLAST DIRECTION, ROADSIDE RACK (NASTRAN)

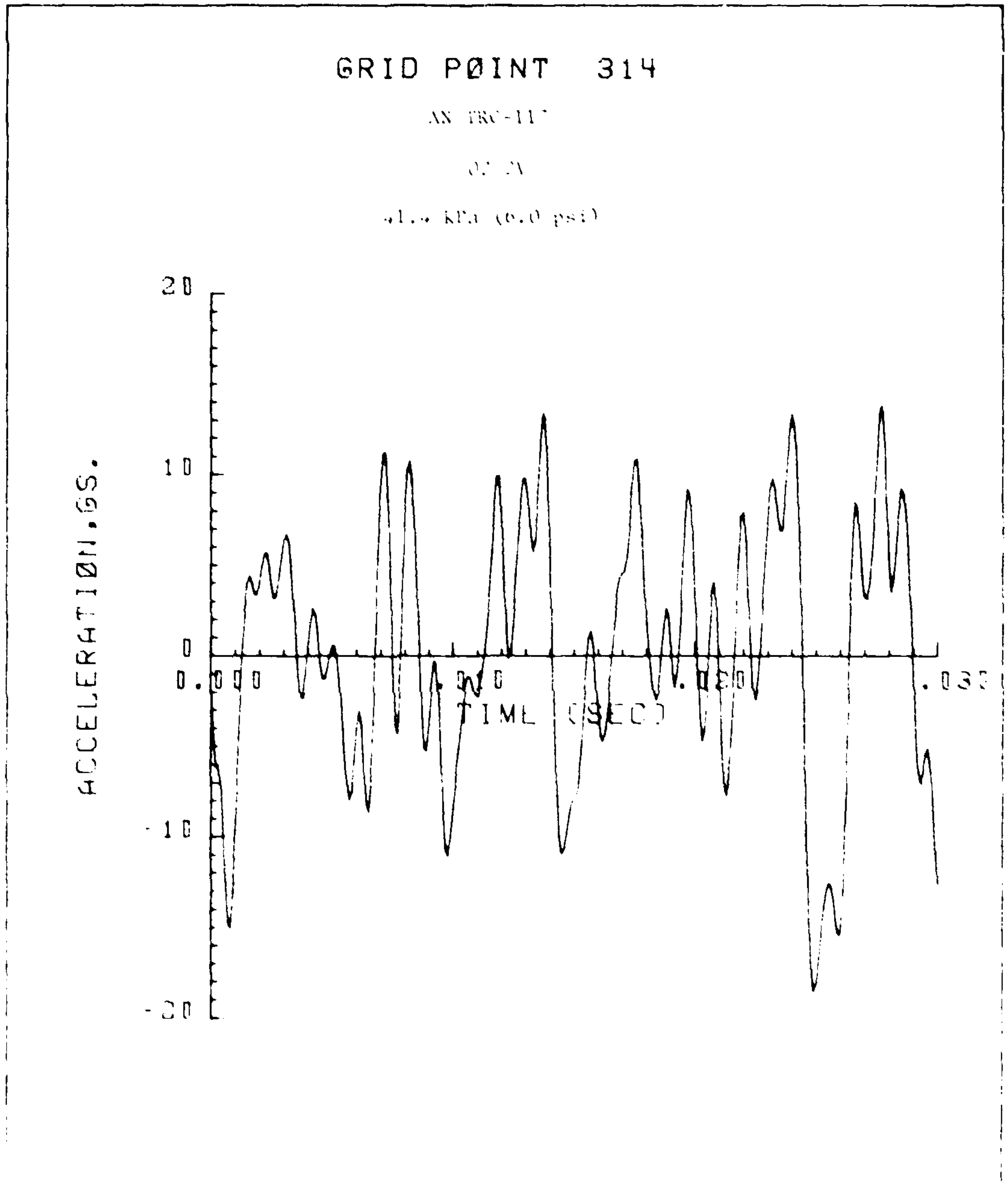
GRID PØINT 314
20
10
0
-10
-20
ACCELERATIØN,GS.
0.000
.010
.020
.030
TIME (SEC)

AD-A085 759 KAMAN AVIDYNE BURLINGTON MA F/G 17/2
STRUCTURAL MODELING AND RESPONSE OF COMMAND, CONTROL AND COMMUN--ETC(U)
MAR 80 J M CALLIGEROS, J P WALSH DAAD05-74-C-0744

UNCLASSIFIED KA-TR-151 ARBRL-CR-00421 NL

3 of 3
AD-A085759

END
DATE
FILMED
7-80
DTIC

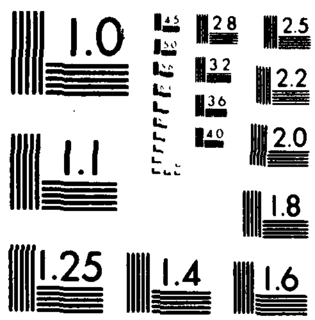

MICROCOPY RESOLUTION TEST CHART

NATIONAL BUREAU OF STANDARDS 1963 A

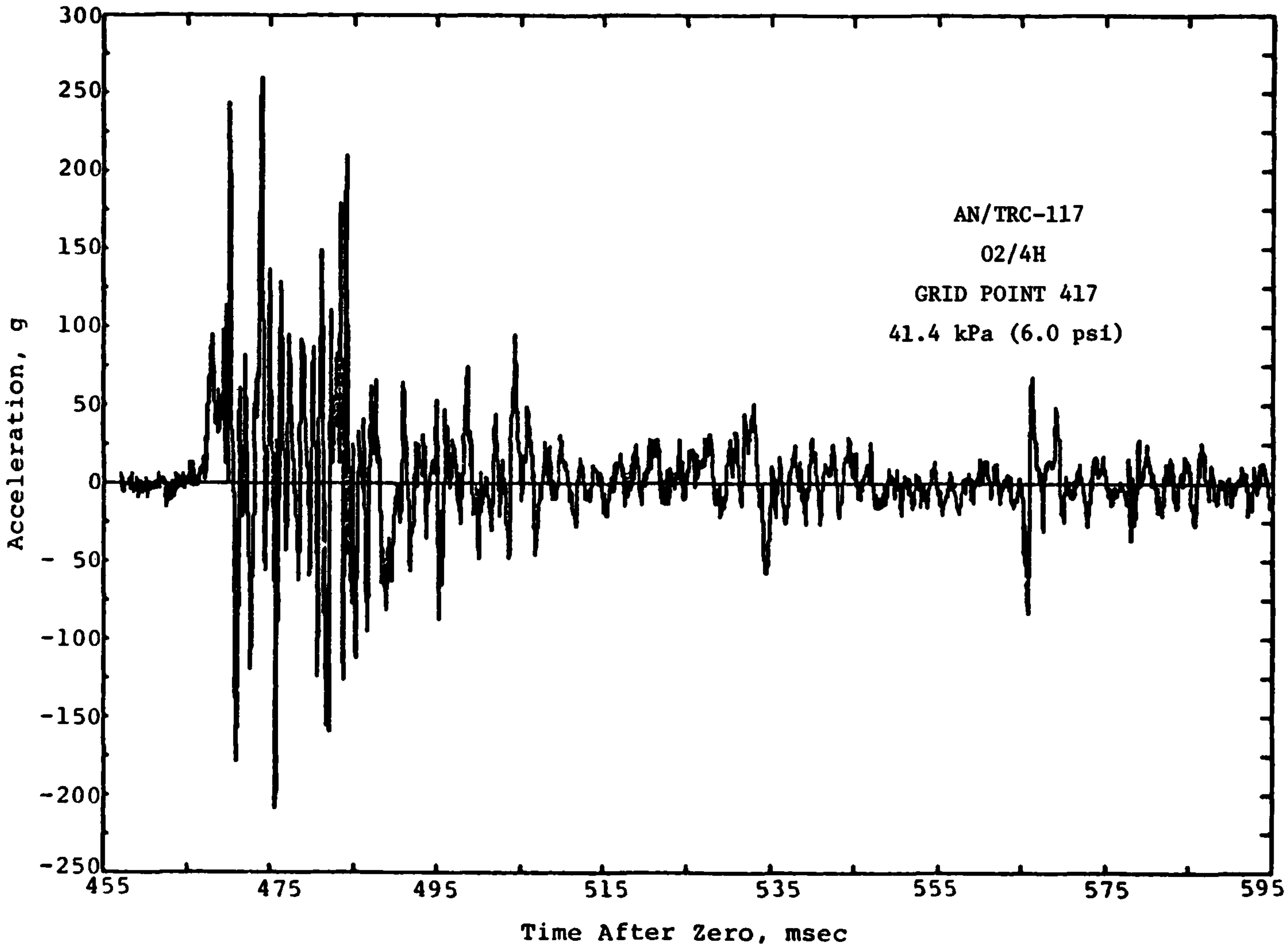

FIGURE 3.72. MEASURED ACCELERATION TIME HISTORY IN BLAST DIRECTION, FRONT END RACKS

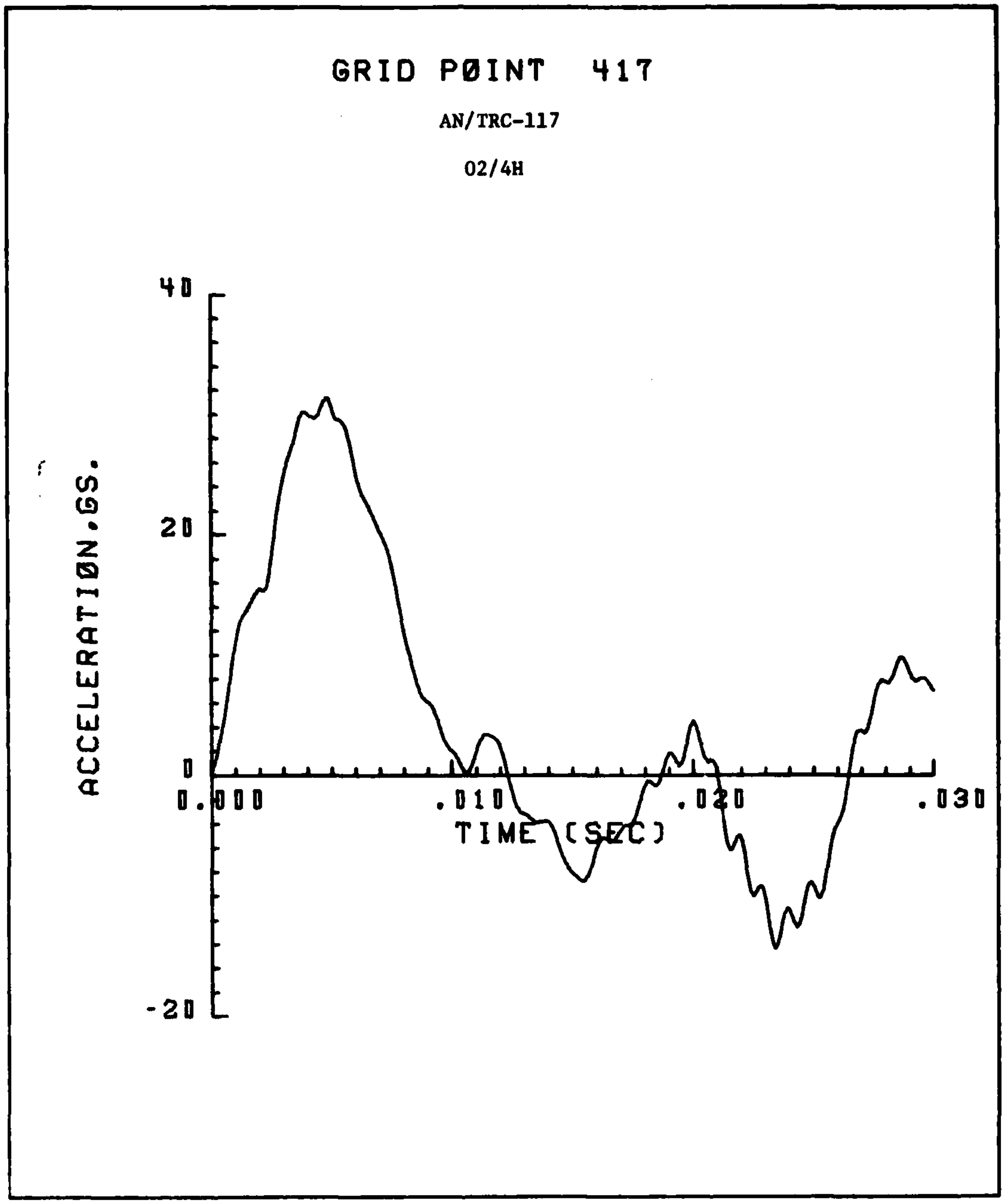

FIGURE 3.73. ACCELERATION TIME HISTORY IN BLAST DIRECTION, FRONT END RACK (NASTRAN)

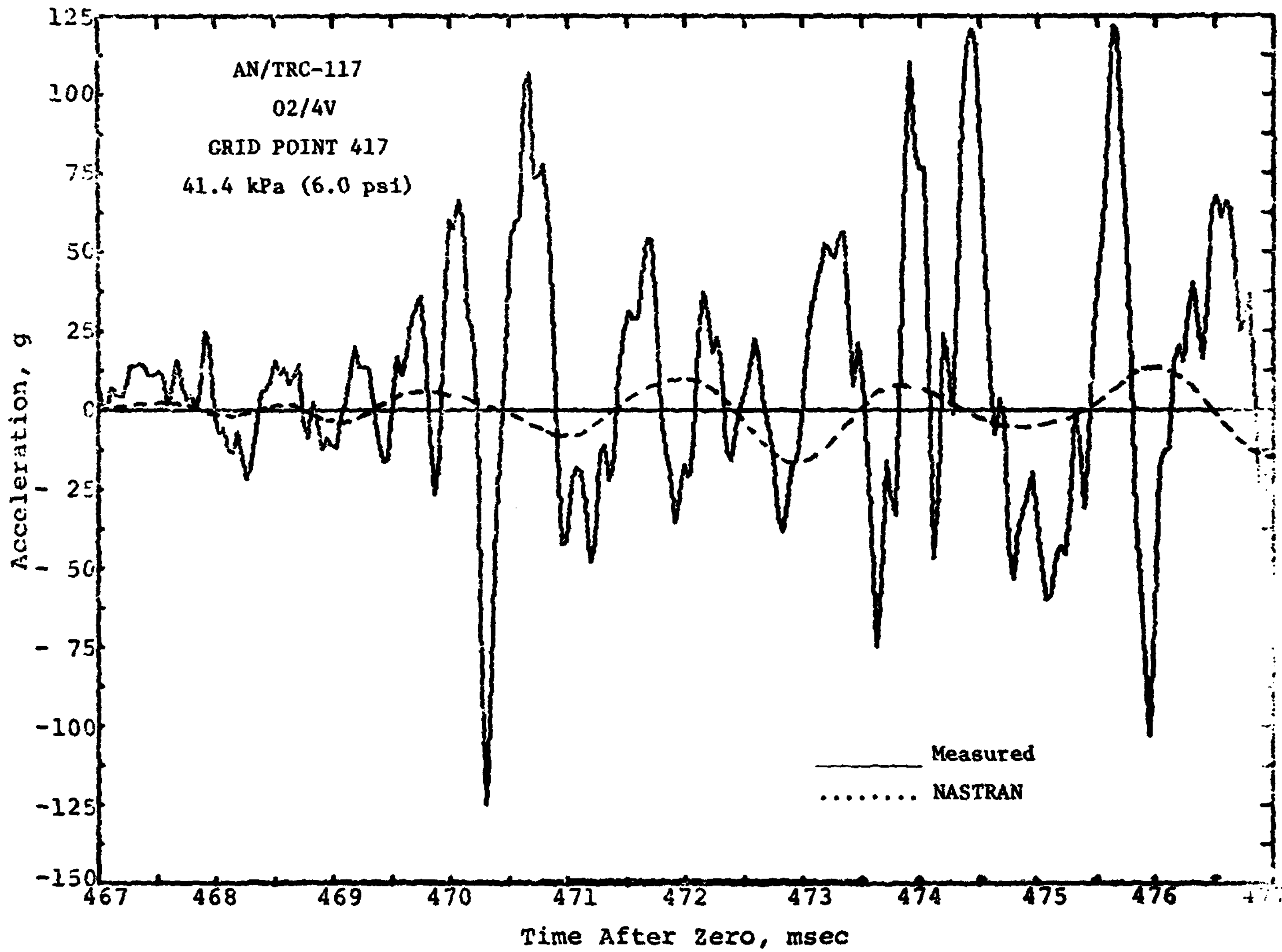

FIGURE 3.74. COMPARISON OF VERTICAL ACCELERATION TIME HISTORIES, FRONT END RACK

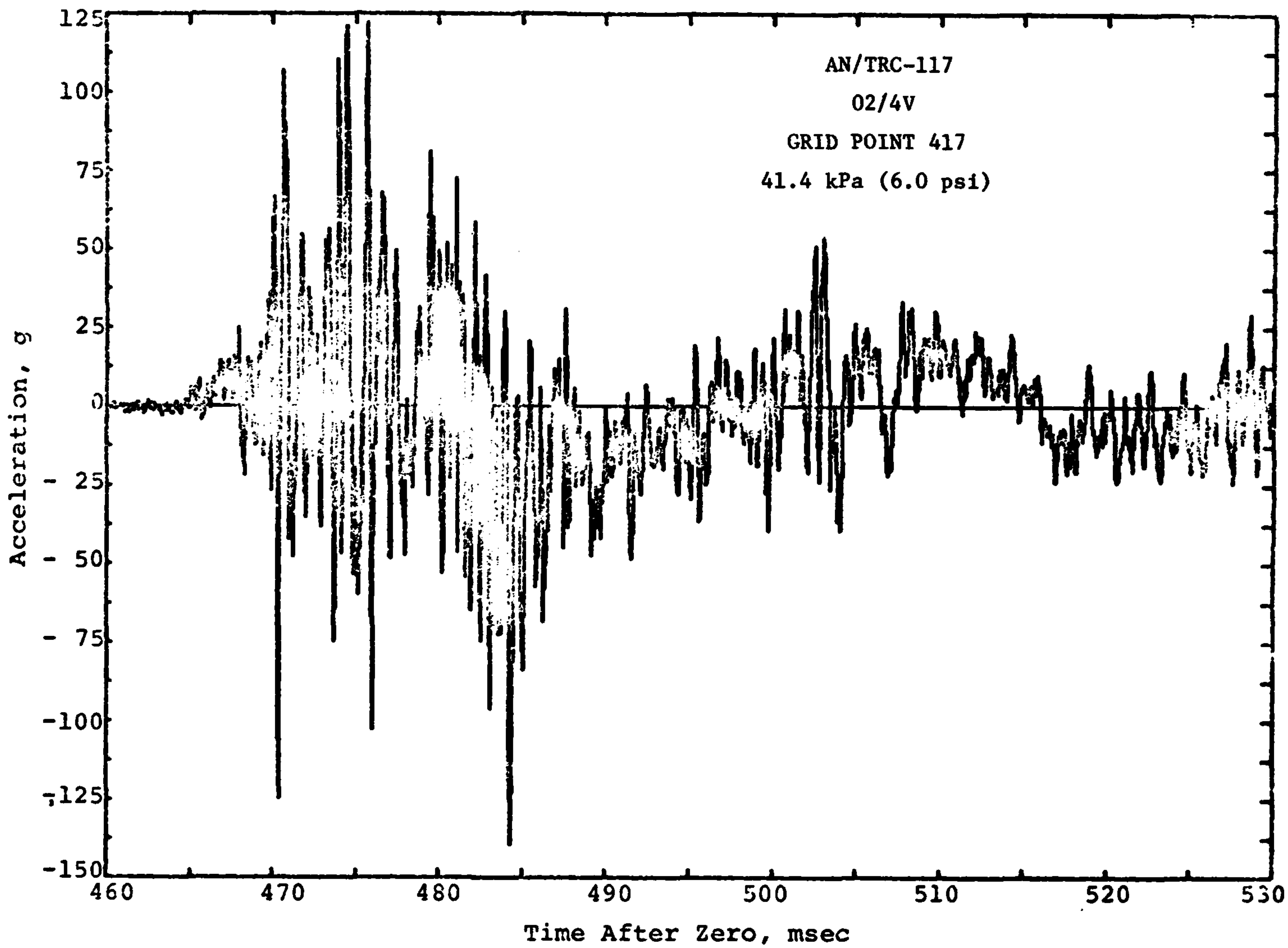

FIGURE 3.75. MEASURED VERTICAL ACCELERATION TIME HISTORY, FRONT END RACK

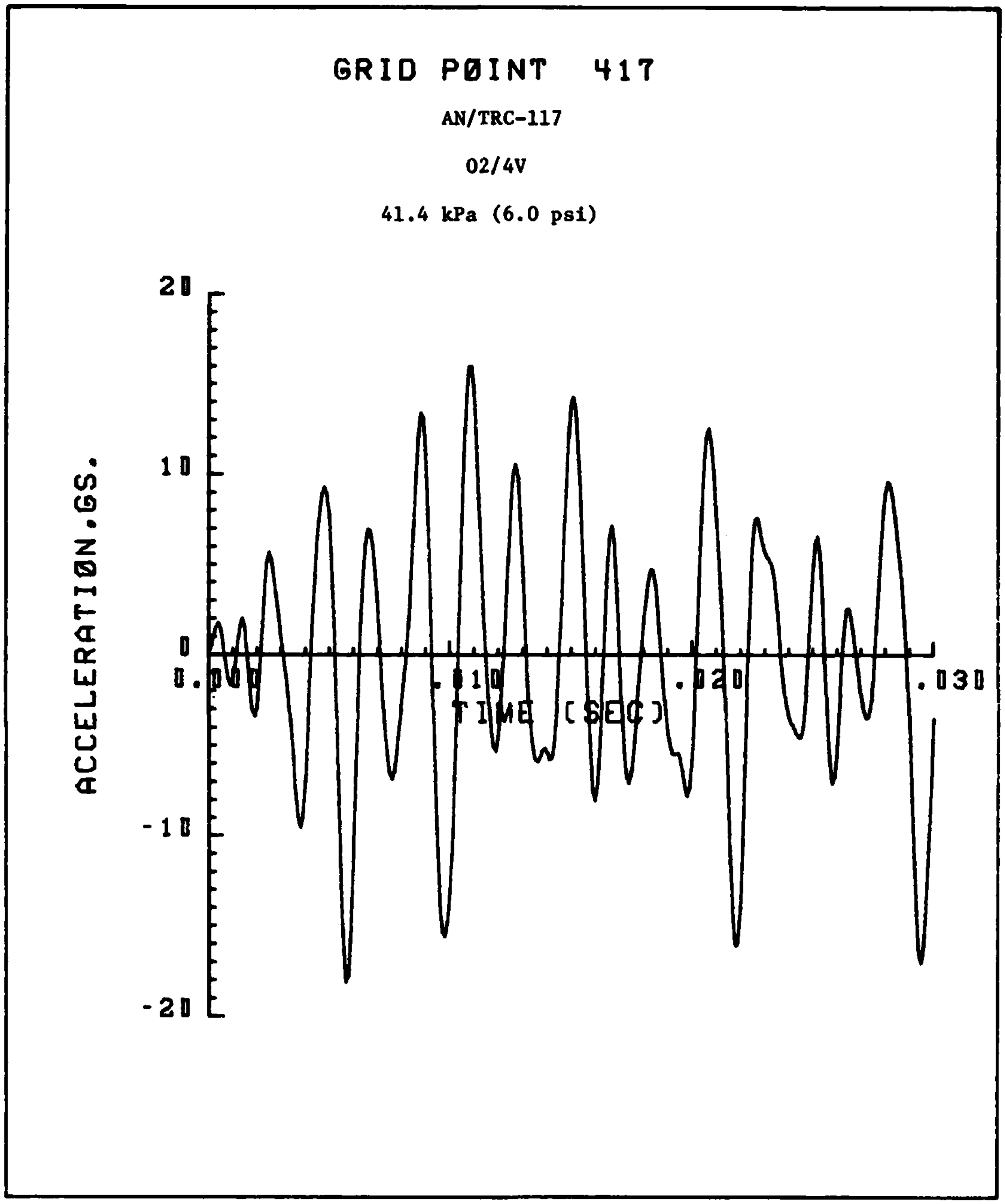

FIGURE 3.76. VERTICAL ACCELERATION TIME HISTORY, FRONT END RACK (NASTRAN)

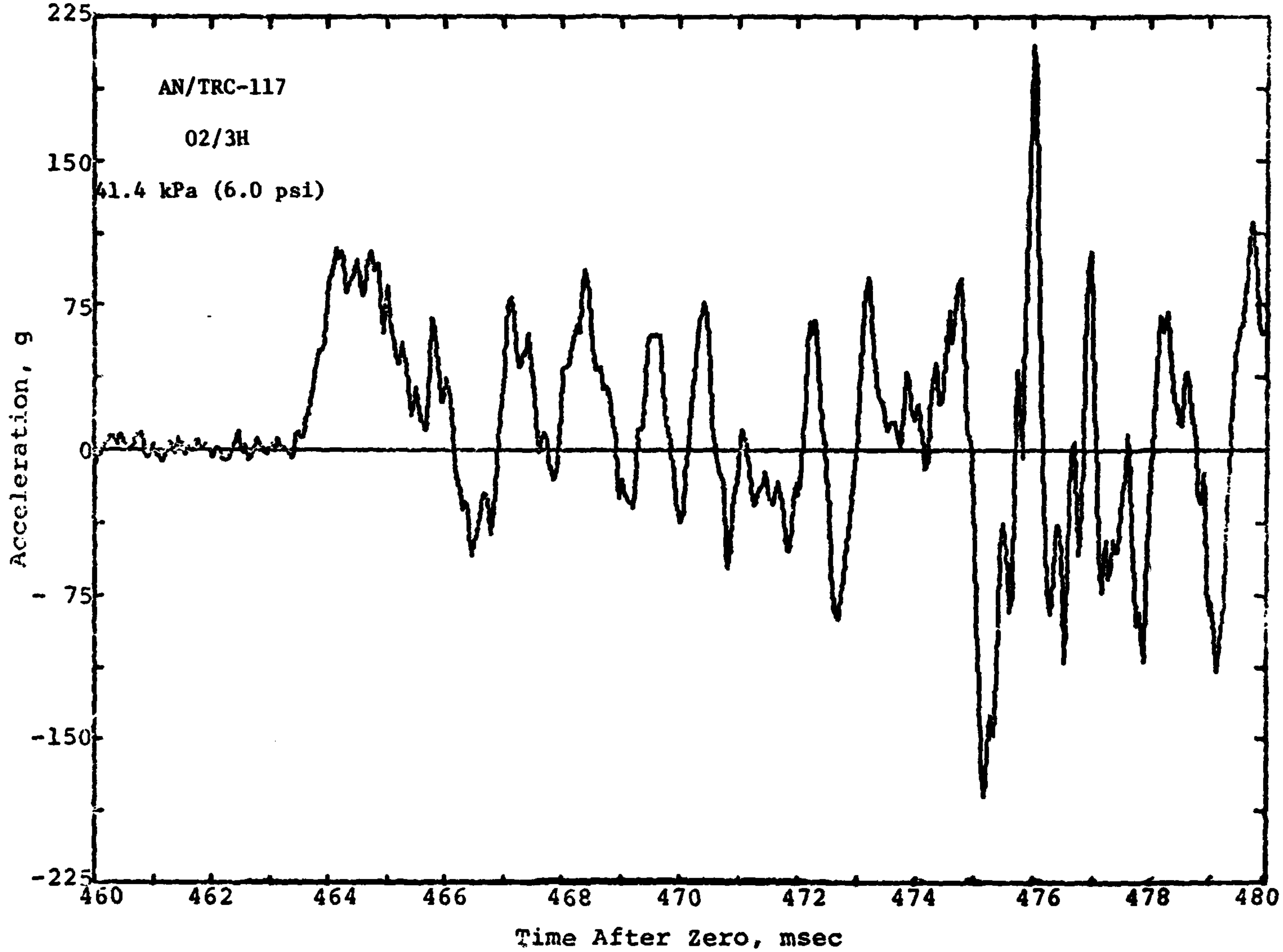

FIGURE 3.77. MEASURED ACCELERATION TIME HISTORY IN BLAST DIRECTION, CENTER OF FLOOR

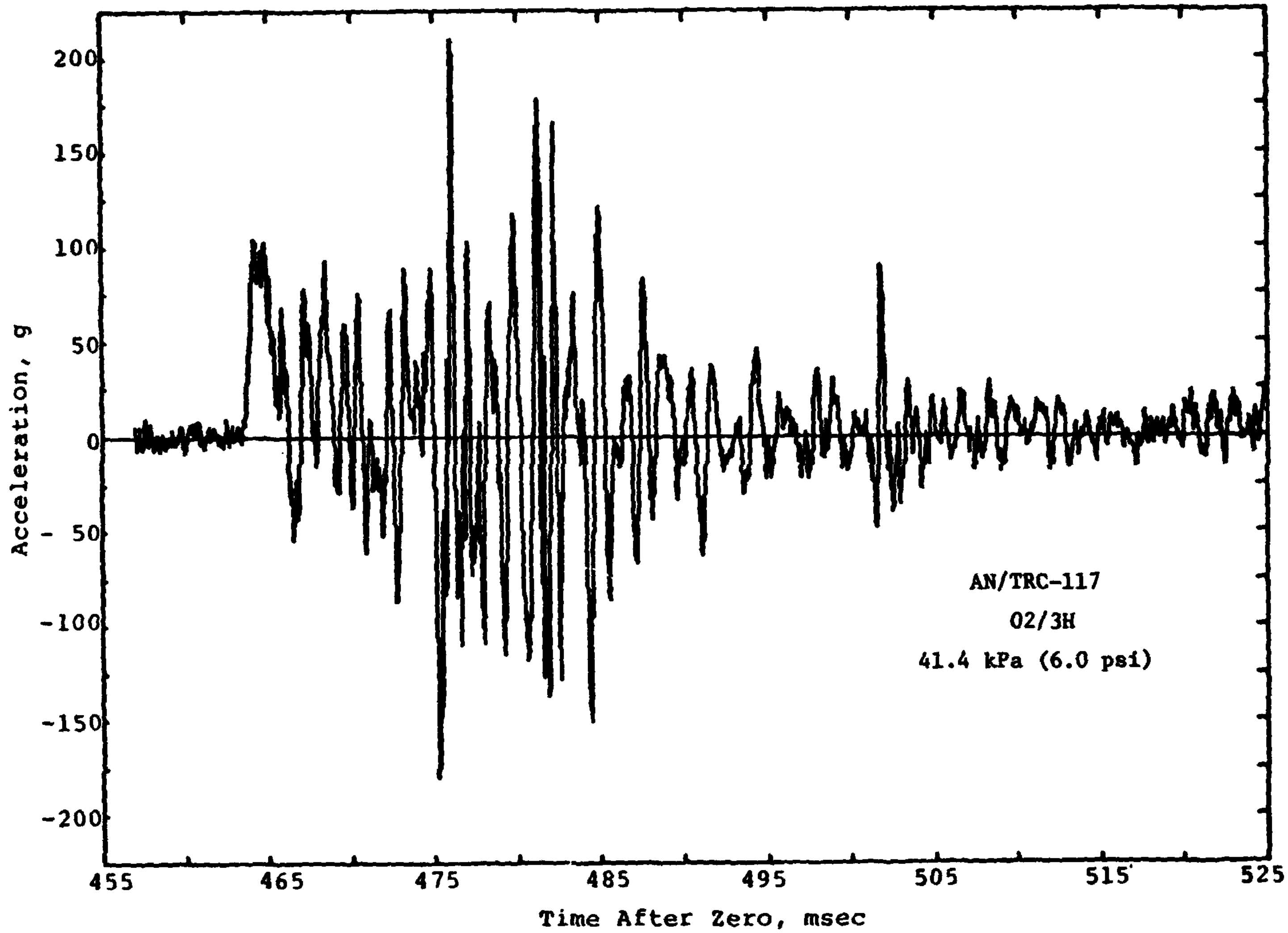

FIGURE 3.78. MEASURED ACCELERATION TIME HISTORY IN BLAST DIRECTION, CENTER OF FLOOR

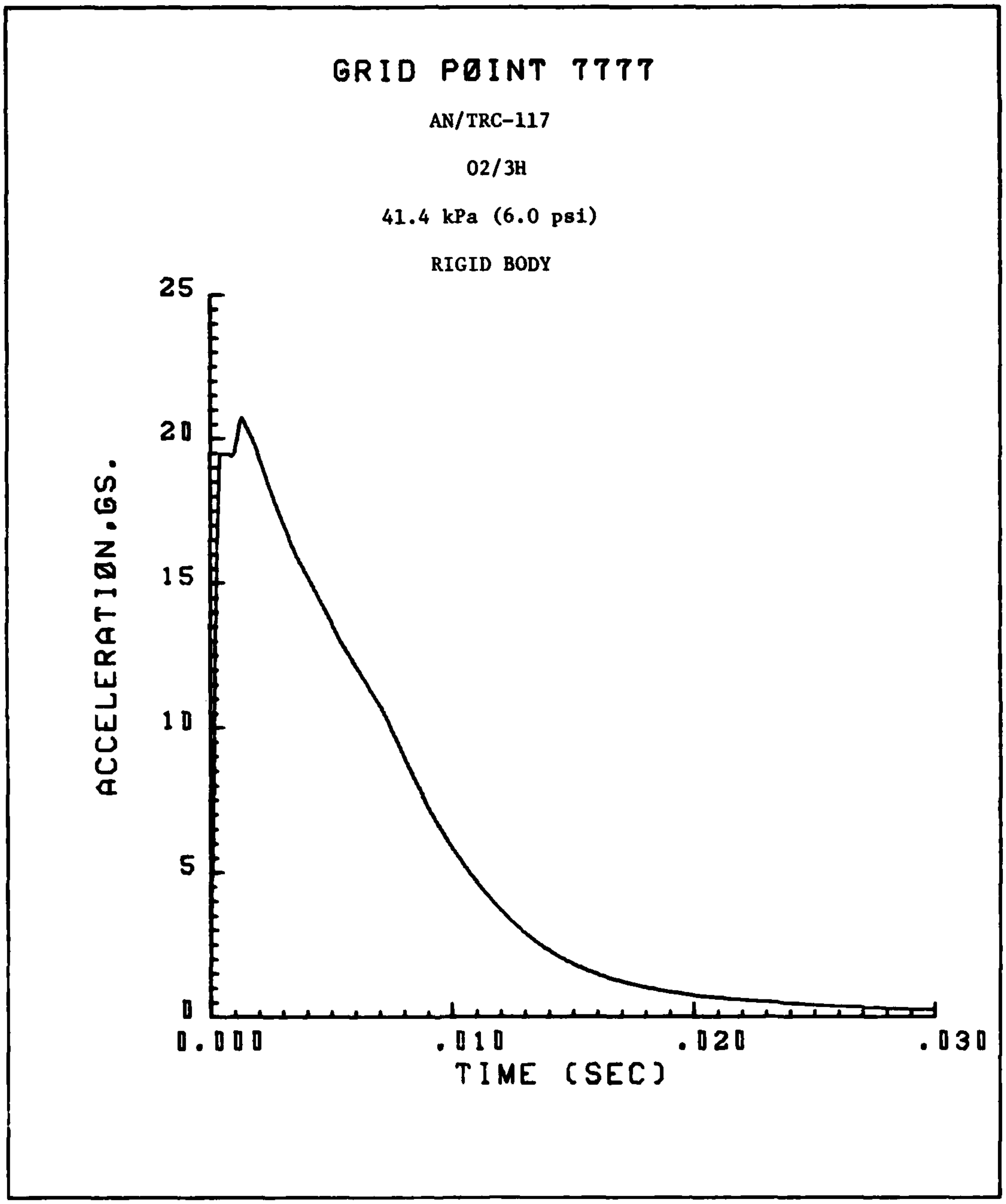

FIGURE 3.79. ACCELERATION TIME HISTORY IN BLAST DIRECTION, CENTER OF FLOOR (NASTRAN)

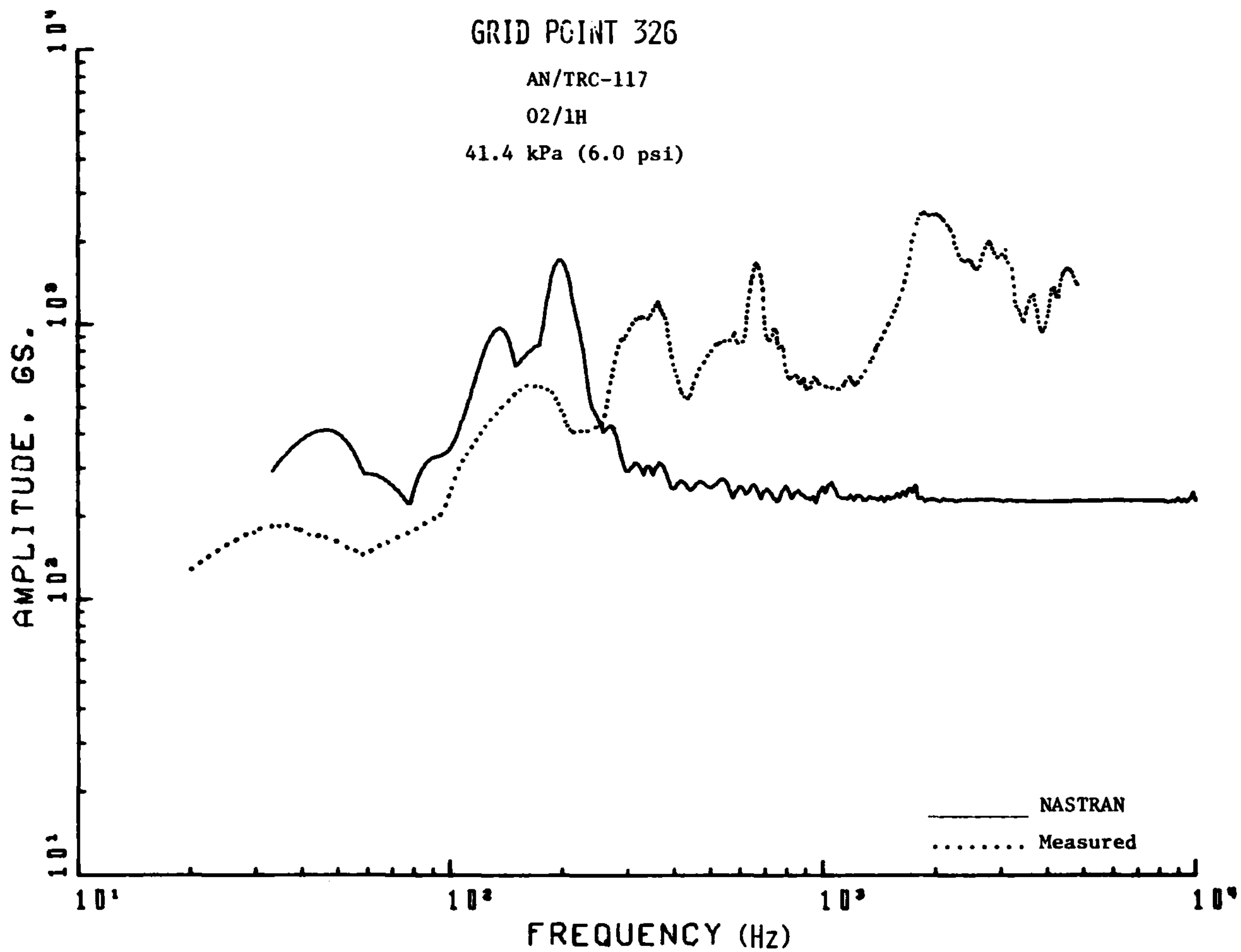

FIGURE 3.80. COMPARISON OF SHOCK SPECTRA BASED ON MEASURED AND ANALYTICAL ACCELERATION TIME HISTORIES IN BLAST DIRECTION, ROADSIDE RACK

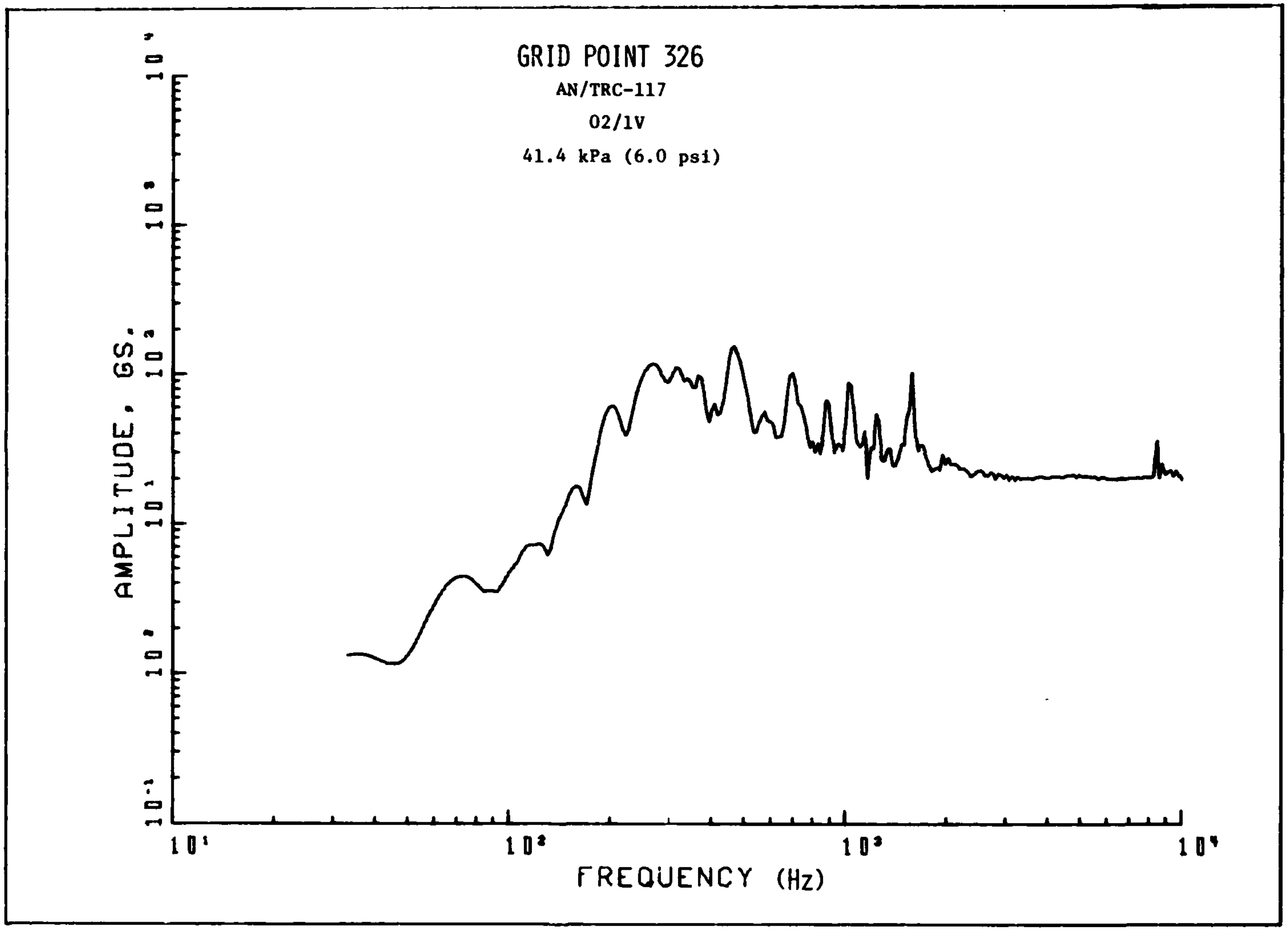

FIGURE 3.81. SHOCK SPECTRUM BASED ON ANALYTICAL VERTICAL ACCELERATION TIME HISTORY, ROADSIDE RACK (NASTRAN)

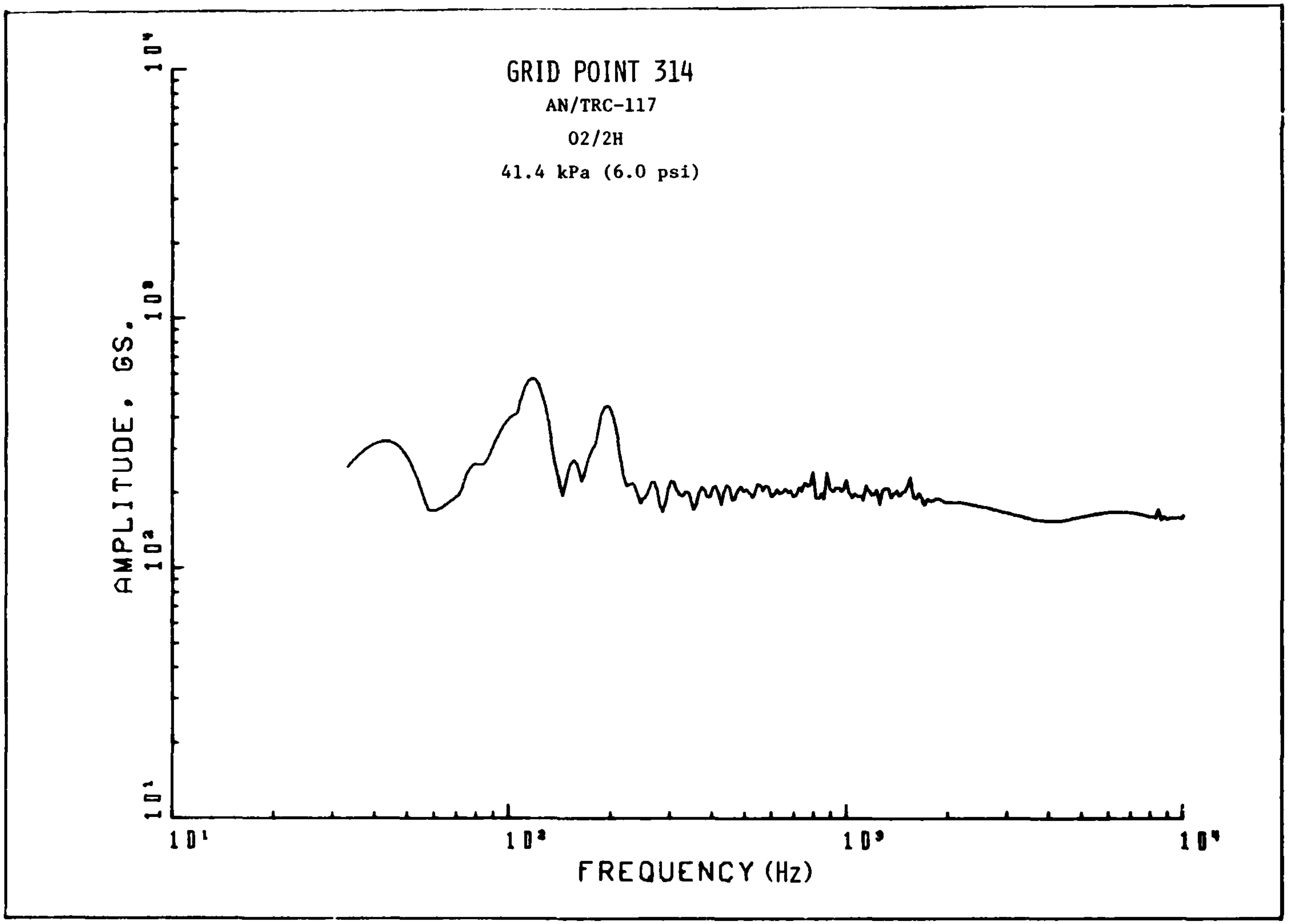

FIGURE 3.82. SHOCK SPECTRUM BASED ON ANALYTICAL ACCELERATION TIME HISTORY IN BLAST DIRECTION, ROADSIDE RACK (NASTRAN)

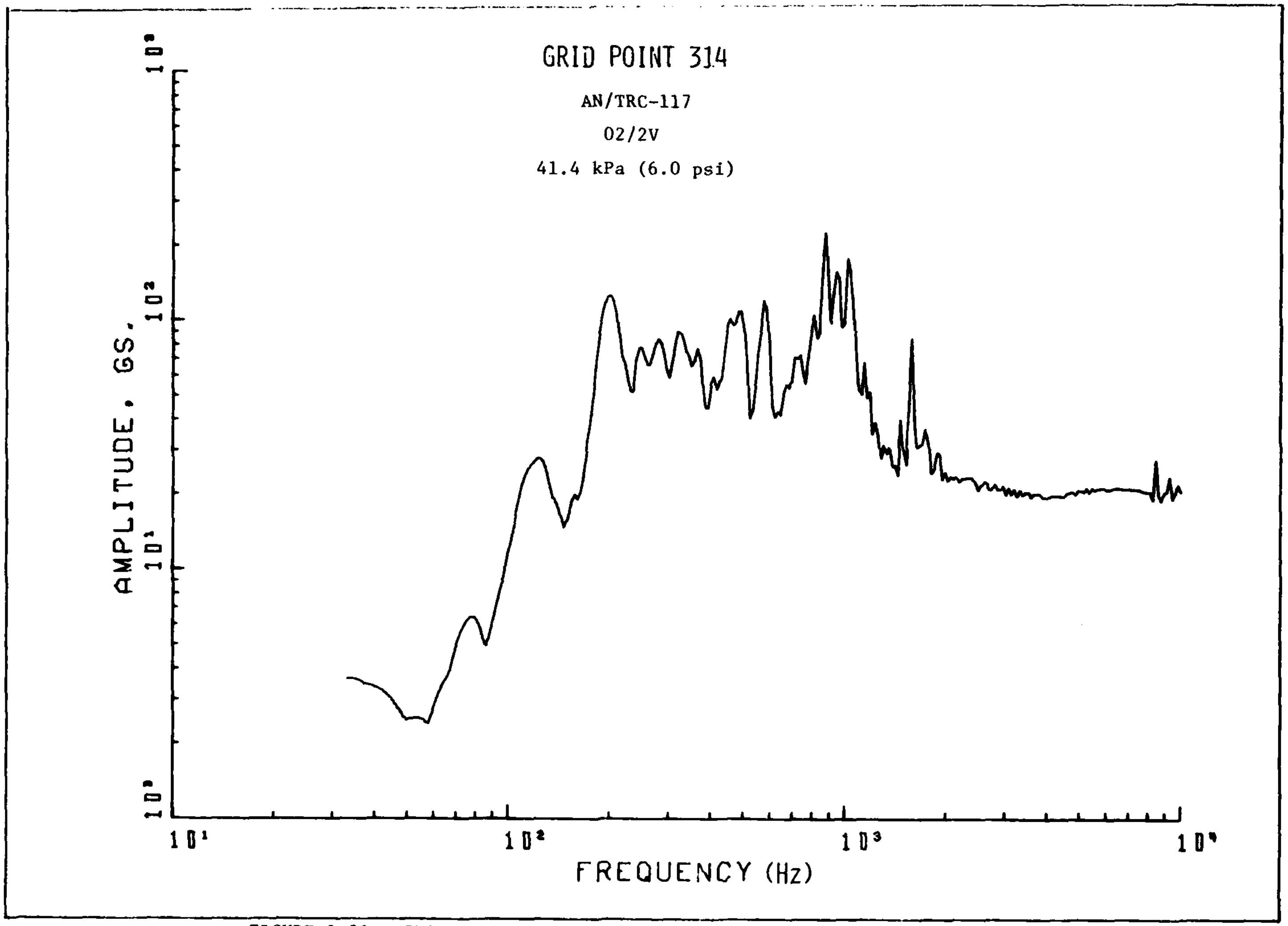

FIGURE 3.83. SHOCK SPECTRUM BASED ON ANALYTICAL VERTICAL TIME HISTORY, ROADSIDE RACK (NASTRAN)

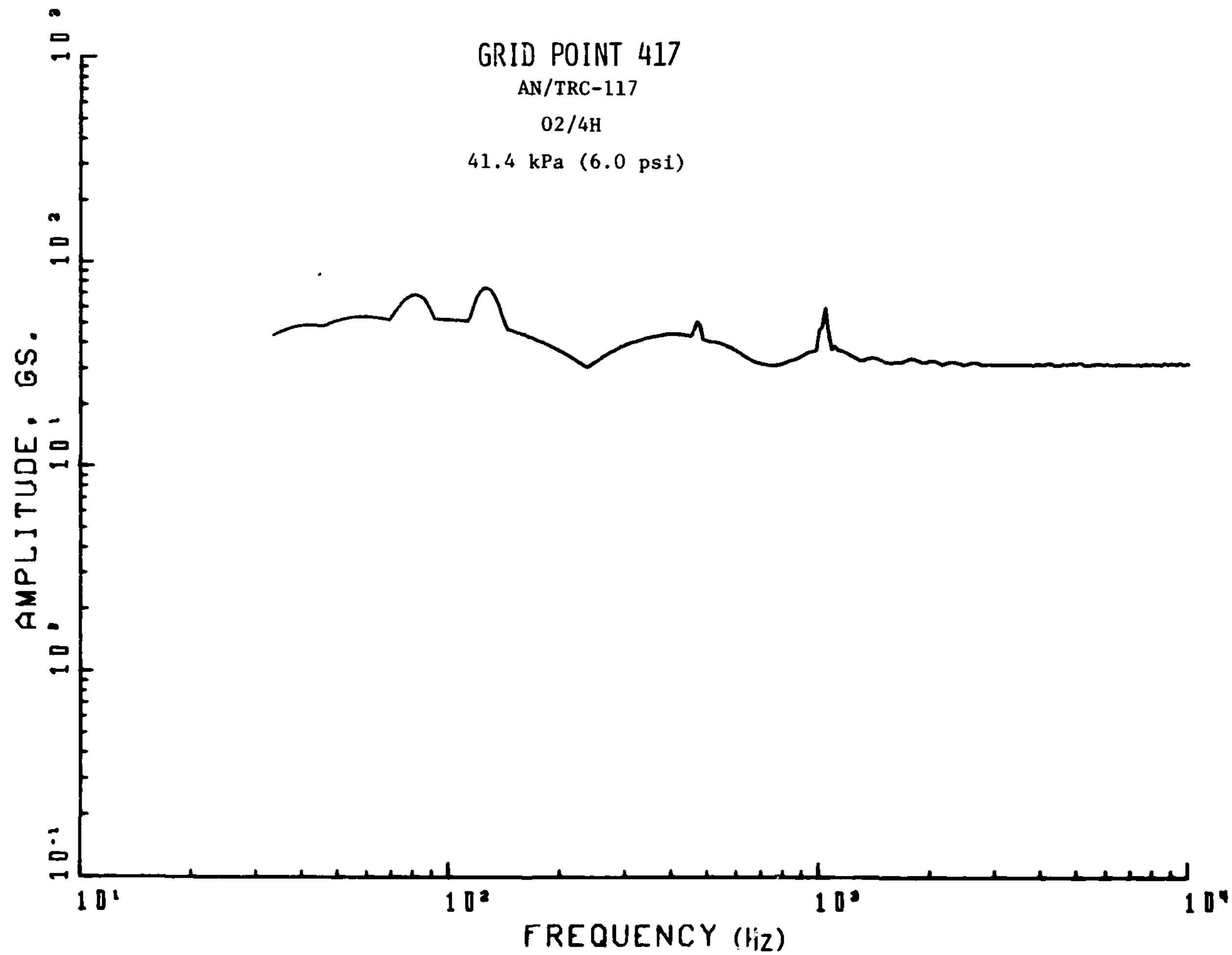

FIGURE 3.84. SHOCK SPECTRUM BASED ON ANALYTICAL ACCELERATION TIME HISTORY IN BLAST DIRECTION, FRONT END RACK (NASTRAN)

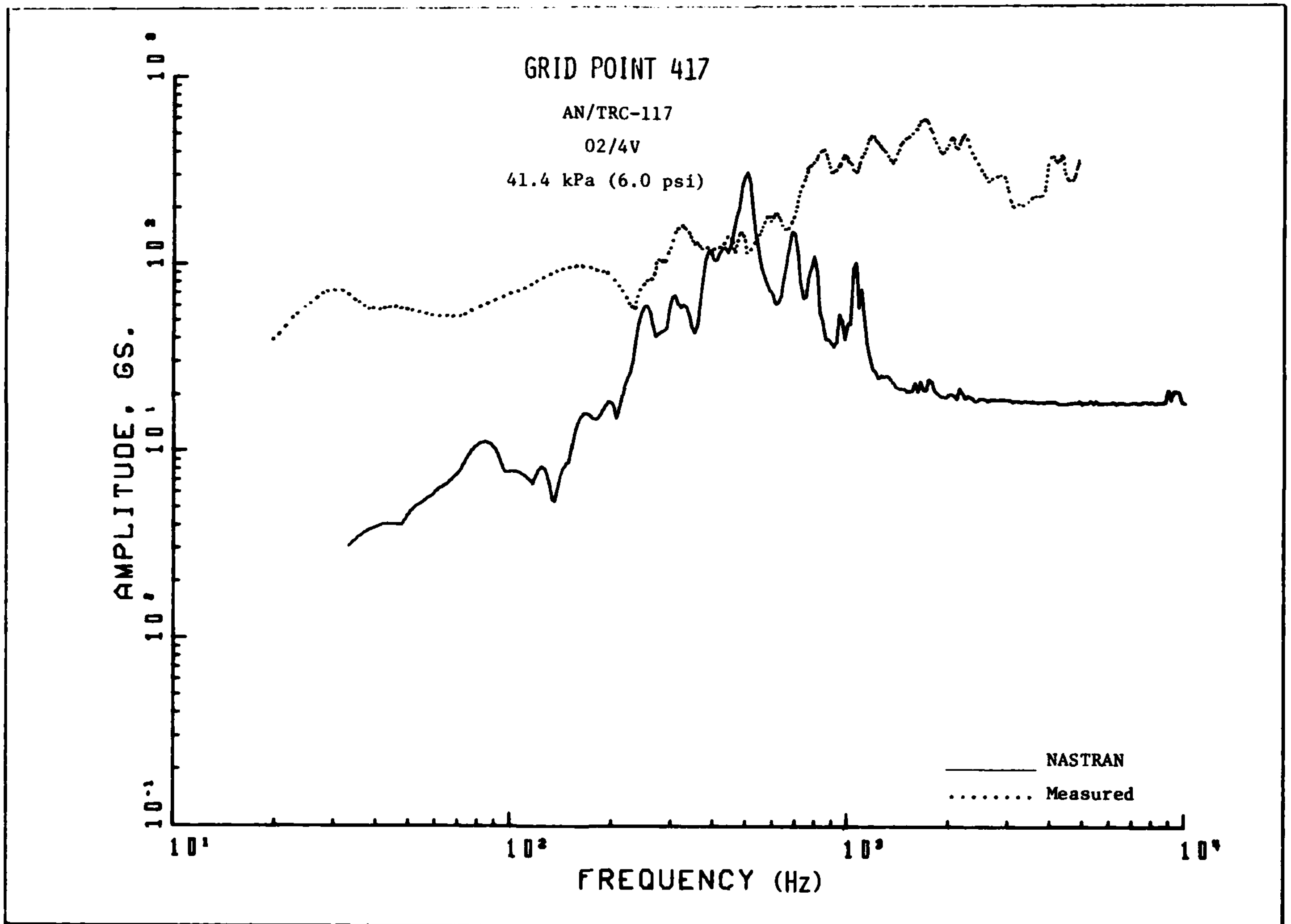

FIGURE 3.85. COMPARISON OF SHOCK SPECTRA BASED ON MEASURED AND ANALYTICAL VERTICAL ACCELERATION TIME HISTORY, FRONT END RACK

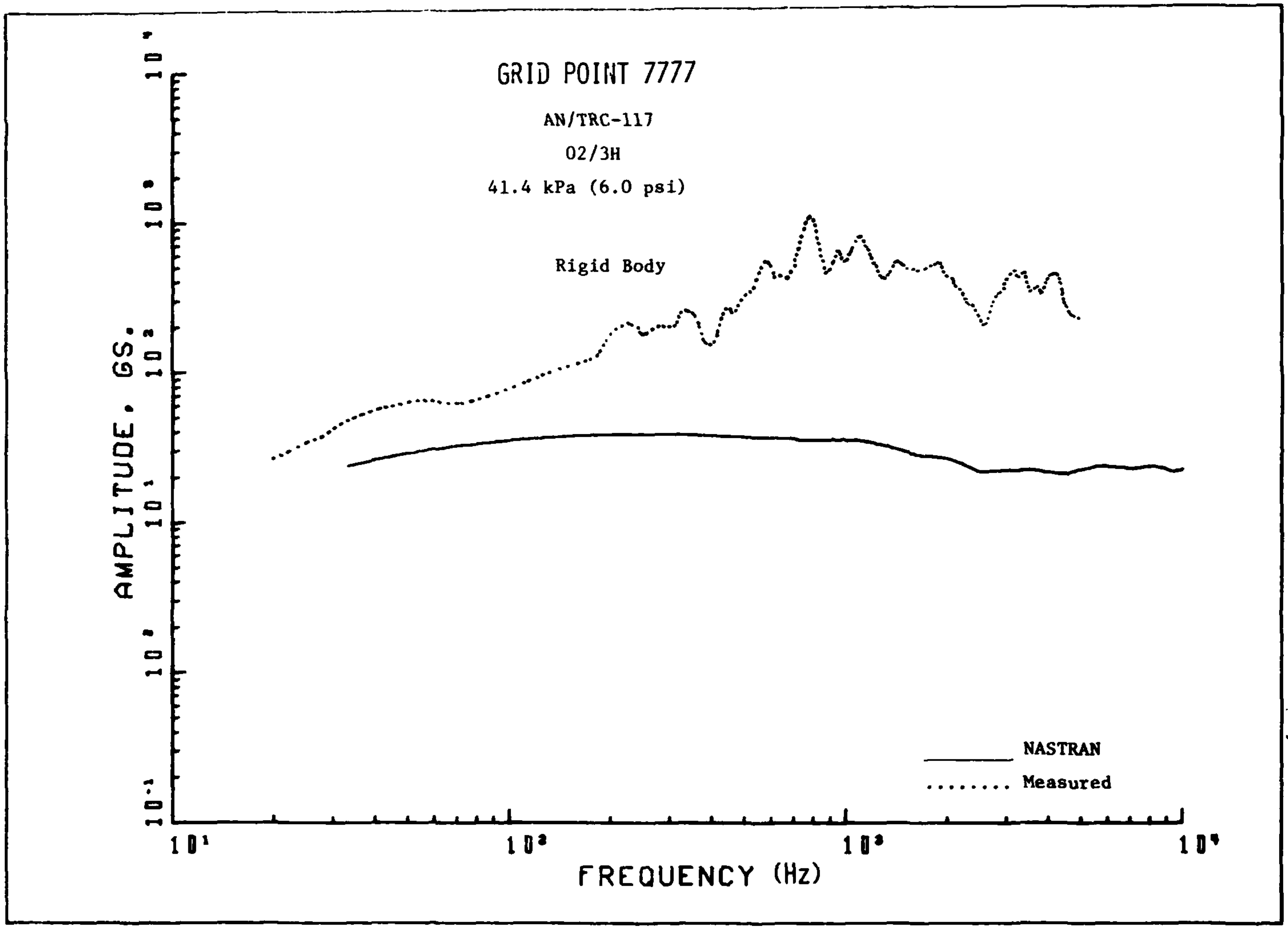

FIGURE 3.86. COMPARISON OF SHOCK SPECTRA BASED ON MEASURED AND ANALYTICAL ACCELERATION TIME HISTORIES IN BLAST DIRECTION, CENTER OF FLOOR

TABLE 3.4

FREQUENCY CONTENT AND ACCELERATIONS OF MEASURED

AND PREDICTED RESPONSES FOR THE AN/TRC-117

GAGE	APPROXIMATE DOMINANT FREQUENCY (Hz)		ACCELERATION AMPLITUDE RATIO
	MEASURED	PREDICTED	MEASURED/PREDICTED
02/1H	2000	170	2
02/1V	700	400	30
02/2H	2500	120	11
02/2V	-	1000	-
02/4H	1500	130	8
02/4V	1500	500	6
02/3H	1000	rigid body	5

The higher frequency content of the measured data may be due to structural accelerations which are being sensed by the accelerometer gage at its mounting location. This is evidenced by gage 02/3H (Figures 3.77 and 3.78) which was installed for the purpose of measuring the rigid body acceleration of the center of the shelter floor. The high frequency content at gage 02/3H is not representative of a rigid body response but rather is characteristic of a response containing localized structural frequencies. The corresponding analytical rigid body response is shown in Figure 3.79, having a peak one fifth of the measured peak and decaying to nearly zero after 30 msecs.

The complete set of shock spectra plots is given in Figures 3.80-3.86 for the AN/TRC-117. Comparisons are shown in Figures 3.80, 3.85 and 3.86, using the corresponding measured and analytical acceleration time histories in Figures 3.63-3.76. The disparity noted earlier between the measured time-history data and the analytical predictions is also reflected in the shock spectra, i.e., the experimental shock spectra are significantly higher than the analytical predictions over most of the frequency range. The closest agreement is in the frequency range between 100 Hz and 300 Hz in Figure 3.80 and between 200 Hz and 700 Hz in Figure 3.85. The shock spectrum comparison in Figure 3.86 is meaningless because the floor accelerometer does not reflect realistically the rigid body response of the system.

The measured and predicted accelerations for the AN/TRC-145 are shown in Figures 3.87-3.97 for the two gages located on the roadside rack, and in Figures 3.98-3.100 for the gage located on the front end rack. A summary of the dominant frequency and acceleration amplitude ratio for each gage as determined from these plots is given in Table 3.5.

The comparison in peak acceleration between measured and predicted responses is much more favorable for the AN/TRC-145 than it was for the AN/TRC-117. As can be seen in Table 3.5, the greatest discrepancy occurs at gage 01/2V, where the measured peak acceleration is 1.8 times greater than the predicted value. Very good comparisons are seen for gages 01/1V and 01/2H. The measured frequencies, however, are significantly greater than the predicted frequencies, as was also the case for the AN/TRC-117. A good comparison in frequency is seen in Figure 3.87, however, at a level of 400 Hz. The measured response in that figure, though, also has a higher frequency of about 2200 Hz which is not present in the predicted curve. As in the case for the AN/TRC-117, the floor gage (01/3H, Figure 3.101) had a high frequency content characteristic of a local structural response rather than the rigid body response. The measured floor acceleration was four times greater than the predicted rigid body acceleration, consistent with the results for the AN/TRC-117.

The shock spectra for the AN/TRC-145 are shown in Figures 3.103-3.109 and comparisons are given in Figures 3.103-3.106. The shock spectra comparisons are generally more favorable for the AN/TRC-145 then they were for the AN/TRC-117 because of the better agreement of the acceleration time histories. This is apparent also at the higher frequencies (1000 Hz or greater). It should be noted that the AN/TRC-145 is inherently a stiffer structure and has higher structural frequencies than the AN/TRC-117 (See Tables 2.21 and 2.40), and this would contribute to a higher shock spectrum at the higher frequencies for the AN/TRC-145.

A post test examination of the shelters revealed that the AN/TRC-117 had received moderate to heavy damage to the roadside wall and moderate to light buckling of the remaining shelter walls. The racks along the roadside wall sustained heavy damage, with the rack upright members bowing outward toward the center. The roadside wall was in contact with the racks in many places. On the other hand, the AN/TRC-145, being a more compact shelter system, received very little damage. The damage to the exterior walls varied from light buckling to no visible damage and the racks appeared to suffer no damage at all.

The damage received by the AN/TRC-117 should thus be considered as a major factor for the poor comparison with analytical predictions. The AN/TRC-145, which had received very little damage, compared much better in the acceleration peaks. However, the measured acceleration time histories for both systems consistency had higher frequencies than the analytical predictions. It is suspected that the gages were sensing localized high frequency structural inputs, as was shown for the gages intended to sense the rigid body response. A lack of greater detail in the structural model would also result in lower frequencies in the analytical results. Increasing the structural modeling detail could result in higher frequencies, at the expense of longer computer running times and storage requirements.

3.5 RESPONSE OF AN/TRC-145 TO A 168 TJ (40 KT BLAST)

The response of the AN/TRC-145 had been found for a 4.2 TJ (1KT) blast at an incident overpressure of 41.4 kPa (6.0 psi). The results were shown in Figures 3.12-3.13 for the gross accelerations and in Figures 3.87-3.102 for the structural accelerations, using the overpressure model of the TRUCK code. It was of further interest to investigate the response of the system to a blast of a higher yield, 168 TJ (40 KT), while maintaining the same incident overpressure of 41.4 kPa. The effect of increasing the yield results in a larger positive phase duration and a more severe loading condition during the drag phase.

The roll angle responses obtained by the TRUCK code at the 168 TJ and 4.2 TJ yields, each at an incident overpressure of 41.4 kPa, are shown in Figure 3.110. It is seen that increasing the yield resulted in a significantly higher roll angle and subsequent overturning of the system due to the greater positive-phase drag forces. At the smaller yield, the roll angle peaked at 0.36 radians and no overturning resulted.

The NASTRAN model of the AN/TRC-145 was also exercised for the 4.2 TJ yield at 41.4 kPa after new loading tables were prepared using the TRUCK pressure model and the corresponding base motion. A comparison with the accelerations for the smaller yield at 41.4 kPa in Figures 3.87-3.102 showed that increasing the yield had generally no discernible effect on the structural accelerations of the walls and racks during the first 30 msecs of response. This result is to be expected since increasing the yield has a minor effect on the early time diffractive loading during which the structural accelerations are excited.

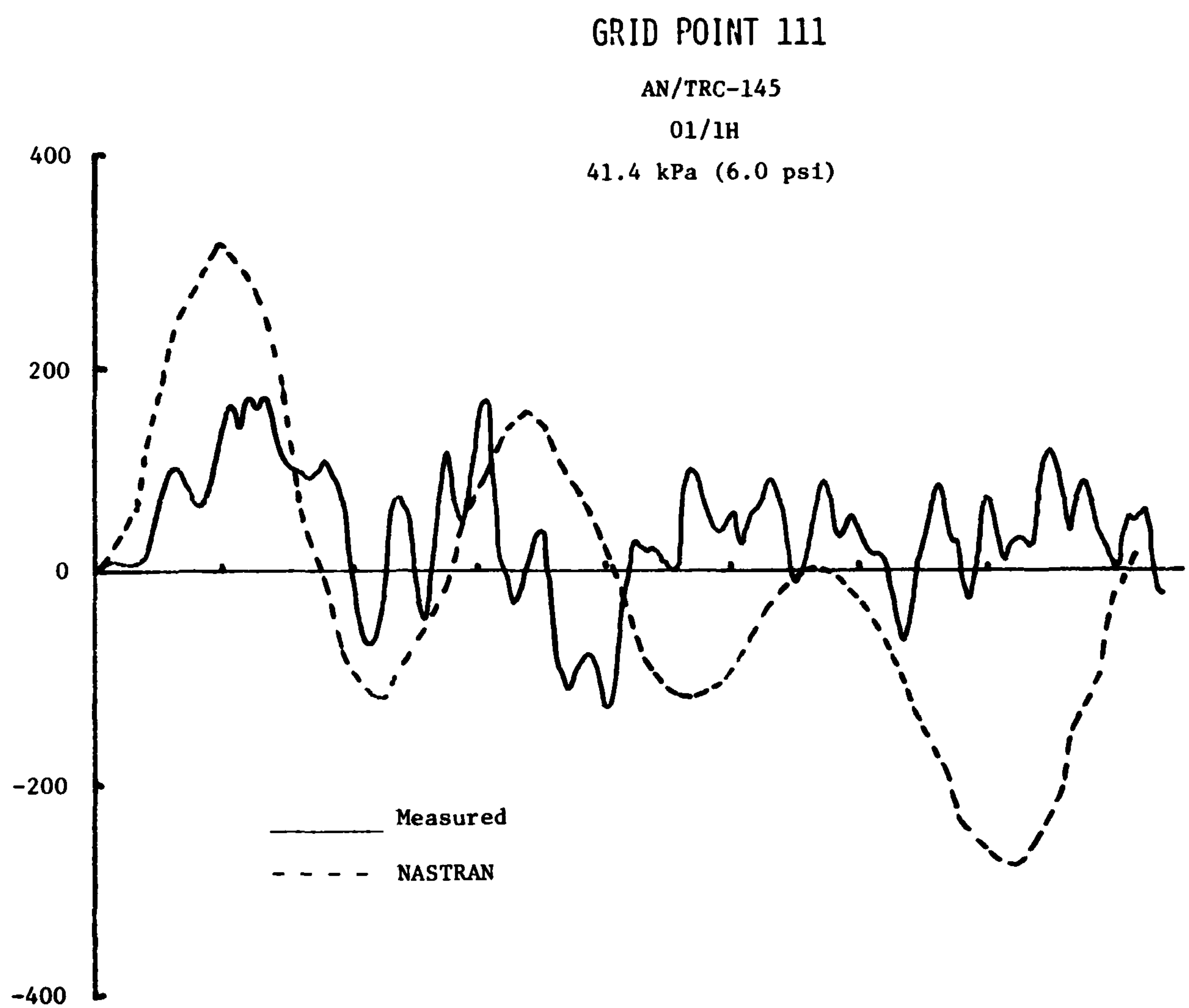

FIGURE 3.87. COMPARISON OF MEASURED AND ANALYTICAL ACCELERATION TIME HISTORIES IN BLAST DIRECTION, ROADSIDE RACK

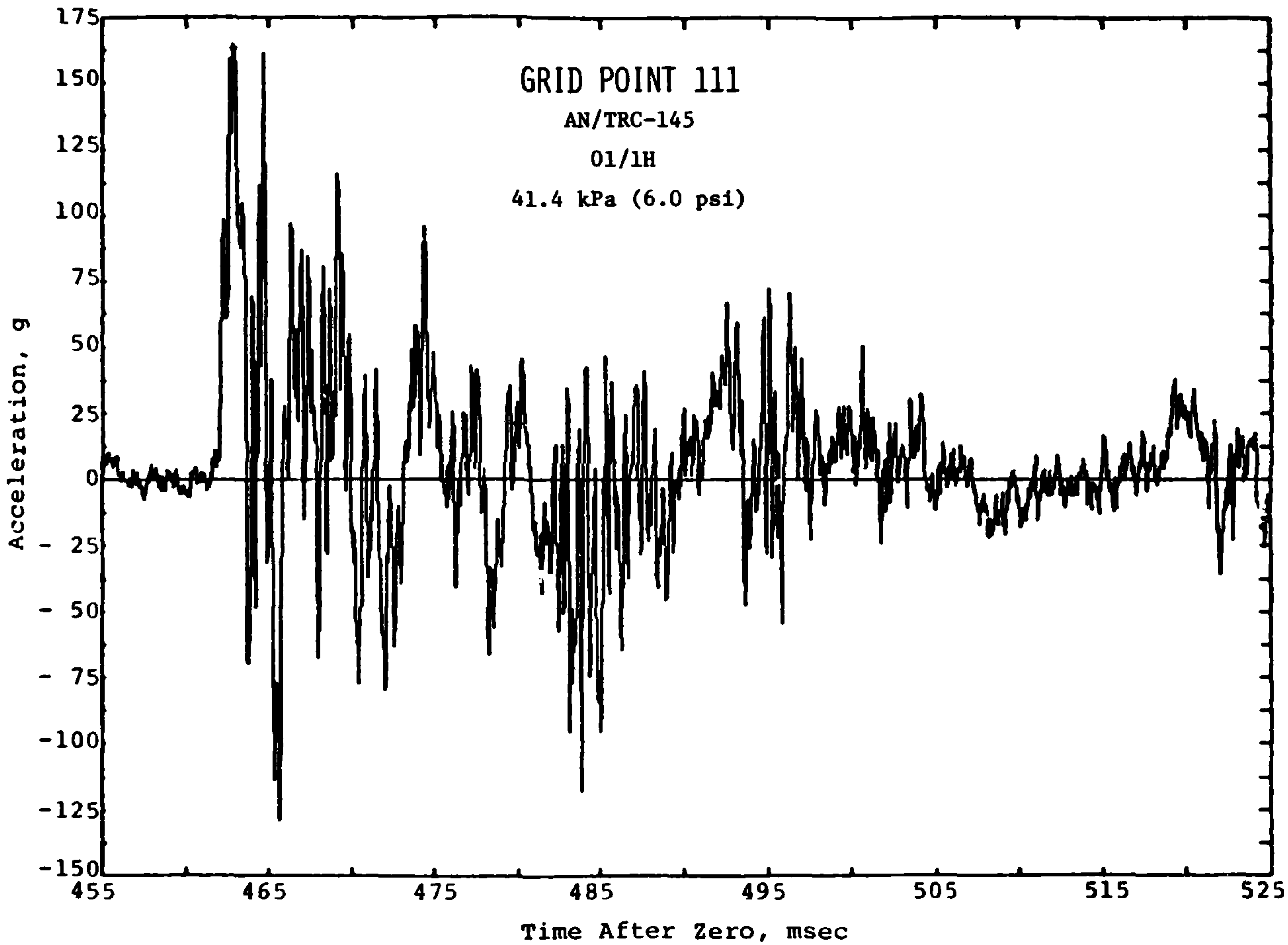

FIGURE 3.88. MEASURED ACCELERATION TIME HISTORY IN BLAST DIRECTION, ROADSIDE RACK

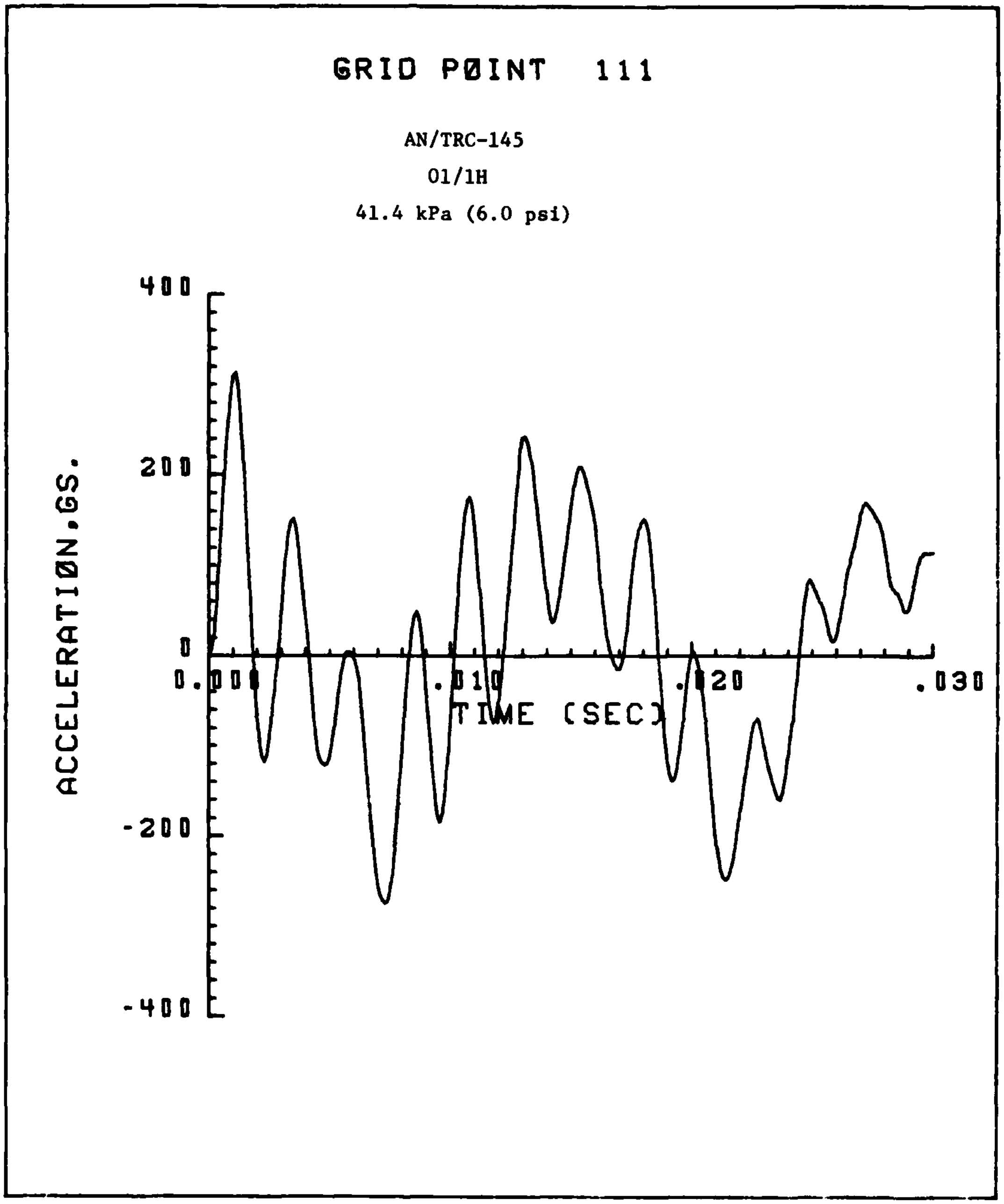

FIGURE 3.89. ANALYTICAL ACCELERATION TIME HISTORY IN BLAST DIRECTION, ROADSIDE RACK (NASTRAN)

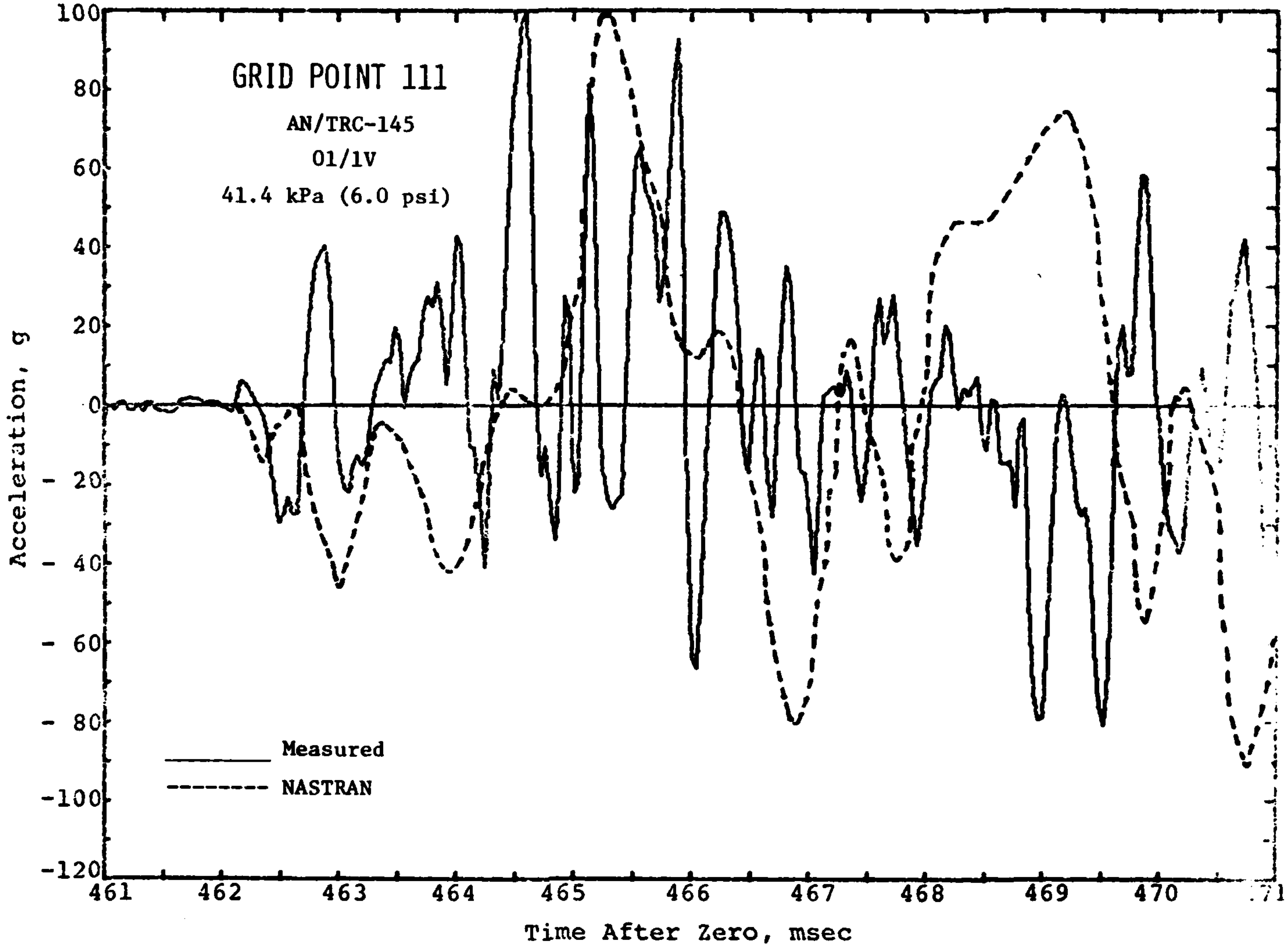

FIGURE 3.90. COMPARISON OF MEASURED AND ANALYTICAL VERTICAL ACCELERATION TIME HISTORIES, ROADSIDE RACK

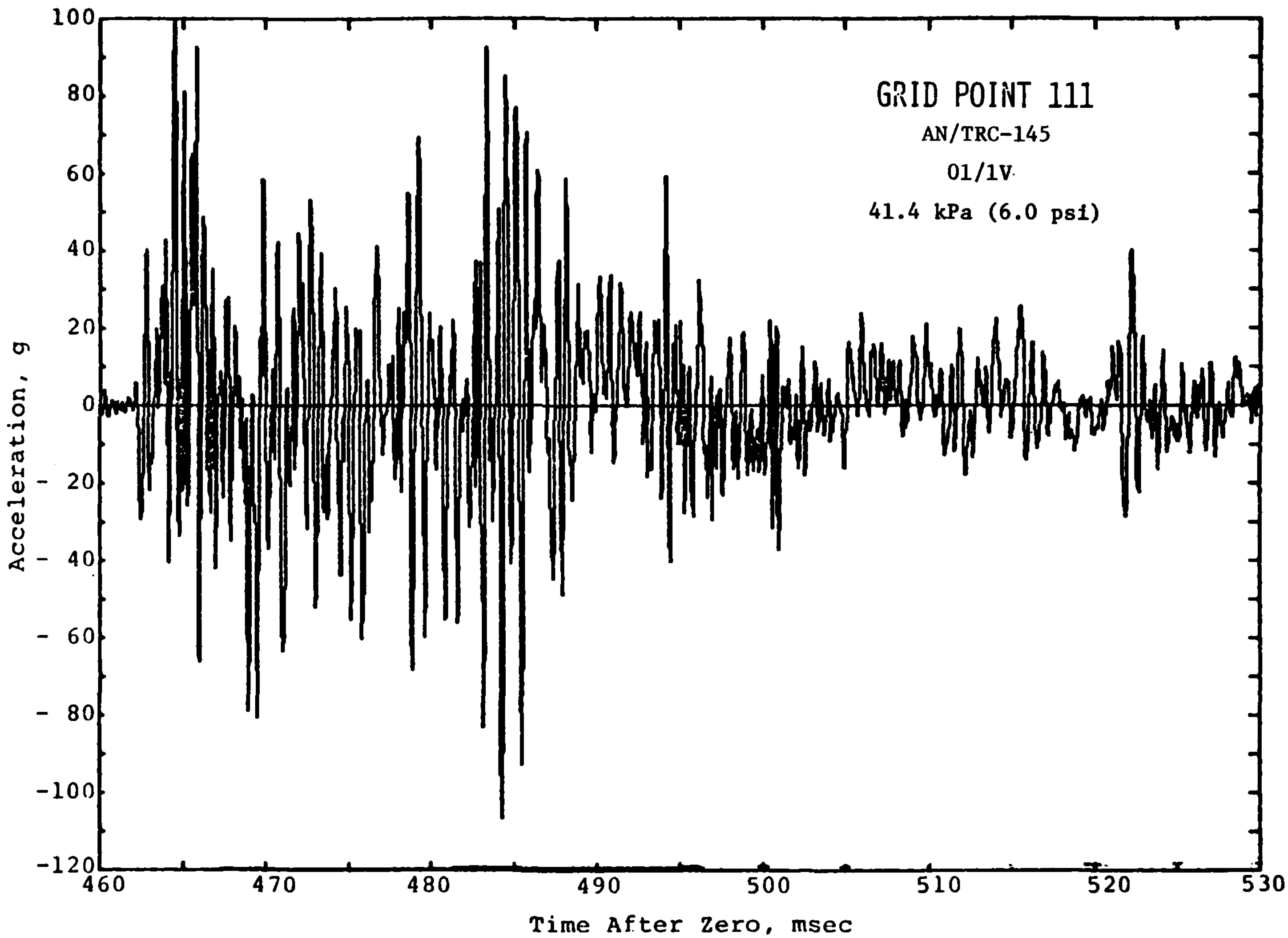

FIGURE 3.91. MEASURED VERTICAL ACCELERATION TIME HISTORY, ROADSIDE RACK

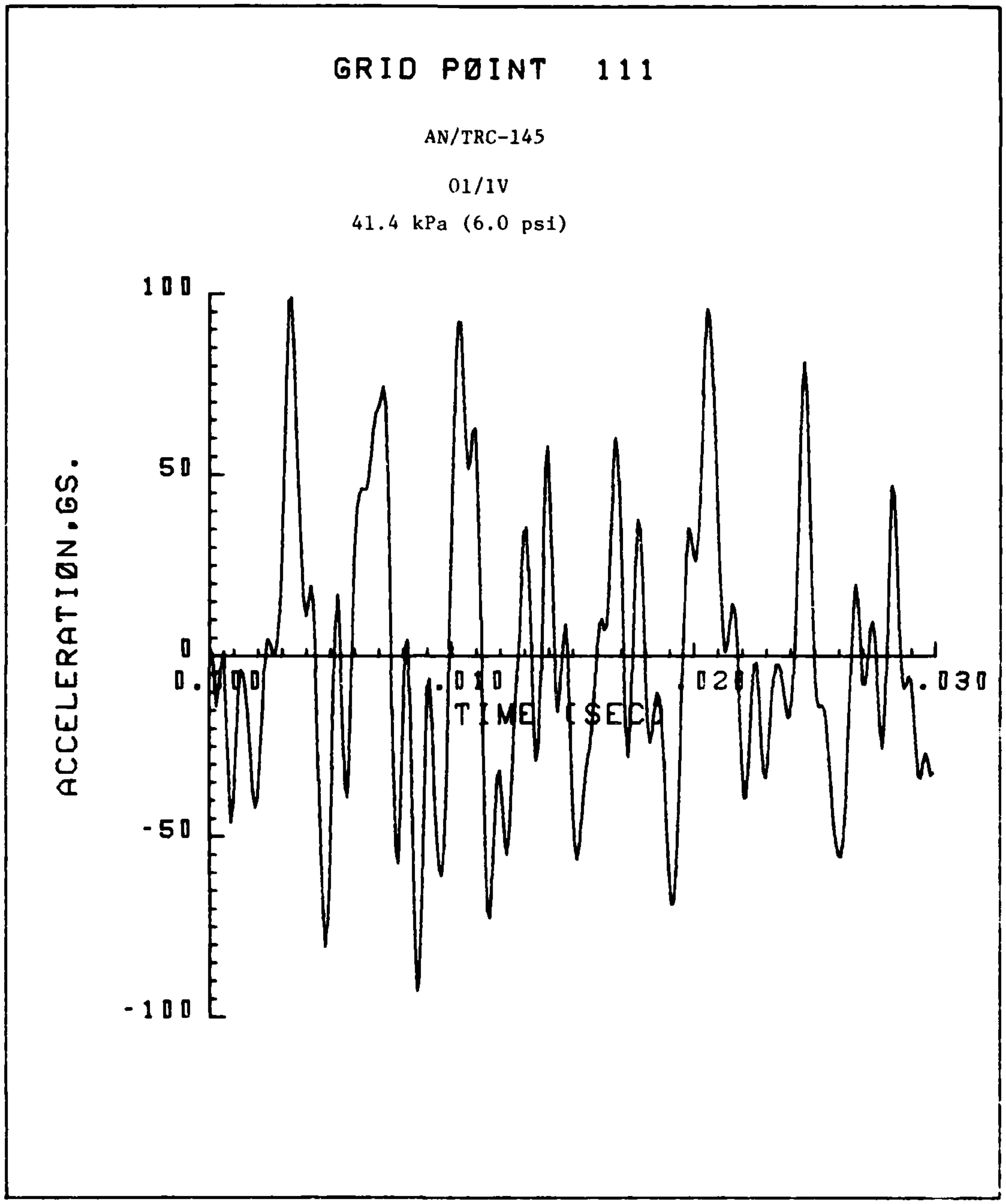

FIGURE 3.92. ANALYTICAL ACCELERATION TIME HISTORY
ROADSIDE RACK (NASTRAN)

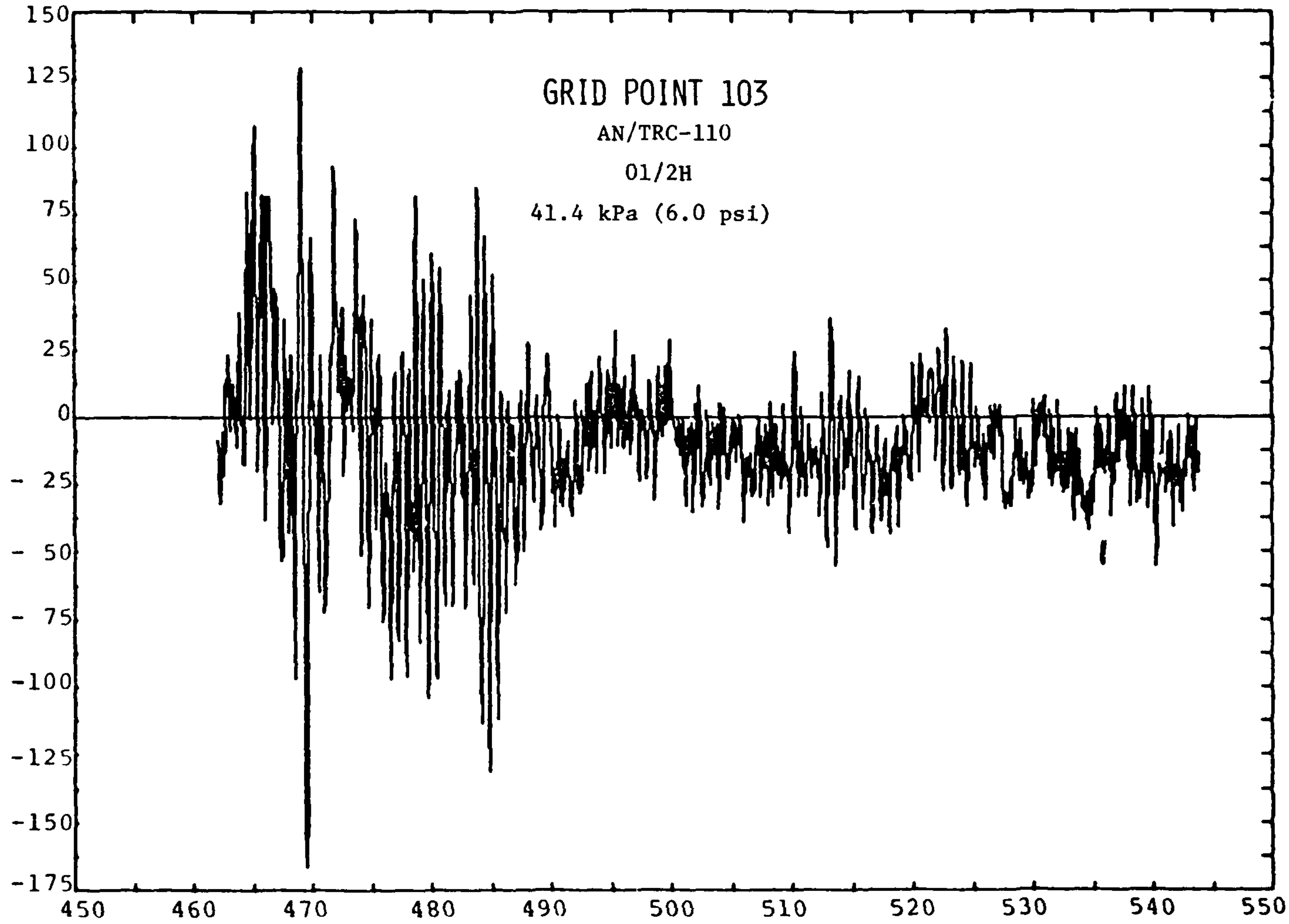

FIGURE 3.93. MEASURED ACCELERATION TIME HISTORY IN BLAST DIRECTION, ROADSIDE RACK

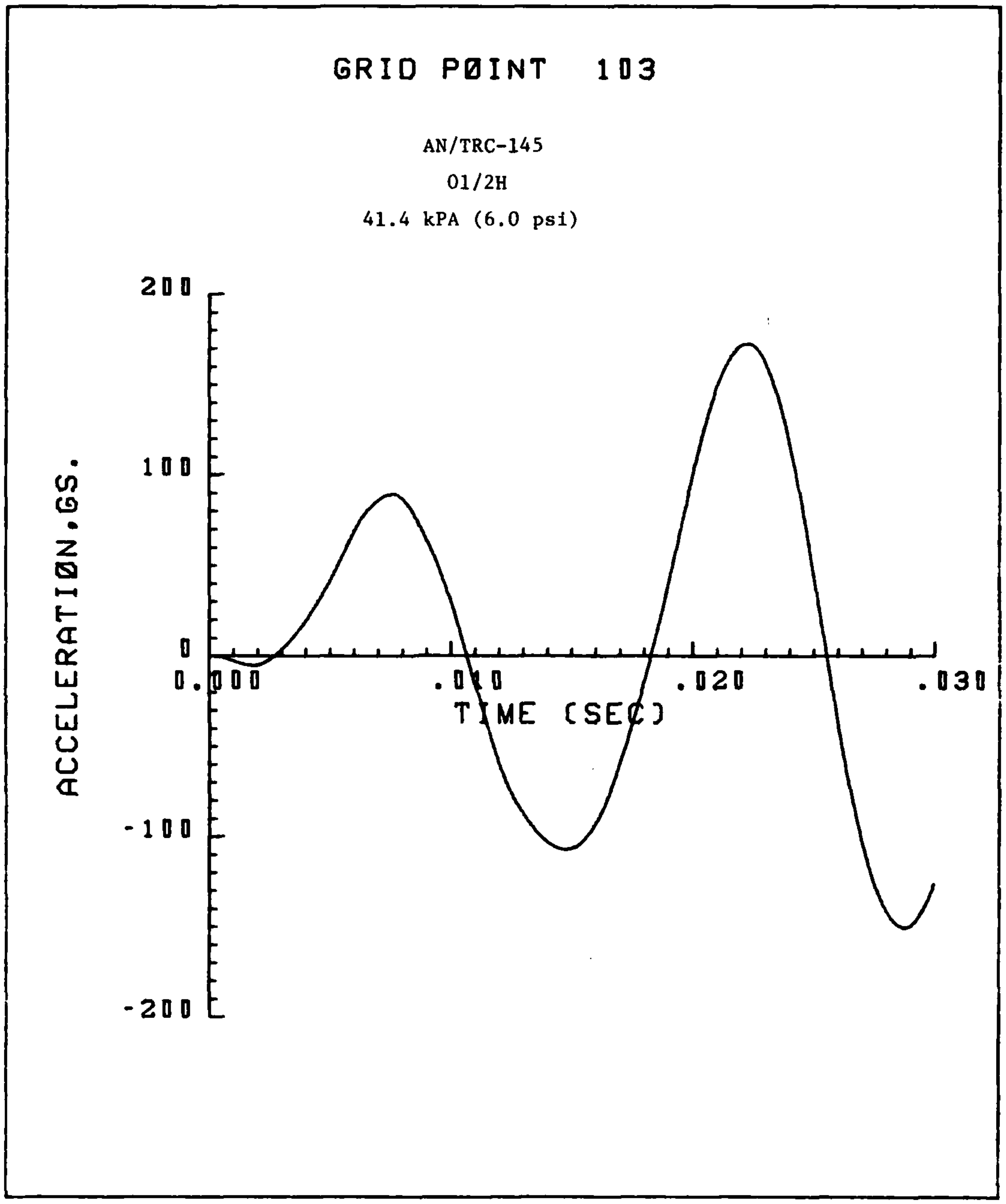

FIGURE 3.94. ANALYTICAL ACCELERATION IN BLAST DIRECTION, ROADSIDE RACK (NASTRAN)

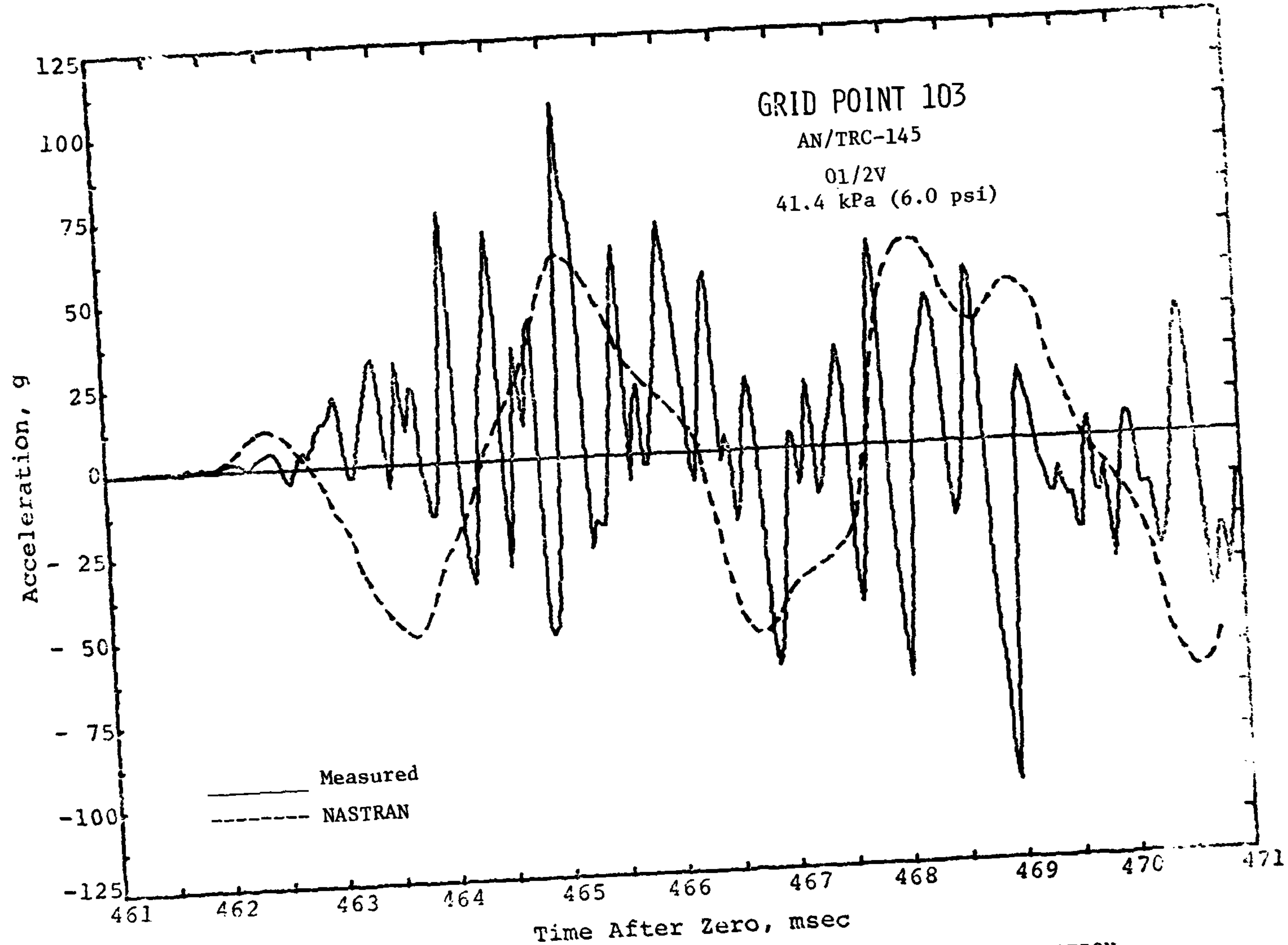

FIGURE 3.95. COMPARISON OF MEASURED AND ANALYTICAL VERTICAL ACCELERATION TIME HISTORIES, ROADSIDE RACK

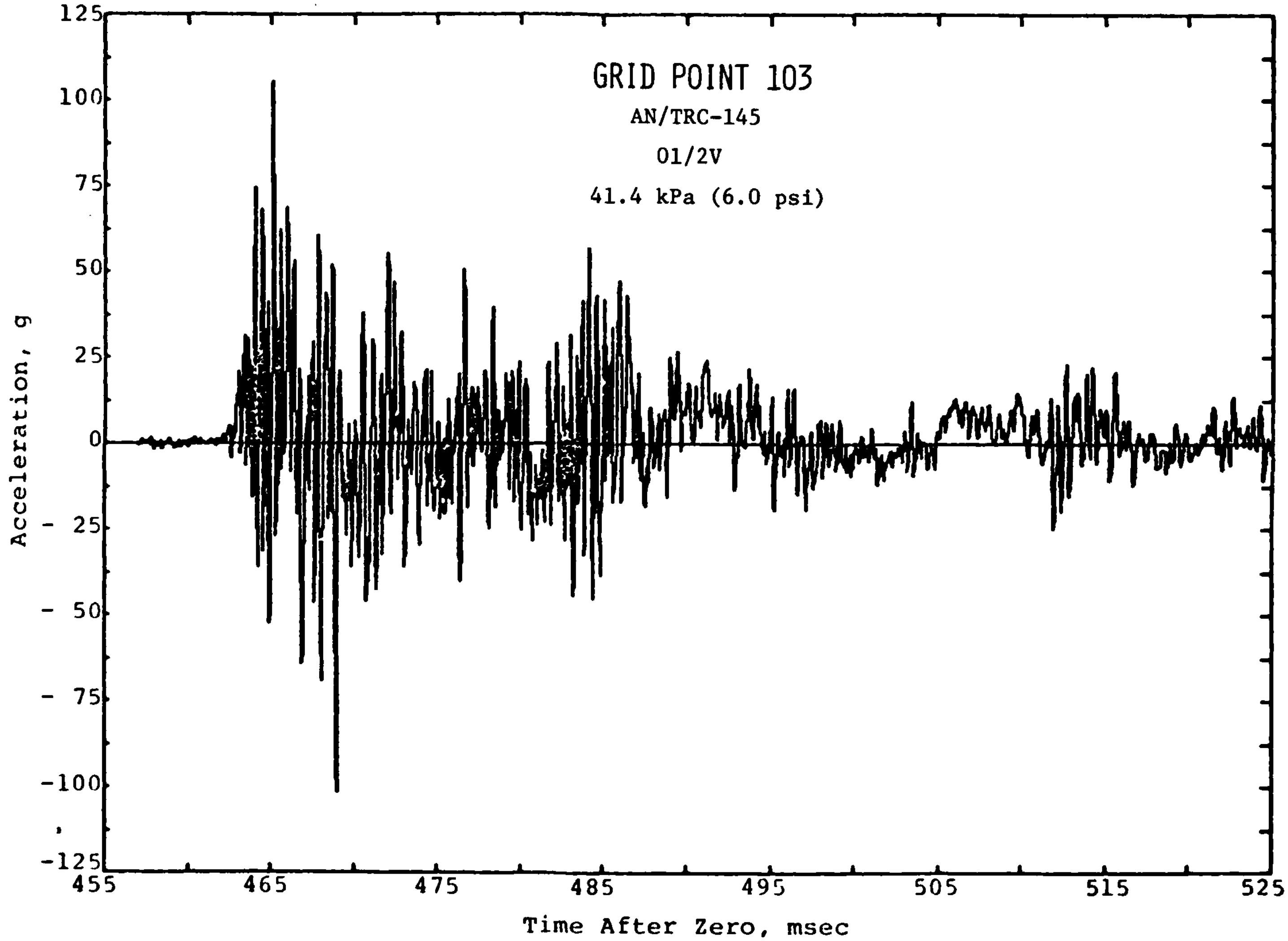

FIGURE 3.96. MEASURED VERTICAL ACCELERATION TIME HISTORY, ROADSIDE RACK

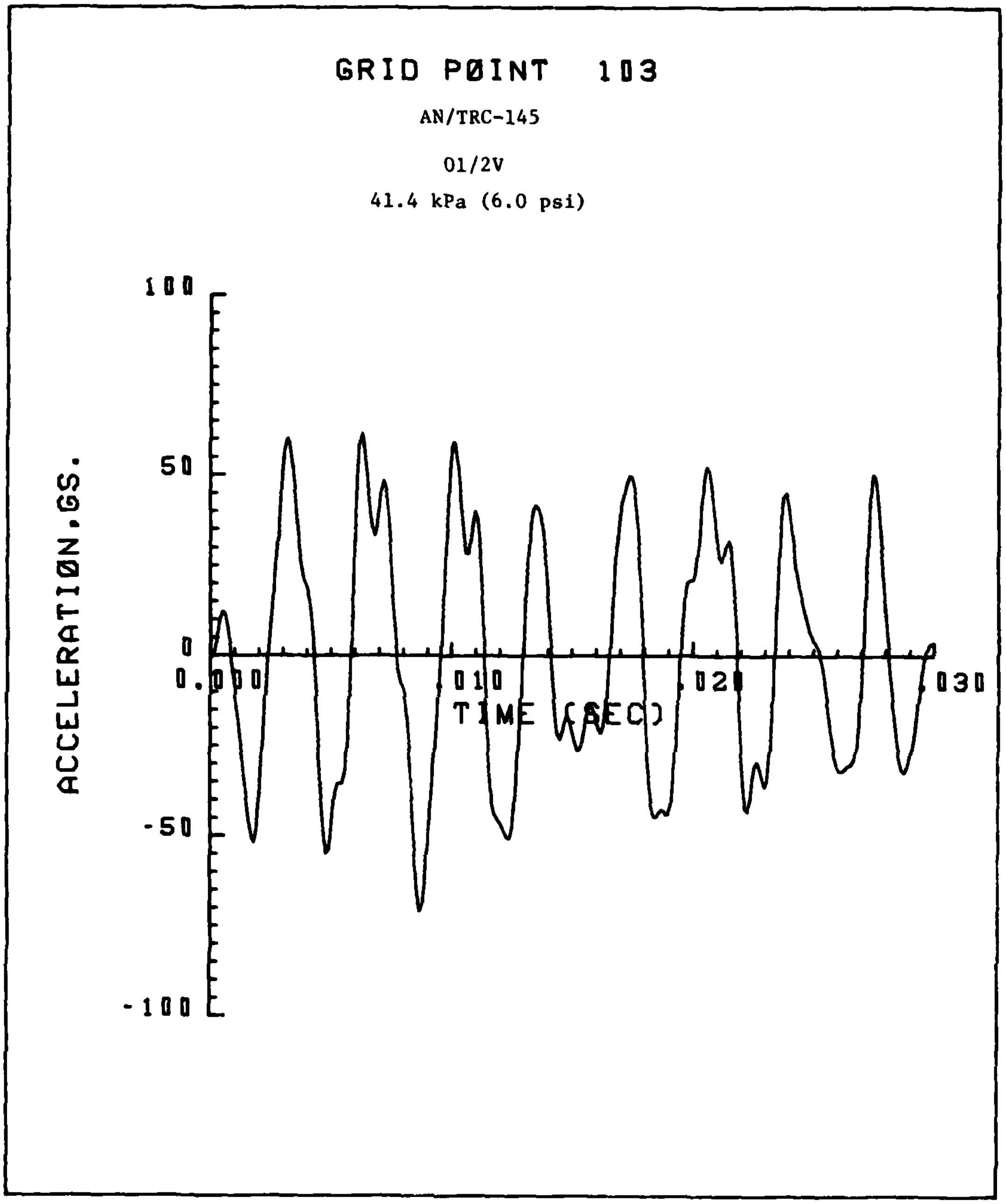

FIGURE 3.97. ANALYTICAL VERTICAL ACCELERATION TIME HISTORY, ROADSIDE RACK (NASTRAN)

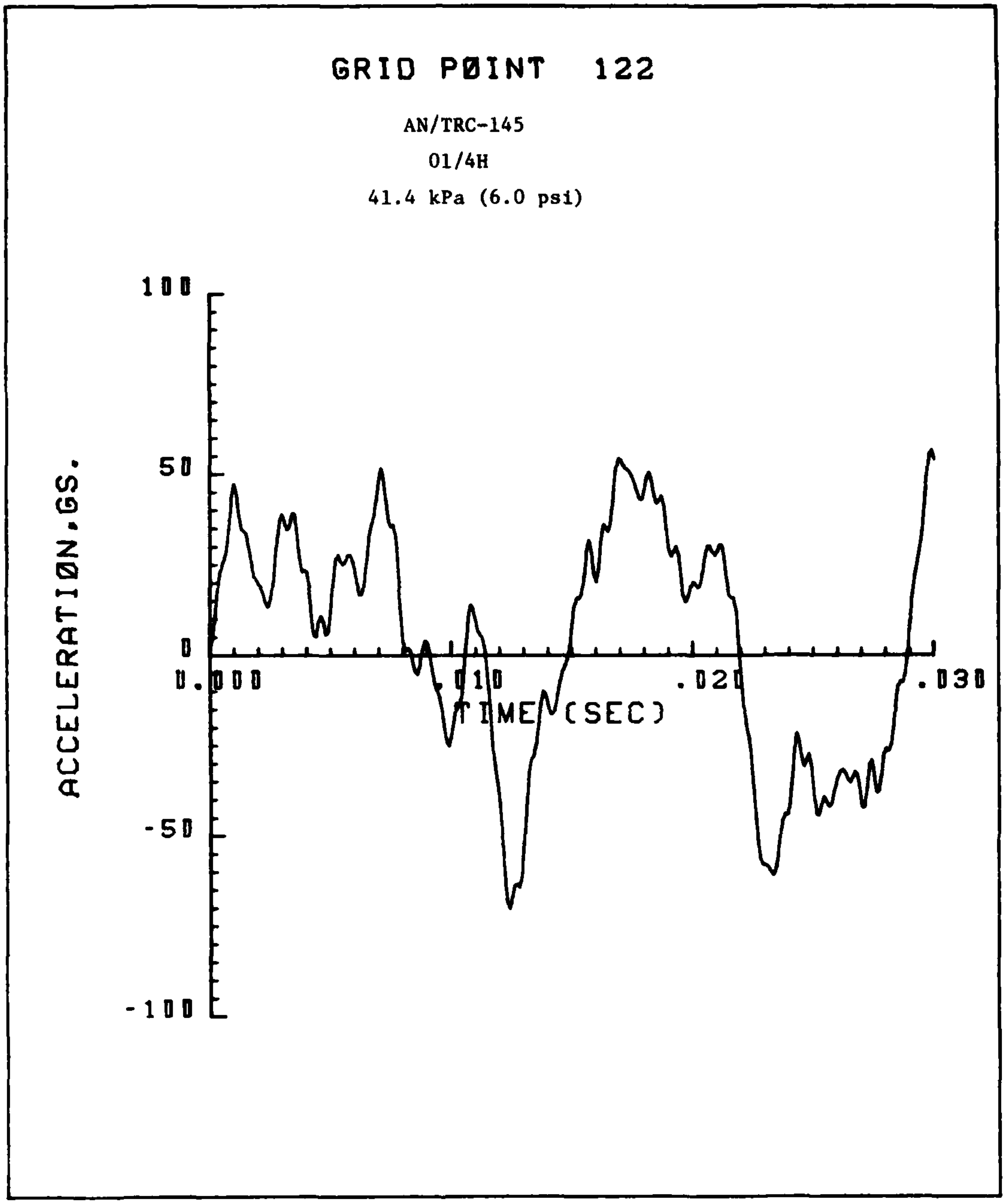

FIGURE 3.98. ANALYTICAL ACCELERATION IN BLAST DIRECTION, FRONT END RACK (NASTRAN)

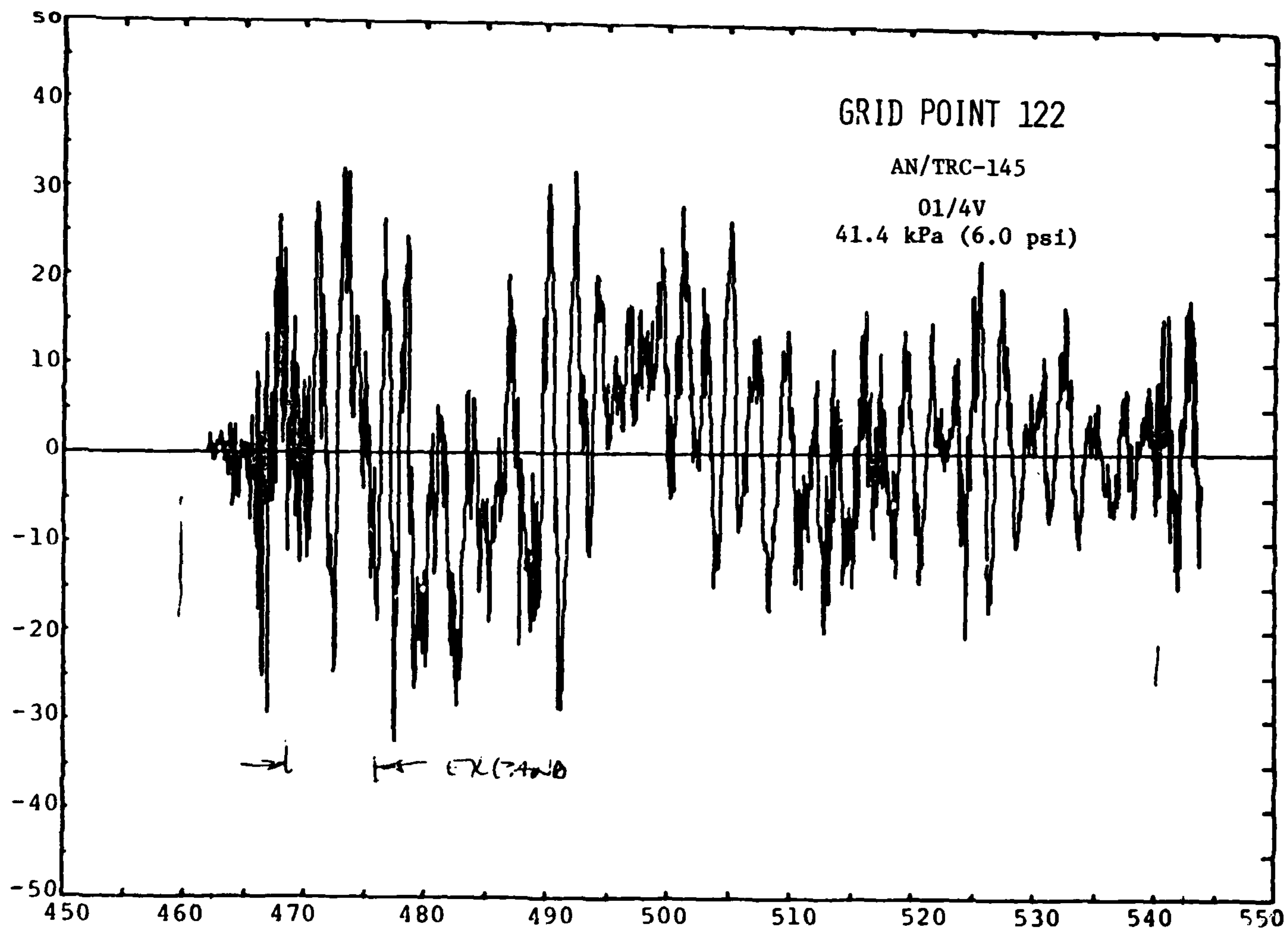

FIGURE 3.99. MEASURED VERTICAL ACCELERATION TIME HISTORY, FRONT END RACK

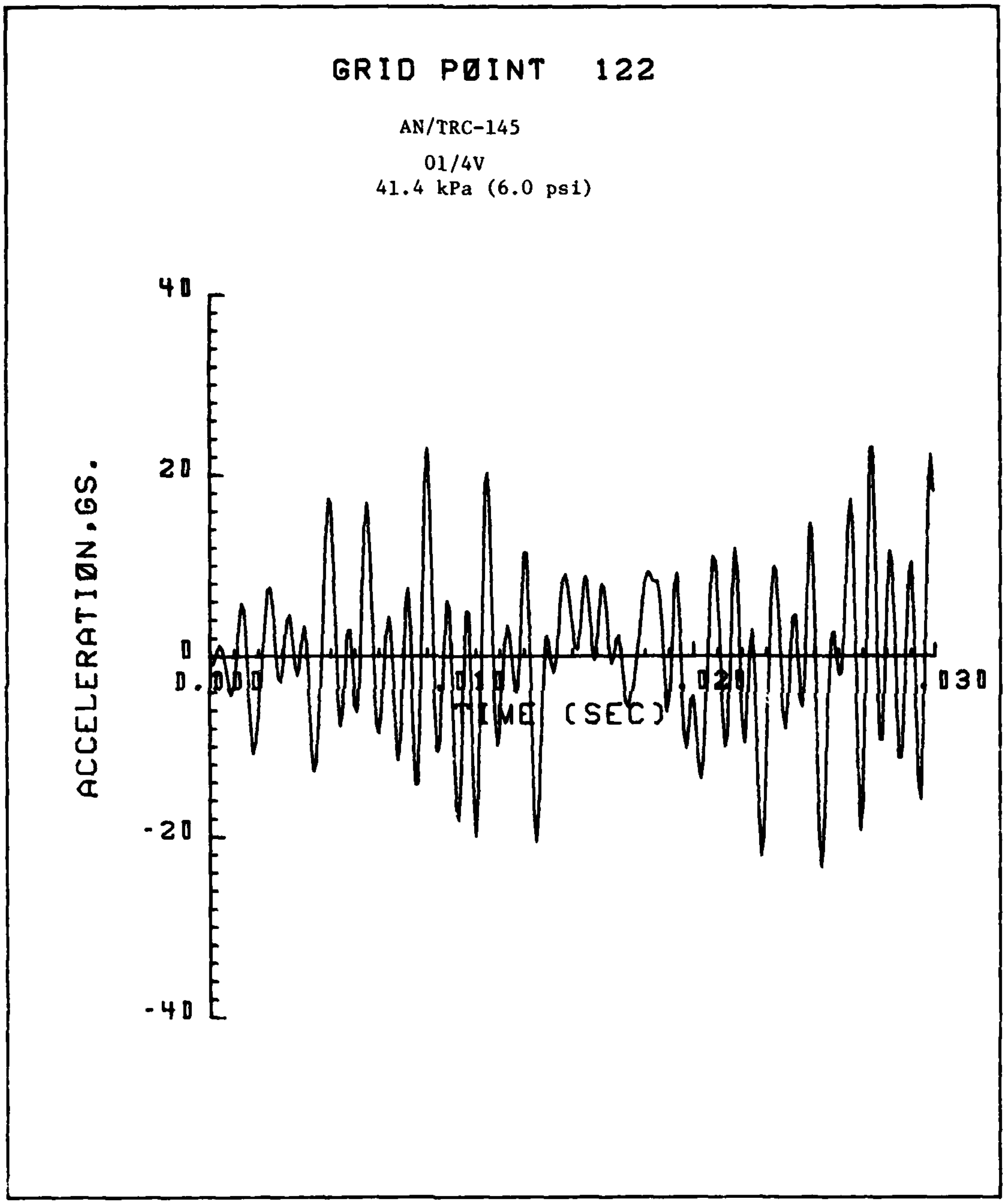

FIGURE 3.100. ANALYTICAL VERTICAL ACCELERATION TIME HISTORY, FRONT END RACK (NASTRAN)

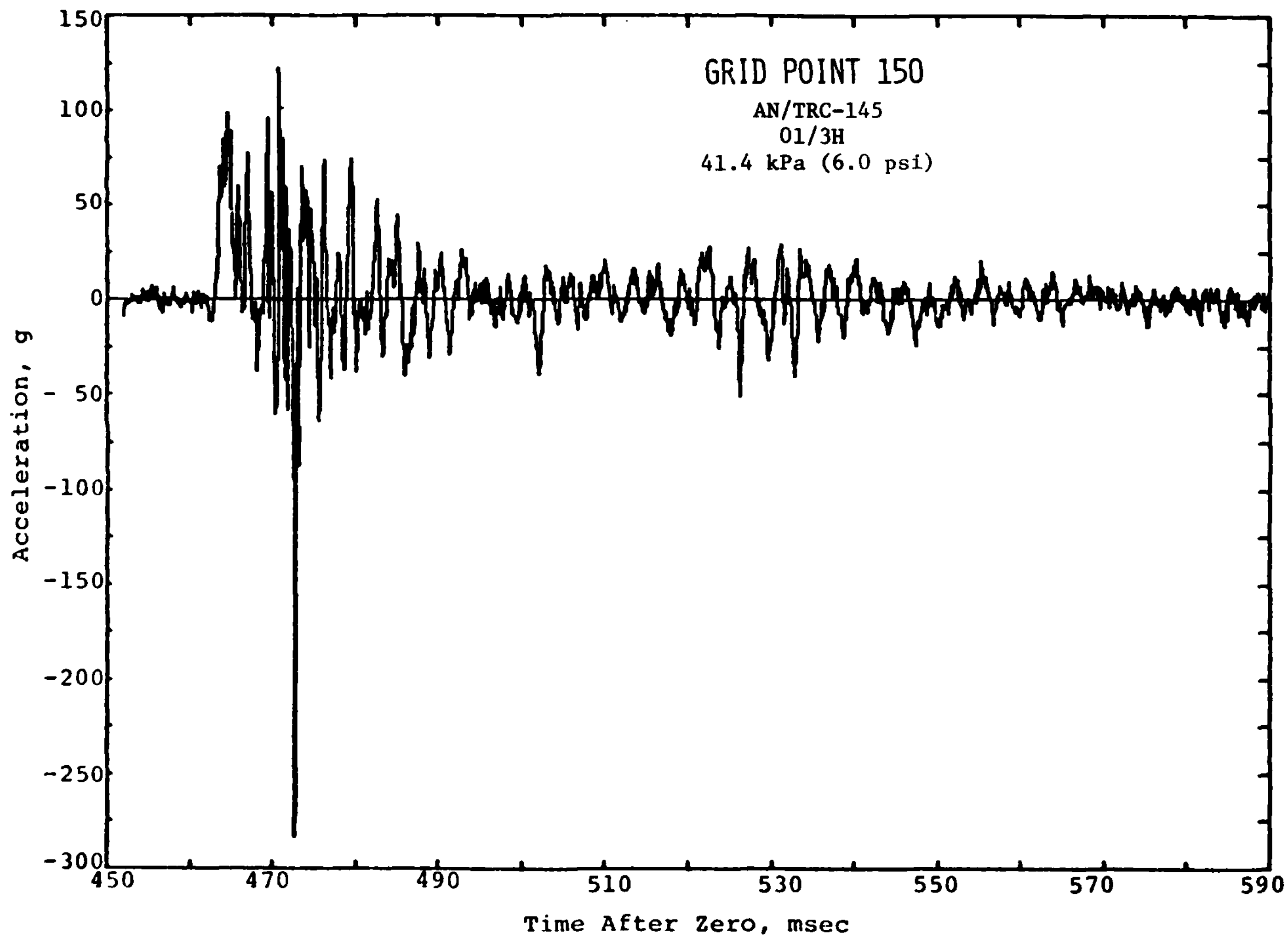

FIGURE 3.101. MEASURED ACCELERATION TIME HISTORY IN BLAST DIRECTION, CENTER OF FLOOR

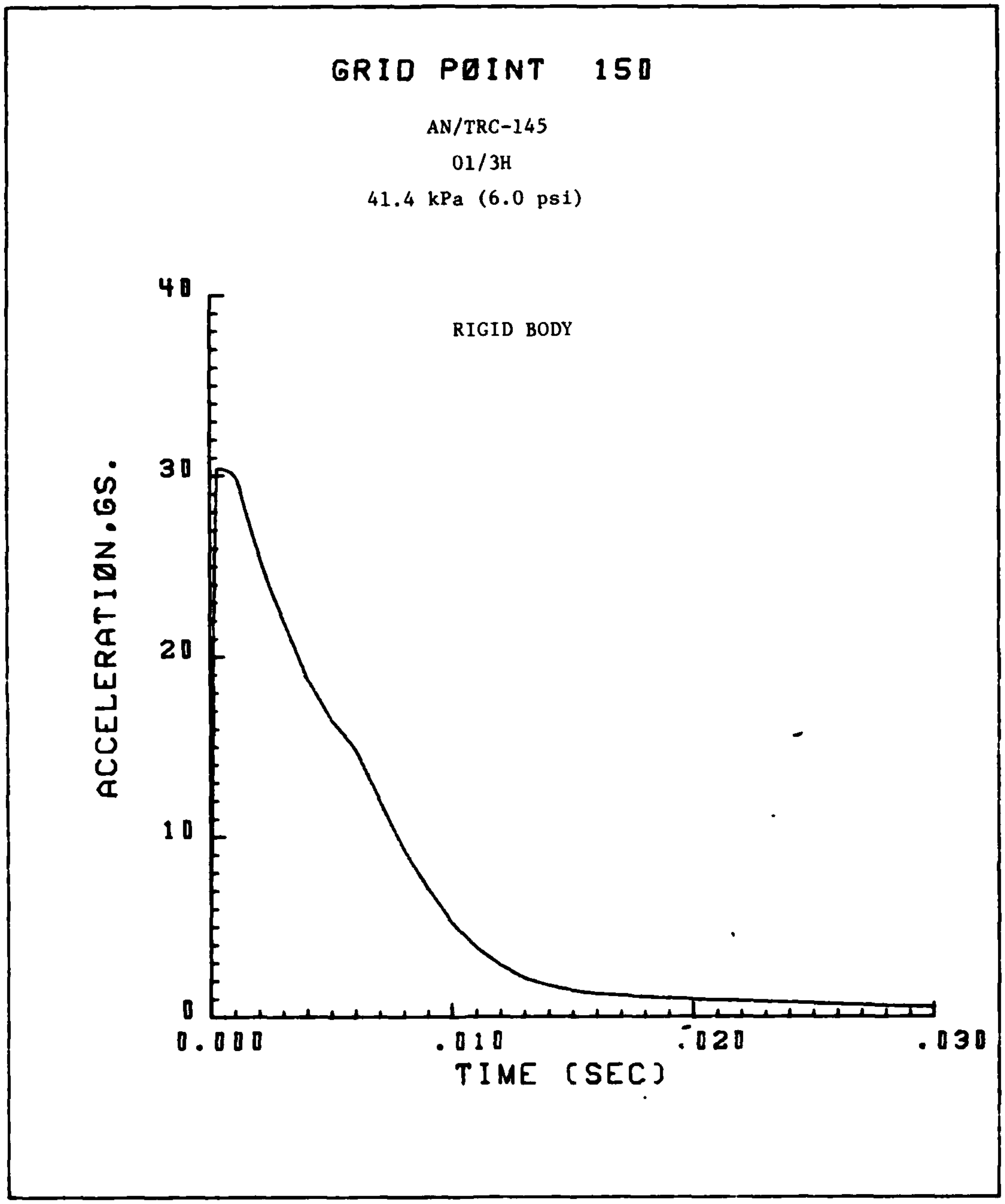

FIGURE 3.102. ANALYTICAL ACCELERATION TIME HISTORY IN BLAST DIRECTION, CENTER OF FLOOR (NASTRAN)

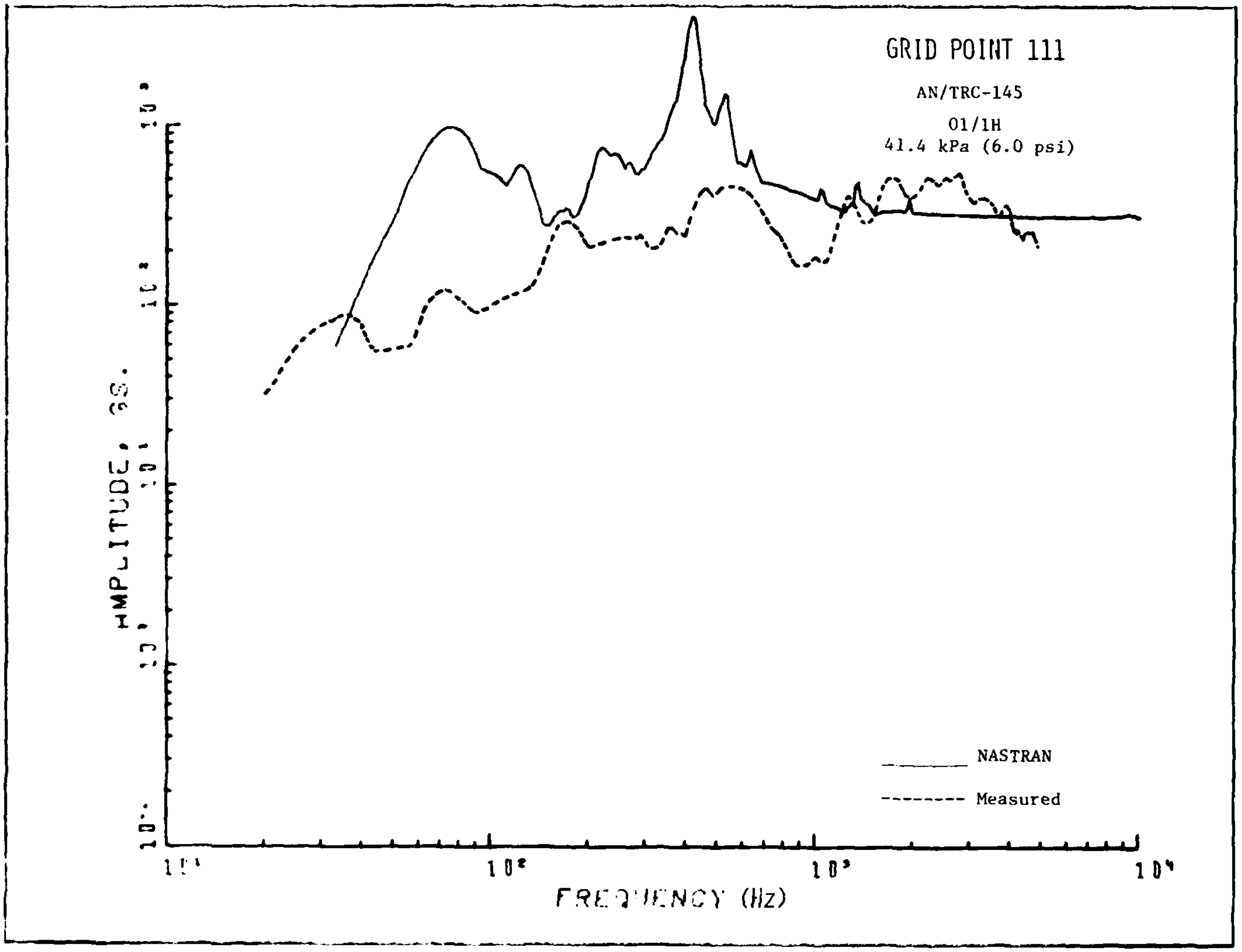

FIGURE 3.103. COMPARISON OF SHOCK SPECTRA BASED ON MEASURED AND ANALYTICAL ACCELERATION TIME HISTORIES IN BLAST DIRECTION, ROADSIDE RACK

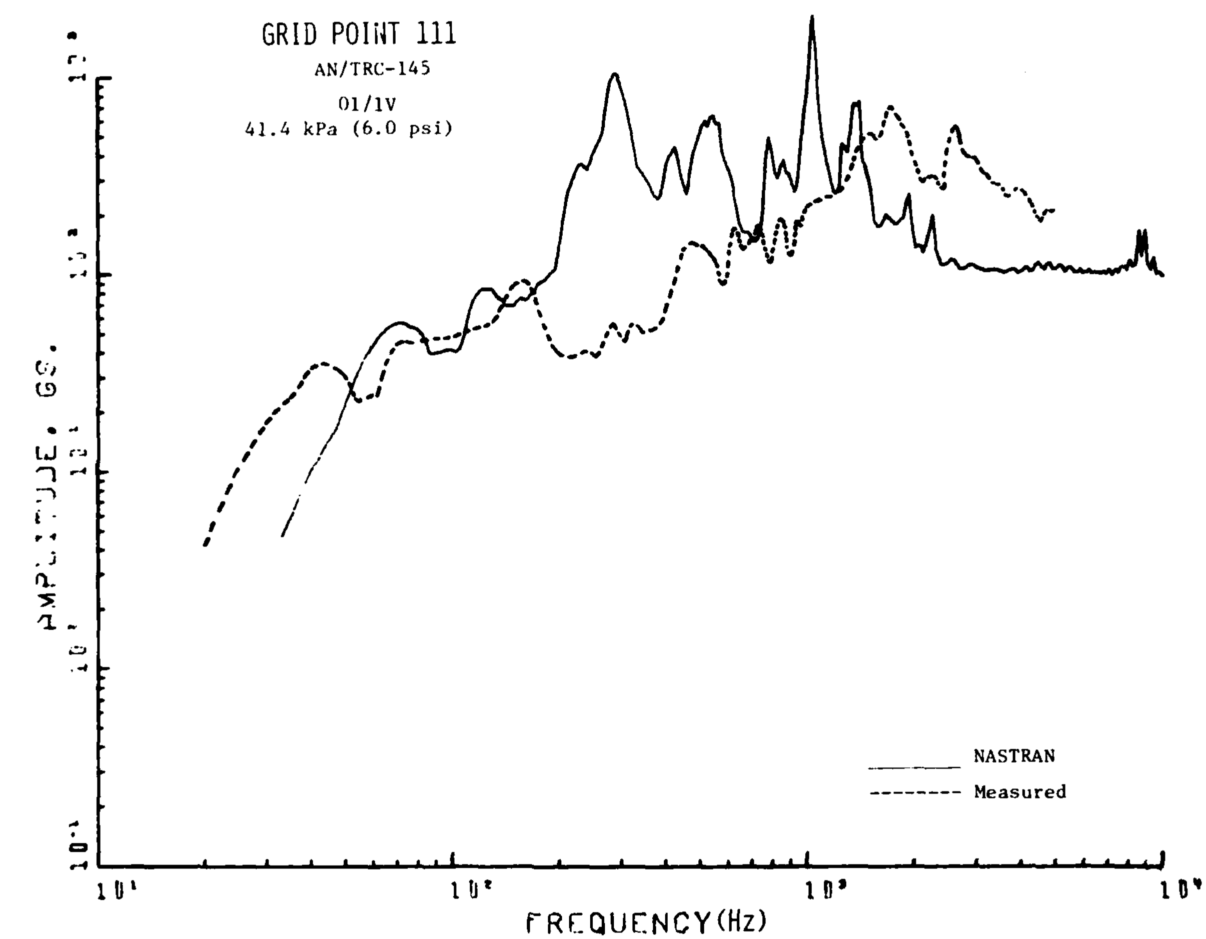

FIGURE 3.104. COMPARISON OF SHOCK SPECTRA BASED ON MEASURED AND ANALYTICAL VERTICAL ACCELERATION TIME HISTORIES, ROADSIDE RACK

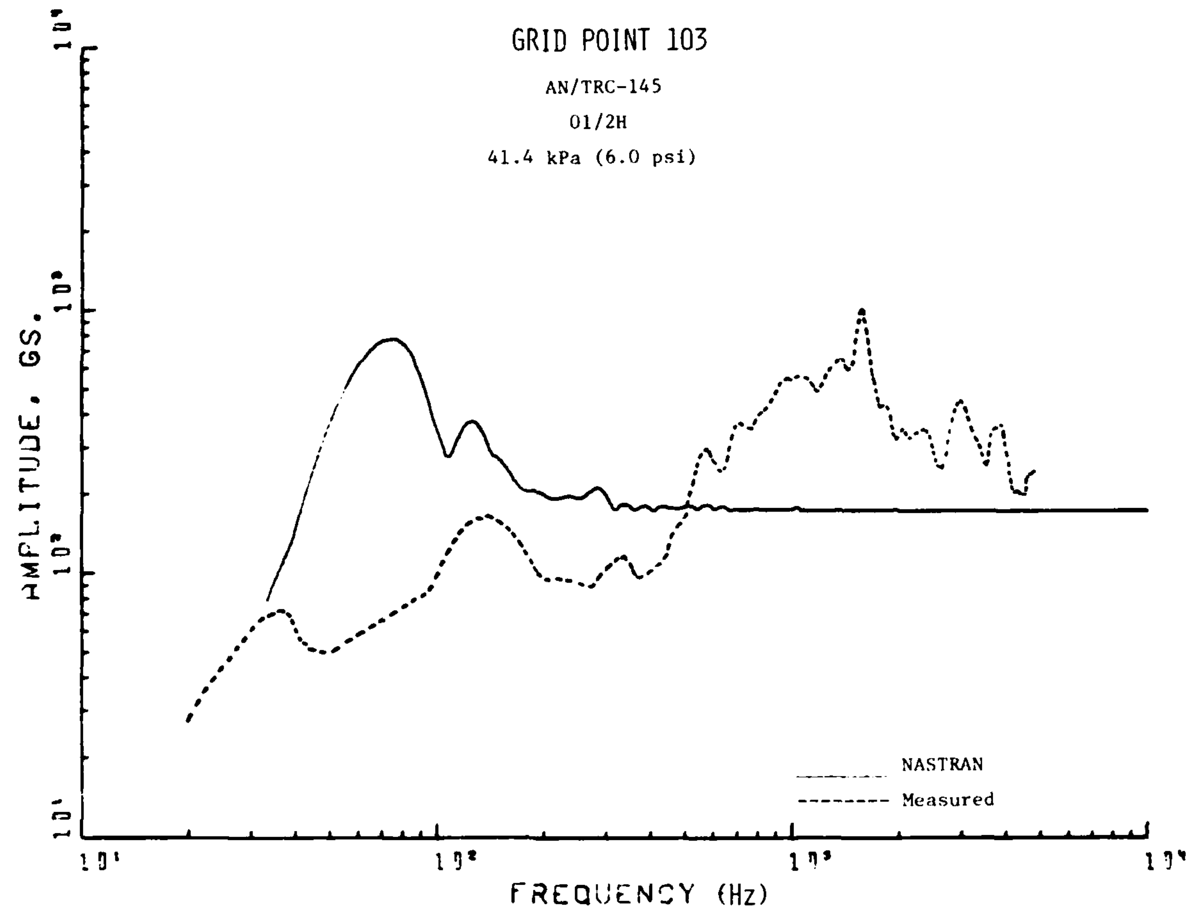

FIGURE 3.105. COMPARISON OF SHOCK SPECTRA BASED ON MEASURED AND ANALYTICAL ACCELERATION TIME HISTORIES IN THE BLAST DIRECTION, ROADSIDE RACK

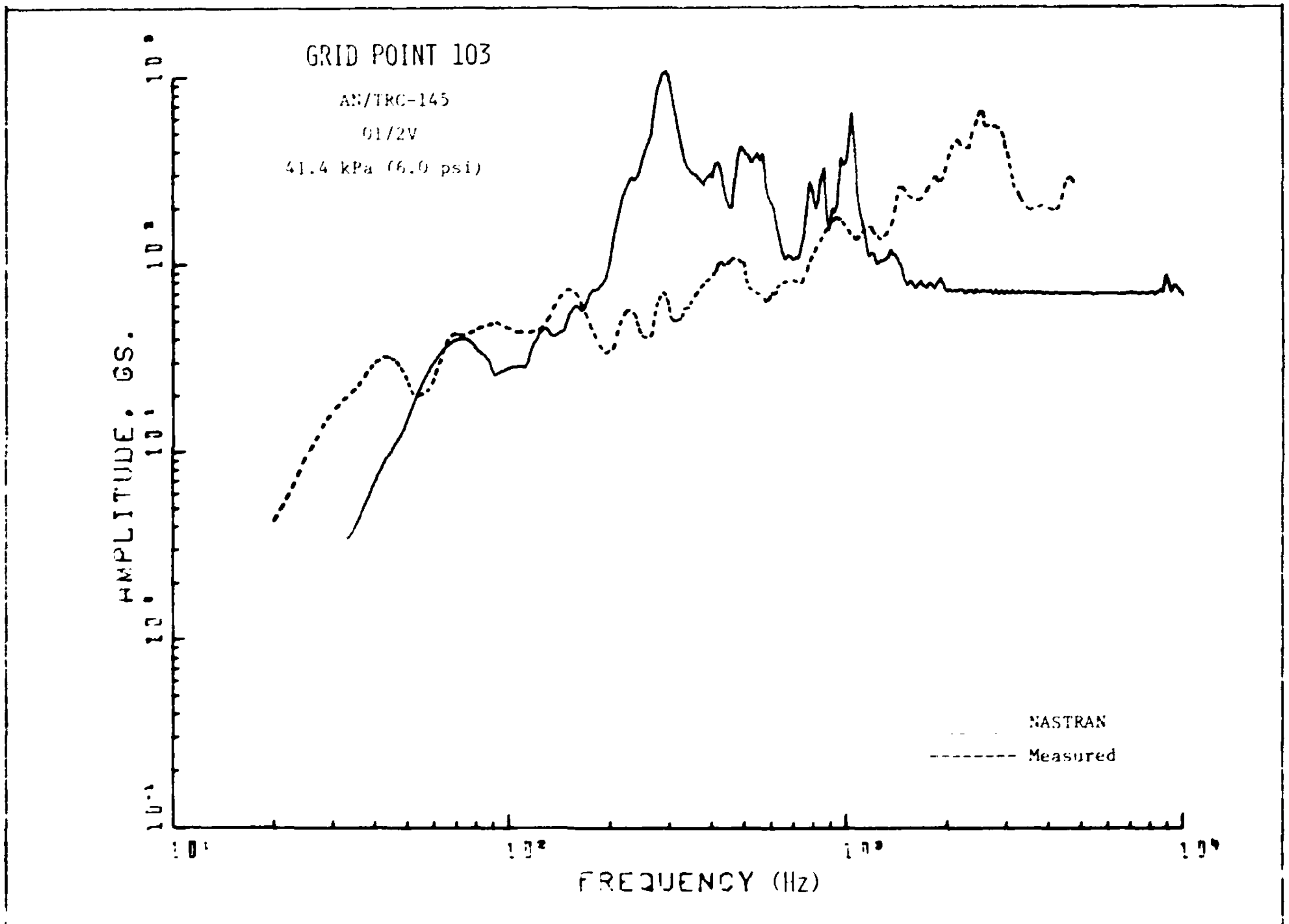

FIGURE 3.106. COMPARISON OF SHOCK SPECTRA BASED ON MEASURED AND ANALYTICAL VERTICAL ACCELERATION TIME HISTORIES, ROADSIDE RACK

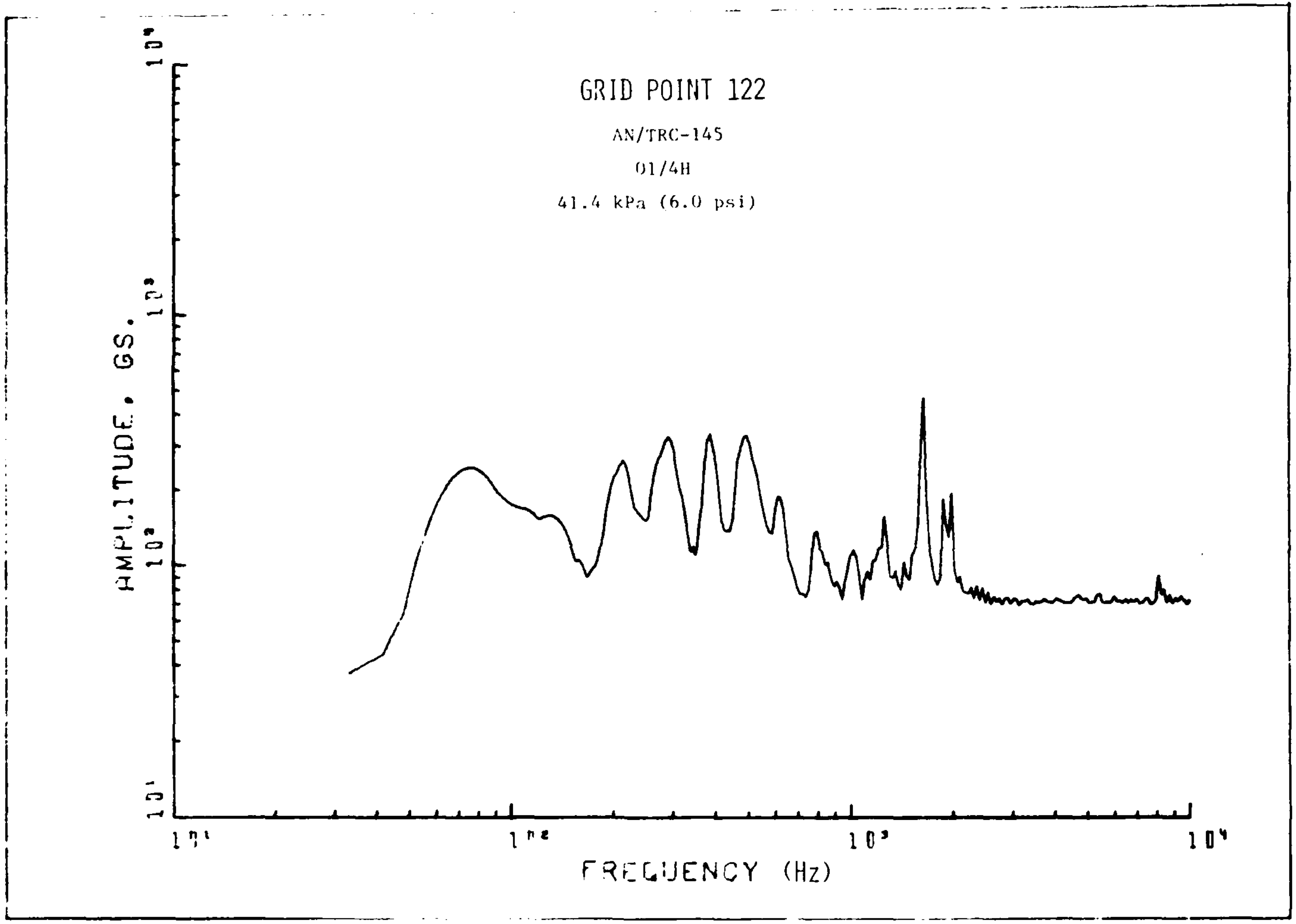

FIGURE 3.107. SHOCK SPECTRUM BASED ON ANALYTICAL ACCELERATION TIME HISTORY IN BLAST DIRECTION, FRONT END RACK (NASTRAN)

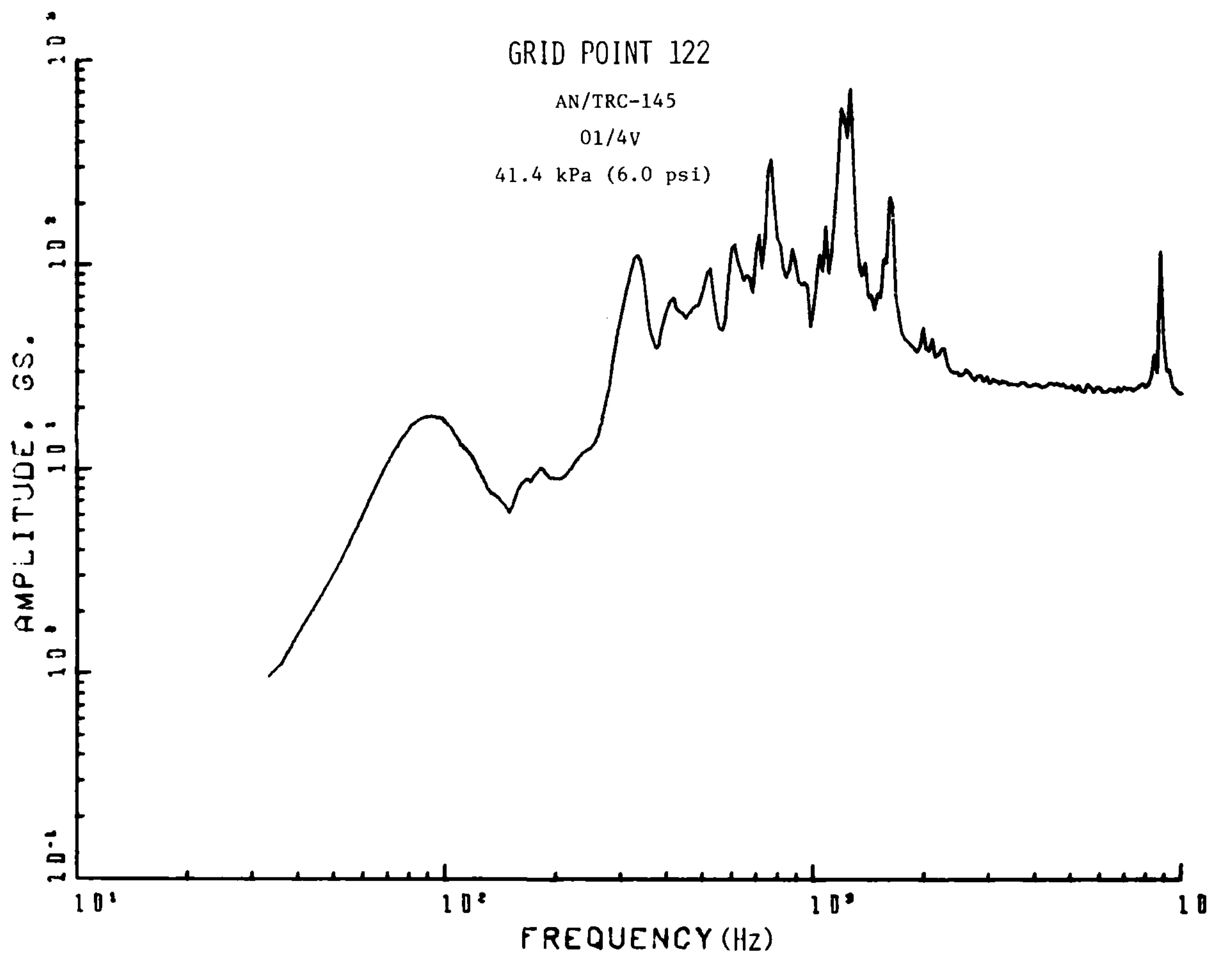

FIGURE 3.108. SHOCK SPECTRUM BASED ON ANALYTICAL VERTICAL ACCELERATION TIME HISTORY, FRONT END RACK (NASTRAN)

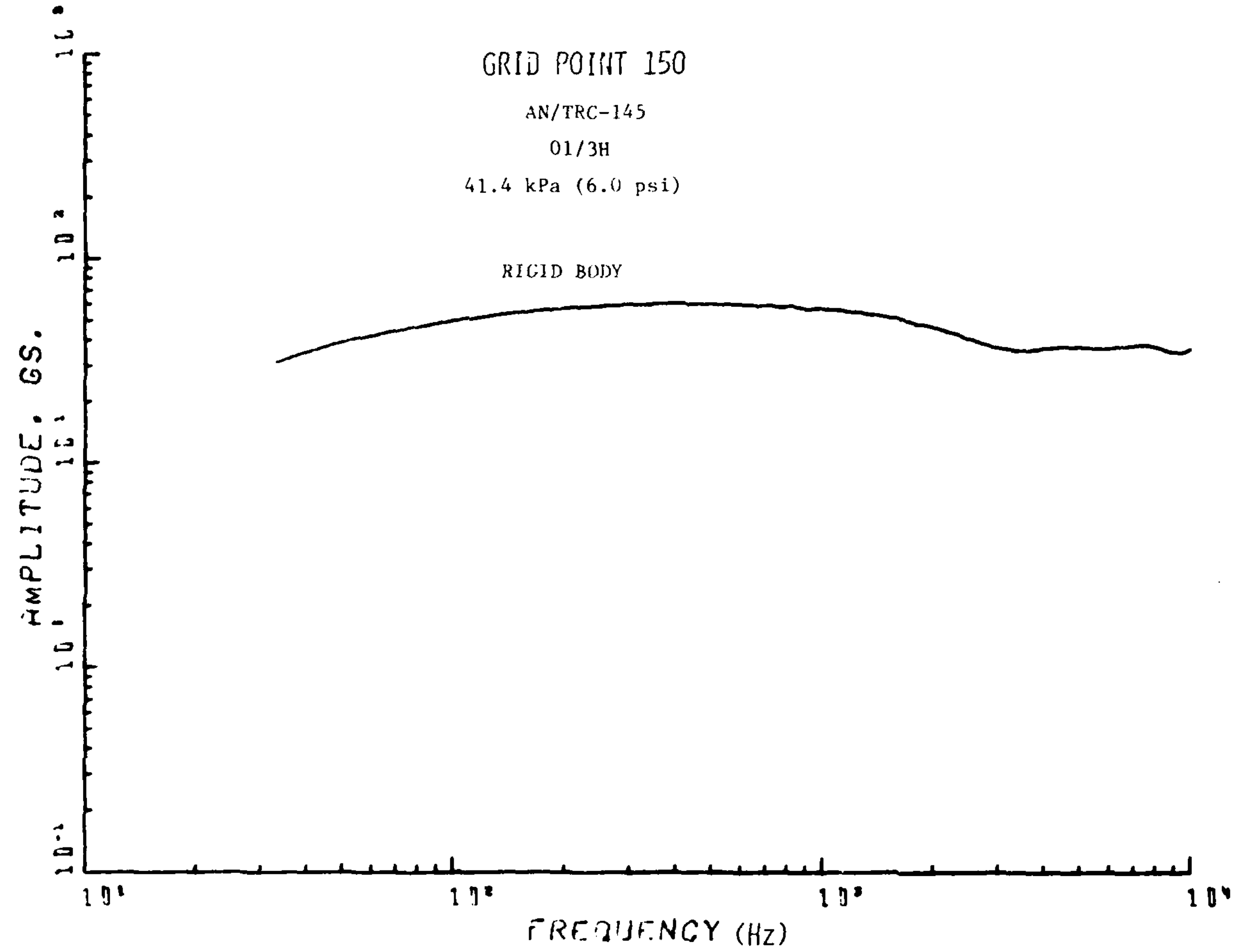

FIGURE 3.109. SHOCK SPECTRUM BASED ON ANALYTICAL ACCELERATION TIME HISTORY IN BLAST DIRECTION, CENTER OF FLOOR (NASTRAN)

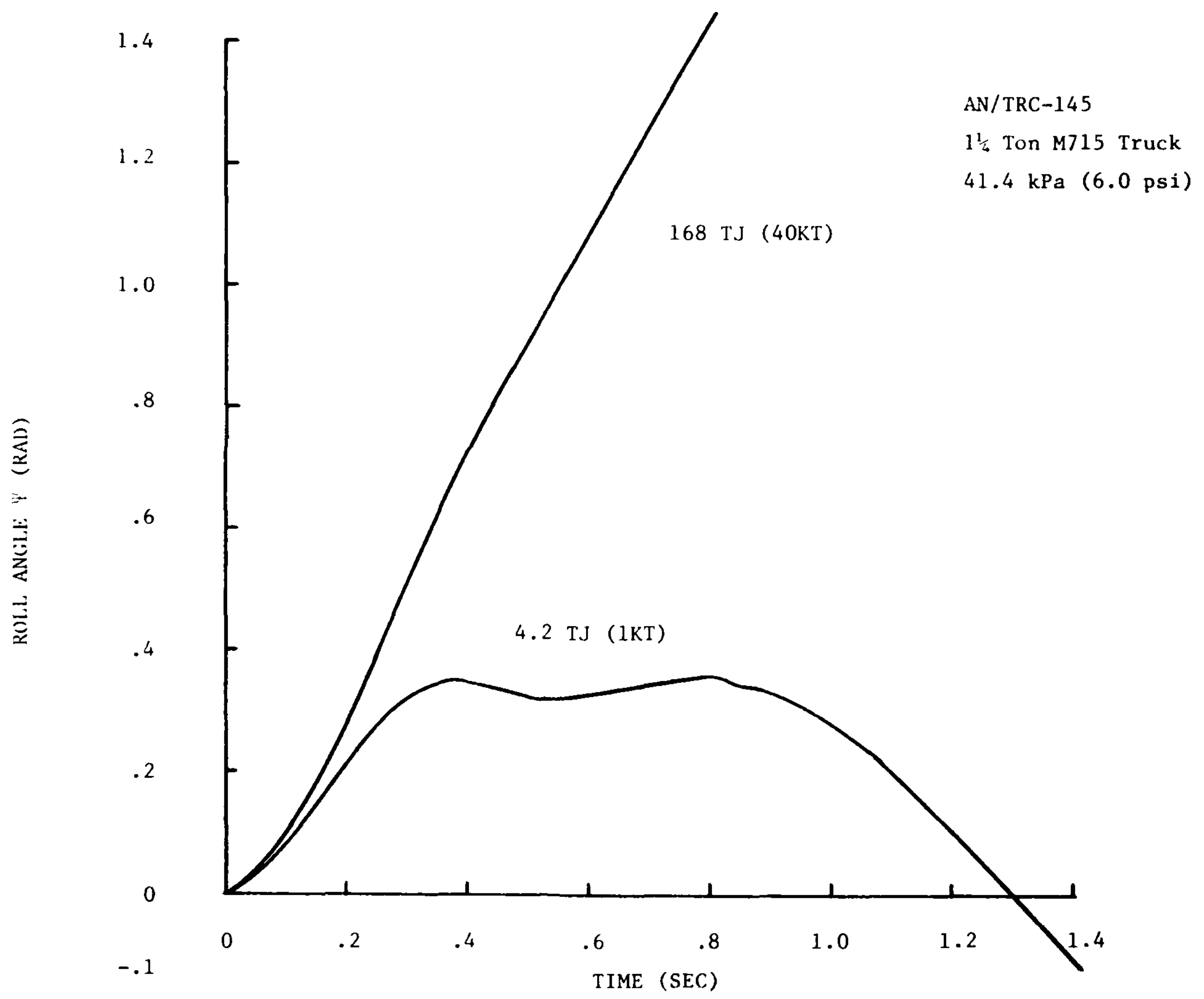

FIGURE 3.110. ROLL ANGLE RESPONSE OF AN/TRC-145 TO INCREASED YIELD AT THE SAME INCIDENT OVERPRESSURE (TRUCK)

TABLE 3.5

FREQUENCY CONTENT AND AMPLITUDE RATIO OF MEASURED

AND PREDICTED RESPONSES FOR THE AN/TRC-145

GAGE	APPROXIMATE DOMINANT FREQUENCY (Hz)		ACCELERATION AMPLITUDE RATIO
	TEST	NASTRAN	MEASURED/PREDICTED
01/1H	400	400 & 2200	.5
01/1V	2000	600	1.0
01/2H	1400	67	.80
01/2V	2500	300	1.8
01/4H	-	500	-
01/4V	2000	1200	1.4
01/3H	1000	rigid body	4

SECTION 4

SUMMARY AND MAJOR CONCLUSIONS

This report has presented a description of the finite element structural models of several Army command, control and communication shelter systems (C^3) that were fielded in the recent DICE THROW test. The models were developed for the AN/TRC-117, AN/TRC-110 and the AN/TCC-61, which utilize the S-280 shelter, and for the AN/TRC-145 which utilizes the S-250 shelter. Various overpressure models were used to prepare loading tables for these systems, and base motion excitation was provided by the TRUCK code. Structural accelerations were determined with the NASTRAN code for several incident overpressure levels experienced in DICE THROW and comparisons with measured responses were made for two systems, the AN/TRC-117 and the AN/TRC-145. In addition to the above mentioned systems, a structural model of the AN/GRC-142B, which also utilizes the S-250 shelter, was developed but no responses were obtained.

The three S-280 systems differed from each other primarily with respect to the internal racks and equipment. This was also the case for the two S-250 systems. It was thus convenient to develop a single S-280 shelter structural model which could be used with the rack configurations of the AN/TRC-117, AN/TRC-110 and the AN/TCC-61. To some extent, a similar procedure was also used for the S-250 shelter model in conjunction with the racks of the AN/TRC-145 and the AN/GRC-142B. Since none of the systems modeled has mass or structural symmetry, it was necessary to model the entire shelter-rack-equipment structure without the benefit of symmetry for reducing the degrees-of-freedom.

The comparison of the measured and analytically determined rack accelerations for the AN/TRC-117 and AN/TRC-145 at an incident overpressure of 41.4 kPa (6.0 psi) revealed the following major conclusions:

1. The comparison for the AN/TRC-117 was poor, with regard to peak accelerations and frequency content. The measured peak accelerations and the frequency content of the measured data exceeded considerably the values for the analytical predictions. The best comparison indicated a factor of 2.0 between the measured and analytical acceleration peaks.

2. The comparison of peak accelerations for the AN/TRC-145 was much more favorable than for the AN/TRC-117. Acceleration peaks compared within a factor 0.5 to 2.0, and even matched closely for two gages. However, as in the case of the AN/TRC-117, the frequency content of the measured accelerations was in general considerably higher than the analytical frequencies.

3. It is suspected that the higher frequency content in the measured data may be due to localized structural frequencies near the gage mount. This is supported by the general high frequency character of the response sensed by the gage intended to pick up the rigid body accelerations for both shelter systems. On the other hand, the lower frequency content in the analytical response can be attributed to insufficient detail of the rack structural model near the gage mount.

4. The AN/TRC-117 racks had sustained considerable damage whereas the AN/TRC-145 racks appeared to suffer no damage. This is also a major consideration for the poor comparison in the AN/TRC-117 acceleration levels.

5. A major uncertainty in the modeling was the unknown distribution of a considerable portion of the total mass of each system. For the AN/TRC-117, for example, this portion represents 40% of the total mass.

6. The base motion does not appear to contribute meaningfully to the structural acceleration response of the shelter walls and equipment racks during the first 30 msecs or so.

7. Increasing the yield while maintaining the overpressure constant, i.e., effectively increasing the drag phase loading without affecting the diffractive loading significantly, resulted in overturning of the AN/TRC-145 system but did not affect the early-time structural response.

8. The AN/TRC-145, by nature of its more compact design, appears to be less vulnerable to blast-induced structural damage than the larger, more flexible, S-280 systems.

APPENDIX A

DATA LISTINGS FOR TRUCK CODE

AN/TRC-117 & AN/TRC-110

AN/TCC-61

AN/TRC-145

DATA LISTING FOR AN/TRC-117 AND AN/TRC-110

```
M35A2-S280 SHELTER,SHELTER AND HEAVY RACKS RIG. ATTACHED.  (110, 117)
              0
              0            0            0            3            1            0
              1            2            2
              2            1            1
32.67         0.           39.04        -99.38
3.705         0.           1.           0.
4.485         0.           0.           -130.
4.465         0.           0.           -178.
-32129.
224951.       215959.      53400.
312.          2952.        2844.
93.26         3381.        3960.
93.26         3381.        3960.
15.4          10.8         0.0          15.4         5.6          0.0
15.4          11.19        -10.76       15.4         -1.4         -5.24
20.24         5.0          -130.0       20.24        0.0          -130.0
20.24         5.0          -178.0       20.24        0.0          -178.0
0.0           0.0
33.675
0.0           -130.0
29.266        40.75
0.0           -175.0
29.266        40.75
              2     20.24
              5
-10000.       42000.       0.0          0.0          10000.       -82000.
              4
-10000.       160000.      0.0          0.0          10000.       -328000.
              2
-10000.       0.           10000.       0.
              2
-10000.       0.           10000.       0.
              4
-10000.       84000.       0.0          0.0          10000.       -164000.
2.48          2.48
              5
-6.2          6243.        0.0          0.0          100.         -100700.
              2
-100.         0.0          100.         0.0
              2
-5.0          0.0          100.         0.0
              2
-5.0          0.0          100.         0.0
              5
-6.2          7161.        0.0          0.0          100.         -115500.
              5
-8.5          26900.       -.125        80.0         0.0          0.0
              5
0.0           0.0          .125         32.5         10.0         12700.
20.375        7.6          386.0
0.0           0.0          1000.
.05           .00015
              6
              3            1
              1            1            1
              4
```

DATA LISTING FOR AN/TRC-117 AND AN/TRC-110 (CONT'D)

29.57	12.36	6.06	1285.9
26.02	37.07	78.06	12.36
29.57	37.07	6.06	1285.9
26.02	12.36	78.06	37.07
29.57	37.07	-43.96	1285.9
78.06	12.36	26.02	37.07
29.57	12.36	-43.96	1285.9
78.06	37.07	26.02	12.36
	4		
21.25	15.89	34.08	1350.2
63.75	33.54	17.95	15.89
-21.25	15.89	34.08	1350.2
17.95	33.54	63.75	15.89
-14.79	40.60	34.08	521.9
14.79	6.83	44.36	40.59
14.79	40.60	34.08	521.9
44.36	6.83	14.79	40.59
	0		
	1		
0.0	49.42	-17.96	8846.0
	1		
0.0	0.0	-17.96	8846.0
	6		
46.5	11.0	-200.5	1122.0
127.5	101.17	25.5	11.0
46.5	11.0	-149.5	1122.0
76.5	101.17	76.5	11.0
46.5	11.0	-98.5	1122.0
25.5	101.17	127.5	11.0
46.5	33.0	-98.5	1122.0
25.5	79.17	127.5	33.0
46.5	33.0	-149.5	1122.0
76.5	79.17	76.5	33.0
46.5	33.0	-200.5	1122.0
127.5	79.17	25.5	33.0
	4		
-44.5	15.89	-73.0	127.1
2.0	96.28	91.0	15.89
-38.04	57.89	-73.0	207.1
8.47	74.29	84.54	37.89
38.04	57.89	-73.0	207.1
84.54	74.29	8.47	37.89
44.5	15.89	-73.0	127.1
91.0	96.28	2.0	15.89
	4		
23.25	11.0	-226.0	1023.0
23.25	101.17	69.75	11.0
23.25	33.0	-226.0	1023.0
23.25	79.17	69.75	33.0
-23.25	33.0	-226.0	1023.0
69.75	79.17	23.25	33.0
-23.25	11.0	-226.0	1023.0
69.75	101.17	23.25	11.0

DATA LISTING FOR AN/TRC-117 AND AN/TRC-110 (CONCL'D)

	4				
44.65	30.0	-149.5	566.67		
0.0	30.0	-75.73	466.47		
-44.65	30.0	-149.5	566.67		
0.0	30.0	-223.28	466.47		
	1				
0.0	0.0	-149.5	14229.0		
	6				
42.80	61.04	-196.87	1614.49		
118.42	51.13	23.68	61.04		
42.80	61.04	-149.50	1614.49		
71.05	51.13	71.05	61.04		
42.80	61.04	-102.13	1614.49		
23.68	51.13	118.42	61.04		
42.80	95.13	-102.13	1614.49		
23.68	17.04	118.42	95.13		
42.80	95.13	-149.50	1614.49		
71.05	17.04	71.05	95.13		
42.80	95.13	-196.87	1614.49		
118.42	17.04	23.68	95.13		
	3				
36.18	78.09	-78.45	901.55		
78.98	34.08	6.62	78.09		
0.0	80.80	-78.45	3711.04		
42.80	31.37	42.80	80.80		
-36.18	78.09	-78.45	901.55		
6.62	34.08	78.98	78.09		
	4				
-21.40	61.04	-220.55	1458.67		
64.19	51.13	21.40	61.04		
21.40	61.04	-220.55	1458.67		
21.40	51.13	64.19	61.04		
21.40	95.13	-220.55	1458.67		
21.40	17.04	64.19	95.13		
-21.40	95.13	-220.55	1458.67		
64.19	17.04	21.40	95.13		
	1				
0.0	112.17	-149.5	12162.34		
	0				
	0	1			
6.	0.	0.	0.	0.8	4250.

END

DATA LISTING FOR AN/TCC-61

M35A2-5240 SHELTER,SHELTER AND HEAVY RACKS RIG. ATTACHED.

0 (61) (ENGULF UK2)

	0	0	0	5	1	0
	1	2	2			
	2	1	1			
33.7	0.	39.96	-100.94			
3.705	0.0	1.0	0.0			
4.483	0.0	0.0	-130.0			
4.483	0.0	0.0	-178.0			
-33657.						
231538.	222210.	56067.				
312.0	2952.0	2844.0				
93.26	3381.0	3960.0				
93.26	3381.0	3960.0				
15.4	10.8	0.0	15.4	5.6	0.0	
15.4	11.19	-10.76	15.4	-1.4	-5.24	
20.24	5.0	-130.0	20.24	0.0	-130.0	
20.24	5.0	-178.0	20.24	0.0	-178.0	
0.0	0.0					
33.875						
0.0	-130.0					
29.266	40.75					
0.0	-178.0					
29.265	40.75					
	2 20.24					
	5					
-10000.	42000.	0.0	0.0	10000.	-82000.	
	5					
-10000.	168000.	0.0	0.0	10000.	-328000.	
	2					
-10000.	0.	10000.	0.			
	2					
-10000.	0.	10000.	0.			
	5					
-10000.	84000.	0.0	0.0	10000.	-164000.	
2.48	2.48					
	5					
-6.2	6243.	0.0	0.0	100.	-100700.	
	2					
-100.	0.0	100.	0.0			
	2					
-5.0	0.0	100.	0.0			
	2					
-5.0	0.0	100.	0.0			
	5					
-6.2	7161.	0.0	0.0	100.	-115500.	
	5					
-8.5	25900.	-.125	80.0	0.0	0.0	
	5					
0.0	0.0	.125	32.5	10.0	12700.	
20.575	0.5	385.0				
0.0	0.0	1000.				
.05	.0001					
	10					
	5	1				
	1	1	1			
	4					

DATA LISTING FOR AN/TCC-61 (CONT'D)

29.57	12.35	8.06	1285.9
26.02	37.07	78.06	12.36
29.57	37.07	8.06	1285.9
26.02	12.35	78.06	37.07
29.57	37.07	-45.98	1285.9
78.06	12.35	26.02	37.07
29.57	12.35	-45.98	1285.9
78.06	37.07	26.02	12.36
	4		
21.25	15.89	34.08	1350.2
63.75	33.54	17.93	15.89
-21.25	15.89	34.06	1350.2
17.93	33.54	63.75	15.89
-14.79	40.50	34.08	521.9
14.79	8.83	44.36	40.59
14.79	40.60	34.98	521.9
44.36	8.83	14.79	40.59
	0		
	1		
0.0	49.42	-17.96	6840.0
	1		
0.0	0.0	-17.96	8040.8
	6		
46.5	11.0	-200.5	1122.0
127.5	101.17	25.5	11.0
46.5	11.0	-149.5	1122.0
76.5	101.17	76.5	11.0
46.5	11.0	-98.5	1122.0
25.5	101.17	127.5	11.0
45.5	33.0	-98.5	1122.0
25.5	79.17	127.5	33.0
46.5	33.0	-149.5	1122.0
76.5	79.17	76.5	33.0
45.5	33.0	-200.5	1122.0
127.5	79.17	25.5	33.0
	4		
-44.5	15.89	-73.0	127.1
2.0	96.23	91.0	15.89
-38.04	37.89	-73.0	207.1
8.47	74.29	84.54	37.89
38.04	37.89	-73.0	207.1
84.54	74.29	8.47	37.89
44.5	15.89	-73.0	127.1
91.0	96.28	2.0	15.89
	4		
23.25	11.0	-226.0	1023.0
23.25	101.17	69.75	11.0
23.25	33.0	-226.0	1023.0
23.25	79.17	69.75	33.0
-23.25	33.0	-226.0	1023.0
69.75	79.17	23.25	33.0
-23.25	11.0	-226.0	1023.0
69.75	101.17	23.25	11.0

```
                4
44.65           30.0           -149.5          566.87

0.0             30.0           -75.73          466.47

-44.65          30.0           -149.5          566.87

0.0             30.0           -223.28         466.47

                1
0.0             0.0            -149.5          14229.0

                6
42.80           61.04          -196.87         1614.49
118.42          51.13          23.68           61.04
42.80           61.04          -149.50         1614.49
71.05           51.13          71.05           61.04
42.80           61.04          -102.13         1614.49
23.68           51.13          118.42          61.04
42.80           95.13          -102.13         1614.49
23.68           17.04          118.42          95.13
42.80           95.13          -149.50         1614.49
71.05           17.04          71.05           95.13
42.80           95.13          -196.67         1614.49
118.42          17.04          23.68           95.13
                5
36.16           78.09          -78.45          901.55
78.98           34.08          6.62            78.09
0.0             80.80          -78.45          3711.04
42.80           31.37          42.80           80.80
-36.18          78.09          -78.45          901.55
6.62            34.08          78.98           78.09
                4
-21.40          61.04          -220.55         1458.67
64.19           51.13          21.40           61.04
21.40           61.04          -220.55         1458.67
21.40           51.13          64.19           61.04
21.40           95.13          -220.55         1458.67
21.40           17.04          64.19           95.13
-21.40          95.13          -220.55         1458.67
64.19           17.04          21.40           95.13
                1
0.0             112.17         -149.5          12162.34

                0
                0              1
2.0             0.             0.              0.              1.              E6 4250.

END
```

DATA LISTING FOR AN/TRC-145

715 WITH S250 RIGIDLY ATTACHED, RACKS RIGIDLY MOUNTED (DICE THROW)

	1					
	0	0	0	2	0	0
	2	5				
	2	2				
15.87	0.0	30.03	-77.62			
1.91	0.0	0.0	0.0			
1.91	0.0	0.0	-126.0			
-9753.						
44847.	34686.	17086.				
0.	2591.	2591.				
0.	2759.	2759.				
25.13	9.78	0.0	17.6	1.28	0.0	
17.8	15.52	-3.07	17.8	-2.07	-3.07	
25.13	11.11	-126.0	25.13	4.61	-126.0	
18.32	10.88	-137.26	18.32	-3.10	-128.05	
0.	0.					
33.5	33.5					
0.	-126.0					
33.5	33.5	33.5				
	6					
-10000.	9610.	-13.3	47.	-4.7	25.	
0.0	0.0	4.7	-56.	10000.	-16000.	
	6					
-10000.	38043.	-13.3	183.	-4.7	102.	
0.0	0.0	4.7	-226.	10000.	-64100.	
	5					
-10000.	7740.	-13.3	26.	0.0	0.0	
4.7	-32.	10000.	-13400.			
	5					
-10000.	30963.	-13.3	103.	0.0	0.0	
4.7	-130.	10000.	-53700.			
1.36	1.36					
	7					
-8.5	6130.	-3.0	1750.	-0.125	250.	
0.0	0.0	100.	-30000.			
	2					
-100.	0.0	100.	0.0			
	7					
-8.5	6200.	-3.0	2360.	-0.125	300.	
0.0	0.0	100.	-50000.			
	2					
-100.	0.0	100.	0.0			
	3					
-8.5	8568.	-0.125	25.5	0.0	0.0	

DATA LISTING FOR AN/TRC-145 (CONT'D)

	3				
0.0	0.0	0.125	10.2	10.0	4046.
17.0	0.8	386.			
0.0	0.0	1000.			
.05	.0001				
	10				
	2	1			
	1	1			
	4				
41.5	9.75	1.9	999.4		
25.6	29.2	76.9	9.75		
41.5	9.75	-49.4	999.4		
76.9	29.2	25.6	9.75		
41.5	29.25	1.9	999.4		
25.6	9.75	25.6	29.2		
41.5	29.25	-49.4	999.4		
76.9	9.75	76.9	29.2		
	2				
-20.8	19.5	27.5	1618.5		
20.8	19.5	62.2	19.5		
20.8	19.5	27.5	1618.5		
62.2	19.5	20.8	19.5		
	2				
40.75	19.5	-75.0	58.5		
.75	19.5	82.25	19.5		
-40.75	19.5	-75.0	58.5		
85.25	19.5	.75	19.5		
	1				
0.0	39.	-23.5	8466.		
	1				
0.0	0.0	-23.5	8466.		

```
                 9
40.              15.25          -95.8          904.8
123.3            28.            74.2           15.25
40.              15.25          -125.5         904.8
153.             50.4           44.5           15.25
40.              15.25          -155.2         904.8
183.             76.25          14.8           15.25
40.              45.75          -95.8          904.8
14.8             45.75          74.2           45.75
40.              45.75          -125.5         904.8
44.5             45.75          44.5           45.75
40.              45.75          -155.2         904.8
74.2             45.75          14.8           45.75
40.0             76.25          -95.8          904.8
14.8             15.25          74.2           76.25
40.              76.25          -125.5         904.8
44.5             15.25          44.5           76.25
40.              76.25          -155.2         904.8
74.2             15.25          14.8           76.25
                 2
-20.             65.25          -81.           2100.
20.              26.25          60.            65.25
20.              65.25          -81.           2100.
60.              26.25          20.            65.25
                 4
20.              22.9           -170.          1830.
20.              68.6           60.            22.9
-20.             22.9           -170.          1830.
60.              68.6           20.            22.9
20.              68.6           -170.          1830.
20.              22.9           60.            68.6
-20.             68.6           -170.          1830.
60.              22.9           20.            68.6
                 1
0.               91.5           -125.5         6920.

                 1
0.               0.             -125.5         6920.

                 0              1
6.0              0.             0.             0.             0.8            4250.
0.0
END
```

APPENDIX B

ACCELERATION TIME HISTORIES FOR AN/TRC-145

34.5 kPa (5.0 psi)

20.7 kPa (3.0 psi)

SHELTR LOADING MODEL

GRID POINT 13

AN/TRC-145

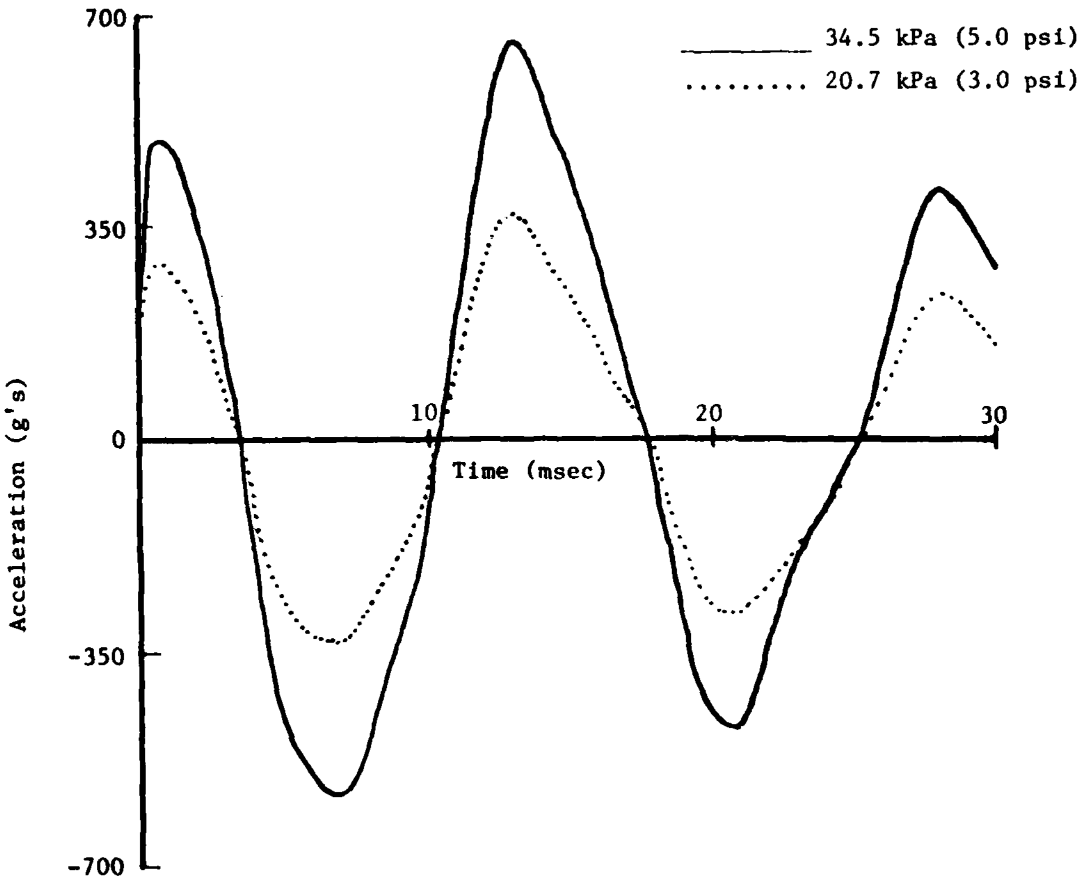

FIGURE B.1. ACCELERATION TIME HISTORY IN BLAST DIRECTION NEAR CENTER OF ROADSIDE WALL PANEL

GRID POINT 103

AN/TRC-145

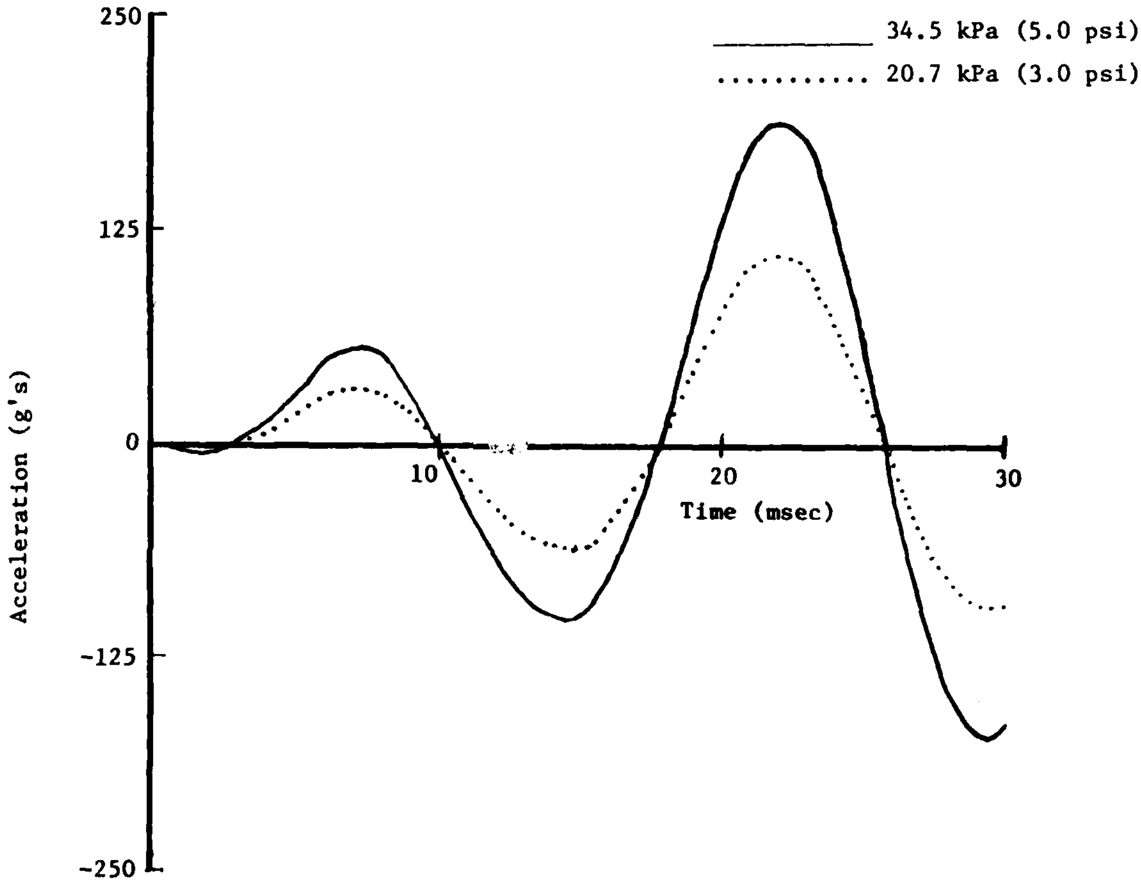

FIGURE B.2. ACCELERATION TIME HISTORY IN BLAST DIRECTION, ROADSIDE RACK

GRID POINT 103

AN/TRC-145

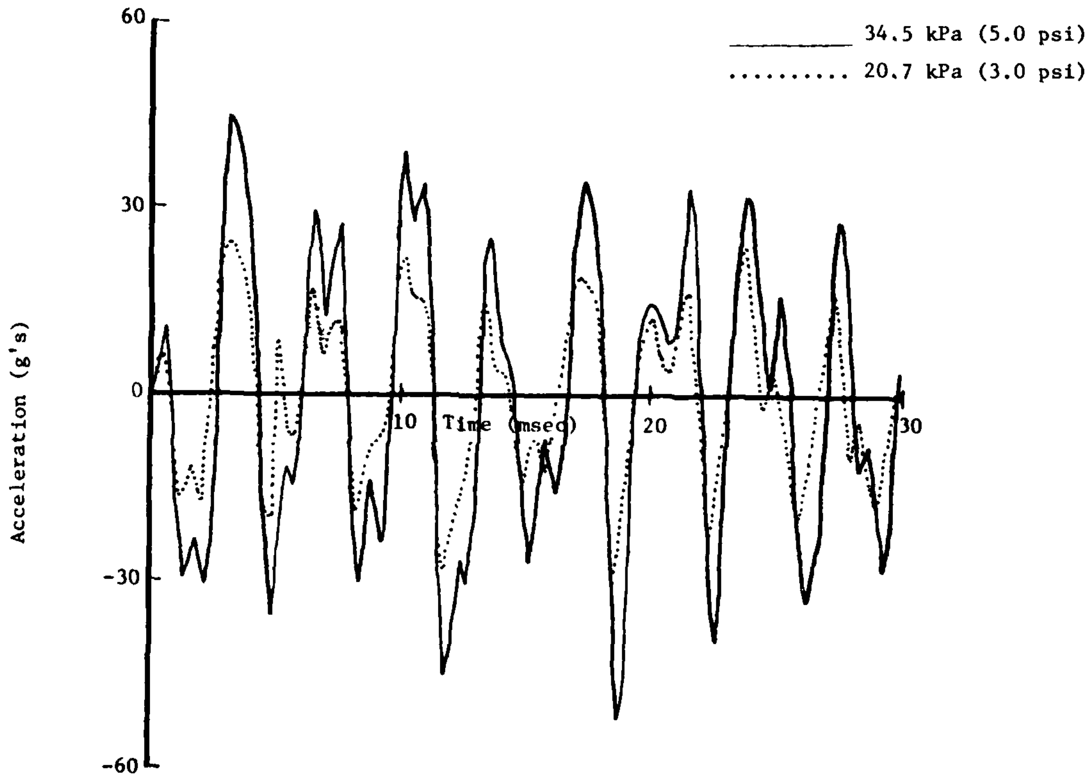

FIGURE B.3. VERTICAL ACCELERATION TIME HISTORY, ROADSIDE RACK

GRID POINT 111

AN/TRC-145

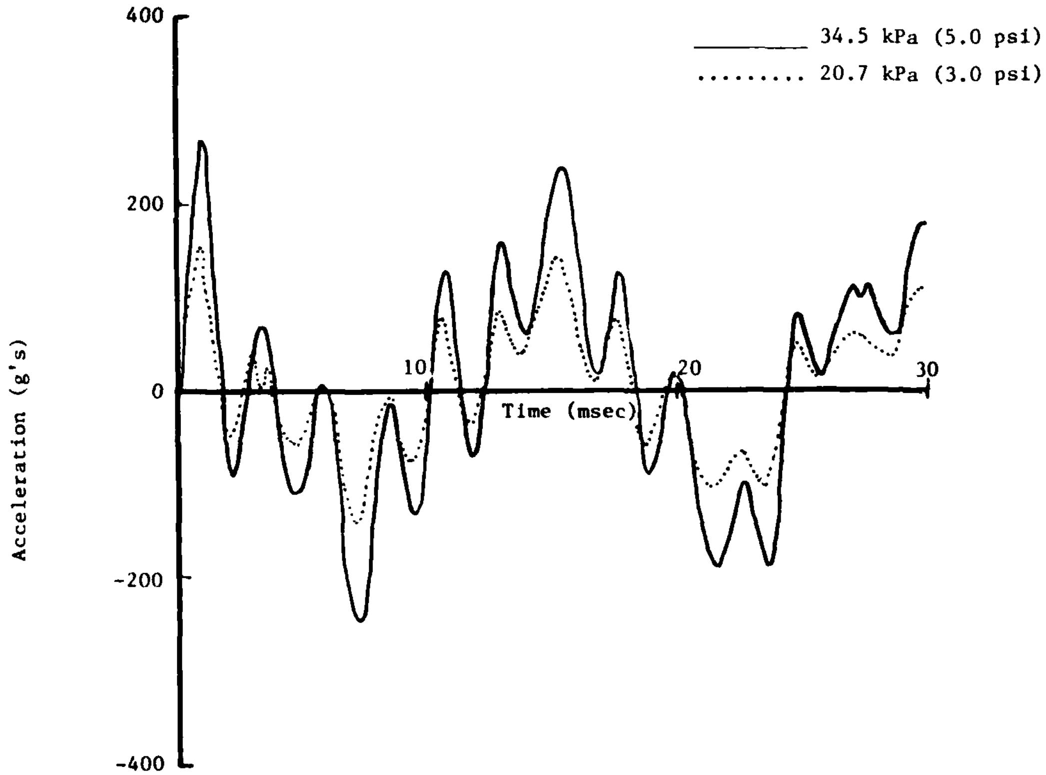

FIGURE B.4. ACCELERATION TIME HISTORY IN BLAST DIRECTION, ROADSIDE RACK

GRID POINT 111

AN/TRC-145

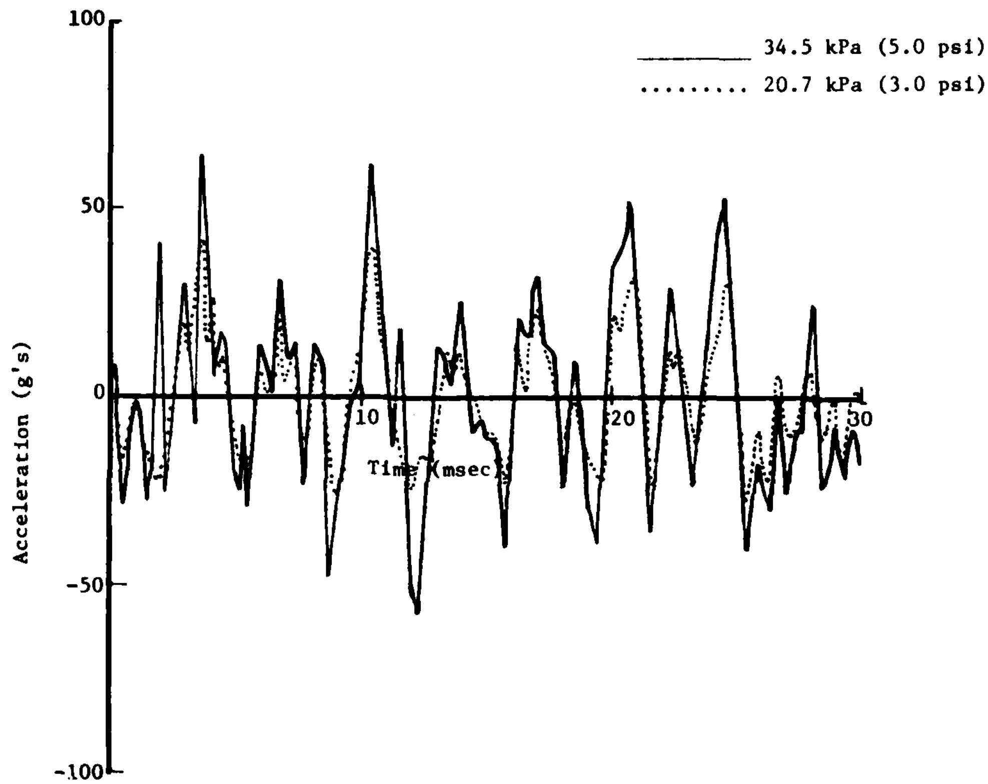

FIGURE B.5. VERTICAL ACCELERATION TIME HISTORY, ROADSIDE RACK

GRID POINT 122

AN/TRC-145

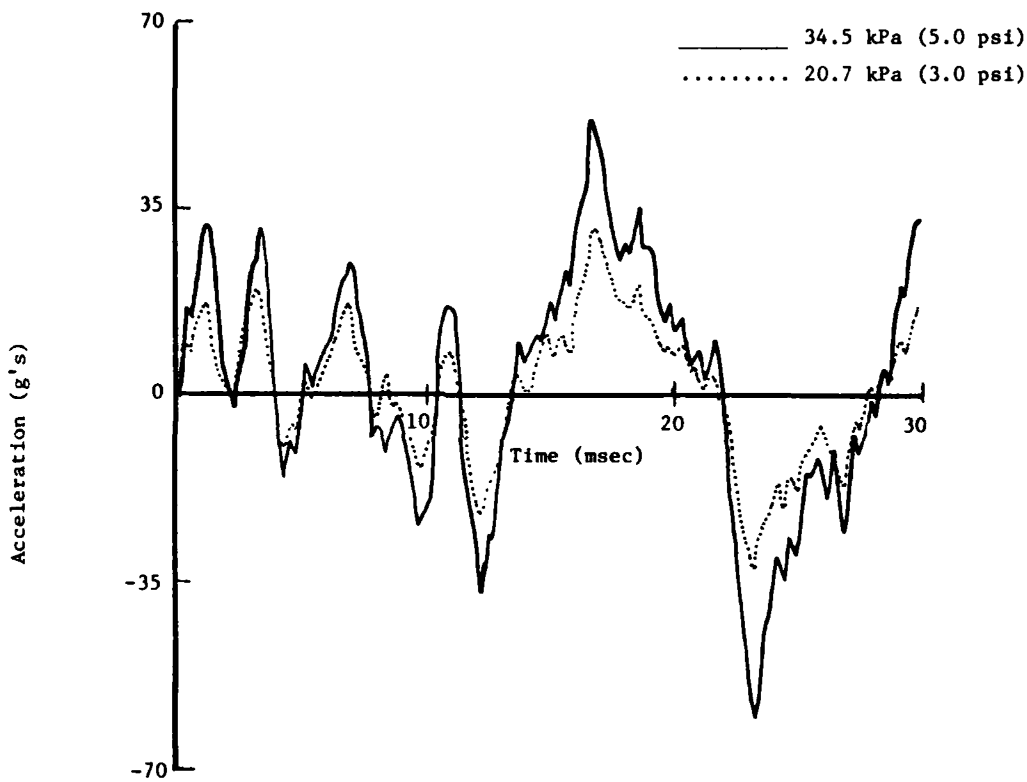

FIGURE B.6. ACCELERATION TIME HISTORY IN BLAST DIRECTION, FRONT WALL RACK

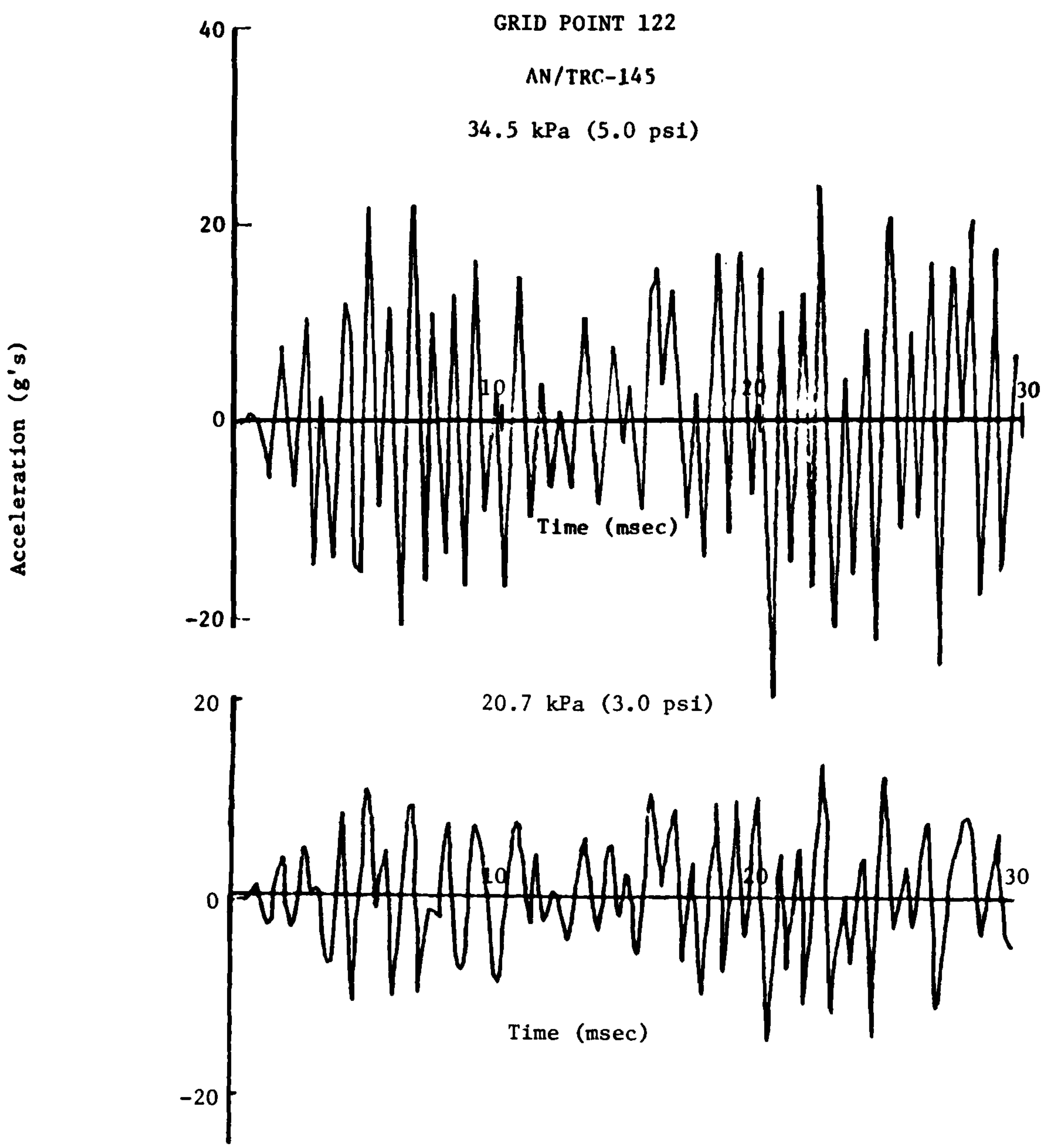

FIGURE B.7. VERTICAL ACCELERATION TIME HISTORY, FRONT WALL RACK

LIST OF SYMBOLS

A	Cross sectional area
CBAR	Beam element
CELAS2	Linear spring element
CONM2	Concentrated mass
CQUAD1	Quadrilateral plate element
D.O.F.	Degrees of freedom
E	Modulus of elasticity of wall panel
E_K	Modulus of elasticity of Kevlar 49
G	Shear modulus of wall panel
G_F	Shear modulus of urethane foam
G_{HC}	Shear modulus of honeycomb core
GRID	Grid point
I_{xx}	Moment of inertia about x centroidal axis
I_{yy}	Moment of inertia about y centroidal axis
I_{yz}	Cross moment of inertia
I_{zz}	Moment of inertia about z centroidal axis
J	Torsional constant
k_y	Transverse shear stiffness coefficient in y-direction
k_z	Transverse shear stiffness coefficient in z-direction
MPC	Multipoint constraint
OMIT	Coordinates omitted from inertia forces
SPC	Single point constraint
t_F	Urethane foam thickness
t_s	Skin thickness

LIST OF SYMBOLS (Cont.)

T_1	Reference membrane thickness
T_3	Transverse shear thickness
V_s	Shock wave velocity
$\left.\begin{matrix} x_{cg} \\ y_{cg} \\ z_{cg} \end{matrix}\right\}$	Mass centroidal coordinates in x, y, z directions, respectively
β	Yaw angle of truck-shelter system
Δp_i	Incident overpressure
Δp_r	Reflected overpressure
ν	Poisson's ratio
ρ	Sandwich panel mass density
ρ_F	Urethane foam mass density
ρ_{HC}	Honeycomb core mass density
ρ_K	Kevlar 49 mass density
ρ_S	Skin mass density
ϕ	Pitch angle of truck-shelter system
χ	Roll angle of truck-shelter system

REFERENCES

1. Private Communication from Mr. Joe Roma of ECOM, Fort Monmouth, N.J.

2. Organization, DS, GS, and Depot Maintenance Manual For Medium Capacity Tactical Radio Relay System, Department of the Army Technical Manual TM-11-5895-456-15, Headquarters Department of the Army, July 1967.

3. Radio Terminal Sets AN/TRC-145(V) 1, AN/TRC-145(V)2, AN/TRC-145(V)3, AN/TRC-145A(V)2, AN/TRC-145A(V)2, and AN/TRC-145A(V)3 (FSN 5895-791-3365), Department of the Army Technical Manual 7M 11-5895-453-14, January 1973.

4. Radio Teletypewriter Sets AN/GRC-142, AN/GRC-142A, AN/GRC-142B, AN/GRC-122, AN/GRC-122A and AN/GRC-122B, Department of the Army Technical Manual TM 11-5815-334-12, May 1970.

5. Hobbs, N.P., et al, TRUCK - A Digital Computer Program for Calculating the Response of Army Vehicles to Blast Waves, Kaman AviDyne TR-136, March 1977.

6. Lottero, R.E., Computational Predictions of Shock Diffraction Loading on an S-280 Electrical Equipment Shelter, U.S. Army Ballistic Research Laboratory, Aberdeen Proving Ground, BRL MR 2599, March 1976. (AD#A022804).

7. Calligeros, John M., and Walsh, John P., Finite Element Modeling of Army Electronic Equipment Shelters Subjected to Blast Loading, U.S. Army Ballistic Research Laboratory, Aberdeen Proving Ground, BRL CR 281, Dec. 1975. (AD#B008904L).

DISTRIBUTION LIST

No. of Copies	Organization
12	Commander Defense Technical Info Center ATTN: DDC-DDA Cameron Station Alexandria, VA 22314
4	Director of Defense Research & Engineering ATTN: DD/TWP DD/S&SS DD/I&SS AD/SW Washington, DC 20301
2	Asst. to the Secretary of Defense (Atomic Energy) ATTN: Document Control Donald R. Cotter Washington, DC 20301
3	Director Defense Advanced Research Projects Agency ATTN: Tech Lib NMRO PMO 1400 Wilson Boulevard Arlington, VA 22209
2	Director Defense Civil Preparedness Agency ATTN: Mr. Goerge Sisson/RF-SR Technical Library Washington, DC 20301
4	Director Defense Intelligence Agency ATTN: DT-1B DB-4C/E.O. Farrell DT-2/Wpns & Sys Div RDS-3A4 Washington, DC 20301
1	Director Weapons Systems Evaluation Group ATTN: Document Control Washington, DC 20305
1	Director National Security Agency ATTN: E.F. Butala, R15 Ft. George G. Meade, MD 20755
3	Director Joint Strategic Target Planning Staff JCS ATTN: Sci & Tech Info Lib JLTW-2 DOXT Offut AFB Omaha, NB 68113
1	Director Defense Communications Agency ATTN: Code 930 Washington, DC 20305
5	Director Defense Nuclear Agency ATTN: STSI/Archives SPAS/Mr.J. Moulton STSP STVL/Dr.La Vier RATN Washington, DC 20305
6	Director Defense Nuclear Agency ATTN: DDST/Dr. Conrad DDST/Dr. Oswald STTL/Tech Lib (2 cys) SPSS (2 cys) Washington, DC 20305
2	Commander Field Command, DNA ATTN: FCPR FCTMOF Kirtland AFB, NM 87115

DISTRIBUTION LIST

No. of Copies	Organization
1	Commander Field Command, DNA Livermore Branch ATTN: FCPRL P.O. Box 808 Livermore, CA 94550
1	Director Institute for Defense Analysis ATTN: IDA Librarian, Ruth S. Smith 400 Army-Navy Drive Arlington, VA 22202
2	HDQA (DAMA-AR; NCL Div) Washington, DC 20310
1	Program Manager US Army BMD Program Office ATTN: John Shea Alexandria, VA 22333
2	Director US Army BMD Advanced Technology Center ATTN: CRDABH-X CRDABH-S Huntsville, AL 35807
1	Commander US Army BMD System Command ATTN: BDMSC-TFN/N.J. Hurst P.O. Box 1500 Huntsville, AL 35807
2	Deputy Chief of Staff for Operations and Plans ATTN: Technical Library Director of Chemical and Nuclear Operations Department of the Army Washington, DC 20310

No. of Copies	Organization
2	Office, Chief of Engineers Department of the Army ATTN: DAEN-MCE-D DAEN-RDM 890 South Pickett Street Alexandria, VA 22304
1	Commander US Army Engineering Center ATTN: ATSEN-SY-L Fort Belvoir, VA 22060
1	Division Engineer US Army Engineering Division ATTN: HNDSE-R/M.M. Dembo Huntsville Box 1600 Huntsville, AL 35804
1	Division Engineer US Army Engineering Division Ohio River ATTN: Docu Cen P.O. Box 1159 Cincinnati, OH 45201
5	Commander US Army Engineer Waterways Experiment Station ATTN: Technical Library William Flathau John N. Strange Guy Jackson Leo Ingram P.O. Box 631 Vicksburg, MS 39180
1	Commander US Army Materiel Development & Readiness Command ATTN: DRCDMD-ST 5001 Eisenhower Avenue Alexandria, VA 22333

DISTRIBUTION LIST

No. of Copies	Organization
1	Commander US Army Materiel Development & Readiness Command ATTN: Technical Library 5001 Eisenhower Avenue Alexandria, VA 22333
3	Commander US Army Armament Research & Development Command ATTN: DRDAR-LCN-F, W. Reiner DRDAR-TSS (2 cys) Dover, NJ 07801
1	Director US Army ARRADCOM Benet Weapons Laboratory ATTN: DRDAR-LCB-TL Watervliet, NY 12189
1	Commander US Army Armament Materiel Readiness Command ATTN: DRSAR-LEP-L, Tech Lib Rock Island, IL 61299
1	Commander US Army Aviation Research & Development Command ATTN: DRSAV-E P.O. Box 209 St. Louis, MO 63166
1	Director US Army Air Mobility Research & Development Laboratory Ames Research Center Moffett Field, CA 94035
1	Commander US Army Communications Research & Development Command ATTN: DRDCO-PPA-SA Fort Monmouth, NJ 07703
6	Commander US Army Electronics Research & Development Command ATTN: DELSD-L DELEW-E, W.S. McAfee R. Freiberg DELSD-EI, J. Roma DELSD-EM, A. Sigismondi C. Goldy Fort Monmouth, NJ 07703
5	Commander US Army Harry Diamond Labs ATTN: Mr. James Gaul Mr. L. Belliveau Mr. J. Gwaltney Mr. F.N. Wimenitz Mr. Bill Vault 2800 Powder Mill Road Adelphi, MD 20783
5	Commander US Army Harry Diamonds Labs ATTN: DRXDO-TI DRXDO-TI/012 DRXDO-NP DRXDO-RBH/P.Caldwell DELHD-RBA/J. Rosado 2800 Powder Mill Road Adelphi, MD 20783
3	Commander US Army Missile Command ATTN: DRDMI-R DRDMI-YDL Chief Scientist Redstone Arsenal, AL 35809
2	Commander US Army Natick Research & Development Command ATTN: DRXRE/Dr.D. Sieling DRXNM-UE, Arthur Johnson Natick, MA 01762

DISTRIBUTION LIST

No. of Copies	Organization
1	Commander US Army Tank Automotive Research & Development Command ATTN: DRDTA-UL Warren, MI 48090
1	Commander US Army Foreign Science and Technology Center ATTN: Rsch & Concepts Branch 220 7th Street, NE Charlottesville, VA 22901
1	Commander US Army Logistical Center ATTN: ATCL-SCA, Robert Cameron Fort Lee, VA 23801
3	Commander US Army Materials and Mechanics Research Center ATTN: Technical Library John Mescall Richard Shea Watertown, MA 02172
2	Commander US Army Nuclear Agency ATTN: ACTA-NAW Technical Library 7500 Backlick Road, Bldg 2073 Springfield, VA 22150
1	Commander US Army Research Office P.O. Box 12211 Research Triangle Park NC 27709
1	Commander US Army Training and Doctrine Command ATTN: ATCD-SA/Mr. Oscar Wells Fort Monroe, VA 23651
2	Director US Army TRADOC Systems Analysis Activity ATTN: LTC John Hesse ATAA-SL, Tech Lib White Sands Missile Range NM 88002
1	Commander Combined Arms Combat Developments Activity ATTN: ATCA-CO/Mr.L.C. Pleger Fort Leavenworth, KS 66027
1	Chief of Naval Research ATTN: N. Perrone Department of the Navy Washington, DC 20360
2	Chief of Naval Operations ATTN: OP-03EG OP-985F Department of the Navy Washington, DC 20350
1	Chief of Naval Material ATTN: MAT 0323 Department of the Navy Arlington, VA 22217
3	Director Strategic Systems Projects Ofc ATTN: NSP-43, Tech Lib NSP-273 NSP-272 Department of the Navy Washington, DC 02360
1	Commander Naval Electronic Systems Command ATTN: PME 117-21A Washington, DC 20360

DISTRIBUTION LIST

No. of Copies	Organization
3	Commander US Naval Facilities Engineering Command ATTN: Code 03A Code 04B Technical Library Washington, DC 20360
2	Commander Naval Sea Systems Command ATTN: ORD-91313 Library Code 03511 Department of the Navy Washington, DC 20362
4	Officer-in-Charge Civil Engineering Laboratory Naval Constr Btn Ctr ATTN: Stan Takahashi R.J. Odello John Crawford Technical Library Port Hueneme, CA 93041
2	Commander Naval Ship Engineering Center ATTN: Technical Library NSEC 6105G Hyattsville, MD 20782
1	Commander David W. Taylor Naval Ship Research & Development Center ATTN: Lib Div, Code 522 Bethesda, MD 20084
1	Commander Naval Surface Weapons Center ATTN: DX-21, Library Br. Dahlgren, VA 22448
3	Commander Naval Surface Weapons Center ATTN: Code WA501/Navy Nuclear Programs Office Code WX21/Tech Lib Code 240/C.J. Aronson Silver Spring, MD 20910
2	Commander Naval Weapons Center ATTN: Code 533/Tech Lib Code 31804/M. Keith China Lake, CA 94555
2	Commander Naval Ship Research & Development Center Facility Underwater Explosions Research Division ATTN: Code 17/W.W. Murray Technical Library Portsmouth, VA 23709
2	Commander Naval Weapons Evaluation Facility ATTN: Document Control R. Hughes Kirtland AFB Albuquerque, NM 87117
2	Director Naval Research Laboratory ATTN: Code 2027/Tech Lib Code 8440/F. Rosenthal Washington, DC 20375
1	Superintendent Naval Postgraduate School ATTN: Code 2124/Tech Rpts Lib Monterey, CA 93940
1	HQ USAF (IN) Washington, DC 20330
1	HQ USAF(PRE) Washington, DC 20330

DISTRIBUTION LIST

No. of Copies	Organization
2	AFSC (DLCAW; Tech Lib) Andrews AFB Washington, DC 20331
1	AFATL (DLYV, P. Nash) Eglin AFB, FL 32542
1	AFATL (DLYV, Jim Flint) Eglin AFB, FL 32542
2	ADTC (ADBRL-2; Tech Lib) Eglin AFB, FL 32542
2	RADC (EMTLD/Docu Lib; EMREC/ R.W. Mair) Griffis AFB, NY 13340
1	AFWL/R. Henny Kirtland AFB, NM 87117
1	AFWL/DE-I Kirtland AFB, MN 87117
1	AFWL/DEX Kirtland AFB, NM 87117
1	AFWL/SUL(Jimmie L. Bratton) Kirtland AFB, NM 87117
1	AFWL/SUL(M.A. Plamondon) Kirtland AFB, NM 87115
1	Interservice Nuclear Weapons School ATTN: Technical Library Kirtland, AFB, NM 87115
2	Commander-in-Chief Strategic Air Command ATTN: NRI-STINFO Lib XPFS Offutt AFB, NB 68113
4	FTD (TDFBD; TDPMG; ETET/ CPT R.C. Husemann; TD-BTA/Lib) Wright-Patterson AFB, OH 45433
1	AFIT (Lib Bldg. 640, Area B) Wright-Patterson AFB OH 45433
1	Director US Bureau of Mines ATTN: Technical Library Denver Federal Center Denver, CO 80225
1	Director US Bureau of Mines Twin Cities Research Center ATTN: Technical Library P.O. Box 1660 Minneapolis, MN 55111
1	US Energy Res & Dev Admin Albuquerque Operations Office ATTN: Doc Control for Tech Lib P.O. Box 5400 Albuquerque, NM 87115
1	US Energy Research & Development Administration Nevada Operations Office ATTN: Doc Control for Tech Lib P.O. Box 14100 Las Vegas, NV 89114
1	Director Lawrence Livermore Lab ATTN: L.W. Woodruft/L-96 P.O. Box 808 Livermore, CA 94550
1	Director Lawrence Livermore Lab ATTN: Jack Kahn/L-7 P.O. Box 808 Livermore, CA 94550

DISTRIBUTION LIST

No. of Copies	Organization
1	Director Lawrence Livermore Lab ATTN: Tech Info Dept L-3 P.O. Box 808 Livermore, CA 94550
1	Director Lawrence Livermore Lab ATTN: R.G. Dong/L-90 P.O. Box 808 Livermore, CA 94550
1	Director Lawrence Livermore Lab ATTN: Ted Butkovich/L-200 P.O. Box 808 Livermore, CA 94550
1	Director Lawrence Livermore Lab ATTN: Robert Schock/L-437 P.O. Box 808 Livermore, CA 94550
1	Director Lawrence Livermore Lab ATTN: J.R. Hearst/L-205 P.O. Box 808 Livermore, CA 94550
4	Director Los Alamos Scientific Lab ATTN: Doc Control for Rpts Lib R.A. Gentry G.R. Spillman Al Davis P.O. Box 1663 Los Alamos, NM 87544

No. of Copies	Organization
6	Sandia Laboratories ATTN: Doc Control for 3141 Sandia Rpt Collection A.M. Chaban M.L. Merritt L.J. Vortman W. Roherty L. Hill P.O. Box 5800 Albuquerque, NM 87115
1	Sandia Laboratories Livermore Laboratory ATTN: Doc Control for Tech Lib P.O. Box 969 Livermore, CA 94550
1	Director National Aeronautics and Space Administration Scientific and Technical Information Facility P.O. Box 8757 Baltimore/Washington International Airport, MD 21240
3	Aerospace Corporation ATTN: Tech Info Services(2 cys) P.N. Mathur P.O. Box 92957 Los Angeles, CA 90009
1	Agbabian Associates ATTN: M. Agbabian 250 North Nash Street El Segundo, CA 90245
1	Applied Theory, Inc. ATTN: John G. Trulio 1010 Westwood Blvd. Los Angeles, CA 90024
1	Artec Associates, Inc. ATTN: Steven Gill 26046 Eden Landing Road Hayward, CA 94545

DISTRIBUTION LIST

No. of Copies	Organization
1	AVCO ATTN: Res Lib A830, Rm 7201 201 Lowell Street Wilmington, MA 01887
1	The BDM Corporation ATTN: Richard Hensley P.O. Box 9274 Albuquerque International Albuquerque, NM 87119
2	The Boeing Company ATTN: Aerospace Library R.H. Carlson P.O. Box 3707 Seattle, WA 98124
1	Brown Engineering Co., Inc. ATTN: Manu Patel Cummings Research Park Huntsville, AL 35807
2	California Research and Technology, Inc. ATTN: Ken Kreyenhagen Technical Library 6269 Variel Avenue Woodland Hills, CA 91364
1	Calspan Corporation ATTN: Technical Library P.O. Box 235 Buffalo, NY 14221
1	Civil/Nuclear Systems Corporation ATTN: Robert Crawford 1200 University N.E. Albuquerque, NM 87102
1	EG&G, Incorporated Albuquerque Division ATTN: Technical Library P.O. Box 10218 Albuquerque, NM 87114

No. of Copies	Organization
1	The Franklin Institute ATTN: Zemons Zudans 20th Street and Parkway Philadelphia, PA 19103
1	General American Trans Corporation General American Research Div ATTN: G.L. Neidhardt 7449 N. Natchez Avenue Niles, IL 60648
1	General Electric Company-TEMPO ATTN: DASIAC P.O. Drawer QQ Santa Barbara, CA 93102
1	General Electric-TEMPO ATTN: E. Bryant 220 S. Main Street, Rm 206 Bel Air, MD 21014
2	Hazeltine Corp. ATTN: Carl Meinen Greenlawn, NY 11740
1	J.H. Wiggins Co., Inc. ATTN: John Collins 1650 South Pacific Cost Highway Redondo Beach, CA 90277
5	Kaman Avidyne ATTN: Dr.N.P. Hobbs (4 cys) Mr. S. Criscione 83 Second Avenue Northwest Industrial Park Burlington, MA 01830
3	Kaman Avidyne ATTN: John Calligeros John P. Walsh Raffi P. Yeghiayan 83 Second Avenue Northwest Industrial Park Burlington, MA 01830

DISTRIBUTION LIST

No. of Copies	Organization
3	Kaman Sciences Corporation ATTN: Library P.A. Ellis F.H. Shelton 1500 Garden of the Gods Road Colorado Spring, CO 80907
1	Lockheed Missiles & Space Co. ATTN: Technical Library P.O. Box 504 Sunnyvale, CA 94088
2	Martin Marietta Aerospace Orlando Division ATTN: G. Fotieo Craig Luongo, Mail Pt 505 P.O.Box 5837 Orlando, FL 32805
3	McDonnell Douglas Astronautics Corporation ATTN: Robert W. Halprin Mr. C. Gardiner Dr. P. Lewis 5301 Bolsa Avenue Huntington Beach, CA 92647
2	Merritt Cases, Inc. ATTN: J.L. Merritt Technical Library P.O. Box 1206 Redlands, CA 92373
1	Meteorology Research, Inc. ATTN: W.D. Green 454 West Woodbury Road Altadena, CA 91001
1	The Mitre Corporation ATTN: Library P.O. Box 208 Bedford, MA 01730

No. of Copies	Organization
1	Pacific Sierra Research Corp ATTN: Dr. Harold Brode 1456 Cloverfield Boulevard Santa Monica, CA 90404
2	Pacifica Technology ATTN: G. Kent R. Bjork P.O. Box 148 Del Mar, CA 92014
4	Physics International Corp. ATTN: Robert Swift Charles Godfrey Larry A. Behrmann Technical Library 2700 Merced Street San Leandro, CA 94577
1	Radkowski Associates ATTN: Peter R. Radkowski P.O. Box 5474 Riverside, CA 92517
2	R&D Associates ATTN: Dr. Albert L. Latter William B. Wright P.O. Box 9695 Marina del Rey, CA 90291
4	R&D Associates ATTN: Jerry Carpenter Sheldon Schuster J.G. Lewis Technical Library P.O. Box 9695 Marina del Rey, CA 90291
1	R&D Associates ATTN: Henry Cooper Suite 500 1401 Wilson Boulevard Arlington, VA 22209

DISTRIBUTION LIST

No. of Copies	Organization
1	The Rand Corporation ATTN: C.C. Mow 1700 Main Street Santa Monica, CA 90406
2	Science Applications, Inc. ATTN: John Cockayne William Layson 1651 Old Meadow Road McLean, VA 22102
1	Science Applications, Inc. Suite 120 2450 Washington Avenue San Leandro, CA 94577
2	Science Applications, Inc. ATTN: Technical Library Michael McKay P.O. Box 2351 La Jolla, CA 92038
4	Systems, Science & Software ATTN: Donald R. Grine Ted Cherry Thomas D. Riney Technical Library P.O. Box 1620 La Jolla, CA 92037
3	Terra Tek, Inc. ATTN: Sidney Green A.H. Jones Technical Library 420 Wakara Way Salt Lake City, UT 84108
2	Tetra Tech, Inc. ATTN: Li-San Hwang Technical Library 630 North Rosemead Blvd. Pasadena, CA 91107
7	TRW Systems Group ATTN: Paul Lieverman Benjamin Sussholtz Norm Lipner William Rowan Jack Farrell Pravin Bhutta Tech Info Ctr/S-1930 One Space Park Redondo Beach, CA 92078
1	TRW Systems Group San Bernardino Operations ATTN: Greg Hulcher P.O. Box 1310 San Bernardino, CA 92402
2	Union Carbide Corporation Holifield National Laboratory Civil Defense Research Proj ATTN: Doc Control for Tech I P.O. Box X Oak Ridge, TN 37830
1	Universal Analytics, Inc. ATTN: E.I. Field 7740 W. Manchester Blvd. Playa del Rey, CA 90291
1	Weidlinger Assoc. Consulting ATTN: M.L. Baron 110 East 59th Street New York, NY 10022
1	Westinghouse Electric Co. Marine Division ATTN: W.A. Votz Hendy Avenue Sunnyvale, CA 94008
2	Battelle Memorial Institute ATTN: Technical Library R.W. Klingesmith 505 King Avenue Columbus, OH 43201

DISTRIBUTION LIST

No. of Copies	Organization
1	California Institute of Technology ATTN: T.J. Ahrens 1201 E. California Blvd. Pasadena, CA 91109
2	Denver Research Institute University of Denver ATTN: Mr. J. Wisotski Technical Library P.O. Box 10127 Denver, CO 80210
3	ITT Research Institute ATTN: Milton R. Johnson R.E. Welch Technical Library 10 West 35th Street Chicago, IL 60616
2	Lovelace Foundation for Medical Education ATTN: Asst. Dir of Research/ Robert K. Jones Technical Library 5200 Gibson Blvd., SE Albuquerque, NM 87109
1	Massachusetts Institute of Tech. Aeroelastic & Structures Rsch Lab ATTN: Dr. E.A. Witmer Cambridge, MA 02139
2	Southwest Research Institute ATTN: Dr. W.E. Baker A.B. Wenzel 8500 Culebra Road San Antonio, TX 78206
2	SRI International ATTN: Dr. G.R. Abrahamson Carl Peterson 333 Ravenswood Avenue Menlo Park, CA 94025
1	University of Dayton Industrial Security Super. KL-505 ATTN: H.F. Swift 300 College Park Avenue Dayton, OH 45409
1	University of Illinois Consulting Engineering Services ATTN: Nathan M. Newmark 1211 Civil Engineering Bldg Urbana, IL 61801
2	The University of New Mexico The Eric H. Wang Civil Engineering Research Facility ATTN: Larry Bickle Neal Baum University Station Box 188 Albuquerque, NM 87131
2	Washington State University Administration Office ATTN: Arthur Miles Hohorf George Duval Pullman, WA 99163

Aberdeen Proving Ground

Dir, USAMSAA
ATTN: DRXSY-D
DRXSY-MP, H. Cohen
Ben Cummings
M. Reches

Cdr, USATECOM
ATTN: DRSTE-TO-F

Dir, Wpns Sys Concepts Team
Bldg. E3516, EA
ATTN: DRDAR-ACW

Cdr, USA Ordnance Ctr & School
ATTN: ATSL-CD-CS/LT C.E. Tate
Bldg 3072

USER EVALUATION OF REPORT

Please take a few minutes to answer the questions below; tear out this sheet and return it to Director, US Army Ballistic Research Laboratory, ARRADCOM, ATTN: DRDAR-TSB, Aberdeen Proving Ground, Maryland 21005. Your comments will provide us with information for improving future reports.

1. BRL Report Number ______________________

2. Does this report satisfy a need? (Comment on purpose, related project, or other area of interest for which report will be used.)

____

____

____

3. How, specifically, is the report being used? (Information source, design data or procedure, management procedure, source of ideas, etc.) ______________________

____

____

4. Has the information in this report led to any quantitative savings as far as man-hours/contract dollars saved, operating costs avoided, efficiencies achieved, etc.? If so, please elaborate.

____

____

5. General Comments (Indicate what you think should be changed to make this report and future reports of this type more responsive to your needs, more usable, improve readability, etc.) ______________________

____

____

____

6. If you would like to be contacted by the personnel who prepared this report to raise specific questions or discuss the topic, please fill in the following information.

Name: ______________________

Telephone Number: ______________________

Organization Address: ______________________

____

____

DATE
ILMED
- 8